Contents lists available at [ScienceDirect](https://www.sciencedirect.com)

Earth-Science Reviews

journal homepage: www.elsevier.com/locate/earscirev

Arctic Ocean Mega Project: Paper 1 - Data collection

Anatoly M. Nikishin^{a,*}, Eugene I. Petrov^b, Sierd Cloetingh^c, Andrey V. Korniychuk^d,
 Andrey F. Morozov^b, Oleg V. Petrov^e, Viktor A. Poselov^f, Alexey V. Beziazykov^f,
 Sergey G. Skolotnev^g, Nikolay A. Malyshev^h, Vladimir E. Verzhbitsky^h, Henry W. Posamentierⁱ,
 Sergey I. Freiman^{a,d}, Elizaveta A. Rodina^a, Ksenia F. Startseva^a, Nikolay N. Zhukov^{a,d}

^a Geological Faculty, Moscow State University, Moscow, Russia

^b The Federal Subsoil Resources Management Agency, Moscow, Russia

^c Utrecht University, Utrecht, the Netherlands

^d Geological and Geophysical Survey of Geological Institute, the Russian Academy of Sciences (GEOSURVEY GIN RAS), Moscow, Russia

^e Russian Geological Research Institute (VSEGED), Saint Petersburg, Russia

^f Gramberg All-Russia Scientific Research Institute for Geology and Mineral Resources of the Ocean (VNIOkeangeologia), Saint Petersburg, Russia

^g Geological Institute, Russian Academy of Sciences, Moscow, Russia

^h Rosneft Oil Company, Moscow, Russia

ⁱ Consultant, 25 Topside Row Drive, the Woodlands, TX 77380, USA

ARTICLE INFO

Keywords:

Arctic
 Seismic data
 Subbottom profiler
 Multi-beam bathymetry
 Lomonosov Ridge
 Mendeleev Rise
 Gakkel Ridge
 Podvodnikov Basin
 Icebreaker
 Scientific research submarine
 Seaward dipping reflectors

ABSTRACT

Over a period of the past 15–20 years, the Russian Government implemented the Arctic Mega Project for geological and comprehensive study of the Arctic Ocean. In this paper we discuss the methods that were used in the implementation of this project. In the course of several expeditions, multiple types of data were acquired, which included: (1) seismic data of different types, (2) subbottom profiler data, (3) geological sampling on slopes of the Mendeleev Rise with the use of special equipment, (4) borehole drilling, (5) gravity and magnetic anomalies, (6) offshore geodetic data, (7) multi-beam bathymetry surveys, and (8) field surveys on multiple Arctic islands. Several nuclear icebreakers and a scientific research submarine were deployed in these operations. Specifically, more than 23,000 km of 2D multi-channel seismic lines and more than 4000 km of wide-angle refraction/reflection seismic lines were acquired, in addition to subbottom profiles for the Eurasia Basin and new bathymetric data of the Arctic Ocean. The new database is intended to facilitate the development of new insights into Arctic geology and geodynamics and contribute to a better understanding of the structure and tectonic evolution of the Arctic Ocean as a whole.

1. Introduction

The Arctic Ocean remains one of the most poorly explored regions on Earth. The Arctic is surrounded by multiple countries: USA, Canada, Denmark (Greenland), Norway and Russia. This naturally implies the necessity of cooperation between different countries to investigate and explore the Arctic. A milestone in international scientific cooperation in the Arctic was the First International Polar Year (IPY) (1882–1883), initiated by the Austrian explorer and naval officer Lt. Karl Weyprecht (Weber and Roots, 1990; Stein, 2008). Over the years, Russia has taken active part in national and the international investigation of the Arctic Ocean. The current project takes Arctic investigation to a new level.

The Arctic Ocean comprises the deep-water Arctic Basin and the

continental shelves adjacent to it (Fig. 1). On the Russian side the continental shelf is widest and is represented by the Barents, Kara, Laptev, East Siberian, and Chukchi seas. On the margins of the USA (Alaska), Canada and Greenland, the continental shelves are significantly narrower. The deep-water Arctic Basin is traditionally divided into the Eurasia and Amerasia basins. The boundary between the basins is marked by the Lomonosov Ridge. It has been suggested (Nikishin et al., 2014) that the Amerasia Basin be divided into two subbasins: the South Amerasia and the North Amerasia basins. Key bathymetric features subsequently can be associated with each of these domains; the Canada Basin lies within the South Amerasia domain. The Alpha-Mendeleev Rise is located within the central part of the North Amerasia domain. The Podvodnikov Basin and deep-water Makarov Basin are situated between

* Corresponding author.

E-mail address: nikishin@geol.msu.ru (A.M. Nikishin).

<https://doi.org/10.1016/j.earscirev.2021.103559>

Received 14 September 2020; Received in revised form 4 February 2021; Accepted 12 February 2021

Available online 16 February 2021

0012-8252/© 2021 Elsevier B.V. All rights reserved.

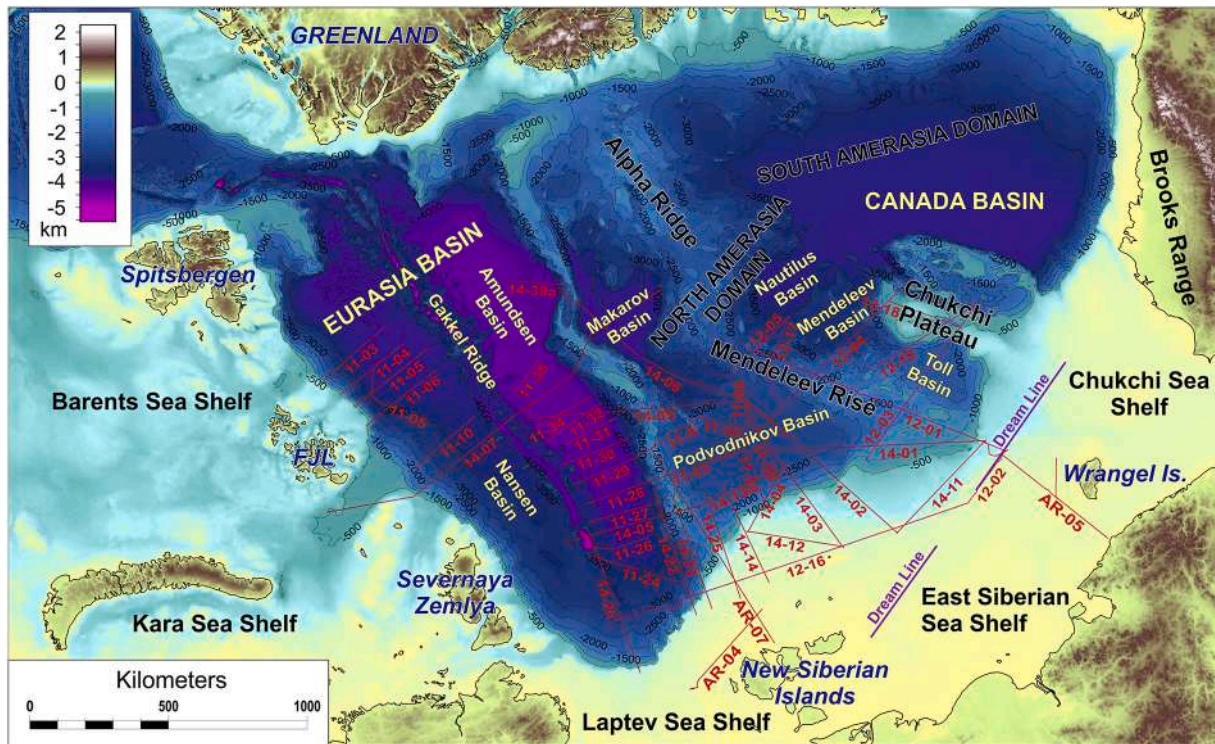


Fig. 1. Topography and bathymetry of the Arctic region (Jakobsson et al., 2012, 2020). Red lines indicate seismic data acquired during the Russian expeditions *Arktika-2011*, *Arktika-2012*, and *Arktika-2014*. (For interpretation of the references to colour in this figure legend, the reader is referred to the web version of this article.)

the Alpha-Mendelev Rise and the Lomonosov Ridge. The deep-water Nautilus and Mendeleev basins are located between the Alpha-Mendelev Rise and the Canada Basin and the Toll Basins is identified between the Mendeleev Rise and the Chukchi Plateau. The Eurasia Basin is divided by the Gakkel Mid-Oceanic Ridge into the Nansen and Amundsen basins. The Eurasia Basin is asymmetric because the Amundsen Basin has a greater water depth than the Nansen Basin (Fig. 1). This asymmetry is also associated with its geological structure (e.g., Nikishin et al., 2018).

The Arctic comprises a considerable part of the Earth's surface. In the past, global plate reconstructions of the evolution of the Earth tended to largely disregard the Arctic simply because of lack of reliable data from that region. The kinematic history of lithospheric plates in the Arctic was developed with data from extra-Arctic regions (for instance, the North Atlantic and the Pacific Ocean) (e.g. Shephard et al., 2013). In order to construct an adequate model of the Mesozoic and Cenozoic global geodynamic history of the Earth, understanding the history of opening of the Arctic Ocean is clearly a prerequisite. The presence of the High Arctic Large Igneous Province (HALIP) complicates Arctic tectonic history. Until this project, limited data on its tectonic structure in the area of the Alpha-Mendelev Rise had been available (e.g., Van Wagoner et al., 1986; Døssing et al., 2013; Coakley et al., 2016; Oakey and Saltus, 2016). Consequently, there were widely different interpretations of this territory, ranging from a continental volcanic area to an oceanic basaltic plateau to a mid-oceanic ridge (e.g., Van Wagoner et al., 1986; Weber, 1990; Dove et al., 2010; Bruvoll et al., 2012; Døssing et al., 2013; Lavrov et al., 2013; Pease et al., 2014; Jokat and Ickrath, 2015; Coakley et al., 2016; Oakey and Saltus, 2016; Petrov and Smelror, 2019; Mukasa et al., 2020).

The ultra-slow spreading Gakkel Mid-Oceanic Ridge is situated in the Eurasia Basin (e.g., Dick et al., 2003; Nikishin et al., 2018). This is a unique geological feature. Its mechanism of formation to account for its ultra-slow spreading nature is poorly known, as is its mineralogical composition (e.g., Dick et al., 2003; Lutz et al., 2018; Jokat et al., 2019).

Also unknown in detail is the exact timing of the initiation of Eurasia Basin opening and whether it was accompanied by magmatism or mantle exhumation during its formation, especially in the area close to the Laptev Sea. Although more than 20 km of sedimentary section has been documented on the Arctic shelves (e.g., the North Chukchi Basin, Nikishin et al., 2014, 2019; Piskarev et al., 2019; Petrov and Smelror, 2019), its origin and the nature of the underlying crustal structure remain unclear.

As recently as 2000, the Arctic Ocean, and especially its Russian part, had been poorly studied and consequently poorly understood. The history of exploration of this ocean has already been reviewed, e.g., in Weber and Roots (1990) Stein (2008), Coakley et al. (2016), Piskarev et al. (2019). Several models for the structure and evolutionary history of the Arctic have been proposed based on available data (e.g., Grantz et al., 1998; Lawver and Scotese, 1990; Embry, 1990; Jokat et al., 1992; Lane, 1997; Vogt et al., 1998; Weber, 1990; Zonenshain et al., 1990; Ziegler, 1988). Based on these studies using limited data control one could incorrectly surmise that the principal models of the Arctic Ocean's evolution had already been formulated. The current study, which incorporates a vast new dataset, has afforded a whole new view of this basin.

Between 1990 and 2000, the Arctic states (Canada, Denmark, Norway, Russia and the USA) faced the challenge of establishing the outer limits of their continental shelves in the Arctic Ocean. The solution to this issue was to be based upon the United Nations Convention on the Law of the Sea (UNCLOS). Many of the requirements for establishing the outer limits of continental shelves involved the mapping of key morphological and geological structures of such offshore territories that are contiguous with the coastal State.

UNCLOS assigns sovereign rights of resources of the seabed and underneath the seabed to the coastal state that lies adjacent. In this context, some of the same information used in establishing extended continental shelf areas can also be indicative of high hydrocarbon potential under the shelves of the Arctic Basin. As a result, several

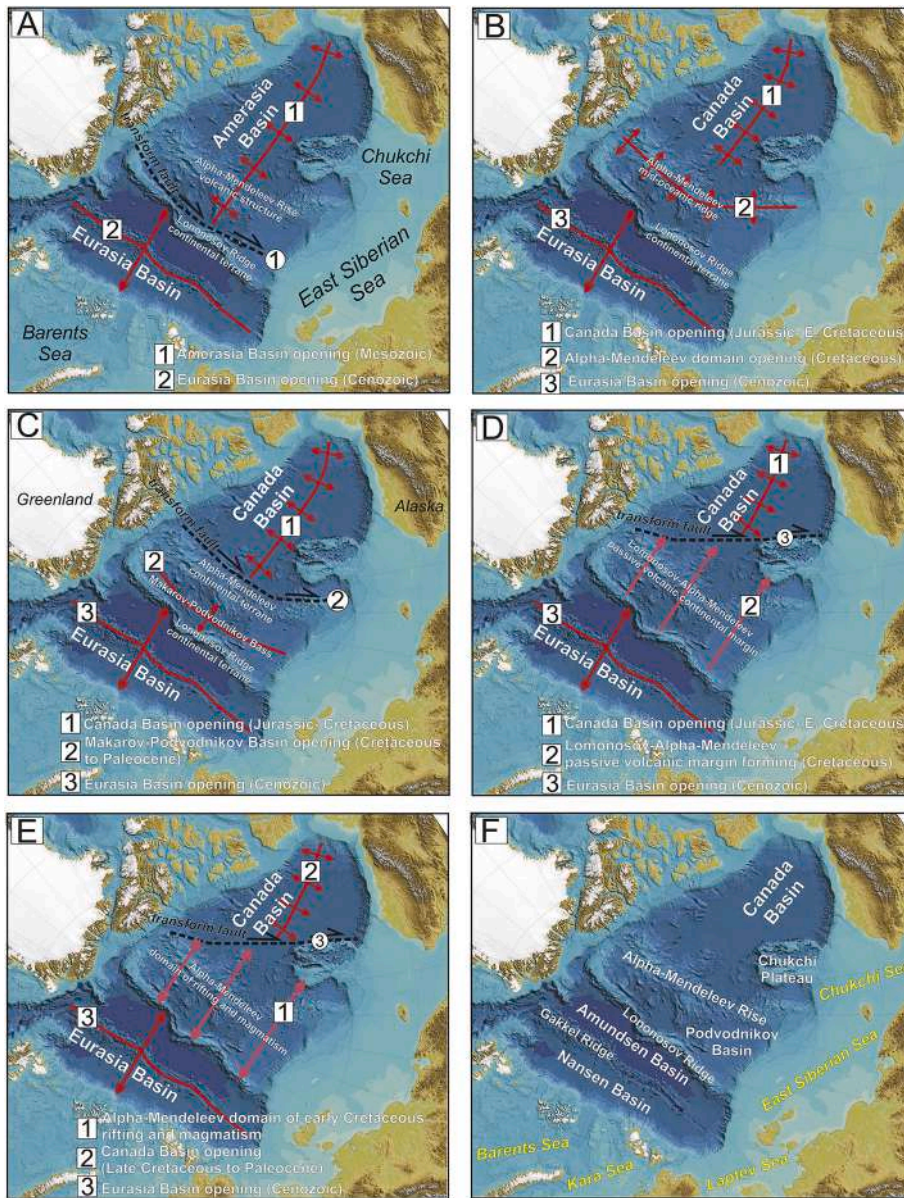


Fig. 2. The five most frequently discussed models of the geological history of the Arctic Ocean. (A) Classical rotation model; (1) (in the square) the opening of the Amerasia Basin in the Jurassic–Cretaceous (the position of the spreading axis is shown), (2) (in the square) the opening of the Eurasia Basin in the Eocene–Quaternary; (1) (in the circle) the main transform fault along Lomonosov Ridge. (B) Model with the Alpha–Mendelev Rise as the mid-oceanic ridge; (1) the opening of the Canada Basin in the Jurassic–Cretaceous, (2) the formation of a mid-oceanic ridge over the mantle plume in the Cretaceous, (3) the opening of the Eurasia Basin in the Eocene–Quaternary. (C) Rotation model with the main transform fault along the Alpha–Mendelev Rise; (1) the opening of the Canada Basin in the Jurassic–Cretaceous, (2) the opening of the Podvodnikov–Makarov basin in the Late Cretaceous–Paleocene, (3) the opening of the Eurasia Basin in the Eocene–Quaternary; (2) (in the circle) the main transform fault. (D) Model with the Alpha–Mendelev Rise as a volcanic continental margin; (1) the opening of the Canada Basin with the main transform fault along the edge of the Chukchi Plateau (Northwind Ridge, shown as 3 in the circle), (2) the formation of the Alpha–Mendelev–Lomonosov area as a volcanic continental margin with large-scale rifting and mantle magmatism in the Cretaceous, (3) the opening of the Eurasia Basin in the Eocene–Quaternary. (E) Model with the Canada Basin as Late Cretaceous to Paleocene structure; (1) rifting and magmatism in the Alpha–Mendelev domain in the Early Cretaceous, (2) opening of the Canada Basin in Late Cretaceous to Paleocene with the main transform fault along the edge of the Chukchi Plateau (Northwind Ridge, shown as 3 in the circle), (3) the opening of the Eurasia Basin in the Eocene–Quaternary. (F) General geography. Based mainly on Dove et al. (2010 and references therein), with additional information from Doré et al. (2015) (model “C”), Miller et al., 2018 (model “E”), Nikishin et al. (2020) (model “D”).

countries started evaluating the economic potential of the Arctic. Concern over issues of global ecology and climatic change became widely relevant in the process.

To further knowledge of the Arctic Ocean, the new Arctic Mega Project was initiated in Russia in 2005. Prior to that time, most geophysical expeditions in the Arctic Ocean were carried out using drifting ice stations. Subsequently, from 2005 to 2020, using additional data collection methods, Russian scientists conducted integrated geological and geophysical surveys designed to produce a regional grid of lines, which would lead to a better understanding of the major Arctic Ocean’s structures (Fig. 1).

For surveying purposes several research vessels (RV) were used, however, most surveys were performed by the special ice-class research vessel *Akademik Fedorov*. In areas with heavy ice conditions, research vessels were accompanied by the nuclear icebreakers *Rossiya*, *Yamal* and *Arktika*. Seismic surveys were conducted in 2011, 2012 and 2014. A substantial number of new 2D seismic lines were collected, including for the first time regional seismic profiles for the Laptev, East Siberian, and Chukchi seas. As of 2020, the database volume accumulated includes 35,000 km of bathymetry profiles, more than 23,000 km of multi-

channel seismic (MCS) lines, more than 4000 km of wide-angle refraction/reflection (WARR) (or deep seismic sounding) lines, and 150 sonobuoy seismic soundings.

Throughout the program, geological sampling was undertaken on different structures of the Amerasia Basin using dredge, ROV and drilling techniques. In 2012, 2014, and 2016, rock samples were collected from the Mendeleev Rise with the support of a nuclear scientific research submarine. In 2019, a subbottom profiler survey was conducted in the Eurasia Basin with in the areas of Gakkel Ridge and Nansen Basin. Given the perennial sea ice conditions and water depths, these wide-scale geological and geophysical surveys in the Arctic Ocean could have been conducted only with the support of a nuclear icebreaker and a nuclear submarine. To date, the Russian Arctic Ocean Mega Project has probably been the most cost-intensive geoscience project in Russia.

We have prepared three papers based on the findings of the Russian Arctic Ocean Mega Project: (1) Data collection; (2) Arctic stratigraphy and regional tectonic structure (Nikishin et al., 2021a); and (3) Mesozoic to Cenozoic geological evolution (Nikishin et al., 2021b).

We will discuss many aspects of the geology of the Arctic in these three papers focusing on two key issues: (1) the structure and formation

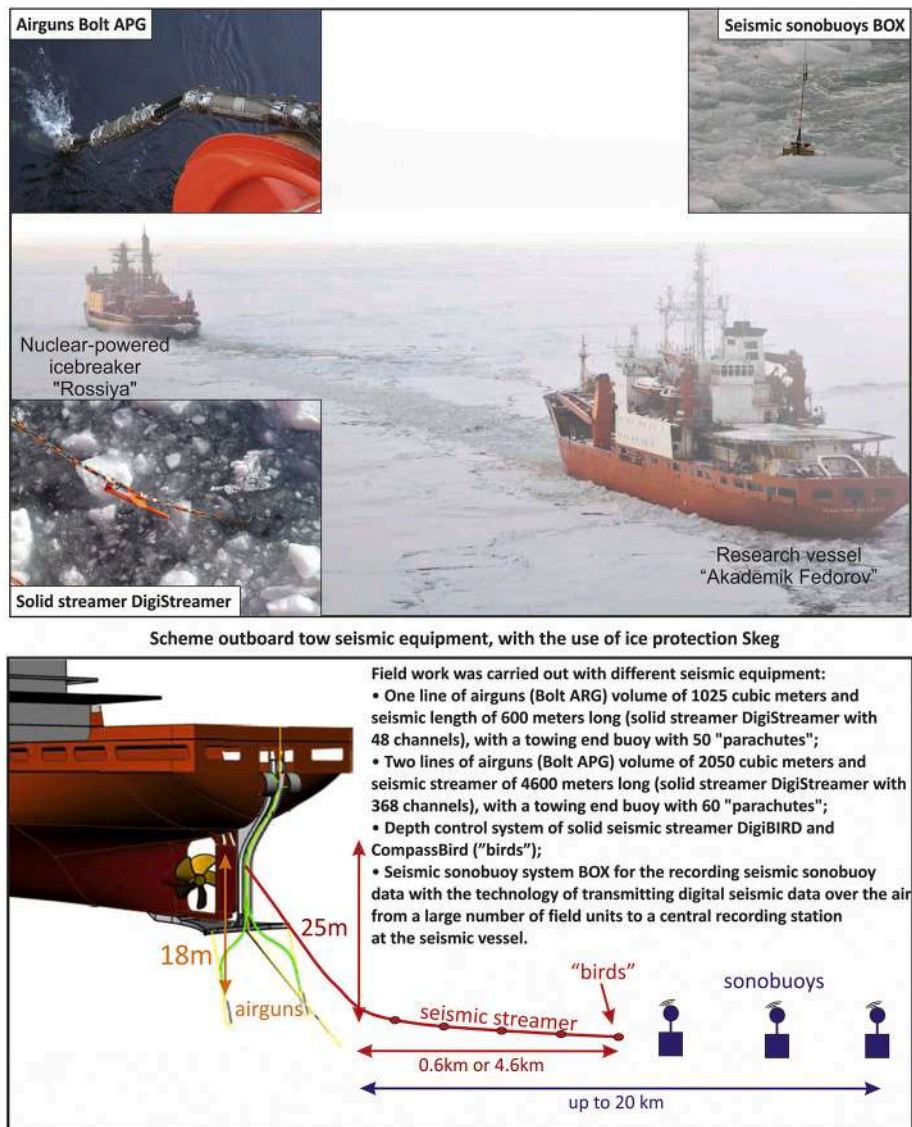


Fig. 3. Example of marine technologies for seismic data acquisition adopted for Russian *Arktika* expeditions, using a combination of a nuclear-powered icebreaker and a research vessel. Information from *Ministry of Natural Resources and Environment of the Russian Federation*.

history of the Alpha-Mendeleev Rise and adjacent deep-water basins and (2) the general chronology of geologic events in the Arctic Ocean's history (Fig. 2). Further insight into these issues will clearly contribute to a better understanding of global geodynamics and of global Earth history for the Meso-Cenozoic.

2. Data types

As briefly mentioned above, a variety of different data types were acquired as part of the Arctic Ocean Mega Project: (1) multiple types of seismic data, (2) subbottom profiler data, (3) geological sampling on the slopes of the Mendeleev Rise with the use of special equipment, (4) borehole data, (5) gravity and magnetic anomaly data, (6) offshore geodetic data, (7) multi-beam bathymetry data, and (8) data from geological surveys on adjacent Arctic islands.

2.1. Seismic data

The Arctic Ocean is characterized by the presence of a solid ice cover with ever-changing properties, both from year to year as well as within the year (the area of ice cover is smaller in summertime and much larger

in wintertime). This characteristic introduces the necessity of corrections both in the timing (season) as well as in the techniques of conducting classical seismic surveys - e.g., in the use of a towed seismic streamer and in the use of seismic stations of different types.

The season for conducting seismic surveys northward of 82°N commonly is limited to a period of a few months, ranging from July to October. During this time, due to the polar day and solar activity, the southern edge of the first-year ice cover retreats farthest northwards, while the multi-year ice cover thaws out to its thinnest within that calendar year.

In solid ice conditions, two vessels sailing one after the other, are used for operations (Figs. 3, 4) along pre-planned seismic acquisition lines. This is a commonly used scheme for geophysical works in the Arctic Ocean (e.g., Hutchinson et al., 2009; Mosher et al., 2013; Piskarev et al., 2019; Petrov and Smelror, 2019). The main task for the lead vessel (the icebreaker) is to create an ice-free channel (a passage without solid ice or with ice crushed into smaller bits). The geophysical data-acquisition vessel follows the icebreaker. In the case of these Russian surveys, a nuclear icebreaker was used as the lead vessel, and the acquisition vessel, equipped with all the geophysical instrumentation, usually armored with some ice protection (e.g., strengthened hull), follows.

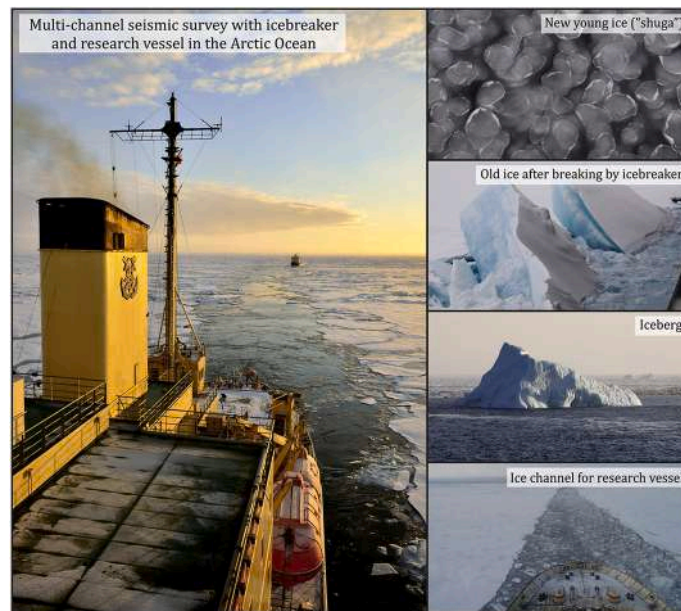


Fig. 4. Photos of seismic data acquisition in the Arctic. An icebreaker is in the front, creating a channel within the ice for the research vessel. The research vessel has all the scientific equipment. Ice conditions are illustrated on the right.

The main task of the data-acquisition vessel (a research vessel (RV), e.g. *Akademik Fedorov*) was to conduct the seismic survey, deploying a towed seismic streamer and seismic stations. Solid ice and pressure ice ridges handicap the constant-speed sailing of the RV, whereas crushed ice does not prevent maintaining a constant speed but can introduce noise on seismic recordings. For conducting surveys with a towed seismic streamer, all equipment trailed from the stern of the research vessel. These include airguns, seismic streamers, and “birds”. RV *Akademik Fedorov* was equipped with a special ice protection system for safe deployment and recovery of the airgun and associated high-pressure lines as well as the seismic streamer. Stable speed of the acquisition vessel was critical to maintaining geometry for acquisition of quality data and to facilitate processing of the data. “Birds” on the seismic streamer helped ensure a constant tow depth.

For conducting multi-channel seismic surveys, the containerized geophysical Arctic-service hardware system with solid-filled and gel-filled seismic streamers of various lengths were used. In different years, seismic equipment included:

- Integrated offshore seismic data acquisition system *ION DigiSTREAMER* or *Sercel SEAL System*;
- Solid-filled seismic streamer *ION DigiSTREAMER* or solid-filled and gel-filled seismic streamers *Sercel SEAL Streamer*;
- *Bolt APG* airguns;
- Control and monitor navigation system *ORCA* or *QINSy*;
- Streamer depth control and positioning system *DigiBIRD* and *DigiCourse*, with the use of special devices (‘birds’) on a seismic streamer;
- Digital airgun controller *DigiSHOT* or *RTS Big Shot*.

In the Arctic Ocean, two versions of seismic streamer lengths were used. A 600 m long solid streamer was used when solid ice cover conditions existed or when an ice channel would close relatively quickly. A streamer 4500 m long and longer (solid or gel-filled) was used in the absence of solid ice cover and when the ice channel remained open for sufficient time for the survey. The streamer towage depth for most of the seismic acquisition was 15 m in order to keep it below any ice keels. The shotpoint spacing on most of the seismic lines was 50 m, with a record length of 12 s.

Additionally, while conducting multi-channel reflection seismic

acquisition, sonobuoy seismic soundings were carried out for refraction data acquisition. These soundings were performed for some seismic lines with the use of floating seismic stations (sonobuoys). In the course of movement of the RV along a seismic line, these sonobuoys were released overboard at certain points, though only during the acquisition of multi-channel seismic data. These sonobuoys were not tied to the vessel in any manner. Thereafter, during the continuation of seismic signal shooting, these sonobuoys recorded seismic signals. These data were immediately transmitted to the research vessel via a wireless communication system. This communication channel continues to operate up to distances of 15–20 km (from RV to sonobuoy). As a consequence, the obtained data contain reflected seismic events; nonetheless, their core value lies in the fact that they also contain refracted seismic events. Refracted seismic events are recorded especially well at offset distances over 10 km. These techniques commonly are used for Arctic Ocean geophysical procedures (e.g., [Mosher et al., 2013](#)).

The main objective of refracted sonobuoy seismic soundings is to obtain a velocity model for seismic profiles that are acquired with the use of a short (600 m) seismic streamer. On these seismic lines, a reflection time-distance graph is too short to place reliance on stack velocities if the Dix formula is used for obtaining a velocity model for the line. That is why on such lines refracted sonobuoy seismic soundings were obtained. Consequently, this enabled velocity models to be computed for lines shot with a long seismic streamer (4500 m and more) where interval velocities could be obtained using the Dix formula. The hardware-software system used for conducting refracted sonobuoy seismic soundings was the radio telemetry seismic data acquisition system *BOX* (*Fairfield Industries*, USA).

Wide-angle reflection and refraction (WARR) surveys were carried out during both dedicated expeditions (*TransArctic-89-91*, *Arktika-2000*, etc.) as well as in conjunction with integrated geophysical expeditions (*Arktika-2012*, *Arktika-2014*). In the early expeditions, seismic receivers were arranged on the water surface (or on ice surface) with the use of airborne landing operations from ice-based RVs. However, subsequently the method of self-emerging 4-component ocean-bottom stations was employed. In most operations, *ADGS-2 M* and *ADSS-5000* stations with *M-K-4-SM26m* recorders (provided by the company *EDB OE RAS*) were used.

The ocean-bottom station is a sphere of 450 mm diameter with a special housing at the top pole. This special housing combines, in terms

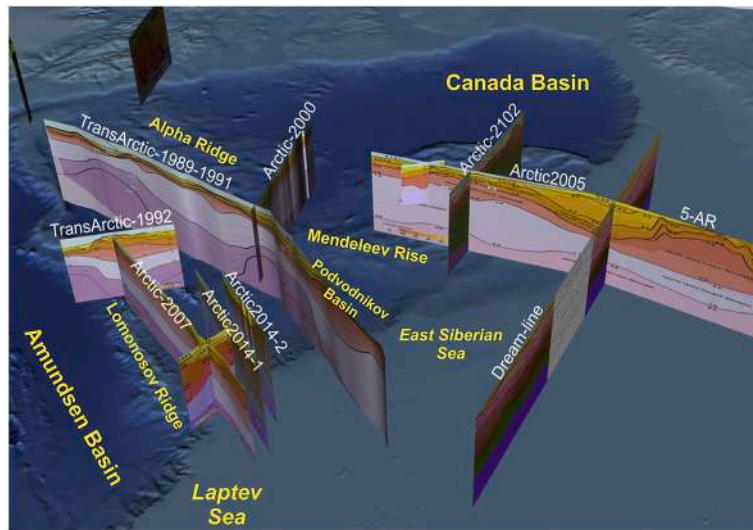


Fig. 5. Location of wide-angle refraction/reflection seismic lines. Presented by VNIIOkeangeologia. For details see Piskarev et al. (2019).

of design, an electrochemical release, a hydroacoustic antenna, and a hydrophone (H component). Components such as a geophone module (X, Y, Z components) and power supply are placed inside the sphere. The encasing sphere of the ocean-bottom station is made of a high-strength aluminum alloy. Single-beam and multi-beam hydrographic echosounders installed on the RV were used for determining coordinates and depth at installation points of ocean-bottom stations.

The seismic signal was produced through blasting TNT charges in early expeditions (*TransArctic-1989–91*, *Arktika-2000* and onwards). Later, starting with the *5-AR* expedition (2008), a special big-volume low-frequency airgun *SIN-6 M* was used, whose specifications are as follows:

- Working pressure – 120-130 atm;
- Volume of pneumatic chamber – 120 l;
- Energy of signal produced – 310 kJ;
- Frequency range – 8-12 Hz;
- Submergence depth – 34-37 m;
- Minimum interval between shots – 150 s;
- Airgun offset distance from vessel hull – 70 m.

Key details of each of the multi-channel seismic acquisition and deep wide-angle refraction/reflection data expeditions are described below.

2.1.1. Multi-channel seismic surveys (MCS)

Under the government-funded *Arktika* program a total of more than 23,000 running km of state-of-the-art seismic lines in the deep-water part of the Arctic Ocean were acquired (Fig. 1). Below is a list of expeditions with associated data volumes produced, equipment used, and specific features of seismic data acquisition.

2.1.1.1. Traverse A-7 expedition. In 2007, the company *MAGE* conducted an MCS of 820 km along a line (parallel to line A-7) from the New Siberian Islands to 83.5° N latitude, along the axial part of the Lomonosov Ridge. *SEAL System* (Sercel, France) recording station, *BoltAPG* (1500 in³, 2000 PSI) guns as seismic source and *SEAL Sentinel Solid* (8100 m length, 648 channels) seismic streamer were used. The record length was 12 s and reached a CDP stacking fold of 108. Positioning was carried out using *GPS Spectra* system with an accuracy of at least 2 m. The main exploration target was the junction of the Lomonosov Ridge and the East Siberian shelf.

2.1.1.2. Traverse 5-AR expedition. Also in 2009, *MAGE* completed a

540 km MCS line from the Chukchi coastline to the edge of the Chukchi shelf using RV *Geolog Dmitry Nalivkin*. *Sercel SEAL System* recording station and *I/O Sleeve* guns (4010 in³, 2000 PSI) as seismic source. The *SEAL Sentinel Solid* (8100 m with 648 channels) seismic streamer was used, with a record length of 15 s, reaching a CDP stacking fold of 81. The seismic navigation system *Spectra* also was used for positioning.

2.1.1.3. Arktika-2011 expedition. In 2011, a MCS survey was undertaken by the company *GNINGI*, using the RV *Akademik Fedorov* and the icebreaker *Rossiya*. The total length of MCS lines was 6300 km. *Sercel SEAL* was utilized with a solid-filled 48-channel streamer of 600 or 4600 m length, one or two air guns *BoltAPG* of 1025 or 2050 in³ volume, and 2050 PSI working pressure. Navigation and positioning was provided by the integrated navigation system *ORCA* and software package *SPRINT*. The data were recorded and pre-processed by telemetric system *BOX*. Record length was 14–15 s and CDP stacking fold for the short streamer was 6 with 46 for the long streamer. The expedition's main objective was to determine the thickness of sedimentary sequences within the Amundsen, Nansen and Podvodnikov basins.

2.1.1.4. Arktika-2012 expedition. In 2012, the geological and geophysical surveys shifted to the Podvodnikov Basin, the Mendeleev Rise, the Chukchi Plateau, and the De Long High, with the company *Sevmorgeo* performing the surveys. The icebreaker *Kapitan Dranitsyn* and RV *Dikson* (a former icebreaker converted to RV, equipped to perform any kind of offshore seismic surveys) were used. The air gun used was a *BoltAPG* of 1600–2000 in³ with 2050 PSI working pressure, and for navigation and positioning a *Trigger Fish* system was used.

Nine lines comprising 5300 linear km were acquired using a long seismic streamer (4500 m – 360 channels) – 1930 km – and a short seismic streamer (600 m – 48 channels) – 3370 km. This expedition's main goal was to study and refine the structure of the sedimentary cover of the Mendeleev Rise.

2.1.1.5. Arktika-2014 expedition. In 2014, MCS surveys were carried out by *MAGE* in the Nansen, Amundsen, Makarov and Podvodnikov basins, across the Lomonosov Ridge and along the margins of the Laptev and East Siberian seas using the RV *Akademik Fedorov* and the icebreaker *Yamal*. The total length of MCS lines acquired was 9900 km.

The MCS complex employed the *DigiStreamer* data acquisition system and solid-fill seismic streamers 600 or 4500 m length. *BoltAPG* air guns with total volumes of 1025/1300/2050 in³ and 2050 PSI working pressure were used as seismic sources. Positioning was performed with

navigation system *QINSy*. The record length was 12 s. and CDP sections were obtained with 6 stacking fold or 45 stacking fold for short and long streamers, respectively.

The main objective of these MCS surveys was to study and refine the structure of the sedimentary cover of the Eurasia and Amerasia basins and the adjacent shelf, and to link with the stratigraphy of the major morphological structures of the region.

2.1.2. Russian wide-angle refraction/reflection (WARR) lines

The main purposes of the WARR surveys were to investigate major structures of the Arctic Ocean and to obtain velocity models of the crust. WARR lines were surveyed along regional lines through the Amerasia Basin (Lomonosov and Alpha ridges, the Mendeleev Rise, the Chukchi Plateau, Podvodnikov and Makarov basins), terminating at the adjacent shelf of Northeast Eurasia (Fig. 5). A brief description of key expeditions undertaken by Russia in the Arctic during the last three decades is presented below. As indicated above, WARR surveys were conducted by two main methods:

- Arranging seismic receivers at the sea surface (including on ice) with the use of airborne operations conducted from ice bases or RVs. This method was used in the *TransArctic-89-91*, *Arktika-2000*, *Arktika-2005* and *Arktika-2007* expeditions.
- Utilization of ocean-bottom stations with participation of RVs. This method was used in the *5-AR*, *Arktika-2012*, *Dream Line*, *Arktika-2014* expeditions.

2.1.2.1. *TransArctic-1989–91*, *TransArctic-92* expeditions. The total length of WARR lines acquired during the *TransArctic 1989–1991* expedition was 1490 km. These lines extended from the Makarov Basin across the Podvodnikov Basin to the East Siberian Shelf. The *TransArctic-1992* WARR line crossed the Lomonosov Ridge approximately along 84°N latitude, including the adjacent Amundsen and Makarov basins. The length of the *Transarctic-1992* line was 280 km.

Acquisition of these *Transarctic* lines was the first Russian experience involving a regular WARR survey in high latitudes of the Arctic. These early data were characterized by sparse intervals between seismic receivers. Consequently, the sedimentary cover over the crust was only poorly studied, controlled as it was by refraction data and modeled based on reflection data. Only high-velocity waves propagating within the crystalline crust were interpreted with some reliability.

Each of WARR lines had three arrays that were characterized by the following parameters:

- 30 receive points with an average spacing of 5–6 km;
- Shot points spaced at 40 km and 50 km;

- Generation of seismic waves by TNT charges weighing 0.2–1.2 tons, with an amount of explosives per entire line of 18 tons.

Seismic waves were recorded by *Delta-Geon-1* digital recorders with the following specifications:

- Number of channels - 3;
- Frequency range 0.2–15 Hz;
- Dynamic range – 100 dB;
- Sampling interval – 7 ms.

2.1.2.2. *Arktika-2000*, *Arktika-2005* and *Arktika-2007* expeditions. The *Arktika-2000* WARR line (500 km long) was routed across the northern part of the Mendeleev Rise and the adjacent Canada and Podvodnikov basins at 82°N. The *Arktika – 2005* WARR line was acquired in 2005 along the axial part of the Mendeleev Rise and its junction with the shelf (500 km). Finally, the *Arktika-2007* regional WARR line (650 km long) was routed from the near-Siberian part of the Lomonosov Ridge to the Laptev Sea Shelf north of the Kotelny Island.

Each of these WARR lines had the same survey parameters as the *TransArctic-89-91* and *TransArctic-92* WARR lines. Seismic waves also were generated by TNT charges. The main airborne operations were supported by helicopters from the research vessel *Akademik Fedorov* accompanied by the nuclear icebreakers *Rossiya* and *Sovetskiy Soyuz*.

2.1.2.3. *5-AR* expedition. This expedition utilized bottom stations to acquire WARR data. The *5-AR* Line (550 km long) extended from Cape Billings (Chukotka coast) to the southern end of the *Arktika-2005* line. Data were acquired by 56 4-component ocean-bottom stations, with 10 km spacing between stations in the receiving array. Generation of seismic signals was done using a *SIN-6 M* airgun. It should be noted that only one station was lost during the *5-AR* line survey.

Two main types of ocean-bottom stations were used – ‘boomerang’ and ‘buoy-based’ stations. During the survey, it was decided to use boomerang ocean-bottom stations in deep water areas and in water areas with moving ice floes instead of buoy-based stations.

2.1.2.4. *Dream Line* expedition. The WARR line (925 km long) was completed in 2009 by the company *Sevmorgeo* on the East Siberian Sea shelf, under a contract with British Petroleum. WARR data were acquired using self-emerging 4-component ocean-bottom stations (X,Y,Z geophones and H hydrophone).

2.1.2.5. *Arktika-2012* expedition. The 480 km long WARR line ran from the Podvodnikov Basin to the Chukchi Plateau, crossing the southern part of the Mendeleev Rise. WARR data were acquired by *Sevmorgeo* using 4-component ocean-bottom stations of ‘boomerang’ type. The

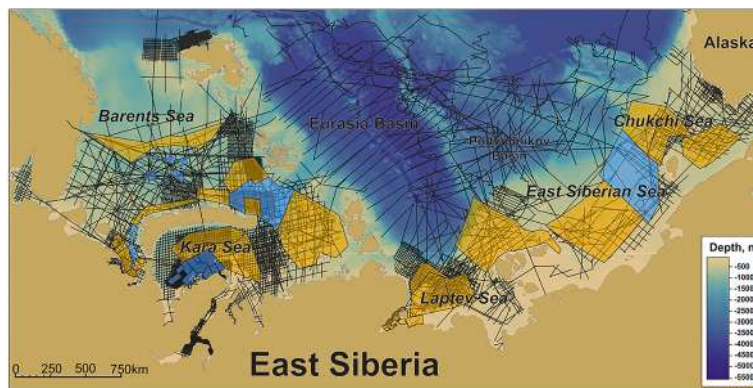


Fig. 6. Location of the main part of the seismic lines in the Arctic Ocean with greater detail over the Russian shelves. Yellow blocks – *Rosneft* licenses. Blue blocks – *Gazprom* licenses. Licensed blocks have many new seismic and other geophysical data. (For interpretation of the references to colour in this figure legend, the reader is referred to the web version of this article.)

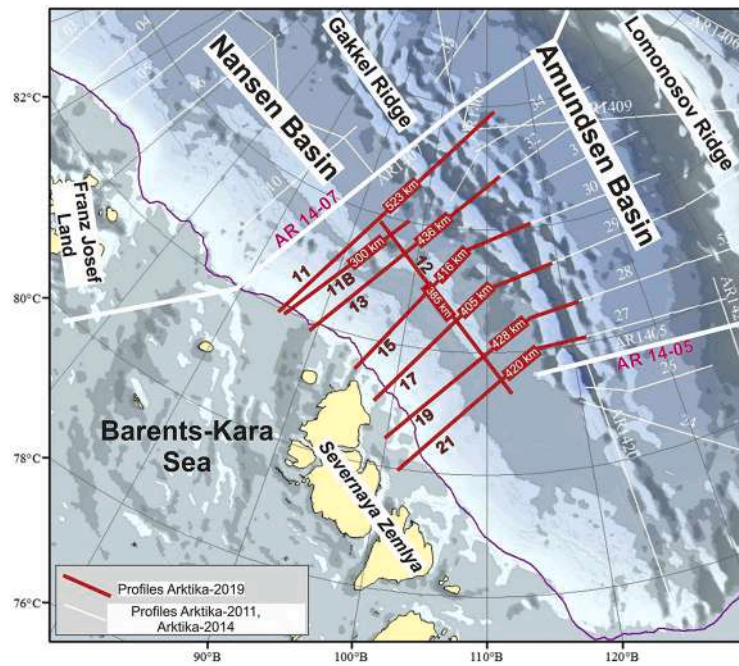


Fig. 7. Location of subbottom profiles of expedition *Arktika-2019* and location of some seismic lines.

survey was carried out by the diesel electric icebreaker *Dikson*.

Generation of seismic signals was carried out using a *SIN-6 M* airgun with working pressure of 120–130 atm and pneumatic chamber volume of 120 l. In the course of the work, one receiver array of seismic stations was set up with 30 seismic stations. Parameters of the acquisition geometry and of seismic signal recording were:

- Shot points spacing – 312 m;
- Receive points spacing in the receiver array – 10–20 km;
- Length of time-distance graph – not less than 150 km;
- Record length – 60 s.

2.1.2.6. *Arktika-2014* expedition. This WARR survey was undertaken by *MAGE* using the RV *Nikolay Trubyachinsky* and consisted of two lines (250 km and 350 km). 4-component ocean-bottom stations of ‘boomerang’ type and a 7300 in³ airgun were utilized. These WARR lines were located in the De Long High and the associated linkage area. The survey aimed to investigate the continuity and structure of the crustal complexes. Parameters of the acquisition geometry and seismic signal recording were:

- Interval between excitations - 150 s;
- Receive points spacing in the receiver array – 6–8.5 km;
- Length of time-distance curve – not less than 150 km;
- Record length – 60 s.

2.1.3. Other new 2D and 3D seismic data for the Russian Arctic shelf

As mentioned above, during the past two decades, many 2D seismic lines have been acquired in the Russian deep-water part of the Arctic continental shelf (Fig. 6). Prior to that, the continental shelves of the Laptev, East Siberian, Chukchi and North Kara seas had been poorly studied. All seismic data in the deep-water part of the Arctic Ocean belong to the *Ministry of Natural Resources and Environment of the Russian Federation* and are open to Russian investigators as well as foreign investigators involved in international scientific projects.

On the Russian part of the shelf, the Russian companies *Rosneft* and *Gazprom* have vast licensed blocks (Fig. 6). For these blocks, a new dense grid of 2D seismic lines is now available. However, these data so far remain private. The bulk of the new seismic data was acquired by the

Russian geophysical companies *Rosgeo*, *DMNG*, *SMNG*, *Sevmorgeologia*, *Yuzhmorgeologiya*, and *MAGE*. In addition, many other companies and institutes conducted seismic surveys there as well: *BGR*, *Halliburton*, *British Petroleum*, *ION*, *CGG*, *TGS*, and *PGS*. The Russian geophysical companies published key results of their surveys mainly in Russian. Geologists of scientific institutes of the *Federal Subsoil Resources Management Agency* and the *Russian Academy of Science* developed a modern seismo-stratigraphic framework of the shelf areas. Outside of Russia, *BGR* (Germany) has been a pioneer in investigating the Laptev Sea with the studies by *Franke* (2013).

3D seismic data for the Russian shelf are available for individual licensed blocks of the East Barents and South Kara seas. They were acquired by *Rosneft* and *Gazprom* and afforded the possibility to refine seismic stratigraphic models for these areas. Principal unconformities and major sequences were identified, and the history of the geologic and tectonic evolution was worked out in detail. For the Barents Sea, 3D seismic data demonstrated, for example, evidence of Early Cretaceous intrusions.

The scientific institutes of the *Federal Subsoil Resources Management Agency VSEGEI* and *VNIOkeangeologia* conducted regional geological and geophysical studies in multiple shelf areas. Results of their studies are available in open-source technical reports and were published openly (e.g., <https://vsegei.ru/ru/info/>; <http://vniio.ru/publications/>).

In the Barents and South Kara seas, data from deep boreholes are available and have been tied to seismic lines to provide ground truth calibration (e.g., *Smelror et al., 2009*). Stratigraphic and seismic stratigraphic frameworks for these seas have been extensively established. However, for the Laptev and East Siberian Seas, as no boreholes are available, seismic stratigraphic interpretations remain uncalibrated.

2.2. Subbottom profiler surveys in the Eurasia Basin in 2019

An expedition to the Eurasia Basin involving the acquisition of sub-bottom seismo-acoustic data was conducted in 2019. At the present time, this is the most recent high-latitude integrated geophysical expedition carried out by Russia in the Arctic. These offshore subbottom studies were aimed at obtaining high-quality data on bottom relief and structure of the upper part of the geological section in the area of the Gakkel Ridge. The following tasks were planned:

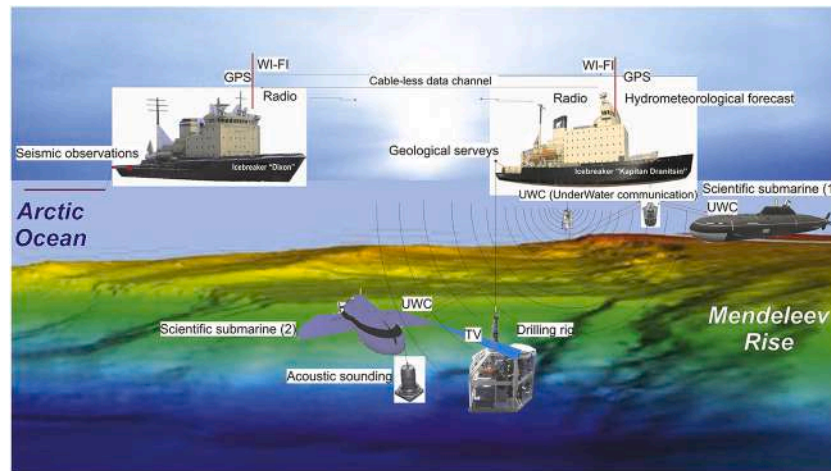


Fig. 8. Comprehensive study of seafloor scarps with bedrock outcrops on the Mendeleev Rise using shallow drilling and the manipulator of the research submarine in 2012 – conceptual scheme (expedition *Arktika-2012*). Data are presented by *Ministry of Natural Resources and Environment of the Russian Federation* and published by [Morozov et al. \(2014\)](#).



Fig. 9. Photos of deep-water drilling unit during the expedition *Arktika-2012*.

- Acquisition of additional data by multi-beam and single-beam echosounders with the purpose of preparing a digital bathymetry database;
- Acquisition of subbottom profiling accompanying the bathymetry surveying.

Two nuclear icebreakers took part in the expedition initially: *Taimyr* and then *50 Let Pobedy*. For research operations, as with earlier integrated geophysical expeditions, the ice-class RV *Akademik Fedorov* was used. Continuous subbottom profiling was conducted with the purpose of studying the upper part of the geological section to a depth up to 100–200 m. The location of profiles is shown in [Fig. 7](#).

New bathymetric data for the Eurasia Basin and data on modern geological processes on the continental slope and on the basin floor were obtained as a result of this expedition. Currently, these data are being processed.

2.3. Rock sampling on slopes of the Mendeleev Rise

To facilitate the geological study of the sedimentary cover and

bedrock on the Mendeleev Rise, within the framework of the expedition *Arktika-2012*, specialized operations were conducted using two icebreakers with additional participation of a scientific research submarine (SRS). Later in 2014 and 2016, deep-water geological expeditions (*Mendeleev-2014* and *Mendeleev-2016*) were conducted with full-scale participation of a nuclear SRS. The full-scale use of the SRS made it possible to replace the use of a RV, and the unique equipment on the SRS allowed rock samples to be taken from the sea floor precisely at the locations intended. The principal research methods utilized in these expeditions are described below.

2.3.1. *Arktika-2012* expedition

On the *Arktika-2012* expedition the objective was to sample bedrock on the slopes of the Mendeleev Rise. The expedition was undertaken by *Sevmorgeo*. Seabed sampling and deep-water drilling were conducted from the icebreaker *Kapitan Dranitsyn*. In conventional dredging, rock samples brought from the seabed usually are derived from “exotic” debris transported to the sampling site by ice rafting processes. The principal challenge was to make certain that the rock samples taken were in situ on the seabed, and shallow drilling with the use of an ice-



Fig. 10. Photos of bottom grab during the expedition *Arktika-2012*.

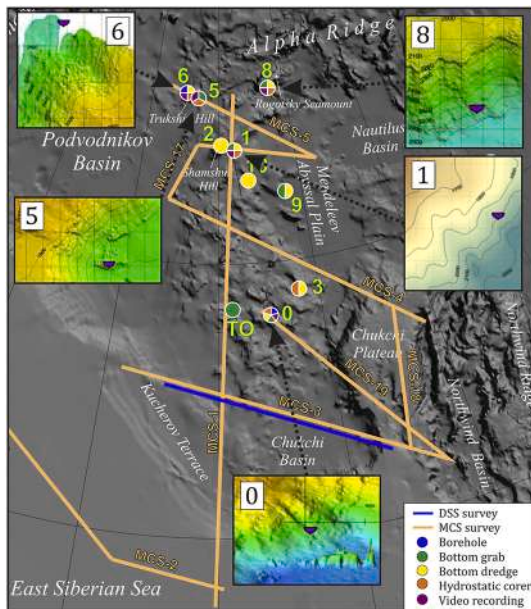


Fig. 11. Locations of polygons of the *Arktika-2012* expedition on the Mendeleev Rise. The various sampling methods are shown with colour. Bathymetry of polygons is illustrated in greater detail. Data are provided by the *Ministry of Natural Resources and Environment of the Russian Federation*.

class deep-water drilling unit ensured this objective. Sampling of bottom rock material was carried out using a hydrostatic corer, a grab sampler and a bottom dredge. For all of these operations the SRS was used.

In accordance with the sampling plan, the following tasks were designated for surveying areas of 10×10 km size as envisaged during the pre-project planning:

1. Detecting locations of bedrock exposure projecting through the surficial cover of loose sediments in areas using a grid size of 2×2 km;
2. Determining site parameters for positioning the drilling unit within the selected locations: seabed slope angle, current speed vector, dimensions of the revealed sites;
3. Video-photometric and sonar documentation of the selected sites for geological sampling and deep-water drilling.

The suite of studies included the following methods and equipment: in 10×10 km areas – multi-beam surveying; in 2×2 km areas – sub-bottom profiler and side-scan sonar surveying. In the final stage of the studies, visual and video inspection of the sites where sampling was to be conducted was performed. Results of these inspections were decisive

in selecting the appropriate seabed sampling method (Fig. 8).

Within the framework of the *Arktika-2012* expedition, 11 polygons (10×10 km) were surveyed. With the use of the SRS, six polygons (Nos. 0, 1, 3, 5, 6, 8) and designated as the top priority targets, with the remaining five polygons to be sampled using alternative equipment. Polygons No. 0 and No. 6 were selected for core drilling. Shallow drilling with video tracking was conducted at four sites (KD12-06-21b on Polygon 6, KD12-00-31b, KD12-00-32b and KD12-00-33b on Polygon 0). On sites KD12-01-29b, KD12-06-31b, KD12-00-33b, bedrock cores were drilled; the lengths of cores recovered at these three stations were 60, 40, and 15 cm respectively.

Drilling was conducted using the ice-class deep-water drilling unit *GBU-2/4000 L* (Fig. 9) developed by *Sevmorgeo*. It was designed in 2012 especially for operations in the Arctic, capable of drilling holes up to 2 m in depth with 76 mm diameter tool and up to a water depth of 4000 m. During this expedition, operations with the deep-water drilling unit were conducted for the first time at negative ambient temperatures and in hazardous ice conditions. The drilling unit was installed at water depths over 2000 m. The icebreaker equipped with additional deployment and hoisting equipment was used for the first time as a RV.

A bottom dredge developed by *VNIIOkeangeologia*, had a rectangular shape with a size of 1×0.5 m and a mass of 500 kg. The dredging method is standard for marine geology. The dredging sites were selected following the recommendations based on surveys of the sea floor acquired by the SRS, coupled with analyses of seabed geomorphology within the work polygon. In total, 9 sites were sampled.

For bottom rock sampling, the clamshell-type grab sampler *DG-1-TV* also was used (Fig. 10). It was developed more than twenty-five years ago and is widely utilized for seabed sampling. It consists of two half-scoops mounted on a frame equipped with a remote video system. From the nine locations sampled, bottom sediment samples weighing between 200 and 450 kg were obtained from seven of the locations. Video recordings of lowering and reaching the bottom were made at five sites. Finally, the hydrostatic corer *E414M/01-00.000* was used for bottom sampling at total of 6 locations.

The combined sampling methodology using all available sampling tools resulted in the collection of a large body of material, including more than 20,000 fragments of gravel-to-block size clasts (Fig. 11). The main results of the *Arktika-2012* expedition were published in subsequent years (Morozov et al., 2013; Petrov et al., 2016; Vernikovskiy et al., 2014; Kossovaya et al., 2018; Petrov and Smelror, 2019). They showed that dredging of slopes and shallow (up to 2 m) drilling resulted in recovery of primarily loose sediments. Consequently, there was no guarantee that samples thus taken were actually basement bedrock. As a result, many Arctic researchers assumed that the dredged sedimentary rocks were the product of ice rafting.

2.3.2. Deepwater geological expeditions in 2014 and 2016

The deep-water geological expeditions of 2014 and 2016 (*Mendeleev-2014* and *Mendeleev-2016*) were able to reproduce the concept of “a field geologist with a hammer” analogous to the classical approach applicable to onshore surveys. The *Geological Institute of the Russian Academy of Sciences (GIN RAS)* and *Geological and Geophysical Survey of GIN RAS (GEOSURVEY GIN RAS)* have developed novel methodologies for comprehensive bottom surveys using the scientific research submersible (SRS). Bedrock samples from outcrops on the seabed were leveraged to produce stratigraphic columns similar to what could be obtained from deep drilling. This approach ensures that rock samples collected were indeed from bedrock. The most important aspect of this comprehensive methodology is the direct sampling of rocks from recognized bedrock outcrops by means of manipulators, thus excluding ice rafted debris. To accomplish this, a field geologist (Sergey Skolotnev) was submerged to the seafloor in a special manned deep-water vehicle where he could visually confirm outcrops presence and extract rock samples with the use of special manipulators.

To fulfill this mission a special purpose-equipped SRS was used. The

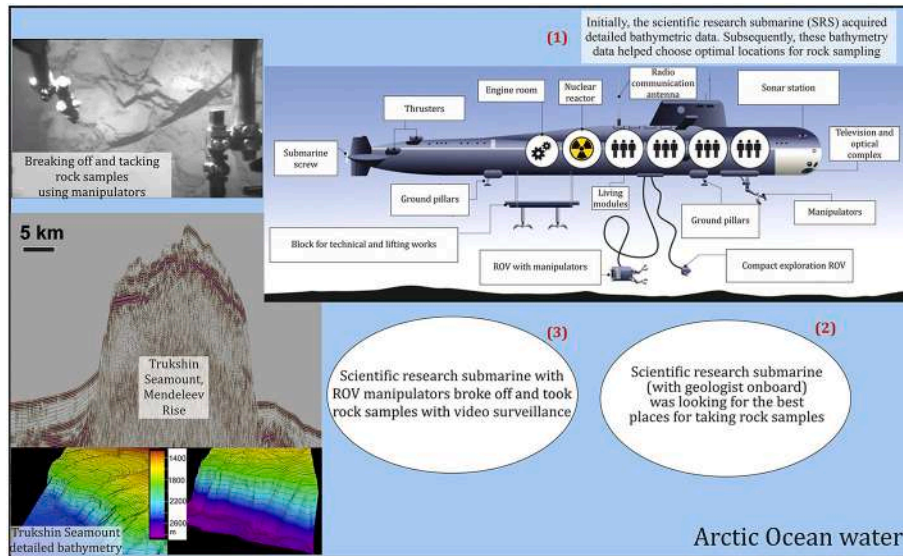


Fig. 12. Conceptual scheme of rock samples taking during *Deepwater Geological Expeditions* to the Mendeleev Rise in 2014 and 2016. Numbers 1, 2, 3 show the sequence of events.

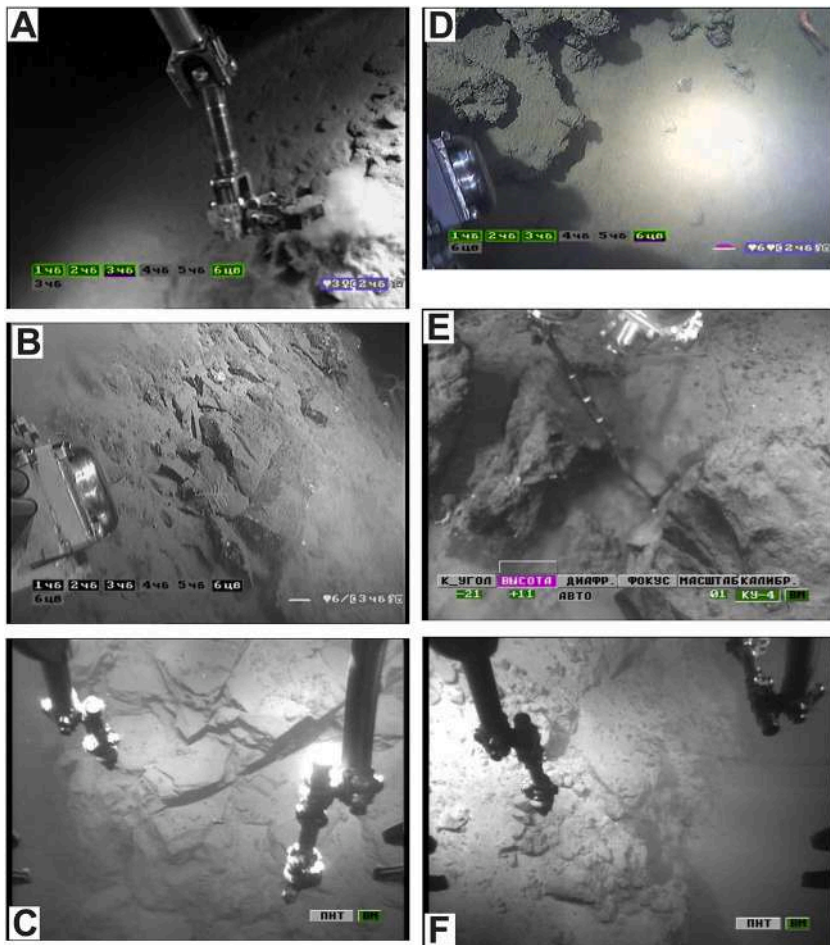


Fig. 13. Submarine bedrock outcrops on the slopes of the Mendeleev Rise. A – sandstone (sample 14–09) (78° 10,8' N, 179° 07,0' W, water depth 1229 m). B – andesite (14–02, 78° 10,3' N, 179° 07,5' W, water depth 1484 m). C – dolomite (1601/22) (79° 00,8' N, 174° 43,0' W, water depth 2343 m). D – limestone (14–10, 78° 10,9' N, 179° 03,3' W, water depth 1282 m). E – andesite basalt (1601/14) (79° 01,4' N, 174° 51,6' W, water depth 2205 m). F – volcanic tuff (1601/25) (79° 00,5' N, 174° 43,4' W, water depth 2111 m). The photos were taken by a manned underwater vehicle. Data are provided by the *Ministry of Natural Resources and Environment of the Russian Federation*, and partly from [Skolotnev et al. \(2019\)](#).

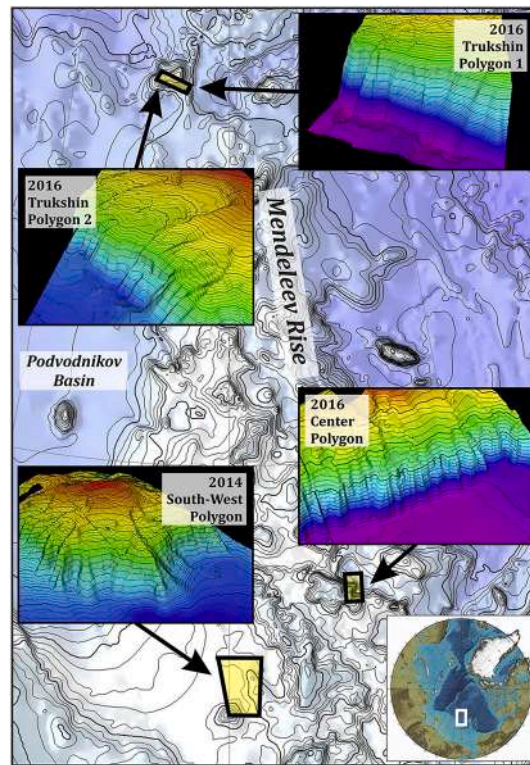


Fig. 14. Locations of polygons of Deepwater Geological Expeditions to the Mendeleev Rise in 2014 and 2016, modified after Skolotnev et al. (2019). Background map is bathymetry data from the International Bathymetric Chart of the Arctic Ocean (Jakobsson et al., 2012). More detailed bathymetry data of polygons are provided by the *Geological and Geophysical Survey of the Geological Institute of the Russian Academy*.

SRS was equipped with a multi-beam echosounder, a subbottom profiler, searchlights, photo and video cameras to detect rock outcrops and document the sampling process. The SRS also was equipped with special manipulators for rock sampling (Fig. 12).

This unique methodology used on the *Mendeleev-2014* and *Mendeleev-2016* expeditions involved six consecutive steps:

- Select polygons for rock sampling based on outcrops detected using seismic sections;
- Undertake a bathymetric survey followed by subbottom profiling of the slope in order to ascertain the precise locations of exposed rocks on the seafloor;
- Have an experienced geoscientist observe the seafloor using video recordings of the nature of rock outcrops, and select sampling locations;
- Recover bedrock samples from seafloor outcrops;
- Identify and record photographically collected rock samples (Fig. 13);
- Process in-lab (e.g., petrographic description and microscopic examination of rocks, X-ray phase analysis, chemo-analytical studies, rock dating) and construct composite geological cross-sections.

The field trial studies conducted in 2014 in the southwestern part of the Mendeleev Rise were aimed at validating a methodology for constructing geological cross-sections across seafloor structures in the Arctic Ocean. For the first time, rock samples were taken at substantial depths (1600 m) directly from bedrock exposures on the Mendeleev Rise (supported with photo- and video-recording and ties to geophysical data). The 2014 field trials helped to work out the best possible suite of methods for reliable characterization of bedrock exposures. An important advantage of this methodology was that a geologist was able to monitor while sampling was being conducted.

The *Mendeleev-2016* expedition successfully employed a SRS to

recover rock samples from bedrock exposures within three polygons. The bedrock geology at the Mendeleev Rise was sampled at greater depths (2000–2400 m) and an improved sampling technique was applied. This work considerably expanded knowledge of the temporal and spatial limits of the geological record of the Mendeleev Rise, which is critically important for correlation with adjacent Arctic coastal geology.

Thus, in the course of two expeditions, four separate steep slopes on the Mendeleev Rise were surveyed (Fig. 14). A principal aspect of this methodology is that rocks were sampled at regular depth intervals along such outcrops specifically for the purpose of constructing a geological cross-section. In total, 77 sites were sampled (Skolotnev et al., 2017, 2019).

The prime conclusion was that all four slopes on the Mendeleev Rise have similar Paleozoic sections, which are represented mainly by shelf carbonate and clastic deposits, and the distance from the southernmost point to the northernmost point is more than 500 km. It is highly likely that the entire Mendeleev Rise has a Paleozoic sedimentary cover. The findings of the *Mendeleev-2014* and *Mendeleev-2016* expeditions confirmed that the recovered bottom rock material during expedition *Arktika-2012* was likely not of ice rafting origin, which is consistent with the paleontological data acquired during the previous *Arktika-2012* expedition (Kossovaya et al., 2018).

2.4. Borehole data

The Arctic Ocean is relatively poorly studied by deep drilling. This is especially true for its deep-water part within which only one borehole has been available. The first scientific drilling expedition to the central Arctic Ocean was completed in September 2004. *Integrated Ocean Drilling Program Expedition (IODP) Leg 302, Arctic Coring Expedition (ACEX)*, recovered sediment cores up to 428 m below seafloor in water depths of ~1300 m, 250 km from the North Pole (Backman et al., 2006). Results of

studies of these boreholes have previously been published (e.g., Moran et al., 2006; Jakobsson et al., 2007).

Several commercial wells (*Popcorn*, *Crackerjack*, *Klondike*, *Burger*, *Diamond*) have been drilled in the Chukchi Sea, located in the American part of the Arctic region (Craddock and Houseknecht, 2016; Homza and Bergman, 2019; Houseknecht et al., 2016; Houseknecht and Wartes, 2013; Ilhan and Coakley, 2018; Kumar et al., 2011; Sherwood et al., 2002). Based on data from these wells, a stratigraphic scheme for Late Paleozoic to Cenozoic was developed for the Alaska shelf (Sherwood et al., 2002; Homza and Bergman, 2019). In Alaska, two wells were drilled on the margin of the Hope Basin in the Chukchi Sea (Bird et al., 2017). These wells penetrated Neogene to Eocene deposits. This sedimentary section overlies Paleozoic carbonates. In the Russian part of the Chukchi Sea, one well was drilled on Ayon Island near the Chukchi Peninsula (Aleksandrova, 2016). The well penetrated deposits from the Quaternary to the Paleocene.

In 2014, *Rosneft* and its US partner *ExxonMobil* successfully completed drilling of the world's northernmost Arctic vertical well *Universitetskaya-1* in the Kara Sea (the well TD is 2.1 km). Multiple companies participated in the drilling of this well, including *ExxonMobil*, *Nord Atlantic Drilling*, *Schlumberger*, *Halliburton*, *Weatherford*, *Baker*, *Trendsetter*, and *FMC*. A new oil field, *Pobeda*, was discovered and the section comprising Jurassic, Cretaceous and Cenozoic deposits was studied in detail.

In 2017, *Rosneft* drilled the 2363 m deep well *Tsentralno-Olginskaya* in the Khatanga Gulf of the Laptev Sea. The well penetrated deposits of the Cretaceous, Jurassic, Triassic and Upper Paleozoic. Results of this drilling have resulted in a refinement of the stratigraphic model for the Laptev Sea. In the Russian part of the Barents Sea, several boreholes from the Soviet era are available and in the Norwegian part of the Barents Sea several new boreholes also are available. For the Barents Sea, a well-worked-out stratigraphy and seismic-stratigraphic framework for Mesozoic and Cenozoic deposits is available (e.g. Smelror et al., 2009). In the Russian part of the Barents Sea, Cenozoic deposits are largely absent, having been glacially eroded.

On the whole, data derived exclusively from drilling on the shelves of the Arctic Ocean are insufficient to assemble an integrated seismic-stratigraphic framework for the entire Arctic Ocean.

2.5. Gravity and magnetic data

Within the framework of the geophysical expeditions in the Arctic Ocean, a shipboard gravity survey was conducted during the *Arktika-2014* expedition in combination with multi-channel seismic surveying. For gravity data acquisition two gravimeters *Chekan-AM* and *Shelf-E*, produced by the company *Elektrobribor*, were used. These gravimeters were positioned on two research vessels taking part in the *Arktika-2014* expedition.

Data from the gravimetric sensors and gyro stabilization systems of the gravimeters were recorded using of *SeaGrav* software. For the *Shelf-E* gravimeter, data from the thermo-stabilization system of the gravimetric sensor were also recorded. The sampling rate of the primary gravimeter data, which were processed in-office, was 0.1 s. Recording of navigation data from the *Trimble SPS 461* onboard satellite receiver also was made with the use of *SeaGrav* software for quality control of the gravimetric equipment, with a sampling rate of navigation data of 1 s.

For in-office processing of gravity data we used data from the files in the format of the international exchange of geophysical data P1/90. These files contain navigation (latitude, longitude) and bathymetric (sea depth) information with 50 m (25 m) discretization. Gravimeters were placed in the specialized equipment rack near the vessel's center, with the place of gravimeter installation determined relative to the reference

point. The sensitive element of the gravimeter was located at the water level.

Primary processing of gravimeter output data was made in real time mode with the use of the *SeaGrav* software module. The *SeaGrav* module results yield gravity increments with corrections for the gravimeter's zero drift. The delay of resultant data caused by the time constant of the gravimeter and the digital filters was also taken into account in the processing. The quality of gravimetric observations was evaluated in real time in the course of data acquisition. Within the framework of the *Arktika-2014* expedition, gravimetric data along the pre-planned geophysical lines were obtained, with 9900 km total length. Precise gravimetric data in the area near the point of the Geographic North Pole were obtained for the first time ever.

All other key data on gravity and magnetic anomalies have been summarized in the course of various international projects (e.g., Gaina et al., 2011; Saltus et al., 2011). In particular, the most comprehensive map of anomalous magnetic fields of the Arctic and the grid of magnetic anomalies with 2×2 km cell size were produced by the *Geological Survey of Norway* as part of the *CAMP-GM* Project (Gaina et al., 2011). This group also produced a composite digital map of gravity field anomalies and a digital model with 10×10 km cell size (Gaina et al., 2011).

It is worth noting that a vast portion of the Russian shelf has been licensed for exploration by petroleum companies (Fig. 6) and for most of them, new commercial gravity and magnetic surveys have been conducted. All these data will become open source after several years. The new data have confirmed the anomalies known earlier and there are no fundamental changes in the regional character of magnetic and gravity anomalies. With these new data, the structure of the sedimentary basins of the Russian continental shelves can be resolved in more detail. An important discovery is the likely identification of new igneous provinces. Evidence for a large-size igneous province with volcanics at the base of the sedimentary basin and numerous probable intrusions within the stratigraphic section of the Chukchi Sea north of Wrangel Island have been found (its contours approximately correspond to the previously known magnetic anomaly). The igneous province in the area of De Long Islands was studied. Its area turned out to be larger than previously assumed. A new igneous province appears to be present in the area at the junction of the East Siberian Sea and the Lomonosov Ridge, as well as on the shelf along the western edge of the Eurasia Basin. The new magnetic and gravity data showed that magmatism played a key role in the formation history of the North Chukchi Basin and basins of the Laptev Sea. For the East Barents Sea, belts of Cretaceous dykes are readily detectable.

2.6. Offshore geodetic operations

An important aspect of the integrated geophysical surveys is the accurate determination of coordinates (positioning) of the research vessel. For this purpose two independent positioning systems for determining vessel position were used.

The primary system was the *SeaPath 330* satellite integrated navigation system using signals from the GPS/GLONASS satellite positioning systems. Due to the fact that the study area is situated in the Earth's high-latitude zone and hence beyond the zone of reception of any systems improving vessel positioning accuracy, data were collected in an autonomous mode, and no differential corrections were incorporated.

The secondary systems, *C-Nav-2050R* and *C-Nav-3050*, were used in order to corroborate and confirm location readings as well as for backup. During the mobilization period before the start of combined survey operations, calibration and accuracy checks were performed for these systems. These calibration operations also were carried out periodically for the entire period of the expeditions. However, the confidence zone of

these operations ends at approximately 78° N, a location farther south than the survey areas. For this reason, in the period between the expeditions and receipt of corrections, an evaluation of accuracy characteristics of the primary positioning system relative to the secondary positioning system was made. Calculations were also performed on the positioning uncertainties by difference in coordinates obtained from these two systems. From the results of control tests in the expeditions *Arktika-2011*, *Arktika-2012* and *Arktika-2014*, the accuracy of operation of the main vessel positioning system was determined as being better than ± 5 m with confidence level of 95%.

Instantaneous sea level was used as the elevation datum for geophysical surveys. Water depths in the survey's area varied within the range of 700–4500 m. Tide variations were not accounted for as this is not required by the IHO S-44 standard for depths in excess of 200 m for bathymetry surveys and hence for geophysical surveys as well.

2.7. Multi-beam bathymetric surveying

In the course of the bathymetric expedition *Arktika-2010* and the integrated geophysical expeditions *Arktika-2011* and *Arktika-2014*, bottom relief was surveyed from the RV *Akademik Fedorov* with support of the nuclear icebreakers *Yamal* and *Rossiya*. Surveys of bottom relief were performed using an *EM122* (*Kongsberg Maritime AS*) multi-beam echosounder. In addition to the multi-beam echosounder, surveying with the single-beam echosounder *EA600* (*Kongsberg Maritime AS*) was also conducted. The main objective of single-beam surveying was the control of data obtained from the multi-beam echosounder as well as depth control at the time of data processing.

Bottom relief surveying was performed by the research vessel *Akademik Fedorov* in severe ice conditions in conjunction with a nuclear icebreaker. Because the main objective of the expeditions *Arktika-2011* and *Arktika-2014* was to obtain good-quality geophysical data, bathymetric surveying was made along the pre-planned geophysical survey lines. Vessel speed during performance of the survey ranged from 4 to 6 knots depending on ice conditions. This vessel speed ensured optimal quality of acoustic coverage of the seabed within the swath, making it possible to obtain a continuous digital model of the relief without considerable blanks.

Computerized multi-beam echosounder control systems using *Sea-floor Information System* software (*Kongsberg Maritime AS*) produced seabed relief surveys. Continuous 24-h monitoring by hydrographers and engineers resulted in uninterrupted round-the-clock operation of positioning/surveying. In addition, data quality monitoring and records of measurements of sound velocity in water were logged. All data were properly marking and annotated, and were maintained in accordance with pre-determined instructions. Hydrographers on watch also maintained scheduled documentation of performance quality with depth reading difference determinations between depths measured by the central beam of the multi-beam echosounder *EM122* and depths measured by the *EA600* single-beam echosounder.

The approach of conducting bathymetric surveying in combination with geodetic operations ensured: (1) implementation of navigation along pre-planned survey lines, (2) quality control of vessel positioning determinations, (3) control of completeness and confidence of obtained bathymetric data, (4) uninterrupted recording of bathymetric data, and (5) obtaining necessary corrections for depth adjustment.

In accordance with the classification of the IHO S-44 Standard, seabed relief surveying was conducted consistent with requirements of the second category of accuracy. The width of the swath covered by regular bathymetry grids was 3–4 km.

2.8. Field surveys on Arctic islands

Since 1937 the *Russian Academy of Sciences* has conducted many field expeditions focused on geological studies of islands and adjacent continental lands of the Arctic region. During the last decade, the geology of almost all islands of the Russian Arctic was re-examined. Most of these operations were organized by the *Federal Subsoil Resources Management Agency* (*VSEGEI* and *VNIOkeangeologia*, Petrov, Proskurnin, Kos'ko, Korago, Sobolev, Gusev, Rekant et al.). Investigations also were conducted by geologists from the *Russian Academy of Sciences* (Sokolov, Kuzmichev, Tuchkova, Danukalova, Karyakin, Lobkovsky, Rogov et al., Moscow; Vernikovskiy, Metelkin, Nikitenko et al., Novosibirsk; Prokopyev, Yakutsk; Akinin, Magadan), *St. Petersburg State University* (Ershova, Khudoley et al.) and *Moscow State University* (Nikishin et al.). During the last 7 years, *Rosneft* has undertaken geological investigations of almost all islands of the Russian Arctic as well as the study of cores from boreholes from the Arctic shelf. As a result, we have had access to: (1) a revised version of the stratigraphy of the Arctic islands, (2) state-of-the-art age dating of almost all igneous complexes on all islands, (3) age dating of detrital zircons from almost all stratigraphic intervals on all islands, (4) new paleomagnetic data, and (5) new models of the geological history of the Arctic islands. All of these new data are vital for better understanding of the geological history of the Arctic Ocean.

3. Collected data summary

All planned surveys within the framework of the Russian Arctic Ocean Mega Project have been completed. As a result of surveys conducted between 2005 and 2020, the database as of today includes 35,000 km of bathymetric profiles, more than 23,000 km of multi-channel seismic (MCS) lines, more than 4000 km of wide-angle refraction/reflection (WARR) data, 150 refracted sonobuoy seismic soundings, approximately 10,000 km of gravity surveys, and a large amount of ocean bottom rock samples. All geophysical surveys along the pre-planned survey lines have been made possible only through the support of nuclear icebreakers.

In total, during three years of expeditions *Arktika-2011*, *Arktika-2012* and *Arktika-2014*, the vast majority of planned MSC lines were successfully acquired. Unfortunately, under conditions of solid ice cover, the long seismic streamer (4500 m and more) could be deployed to a lesser extent than planned. This was especially the case for the *Arktika-2011* expedition when ice conditions were extremely severe. In contrast, for the *Arktika-2014* expedition, more than half of the planned MCS lines could be acquired with the long seismic streamer, owing to improved ice conditions that year.

Taking rock samples on slopes of submarine highs turned out to be a challenging task. Utilization of a bottom dredge and a grab sampler gives no guarantee that samples taken are just bedrock. Drilling 2-m deep boreholes showed that rocky formations have moved along the slope and became intermingled with loose sediments. The most effective method for taking samples of bedrock proved to be through the deployment of the scientific research submarine (SRS) equipped with special manipulators using *GEOSURVEY GIN RAS* methodology in the course of the *Mendeleev-2014* and *Mendeleev-2016* expeditions. Utilization of the SRS made it possible to locate the most reliable places for sampling with manned underwater vehicles. The unique methodology available to the *Mendeleev-2014* and *Mendeleev-2016* expeditions enabled the construction of a composite stratigraphic column comparable to the results produced by deep drilling.

Bathymetric and subbottom surveys used jointly with other methods of studying the bottom of the Eurasia Basin demonstrated a high level of effectiveness, but could only be acquired when a nuclear icebreaker was

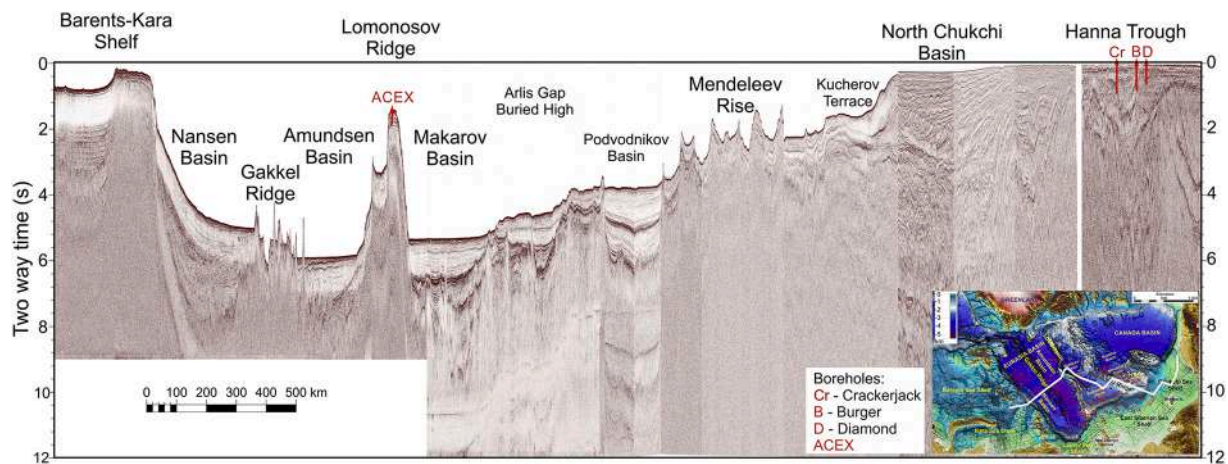


Fig. 15. Composite seismic section running from the Barents-Kara shelf to Alaska shelf. Profile location is shown on the map.

used. The detailed bathymetry and geological structure of the uppermost 100 m were resolvable, facilitating the study of the rift valley area of the Gakkel Ridge as well as present-day geological processes on the continental slope and on the Nansen basin floor.

4. Seismic data processing

Processing of the MSC refracted sonobuoy seismic soundings and WARR seismic data were performed by several Russian and international geophysical companies, in particular *Rosgeo*, *SMNG*, *Sevmorgeo*, *MAGE*, *Geolab*, *GNINGI*, *WGP*. As the processing standard, techniques of the company *ION*, with many years of geophysical experience, were used and many seismic lines were acquired and/or processed with their participation. The participating Russian geophysical companies utilized known and proven software packages (*Paradigm Echos*, *SeisSpace Pro-MAX*, *GEOLAB* and others) and processing was undertaken in accordance with international standards for seismic data processing.

4.1. MCS data processing

The generalized processing sequence for MCS data incorporated modern processing procedures. Interference waves and irregular noise suppression and multiple wave attenuation were the main processing procedures for stable tracking of seismic horizons and acoustic basement.

LIFT (Leading Intelligent Filter Technology) procedure was used to suppress low-speed surface interference waves as well as impulse and irregular noise. LIFT provides effective suppression of interference waves of various types with conservation of signal amplitudes and phase characteristics. This technique is based on the extraction of signal and noise in different frequency ranges from seismic data, attenuation of interference waves to a level less than or equal to the signal in each frequency range using velocity filters, and calculation of the sum of the residual signal components that form the signal part of the seismic data.

Multiple wave energy that is generated in offshore seabed seismic surveys and recorded on seismic records were predicted by combining mathematical extrapolation of the wavefield through the water column and calculation of the reflectivity from the seabed. The WEMA (Wave Equation Multiple Attenuation) procedure was used primarily for simulation and adaptive subtraction of multiple waves. Seabed reflectivity in relation to the amplitudes of upward and downward waves was used to successfully suppress multiple waves. In WEMA, instead of estimating the seabed reflectivity, a least-squares calculation of the space-time variable of the matching filter was performed. No additional assumptions about the nature and complexity of the seabed were required to apply WEMA. Also, multiple wave attenuation was

performed with the surface-related multiple elimination (SRME) as well as Radon transform procedures with the help of FK-transformation. Predictive deconvolution was applied to increase the seismic resolution, the frequency spectrum, and suppress reverberant waves in the shallow water part of the seismic lines.

After seismic stacking 2D-FX deconvolution, spectral and amplitude balancing and two-way coherency filtration were applied. Increased vertical resolution was achieved by applying spectrum alignment. This has allowed for effectively compensating for the non-uniformity of definitive sections primarily within the section characterized by low acoustic velocities.

Several iterations of velocity analyses were performed for the MCS data. In addition, sonobuoy seismic soundings data were used for obtaining final velocity models for each MCS line and for constructing depth sections. The data of sonobuoy seismic soundings were especially helpful for obtaining velocity models for the MCS lines acquired with short seismic streamers. The short seismic streamer records from MCS demonstrated low sensitivity to variations of stacking velocities. In general, stacking, supported by reliable velocity functions from sonobuoy seismic soundings (150 in total), produced good quality seismic sections, especially in the noiseless environment of abyssal seas.

The final processed seismic data were time or depth sections with 6 CDP fold for short seismic streamer data (600 m), and time or depth sections with minimum 45 CDP fold for long seismic streamer data (4500 m. and longer).

4.2. Seismic data interpretation

In Russia, interpretation of the seismic lines of the *Arktika* expeditions was conducted mainly by three groups: (1) the *VSEGEI* (St. Petersburg) group (e.g., [Daragan-Sushchova et al., 2015](#); [Petrov, 2017](#); [Petrov and Smelror, 2019](#)), (2) the *VNIIOkeangeologia*, St. Petersburg group (e.g. [Poselov et al., 2012](#); [Piskarev et al., 2019](#)), (3) the so-called Moscow group (*Moscow State University*, *Rosneft* and *GEOSURVEY GIN RAS*) (e.g. [Nikishin et al., 2014, 2018, 2019](#)). Our Paper-2 summarizes the principal results of the interpretation of Russian seismic lines for the Arctic ([Nikishin et al., 2021a](#)).

Sonobuoy seismic soundings data were obtained for most seismic lines. A part of the processing results has been presented elsewhere ([Daragan-Sushchova et al., 2015](#); [Petrov, 2017](#); [Piskarev et al., 2019](#); [Butsenko et al., 2019](#); [Petrov and Smelror, 2019](#)). Results of wide-angle refraction/reflection surveys were processed and published ([Lebedeva-Ivanova et al., 2011, 2019](#); [Poselov et al., 2012](#); [Petrov et al., 2016](#); [Petrov, 2017](#); [Kashubin et al., 2018](#); [Piskarev et al., 2019](#)) and included in international reviews (e.g. [Pease et al., 2014](#); [Lebedeva-Ivanova et al., 2019](#)).

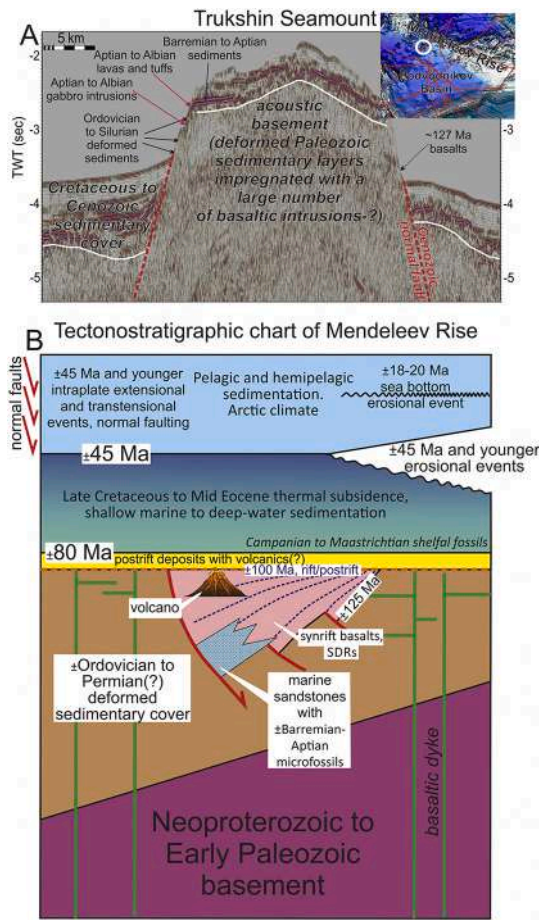


Fig. 16. A. Fragment of seismic section ARC-12-05 for the Trukshin Seamount (Mendelev Rise). Location of the section is shown on the map. The seamount is denoted by a white circle. The approximate locations of Russian samples for this seamount are presented. Ages of basalts are after [Morozov et al. \(2013\)](#) and [Skolotnev et al. \(in preparation\)](#). Fossils after [Skolotnev et al. \(2019\)](#). B. Tectonostratigraphic chart of the Mendelev Rise. The ages are based on [Morozov et al. \(2013\)](#), [Skolotnev et al. \(2019\)](#), and [Mukasa et al. \(2020\)](#),

5. International cooperation in the investigation of the Arctic Ocean

Russia has taken part in many international projects aimed at the investigation of the Arctic, including in particular, the first scientific drilling expedition to the central Arctic Ocean in September 2004. Plans for this first-ever event were carefully crafted over several years and included a fleet of three icebreaker-class ships: a drilling vessel, the *Vidar Viking*, which remained at a fixed location and suspended over 1600 m of drill pipe through the water column and into the underlying sediments, a Russian nuclear icebreaker, *Sovetskiy Soyuz*, and the diesel-electric Swedish icebreaker *Oden*. The *Sovetskiy Soyuz* and *Oden* protected the *Vidar Viking* by breaking heavy flows into smaller bits to allow the *Vidar Viking* to stay positioned in order to drill and recover the sediment cores. The *Sovetskiy Soyuz* conducted the first “attack” on oncoming heavy flows, whereas *Oden* was the last defense in protecting the drilling operation against the oncoming ice ([Backman et al., 2006](#)). When conducting seismic surveys in the Arctic Ocean, many international companies participated on a commercial basis.

Field surveys on the Russian Arctic islands were often conducted by international teams of geologists, organized by VSEGEI and institutes of

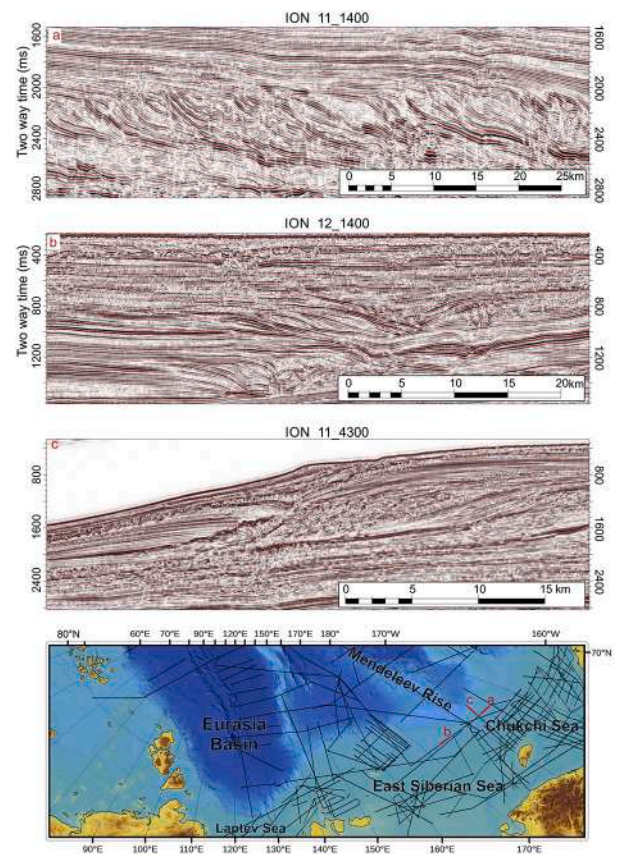


Fig. 17. Examples of seismic sections for shelf and continental slope, North Chukchi Basin.

the *Russian Academy of Sciences*. In these operations geologists took part from Sweden (D. Gee, V. Pease), USA (E. Miller), Germany (C. Brandes, D. Franke et al.), UK (R. Scott) and other countries. Other successful international projects included, for example, the *Swedish-Russian-US Arctic Ocean Investigation of Climate-Cryosphere-Carbon Interactions (SWERUS-C3)*.

One of the products of international cooperation was the *Tectonic Map of the Circumpolar Arctic (TeMar)*, which was compiled under the *International Project Atlas of Geological Maps of the Circumpolar Arctic*. The project has been ongoing since 2004 by geological surveys of the Arctic countries supported by the *UNESCO Commission for the Geological Map of the World (CGMW)* and national programs for scientific substantiation for the *United Nations Commission for the Law of the Sea (UNCLOS)*. The *TeMar* working group coordinated by Russia (VSEGEI) includes leading scientists from geological surveys, universities and national academies of science of Denmark, Sweden, Norway, Russia, Canada, the USA, France, Germany and Great Britain (see [Petrov et al., 2016](#)).

6. Results and discussion

Results of all these operations were consolidated into GIS-projects (e. g. *Petrel*, *ArcGIS*). With 2D seismic data we have been able to construct composite regional seismic profiles for all regions ([Fig. 15](#)) tied to drilling and magnetic and gravity anomalies data. We have also correlated the seismic-based stratigraphy across multiple deep-water and shelf basins. This has enabled the construction of an integrated seismic-stratigraphic framework for the entire Arctic Ocean and its shelves (see *Paper-2*).

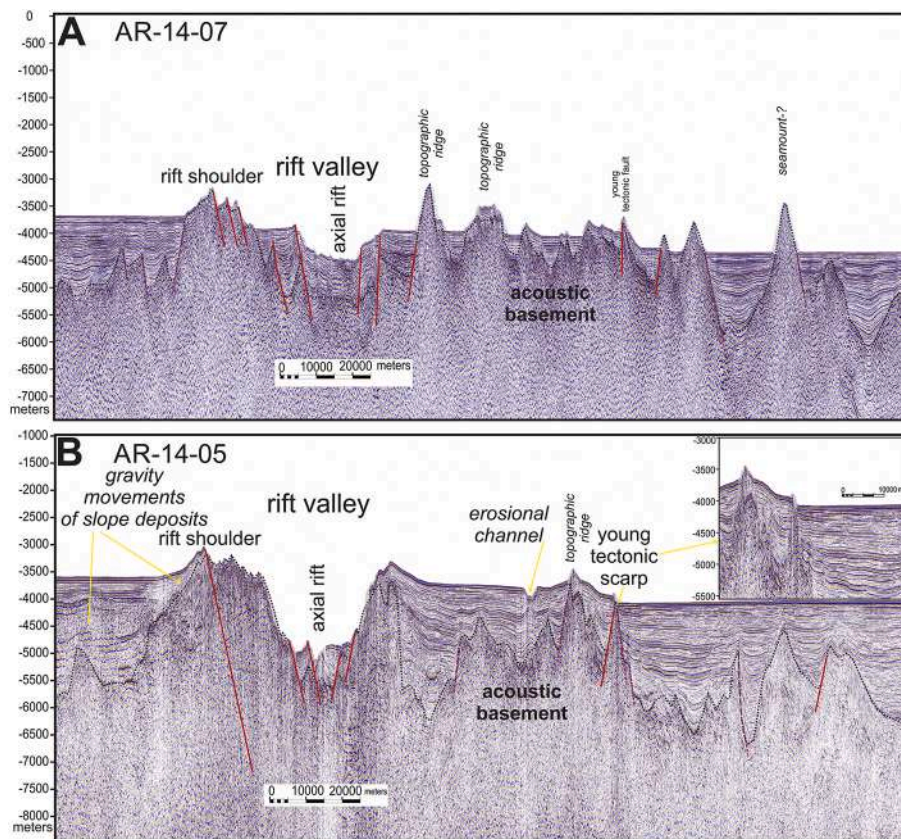


Fig. 18. Seismic sections across the Gakkel Rift valley. For location see Fig. 7. Modified after Nikishin et al. (2018).

Integration of seismic and sampling data from submarine slopes of the Mendeleev Rise acquired by SRS during the *Mendeleev-2014* and *Mendeleev-2016* expeditions has enabled us to construct a model for the structure and stratigraphy of this feature. Skolotnev et al. (2019) suggested that based on subsea observations, Paleozoic deposits appear deformed and are not horizontally oriented (it should be noted that we cannot confirm this one way or the other). It is important to point out that on seismic sections all Paleozoic complexes look like acoustic basement, i.e., opaque, with no apparent coherent internal reflections. This suggests that the Paleozoic deposits are likely to be deformed into folds that image poorly due to their likely steep dip. At one site on the Trukshin Seamount (Skolotnev et al., 2019) samples of sandstones were taken at the base of a section of horizontal architecture that is well imaged on seismic sections. These sandstones were found to have Barremian-Aptian microfossils and detrital zircons with an age of about 120 Ma (Skolotnev et al., in preparation). This might indicate that the development of the sedimentary and volcanic section of the Mendeleev Rise started approximately at the Barremian/Aptian boundary.

It was also found that among exposures of Paleozoic rocks, many instances of basalt, dolerite and basaltic tuff (Skolotnev et al., 2017, 2019) are present with isotopic ages of about 105–124 Ma (Skolotnev et al., in preparation). From the data acquired during the *Arktika-2012* expedition, an isotopic age of approximately 127 Ma was obtained for basalts collected from the Trukshin Seamount (Morozov et al., 2013). The large number of basalt outcrops indicates that the Paleozoic section as well as the entire basement underlying the Mendeleev Rise are impregnated with basaltic intrusions. Arctic Ocean researchers obtained isotopic ages of basalts in the intervals of 118–112, 105–100 and 90–70 Ma at the northern part of the Chukchi Borderland (Mukasa et al., 2020).

Our stratigraphic model of the Trukshin Seamount and the entire Mendeleev Rise is shown in Fig. 16. The main conclusion is that deformed Paleozoic sedimentary deposits cover the continental basement there and that the Paleozoic deposits are impregnated with a large number of basaltic intrusions of Aptian-Albian age. The section covering the Mendeleev Rise comprising sandstones, tuffs and basalts, ranges in age from Barremian to Aptian; the presence of Triassic and Jurassic deposits has not yet been substantiated.

In the North Chukchi Basin and on the continental slope of the Amerasia and Eurasia basins, clinofolds within various sedimentary sequences are well resolved (Fig. 17), and provide the basis for developing the seismic stratigraphic framework for the Cretaceous and Cenozoic of the Arctic Ocean.

The Gakkel Ridge is a classic example of an ultra-slow spreading mid-oceanic ridge (Dick et al., 2003; Nikishin et al., 2018). For this area we acquired several multi-channel seismic lines and subbottom profiler lines (Figs. 18, 19). These data will contribute to a better understanding of the geodynamics of ultra-slow spreading. Seismic sections show that the Gakkel Ridge is asymmetrical and that along the strike of the rift valley, seamounts, which may be of volcanic or tectonic origin, are present. We also observe young normal faults along the Gakkel Ridge trend. These new data will be valuable for further special analysis and new expeditions.

The data collected from the Arctic Ocean confirm the likely presence of volcanoes and volcanic complexes of Cretaceous age, which were detected earlier (e.g. Coakley et al., 2016; Mukasa et al., 2020). For example, our data confirmed that Aptian-Albian lavas and intrusions occur on slopes of the Mendeleev Rise. Seismic data demonstrate the presence of many seaward dipping reflectors (SDR) within sections in

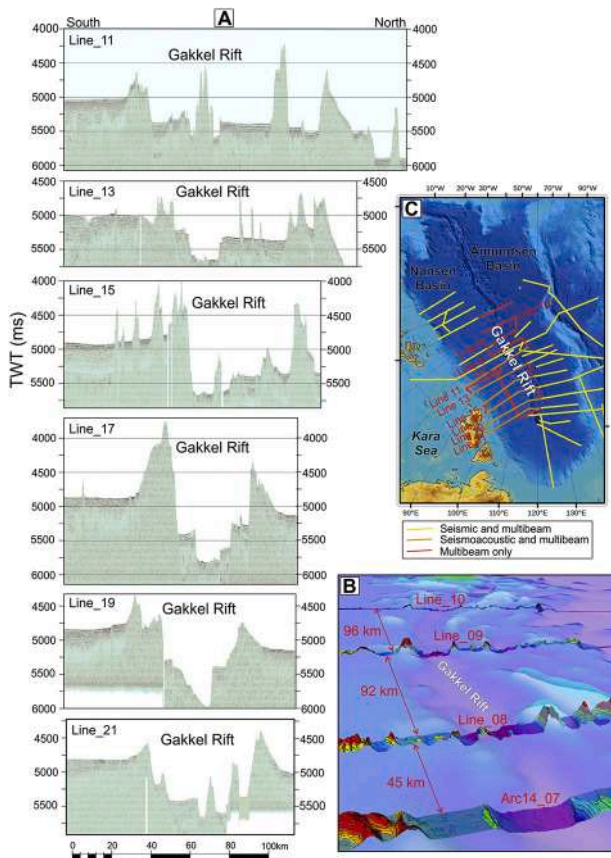


Fig. 19. Subbottom profiler and multibeam data for the Eurasia Basin and Gakkel rift valley. A. Subbottom lines for the Gakkel Rift region (preliminary field processing). B. Multibeam profiles for the Gakkel Rift region. Background colored map is official bathymetry of the Eurasia Basin (IBCAO, Jakobsson et al., 2012). Note the significant difference between the new multibeam data and published bathymetry. C. Location map and data types.

the Mendeleev Rise area and of the adjacent Podvodnikov and Toll basins (Fig. 20). Many buried seamounts, interpreted as volcanic edifices, have been found in the Mendeleev Rise and in the Podvodnikov, Makarov, and Toll basins, as well as on the Lomonosov Ridge (Fig. 21). Our data show the existence of a vast volcanic edifice in the area of the Alpha-Mendeleev Rise, which was predicted by analyses of magnetic anomalies (e.g., Gaina et al., 2011; Saltus et al., 2011; Det et al., 2013; Oakey and Saltus, 2016).

On seismic sections across the deep-water part of the Arctic Ocean, we observe many half-grabens that are characteristic of continental rift systems. At the same time, we found at least two V-shaped structures suggestive of rift valleys not typical of continental rifts (Fig. 22). Alternative interpretations of such structures are presented in Paper-2.

On the shelves of the Russian East Arctic in the Laptev, East Siberian and Chukchi seas, many synrift to postrift sedimentary basins with complex structure are identified. On many regional seismic sections across these basins, the seismic Moho is clear, occurring at depths between 9 and 11 s (Figs. 23, 24). This suggests that for these basins better constrained geometrical models for the structure of rift systems can be constructed for the entire thickness of the crust. The new data therefore make it possible to develop well-constrained models for the origin of these basins.

Thicknesses of sedimentary deposits in excess of 10 s (more than 20 km) have been observed in the North Chukchi Basin (Figs. 15, 24). An obvious and first-order question that will be addressed in Paper-2 is how such super-deep basins originate and what type of underlying crust is associated with them.

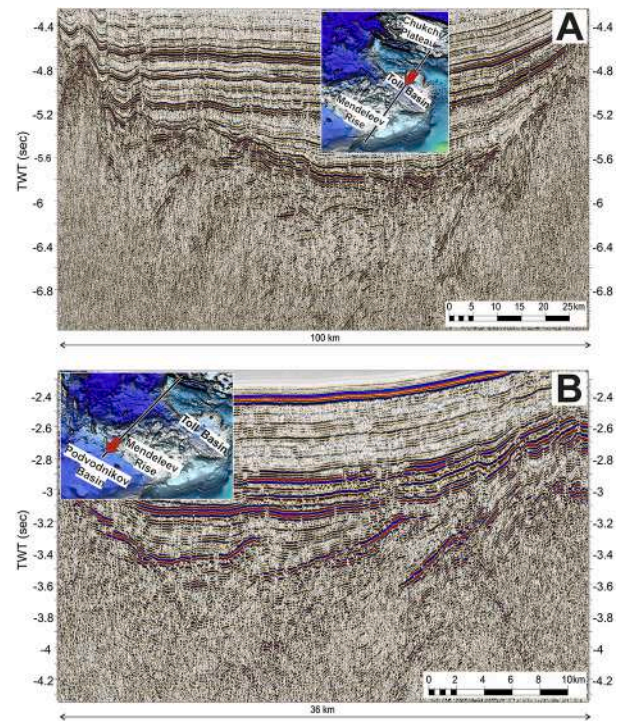


Fig. 20. Examples of seismic sections for regions of the Mendeleev Rise and Toll Basin. SDR-like seismic units are proposed. Possible half-grabens are filled by basalts.

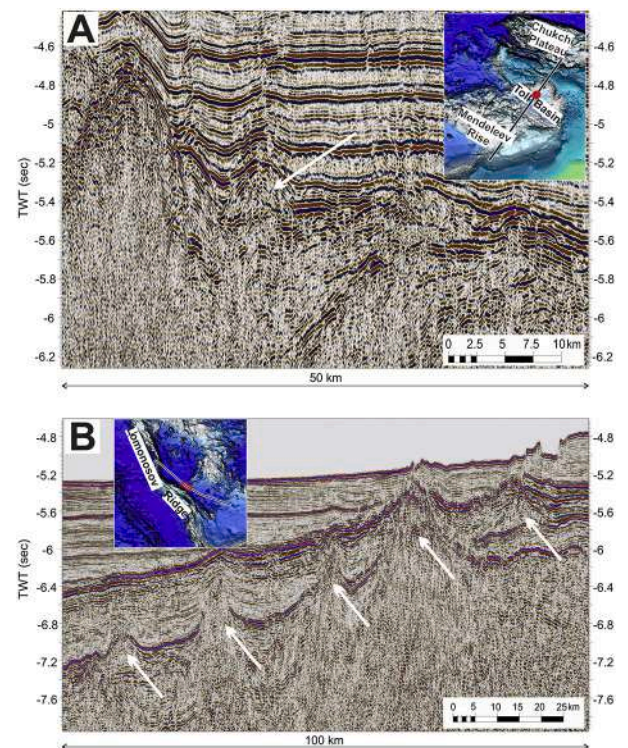


Fig. 21. Examples of seismic sections for regions of the Makarov and Toll basins. Possible volcanic edifices are indicated by arrows.

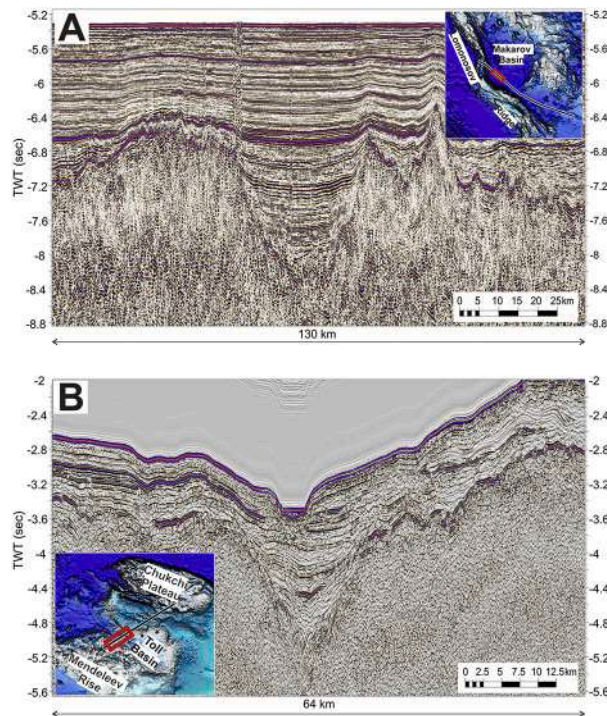


Fig. 22. Example of seismic sections for regions of the Makarov and Toll basins. V-shaped troughs are filled by sediments.

The Arctic Ocean can be called a lake-ocean during some periods of its history (e.g., Stein, 2008). At least from Cretaceous time until the present, it has been situated in the vicinity of the geographic North Pole. Its sediments contain records of paleoclimatic changes for the time period of more than 100 million years. To a large extent, sedimentation and lithology of sediments were controlled by the paleoclimate. On seismic sections we recognize packages of reflections of variable amplitude representing variable lithologies that can be traced regionally. Seismic data allow us to infer different climatic epochs in the history of the Arctic (see Paper-2).

An example of data integration focused on the understanding of the geological structure of the Podvodnikov Basin is shown in Fig. 25. Interpretation of this seismic section shows that synrift and postrift complexes can be identified. The synrift complex contains unidirectional dipping bright reflectors, which can be interpreted as synrift deposits with interbedded basalts (SDR-like units). The velocity model shows that in the synrift complex, rocks with high seismic velocities are present, which can be interpreted as basalt. Data on magnetic and gravity anomalies also exhibit a large anomaly in this basin (the High Arctic Magnetic High Domain of Gaina et al., 2011; Oakey and Saltus, 2016), which is thought to be associated with HALIP basalts (Oakey and Saltus, 2016).

Integration of the entirety of the new data available enables us to develop a comprehensive stratigraphic and regional tectonic structural framework (see Paper-2) and a new model for the Mesozoic-Cenozoic geological evolution of the Arctic Ocean (see Paper-3).

7. Conclusions

The Russian Arctic Ocean Mega Project was undertaken in the past 15–20 years. A very substantial amount of new data was obtained:

- (1) More than 23,000 km of multi-channel seismic lines, enabling the construction of a new comprehensive stratigraphic and regional tectonic structural framework and a new model for the Mesozoic-Cenozoic geological evolution of the Arctic Ocean.

- (2) More than 4000 km of wide-angle refraction/reflection lines enabling the construction of models for the structure of the Earth's crust for various regional features.
- (3) For the Mendeleev Rise, many rock samples were taken on slopes of seamounts in the course of three expeditions. Notably, sampling was undertaken with the use of drilling and a scientific research submarine. These data facilitates creation of a model for the structure of the Mendeleev Rise.
- (4) The Ministry of Natural Resources and Environment of the Russian Federation, as well as Rosneft and Gazprom made a major effort in setting the stage for seismic surveying and the study of magnetic and gravity anomalies. Contributing to this effort were several new commercial wells that have recently come available. Integration of all new data for the shelf provides a robust base for improvement of our understanding of the entire Arctic Ocean.
- (5) New subbottom profiles for the Eurasia Basin have been acquired. This makes it possible to better understand the structure of the Gakkel Ridge and Quaternary processes in the entire Eurasia Basin.
- (6) New data on the bathymetry of the Arctic Ocean have been collected, improving the previously poorly studied bathymetry in major parts of this ocean.
- (7) A large body of additional new data including, for example, bottom dredging, gravity and magnetic anomalies, has been obtained.

Our expeditions demonstrated that for an effective investigation of the Arctic Ocean, deployment of modern icebreakers and submarines is vital.

Declaration of Competing Interest

We have no conflict of interest.

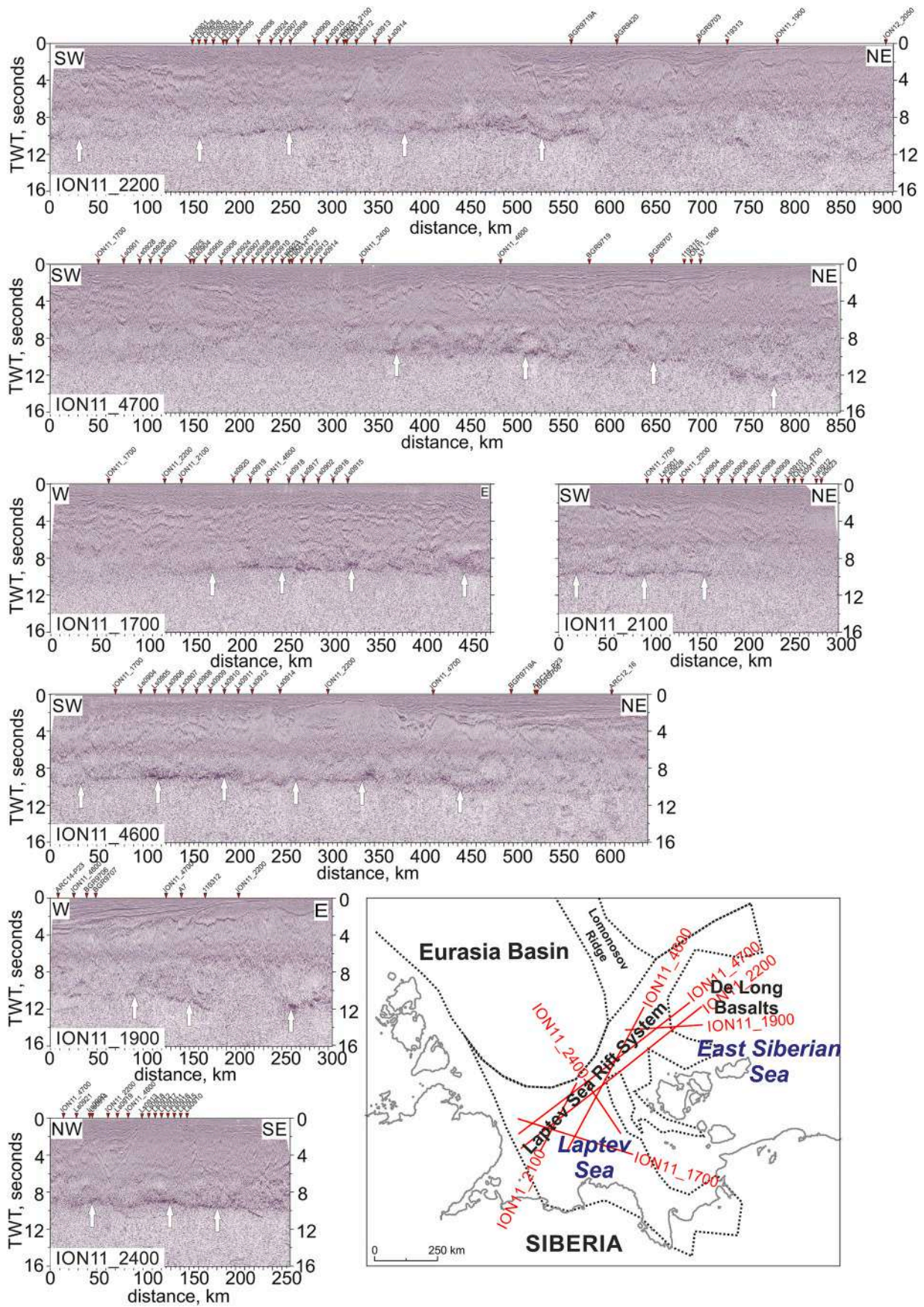


Fig. 23. Examples of seismic sections for the Laptev and East Siberian seas. Seismic Moho (white arrows) is well expressed within the synrift-postrift basins.

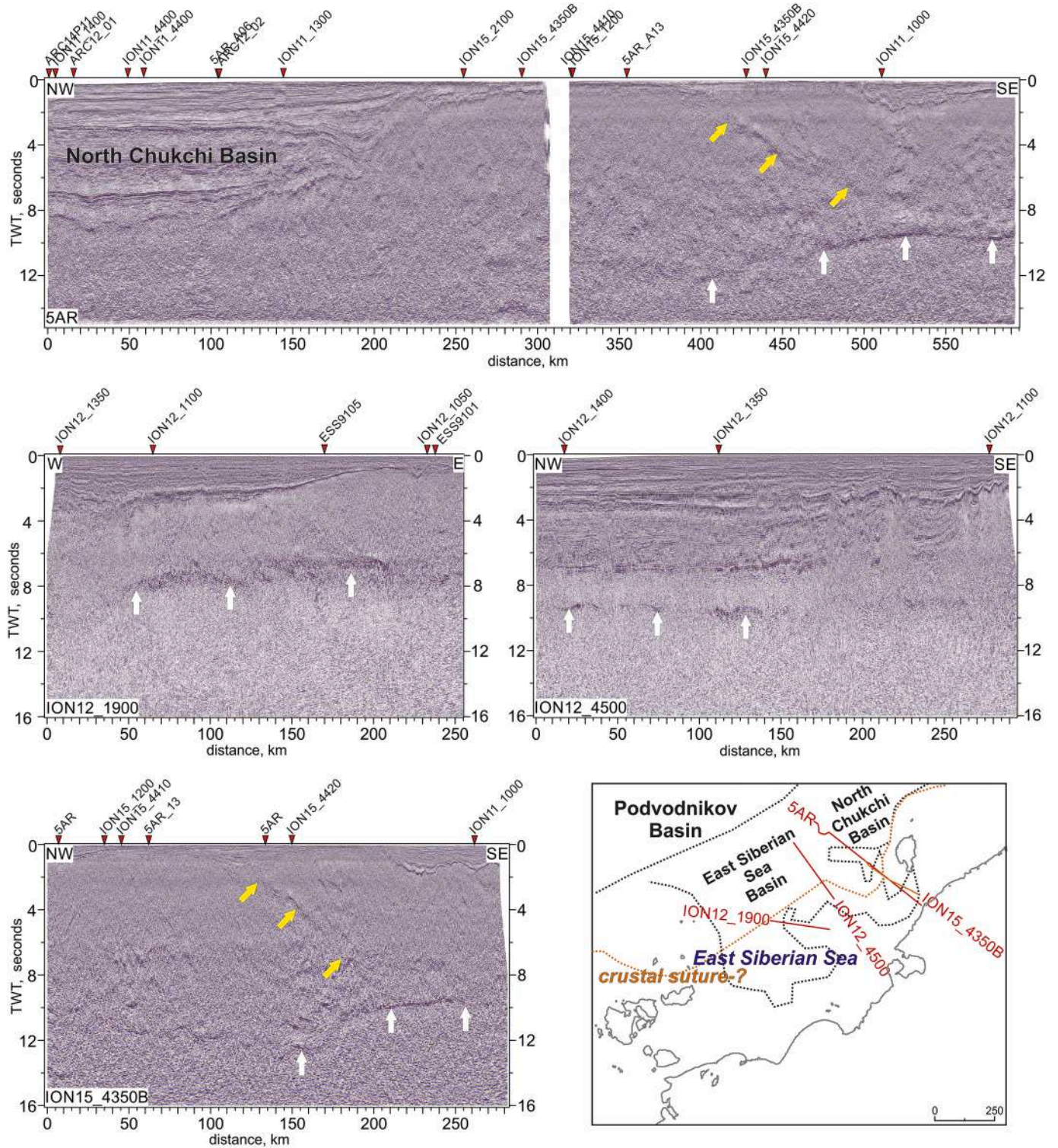


Fig. 24. Examples of seismic sections for the East Siberian and Chukchi seas. Seismic Moho (white arrows) is well recognized for synrift-postrift basins. Yellow arrows show possible crustal suture. (For interpretation of the references to colour in this figure legend, the reader is referred to the web version of this article.)

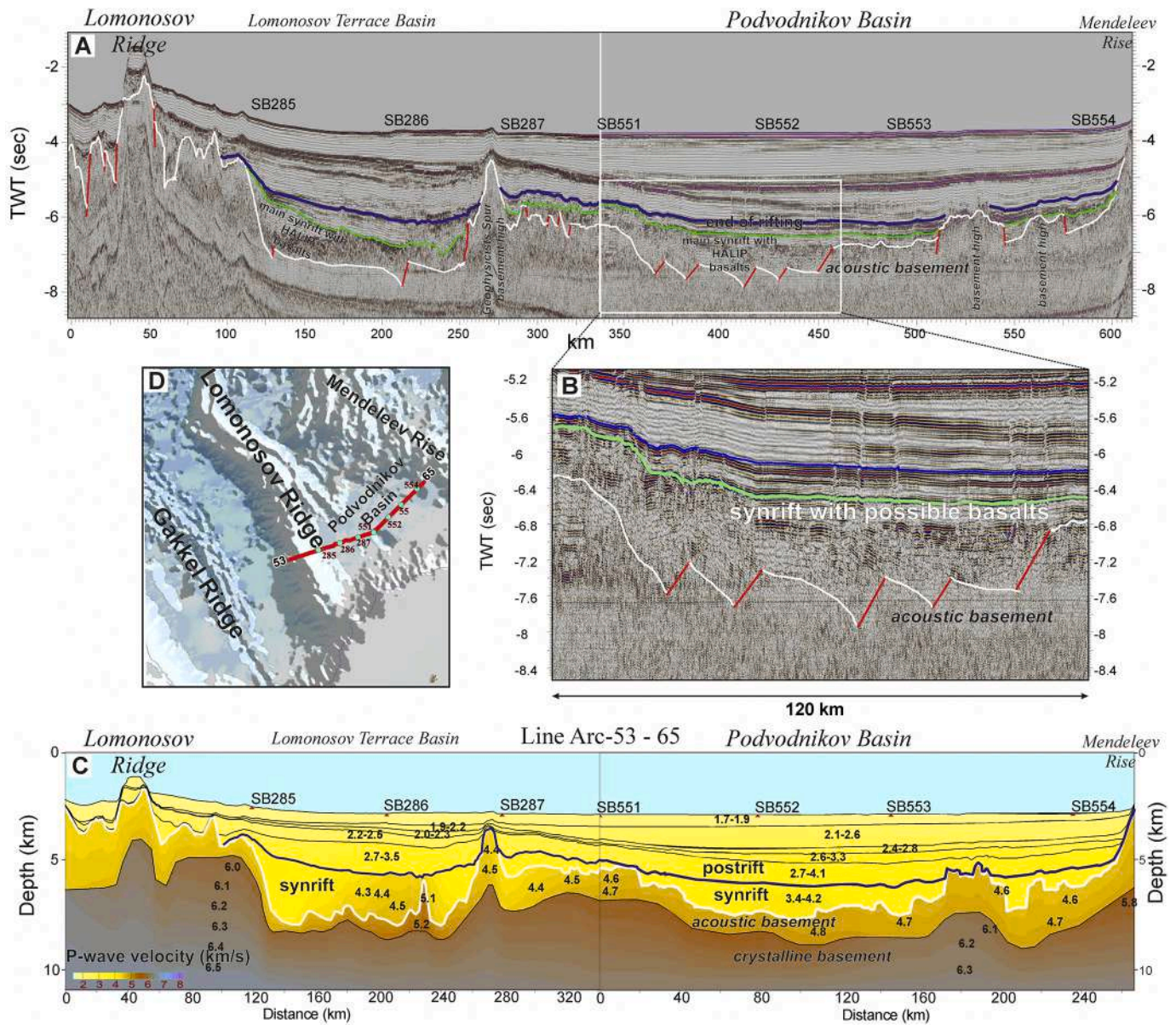


Fig. 25. An example of seismic data interpretation for the Podvodnikov Basin. A. Interpretation of the MCS seismic section (performed at *Moscow State University*). Key elements are synrift and postrift complexes. B. Fragment of this seismic sections with synrift unit and rift/postrift boundary. Synrift complex has bright reflectors dipping in one direction. C. Seismic velocity model along the same seismic sections based on refracted sonobuoys seismic soundings data (carried out by *VNIIO-keangeologia*). Interpretations by two different teams are very similar. Synrift complex has relatively high seismic velocity. We propose that the synrift complex is partly associated with basalts. D. Location of the section. Blue circles are location of sonobuoys and its numbers. (For interpretation of the references to colour in this figure legend, the reader is referred to the web version of this article.)

Acknowledgements

The authors are grateful to the *Ministry of Natural Resources and Environment of the Russian Federation* and to the *Federal Subsoil Resources Management Agency* for the opportunity to publish this paper. We are especially grateful to the professional and dedicated crews of all vessels, submarines, airplanes and helicopters and to all the specialized researchers from different countries taking part in these Arctic Expeditions. Many friends and colleagues, such as the late R. Scott, are in our memory for their pioneering contributions. Processing of all data of many kinds was conducted in different companies in Russia as well as other countries. We express many thanks to Tim Horscroft and Gillian Foulger for the invitation to write this paper. Gillian Foulger proposed the title and general structure of this paper. The work of AMN, SIF, KFS, EAR and NNZ was supported by RFBR grants (18-05-70011 and 18-05-

00495). The work of SGS was supported by RFBR (Russian Foundation for Basic Research, Russia) grant 18-05-70061. We thank the anonymous reviewers for generous, detailed, and constructive criticism and editing of our text.

References

- Aleksandrova, G.N., 2016. Geological evolution of Chauna Depression (North-Eastern Russia) during Paleogene and Neogene. 1. Paleogene. (in Russian). *Bull. Moscow Soc. Nat. Geol. Ser.* 91, 148–164 (in Russian).
- Backman, J., Moran, K., McInroy, D.B., Mayer, L.A., the Expedition 302 Scientists, 2006. *Proc. IODP, 302*. College Station TX (Integrated Ocean Drilling Program Management International, Inc.). <https://doi.org/10.2204/iodp.proc.302.101.2006>.
- Bird, K.J., Houseknecht, D.W., Pitman, J.K., 2017. Geology and assessment of undiscovered oil and gas resources of the Hope Basin Province, 2008. In: Moore, T. E., Gautier, D.L. (Eds.), *The 2008 Circum-Arctic Resource Appraisal*. U.S. Geological Survey Professional Paper 1824, Reston, Virginia, pp. 1–9. <https://doi.org/10.3133/pp1824D>.

- Bruvold, V., Kristoffersen, Y., Coakley, B.J., Hopper, J.R., Planke, S., Kandilarov, A., 2012. The nature of the acoustic basement on Mendeleev and northwestern Alpha ridges, Arctic Ocean. *Tectonophysics* 514–517, 123–145. <https://doi.org/10.1016/j.tecto.2011.10.015>.
- Butsenko, V.V., Poselov, V.A., Zholondz, S.M., Smirnov, O.E., 2019. Seismic attributes of the Podvodnikov basin basement. *Dokl. Earth Sci.* 488 (2), 1182–1185. <https://doi.org/10.1134/S1028334X19100015>.
- Coakley, B., Brumley, K., Lebedeva-Ivanova, N., Mosher, D., 2016. Exploring the geology of the Central Arctic Ocean; understanding the basin features in place and time. *J. Geol. Soc. Lond.* 173, 967–987. <https://doi.org/10.1144/jgs2016-082>.
- Craddock, W.H., Houseknecht, D.W., 2016. Cretaceous–Cenozoic burial and exhumation history of the Chukchi shelf, offshore Arctic Alaska. *Am. Assoc. Pet. Geol. Bull.* 100, 63–100. <https://doi.org/10.1306/09291515010>.
- Daragan-Sushchova, L.A., Petrov, O.V., Sobolev, N.N., Daragan-Sushchov, Yu.I., Grin'ko, L.R., Petrovskaya, N.A., 2015. Geology and tectonics of the Northeast Russian Arctic region, based on seismic data. *Geotectonics* 49, 469–484. <https://doi.org/10.1134/S0016852115060023>.
- Dick, H.J.B., Lin, J., Schouten, H., 2003. An ultraslow-spreading class of ocean ridge. *Nature* 426, 405–412. <https://doi.org/10.1038/nature02128>.
- Doré, A.G., Lundin, E.R., Gibbons, A., Somme, T.O., Tørdubakken, B.O., 2015. Transform margins of the Arctic: a synthesis and re-evaluation. *Geol. Soc. Lond. Spec. Publ.* 431, 63–94. <https://doi.org/10.1144/SP431.8>.
- Dossing, A., Jackson, H.R., Matzka, J., Einarsson, I., Rasmussen, T.M., Olesen, A.V., Brozena, J.M., 2013. On the origin of the Amerasia Basin and the High Arctic large Igneous Province—results of new aeromagnetic data. *Earth Planet. Sci. Lett.* 363, 219–230. <https://doi.org/10.1016/j.epsl.2012.12.013>.
- Dove, D., Coakley, B., Hopper, J., Kristoffersen, Y., Team, H.G., 2010. Bathymetry, controlled source seismic and gravity observations of the Mendeleev ridge; implications for ridge structure, origin, and regional tectonics. *Geophys. J. Int.* 183, 481–502. <https://doi.org/10.1111/j.1365-246X.2010.04746.x>.
- Embry, A.F., 1990. Geological and geophysical evidence in support of anticlockwise rotation of northern Alaska. *Mar. Geol.* 93, 317–329.
- Franke, D., 2013. Rifting, lithosphere breakup and volcanism: Comparison of magma-poor and volcanic rifted margins. *Mar. Pet. Geol.* 43, 63–87. <https://doi.org/10.1016/j.marpetgeo.2012.11.003>.
- Gaina, C., Werner, S.C., Saltus, R., Maus, S., 2011. Chapter 3 Circum-Arctic mapping project: new magnetic and gravity anomaly maps of the Arctic. *Geol. Soc. Lond. Mem.* 35, 39–48. <https://doi.org/10.1144/M35.3>.
- Grantz, A., Clark, D.L., Phillips, R.L., Srivastava, S.P., 1998. Phanerozoic stratigraphy of Northwind Ridge, magnetic anomalies in the Canada Basin, and the geometry and timing of rifting in the Amerasia Basin. *Arctic Ocean. Geol. Soc. Am. Bull.* 110, 801–820.
- Homza, T.X., Bergman, S.C., 2019. A Geologic Interpretation of the Chukchi Sea Petroleum Province. The American Association of Petroleum Geologists, Offshore Alaska, USA. <https://doi.org/10.1306/AAPG119>.
- Houseknecht, D.W., Wartes, M.A., 2013. Clinoform deposition across a boundary between orogenic front and foredeep – an example from the Lower Cretaceous in Arctic Alaska. *Terra Nova* 25, 206–211. <https://doi.org/10.1111/ter.12024>.
- Houseknecht, D.W., Craddock, W.H., Lease, R.O., 2016. Upper Cretaceous and Lower Jurassic strata in shallow cores on the Chukchi Shelf, Arctic Alaska. In: USGS Prof. Pap, 1814, p. 37. <https://doi.org/10.3133/pp1814C>.
- Hutchinson, D.R., Jackson, H.R., Shimeld, J.W., Chapman, C.B., Childs, J.R., Funck, T., Rowland, R.W., 2009. Acquiring marine data in Canada Basin, Arctic Ocean. *EOS Transactions* 90, 197–204.
- Ilhan, I., Coakley, B.J., 2018. Meso–Cenozoic evolution of the southwestern Chukchi Borderland, Arctic Ocean. *Mar. Pet. Geol.* 95, 100–109. <https://doi.org/10.1016/j.marpetgeo.2018.04.014>.
- Jakobsson, M., Backman, J., Rudels, B., Nycander, J., Frank, M., Mayer, L., Jokat, W., Sangiorgi, F., O'Regan, M., Brinkhuis, H., King, J., Moran, K., 2007. The early Miocene onset of a ventilated circulation regime in the Arctic Ocean. *Nature* 447, 986–990. <https://doi.org/10.1038/nature05924>.
- Jakobsson, M., Mayer, L., Coakley, B., Dowdeswell, J.A., Forbes, S., Fridman, B., Hodnesdal, H., Noormets, R., Pedersen, R., Rebecco, M., Schenke, H.W., Zarayskaya, Y., Accettella, D., Armstrong, A., Anderson, R.M., Bienhoff, P., Camerlenghi, A., Church, I., Edwards, M., Gardner, J.V., Hall, J.K., Hell, B., Hestvik, O., Kristoffersen, Y., Marcussen, C., Mohammad, R., Mosher, D., Nghiem, S. V., Pedrosa, M.T., Travaglini, P.G., Weatherall, P., 2012. The International Bathymetric Chart of the Arctic Ocean (IBCAO) Version 3.0. *Geophys. Res. Lett.* 39 <https://doi.org/10.1029/2012GL052219> n/a-n/a.
- Jakobsson, M., Mayer, L.A., Bringenspar, C., et al., 2020. The international bathymetric chart of the Arctic Ocean version 4.0. *Sci. Data* 7, 176. <https://doi.org/10.1038/s41597-020-0520-9>.
- Jokat, W., Ickrath, M., 2015. Structure of ridges and basins off East Siberia along 81°N, Arctic Ocean. *Mar. Pet. Geol.* 64, 222–232. <https://doi.org/10.1016/j.marpetgeo.2015.02.047>.
- Jokat, W., Uenzelmann-Neben, G., Kristoffersen, Y., Rasmussen, T.M., 1992. Lomonosiv Ridge – a double-sided continental margin. *Geology* 20, 887–890.
- Jokat, W., O'Connor, J., Hauff, F., Koppers, A., Miggins, D., 2019. Ultraslow spreading and volcanism at the eastern end of Gakkel Ridge, Arctic Ocean. *Am. Geophys. Union. https://doi.org/10.1029/2019GC008297*
- Kashubin, S.N., Petrov, O.V., Artemieva, I.M., Morozov, A.F., Vyatkin, D.V., Golysheva, Y.S., Kashubina, T.V., Milshtein, E.D., Rybalka, A.V., Erinchek, Y.M., Sakulina, T.S., Krupnova, N.A., Shulgin, A.A., 2018. Crustal structure of the Mendeleev Rise and the Chukchi Plateau (Arctic Ocean) along the Russian wide-angle and multichannel seismic reflection experiment “Arctic-2012.”. *J. Geodyn.* 119, 107–122. <https://doi.org/10.1016/j.jog.2018.03.006>.
- Kossovaya, O.L., Tolmacheva, T.Yu., Petrov, O.V., Isakova, T.N., Ivanova, R.M., Mirolyubova, E.S., Rekant, P.V., Gusev, E.A., 2018. Palaeozoic carbonates and fossils of the Mendeleev rise (Eastern Arctic): study of sea bottom dredged material. *J. Geodyn.* 120, 23–44. <https://doi.org/10.1016/j.jog.2018.05.001>.
- Kumar, N., Granath, J.W., Emmet, P.A., Helwig, J.A., Dinkelman, M.G., 2011. Chapter 33 Stratigraphic and tectonic framework of the US Chukchi Shelf: exploration insights from a new regional deep-seismic reflection survey. *Geol. Soc. Lond. Mem.* 35, 501–508. <https://doi.org/10.1144/M35.33>.
- Lane, L.S., 1997. Canada Basin, Arctic Ocean: evidence against a rotational origin. *Tectonics* 16, 363–387.
- Laverov, N.P., Lobkovsky, L.I., Kononov, M.V., Dobretsov, N.L., Vernikovskiy, V.A., Sokolov, S.D., Shipilov, E.V., 2013. A geodynamic model of the evolution of the Arctic basin and adjacent territories in the Mesozoic and Cenozoic and the outer limit of the Russian Continental Shelf. *Geotectonics* 47, 1–30. <https://doi.org/10.1134/S0016852113010044>.
- Lawver, L.A., Scotese, C.R., 1990. A review of tectonic models for the evolution of the Canadian Basin. In: Grantz, A., Johnson, L., Sweeney, J.F. (Eds.), *The Arctic Ocean region, The Geology of North America*, vol. L, pp. 593–618.
- Lebedeva-Ivanova, N., Gaina, C., Minakov, A., Kashubin, S., 2019. ArcCRUST: Arctic crustal thickness from 3-D gravity inversion. *Geochem. Geophys. Geosyst.* <https://doi.org/10.1029/2018GC008098>, 2018GC008098.
- Lebedeva-Ivanova, N.N., Gee, D.G., Sergeyev, M.B., 2011. Chapter 26 Crustal structure of the East Siberian continental margin, Podvodnikov and Makarov basins, based on refraction seismic data (TransArctic 1989–1991). *Geol. Soc. Lond. Mem.* 35, 395–411. <https://doi.org/10.1144/M35.26>.
- Lutz, R., Franke, D., Berglar, K., Heyde, I., Schreckenberger, B., Klitzke, R., Geissler, W., 2018. Evidence for mantle exhumation since the early evolution of the slowspreading Gakkel Ridge, Arctic Ocean. *J. Geodyn.* <https://doi.org/10.1016/j.jog.2018.01.014>.
- Miller, E.L., Akinin, V.V., Dumitru, T.A., Gottlieb, E.S., Grove, M., Meisling, K., Seward, G., 2018. Deformational history and thermochronology of Wrangel Island, East Siberian Shelf and coastal Chukotka, Arctic Russia. *Geol. Soc. London Spec. Publ.* 460, 207–238. <https://doi.org/10.1144/SP460.7>.
- Moran, K., Backman, J., Brinkhuis, H., Clemens, S.C., Cronin, T., Dickens, G.R., Eynaud, F., Gattacceca, J., Jakobsson, M., Jordan, R.W., Kaminski, M., King, J., Koc, N., Krylov, A., Martinez, N., Matthiessen, J., McInroy, D., Moore, T.C., Onodera, J., O'Regan, M., Pálfi, H., Rea, B., Rio, D., Sakamoto, T., Smith, D.C., Stein, R., St John, K., Suto, I., Suzuki, N., Takahashi, K., Watanabe, M., Yamamoto, M., Farrell, J., Frank, M., Kubik, P., Jokat, W., Kristoffersen, Y., 2006. The Cenozoic palaeoenvironment of the Arctic Ocean. *Nature* 441, 601–605. <https://doi.org/10.1038/nature04800>.
- Morozov, A.F., Petrov, O.V., Kashubin, S.N., Kremenetsky, A.A., Shkatov, M.Y., Kaminsky, V.D., Gusev, E.A., Griukurov, G.E., Rekant, P.V., Shevchenko, S.S., Sergeev, S.A., Shatov, V.V., 2013. New geological data substantiating continental nature of region of Central-Arctic rises. *Reg. Geol. i Metallog.* 55, 34–55.
- Morozov, A.F., Shkatov, M.Yu., Korneev, O.Yu., Kashubin, S.N., 2014. Complex geological and geophysical expedition “Arctic-2012” for continental nature definition of the Mendeleev Rise in Arctic Ocean. *Prospect Protect. Min. Resour.* 3, 22–27 (in Russian).
- Mosher, D.C., Chapman, C.B., Shimeld, J., Jackson, H.R., Chian, D., Hutchinson, D., Lebedeva-Ivanova, N., Verhoef, J., Pedersen, R., 2013. High Arctic marine geophysical data acquisition. *Lead. Edge* 524–536. May, 2013.
- Mukasa, S.B., Andronikov, A., Brumley, K., Mayer, L.A., Armstrong, A., 2020. Basalts from the Chukchi Borderland: 40Ar/39Ar Ages and Geochemistry of submarine intraplate lavas dredged from the western Arctic Ocean. *Am. Geophys. Union. https://doi.org/10.1029/2019JB017604*
- Nikishin, A.M., Petrov, E.I., Malyshev, N.A., 2014. Geological Structure and History of the Arctic Ocean. EAGE Publications bv. <https://doi.org/10.3997/9789462821880>.
- Nikishin, A.M., Gaina, C., Petrov, E.I., Malyshev, N.A., Freiman, S.I., 2018. Eurasia Basin and Gakkel Ridge, Arctic Ocean: Crustal asymmetry, ultra-slow spreading and continental rifting revealed by new seismic data. *Tectonophysics* 746, 64–82. <https://doi.org/10.1016/j.tecto.2017.09.006>.
- Nikishin, A.M., Startseva, K.F., Verzhbitsky, V.E., Cloetingh, S., Malyshev, N.A., Petrov, E.I., Posamentier, H., Freiman, S.I., Lineva, M.D., Zhukov, N.N., 2019. Sedimentary Basins of the East Siberian Sea and the Chukchi Sea and the Adjacent Area of the Amerasia Basin: Seismic Stratigraphy and Stages of Geological history. *Geotectonics* 53, 635–657. <https://doi.org/10.1134/S0016852119060104>.
- Nikishin, A.M., Malyshev, N.A., Petrov, E.I., 2020. The main problems of the structure and history of the geological development of the Arctic Ocean. *Her. Russ. Acad. Sci.* 90 (3), 345–356. <https://doi.org/10.1134/S101933162003003X>, 2020.
- Nikishin, A.V., Petrov, E.I., Cloetingh, S., Freiman, S.I., Malyshev, N.A., Morozov, A.F., Posamentier, H.W., Verzhbitsky, V.E., Zhukov, N.N., Startseva, K.F., Rodina, E.A., 2021a. Arctic Ocean Mega-project: paper 2 – Arctic stratigraphy and regional tectonic structure. *Earth Sci. Rev.* (in press).
- Nikishin, A.V., Petrov, E.I., Cloetingh, S., Freiman, S.I., Malyshev, N.A., Morozov, A.F., Posamentier, H.W., Verzhbitsky, V.E., Zhukov, N.N., Startseva, K., 2021b. Arctic Ocean Mega-project: Paper 3 – Mesozoic to Cenozoic geological evolution. *Earth-Sci. Rev.* (in press).
- Oakey, G.N., Saltus, R.W., 2016. Geophysical analysis of the Alpha–Mendeleev ridge complex: Characterization of the High Arctic Large Igneous Province. *Tectonophysics* 691, 65–84. <https://doi.org/10.1016/j.tecto.2016.08.005>.
- Pease, V., Drachev, S., Stephenson, R., Zhang, X., 2014. Arctic lithosphere — a review. *Tectonophysics* 628, 1–25. <https://doi.org/10.1016/j.tecto.2014.05.033>.
- Petrov, O., Morozov, A., Shokalsky, S., Kashubin, S., Artemieva, I.M., Sobolev, N., Petrov, E., Ernst, R.E., Sergeev, S., Smelror, M., 2016. Crustal structure and tectonic

- model of the Arctic region. *Earth-Sci. Rev.* 154, 29–71. <https://doi.org/10.1016/j.earscirev.2015.11.013>.
- Petrov, O.V., 2017. *Tectonic Map of the Arctic*. VSEGEI Publishing House, St. Petersburg.
- Petrov, O.V., Smelror, M. (Eds.), 2019. *Tectonostratigraphic Atlas of Eastern Arctic (Eastern Russia and Adjacent Areas)*. VSEGEI Publishing House Press, St. Petersburg, 152 p. (in Russian).
- Piskarev, A., Poselov, V., Kaminsky, V. (Eds.), 2019. *Geologic Structures of the Arctic Basin*. Springer International Publishing, Cham. <https://doi.org/10.1007/978-3-319-77742-9>.
- Poselov, V.A., Avetisov, G.P., Butsenko, V.V., Zholondz, S.M., Kaminsky, V.D., Pavlov, S. P., 2012. The Lomonosov Ridge as a natural extension of the Eurasian continental margin into the Arctic Basin. *Russ. Geol. Geophys.* 53, 1276–1290. <https://doi.org/10.1016/j.rgg.2012.10.002>.
- Saltus, R.W., Miller, E.L., Gaina, C., Brown, P.J., 2011. Chapter 4 Regional magnetic domains of the Circum-Arctic: a framework for geodynamic interpretation. *Geol. Soc. Lond. Mem.* 35, 49–60. <https://doi.org/10.1144/M35.4>.
- Shephard, G.E., Müller, R.D., Seton, M., 2013. The tectonic evolution of the Arctic since Pangea breakup: integrating constraints from surface geology and geophysics with mantle structure. *Earth-Sci. Rev.* 124, 148–183. <https://doi.org/10.1016/j.earscirev.2013.05.012>.
- Sherwood, K.W., Johnson, P.P., Craig, J.D., Zerwick, S.A., Lothamer, R.T., Thurston, D. K., Hurlbert, S.B., 2002. Structure and stratigraphy of the Hanna Trough, U.S. Chukchi Shelf, Alaska. In: Miller, E.L., Grantz, A., Klempere, S.L. (Eds.), *Special Paper 360: Tectonic Evolution of the Bering Shelf-Chukchi Sea-Artic Margin and Adjacent Landmasses*. Geological Society of America, Boulder, Colorado, pp. 39–66. <https://doi.org/10.1130/0-8137-2360-4.39>.
- Skolotnev, S., Aleksandrova, G., Isakova, T., Tolmacheva, T., Kurilenko, A., Raevskaya, E., Rozhnov, S., Petrov, E., Korniyuchuk, A., 2019. Fossils from seabed bedrocks: Implications for the nature of the acoustic basement of the Mendeleev Rise (Arctic Ocean). *Mar. Geol.* 407, 148–163. <https://doi.org/10.1016/j.margeo.2018.11.002>.
- Skolotnev, S.G., Fedonkin, M.A., Korniyuchuk, A.V., 2017. New data on the geological structure of the southwestern Mendeleev Rise, Arctic Ocean. *Dokl. Earth Sci.* 476, 1001–1006. <https://doi.org/10.1134/S1028334X17090173>.
- Smelror, M., Petrov, O.V., Larssen, G.B., Werner, S. (Eds.), 2009. *Geological History of the Barents Sea*. Atlas. Geological Survey of Norway, Trondheim.
- Stein, R., 2008. *Arctic Ocean Sediments: Processes, Proxies, and Paleoenvironment*, 1st ed. Elsevier Science.
- Van Wagoner, N.A., Williamson, M.-C., Robinson, P.T., Gibson, I.L., 1986. First samples of acoustic basement recovered from the Alpha Ridge, Arctic Ocean: new constraints for the origin of the ridge. *J. Geodyn.* 6, 177–196.
- Vernikovskiy, V.A., Morozov, A.F., Petrov, O.V., Travin, A.V., Kashubin, S.N., Shokal'sky, S.P., Shevchenko, S.S., Petrov, E.O., 2014. New data on the age of dolerites and basalts of Mendeleev Rise (Arctic Ocean). *Dokl. Earth Sci.* 454, 97–101. <https://doi.org/10.1134/S1028334X1402007X>.
- Vogt, P.R., Jung, W.Y., Brozena, J.M., 1998. Arctic marine gravity highs remain puzzling. *EOS Trans. Am. Geophys. Union* 79 (601), 605–606.
- Weber, J.R., 1990. The structures of the Alpha Ridge, Arctic Ocean and Iceland-Faroe Ridge, North Atlantic: comparisons and implications for the evolution of the Canada Basin. *Mar. Geol.* 93, 43–68.
- Weber, J.R., Roots, E.F., 1990. Historical background; Exploration, concepts, and observations. In: Grantz, A., Johnson, G.L., Sweeney, J.F. (Eds.), *The Arctic Ocean region (pp. 5–36)*. The Geology of North America DNAG L. Geological Society of America, Boulder.
- Ziegler, P.A., 1988. Evolution of the Arctic-North Atlantic and the Western Tethys. *Am. Assoc. Pet. Geol. Mem.* 43, 1–198.
- Zonenshain, L.P., Kuzmin, M.I., Natapov, L.M., 1990. *Geology of the USSR: A Plate-Tectonic Synthesis*, Geodynamics Series. American Geophysical Union, Washington, D. C. <https://doi.org/10.1029/GD021>.



Invited Review

Arctic ocean mega project: Paper 2 – Arctic stratigraphy and regional tectonic structure

Anatoly M. Nikishin^{a,*}, Eugene I. Petrov^b, Sierd Cloetingh^c, Nikolay A. Malyshev^d,
Andrey F. Morozov^b, Henry W. Posamentier^e, Vladimir E. Verzhbitsky^d, Sergey I. Freiman^a,
Elizaveta A. Rodina^a, Ksenia F. Startseva^a, Nikolay N. Zhukov^a

^a Geological Faculty, Moscow State University, Moscow, Russia

^b The Federal Subsoil Resources Management Agency, Moscow, Russia

^c Utrecht University, Utrecht, the Netherlands

^d Rosneft, Moscow, Russia

^e Consultant, 25 Topside Row Drive, The Woodlands, TX 77380, USA

ARTICLE INFO

Keywords:

Arctic
seismic stratigraphy
Lomonosov Ridge
Amundsen Basin
Nansen Basin
Podvodnikov Basin
North Chukchi Basin
Mendeleev Rise
Laptev Sea Basin
East Siberian Sea Basin
Gakkel Ridge
climate change
SDR

ABSTRACT

A seismic stratigraphic framework and basin fill geohistory for Arctic Ocean basins is presented based on data collected by several Russian Government organized expeditions to the Arctic Ocean. This analysis tied together seismic stratigraphic interpretations for the shelf and the deep-water part of the ocean. The stratigraphic framework is based on age data derived from linear magnetic anomalies in the Eurasia Basin, borehole data for the Lomonosov Ridge and Alaska Shelf, and correlations with various regional geological events. Six seismic boundaries were identified and traced regionally over large areas. We present as a hypothesis that the Arctic Ocean probably was formed during four phases with different kinematics: 133-125 Ma – Canada Basin opening, 125-80 Ma – superplume-related tectonics and magmatism in the Alpha-Mendeleev Rise area and adjacent basins, 80-56 Ma - strike-slip fault tectonics, and 56-0 Ma – Eurasia Basin opening. The time interval of 45-20 Ma appears to be a period of large-scale vertical intraplate movements and normal faulting. Climatic events are recorded in the sedimentary cover of the Arctic Ocean.

The analyses were based on a comprehensive dataset that included more than 23,000 km of 2D seismic lines, which were acquired in the deep-water part of the ocean, supplemented by a large number of federal and commercial seismic lines, which were acquired for the Russian shelves during the past 10-15 years. In addition, special multiple Russian expeditions collected samples on scarps of the Mendeleev Rise that served as ground truth for the seismic interpretation.

1. Introduction

The Arctic Ocean has been actively studied in recent years. In this paper we discuss the geological structure of the Arctic Ocean as well as associated aspects of paleoenvironment and paleoclimate. The tectonic structure of the Arctic Ocean has been discussed recently in a series of reviews (e.g., Vernikovskiy et al., 2013; Gaina et al., 2014; Pease et al., 2014; Nikishin et al., 2014; Lobkovsky, 2016; Coakley et al., 2016). Various versions of the stratigraphy of the ocean's sedimentary cover have been presented (Embry and Dixon, 1994; Backman et al., 2008; Bruvold et al., 2010; Grantz et al., 2011; Houseknecht and Bird, 2011; Mosher et al., 2012; Rekant and Gusev, 2012; Døssing et al., 2013;

Franke, 2013; Brumley, 2014; Weigelt et al., 2014; Jokat and Ickrath, 2015; Nikishin et al., 2014, 2017, 2018, 2019; Rekant et al., 2015; Thórarinnsson et al., 2015; Evangelatos and Mosher, 2016; Hutchinson et al., 2017; Petrov, 2017; İlhan and Coakley, 2018; Miller et al., 2018a, 2018b; Homza and Bergman, 2019; Piskarev et al., 2019). Paleoenvironmental and paleoclimatic investigations of the Arctic Ocean during the Cenozoic were based primarily on results of drilling on the Lomonosov Ridge within the framework of the ACEX Project (Brinkhuis et al., 2006; Moran et al., 2006; Jakobsson et al., 2007; Backman et al., 2008; Backman and Moran, 2009; O'Regan et al., 2010; Ehlers and Jokat, 2013; Stein et al., 2015). Prior to the current study reported here, the limited data available, which included information from a single well as

* Corresponding author.

E-mail address: nikishin@geol.msu.ru (A.M. Nikishin).

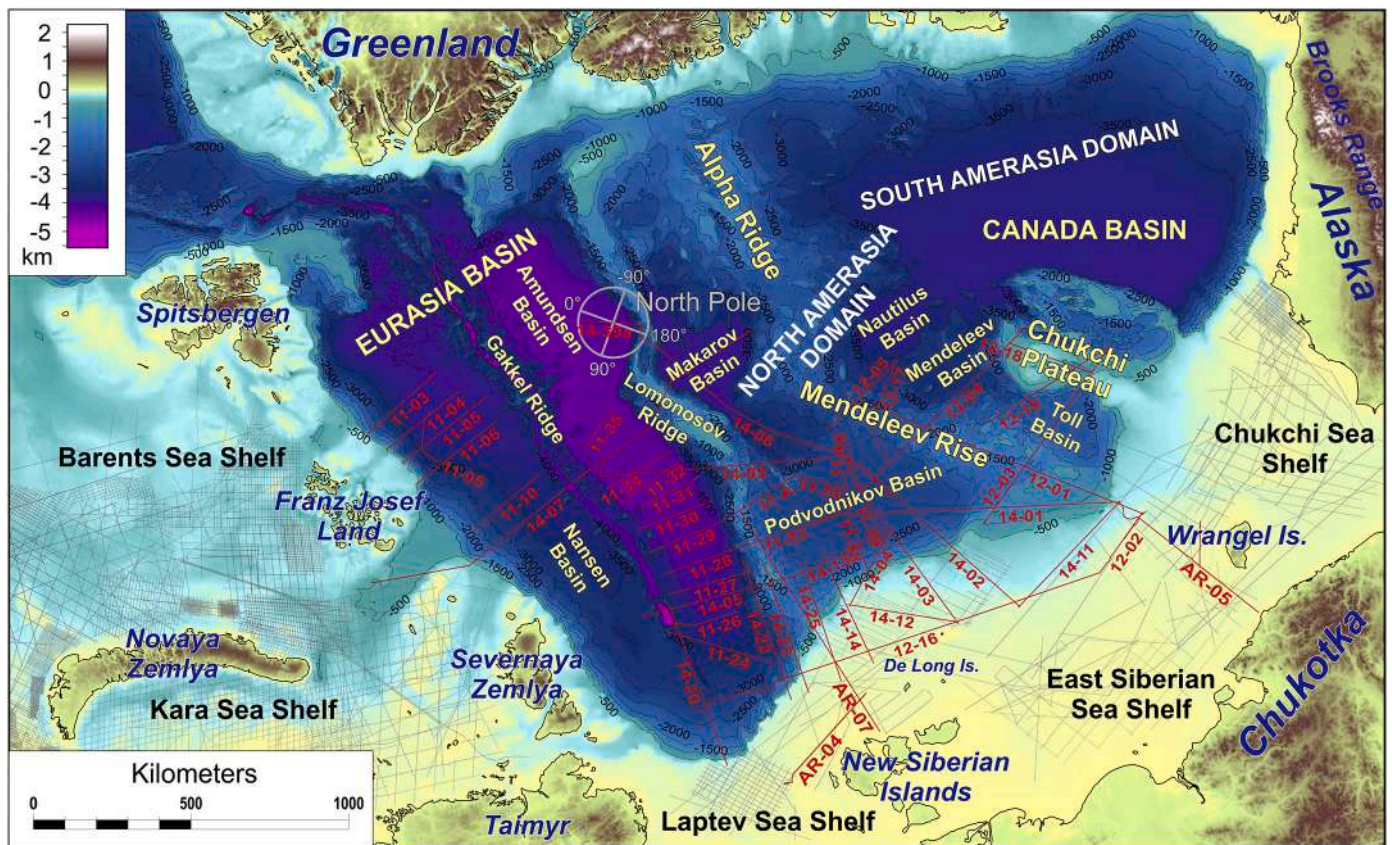


Fig. 1. Location and names of new Russian and other seismic profiles used for the seismic stratigraphic interpretation. The background map illustrates the topography and bathymetry of the Arctic region (Jakobsson et al., 2012, 2020). Red lines indicate seismic data acquired during the Russian Federal projects Arktika-2011, Arktika-2012, and Arktika-2014. Black lines in the shelf areas are federal and commercial profiles used for the regional seismic stratigraphy.

well as several seismic lines (note that the well was not tied to the seismic data), did not allow for compiling a reliable stratigraphic framework of the Arctic Ocean that could lead to a reasonable understanding of its paleogeography and paleotectonics.

In recent years, the Russian Government organized several expeditions to the Arctic Ocean. In this paper we mainly use findings of the projects Arktika-2011, Arktika-2012 and Arktika-2014, which collected more than 23,000 km of 2D seismic lines in the deep-water part of the ocean (see Paper-1, Nikishin et al., 2021a) (Fig. 1). In addition to these data, numerous federal and commercial seismic lines acquired for the Barents, Kara, Laptev, East Siberian and Chukchi shelves during the past 10-15 years (e.g., Drachev et al., 2010; Kumar et al., 2011; Nikishin et al., 2014, 2017, 2018, 2019; Ilhan and Coakley, 2018) also were available. For ground truth, rock samples were taken on sea floor scarps along the Lomonosov Ridge and Mendeleev Rise (Morozov et al., 2013; Petrov et al., 2016; Skolotnev et al., 2017, 2019; Knudsen et al., 2018; Rekant et al., 2019). In this paper we tie together seismic stratigraphic interpretations from the shelf to the deep-water parts of the ocean. Based on this new stratigraphic framework, we will discuss the tectonic structure and formation history of the Arctic Ocean. The improved understanding of Arctic Ocean paleogeography enables further examination of the relationship between the paleoenvironment and global climatic changes of this region.

2. Geological setting and study area

The Arctic Ocean comprises a deep-water basin with complex structure surrounded by multiple shelf seas (Fig. 2, Supplementary Fig. 1). The deep-water basin can be subdivided into two parts, the

Eurasia and Amerasia basins, separated by the Lomonosov Ridge. The Eurasia Basin is a continuation of the North Atlantic Ocean with the ultra-slow spreading Gakkel Mid-Oceanic Ridge running along its axis (Dick et al., 2003). The Lomonosov Ridge, which separates the Eurasia and Amerasia basins, comprises a terrane associated with a continental crust. Based on plate reconstructions, the crust of the Lomonosov Ridge is formed by Paleozoic orogens (a continuation of the Caledonian, Timanian and Taimyr orogens) (Ziegler, 1988; Nikishin et al., 2021a; Knudsen et al., 2018; Miller et al., 2018b; Miller et al., 2018a; Rekant et al., 2019).

In the Amerasia Basin, two domains can be identified: the North Amerasia and the South Amerasia domains (Nikishin et al., 2014). The South Amerasia Domain is represented by the Canada Basin, which is characterized by three principal crustal types. In the central zone, gravity and magnetic anomaly maps clearly indicate the presence of an axial rift zone. It is commonly assumed that typical oceanic crust is present there, whereas continental crust strongly extended by rifting is identified along the basin margins (Mosher et al., 2012; Chian et al., 2016; Hutchinson et al., 2017). In some marginal zones of the basin, the crust has been suggested to be composed of serpentinized mantle (Mosher et al., 2012; Chian et al., 2016). The timing of Canada Basin formation has been the subject of debate with estimates ranging from Early Jurassic to Late Cretaceous (e.g., Embry and Dixon, 1994; Embry, 1990; Grantz et al., 2011; Helwig et al., 2011; Coakley et al., 2016; Hutchinson et al., 2017; Miller et al., 2018b; Miller et al., 2018a; Homza and Bergman, 2019;). The North Amerasia Domain is represented by the Alpha-Mendeleev Rise (we will use this name to collectively refer to the Alpha Ridge and Mendeleev Rise) and the associated conjugate deep basins. Two basins are present between the Alpha-Mendeleev Rise and

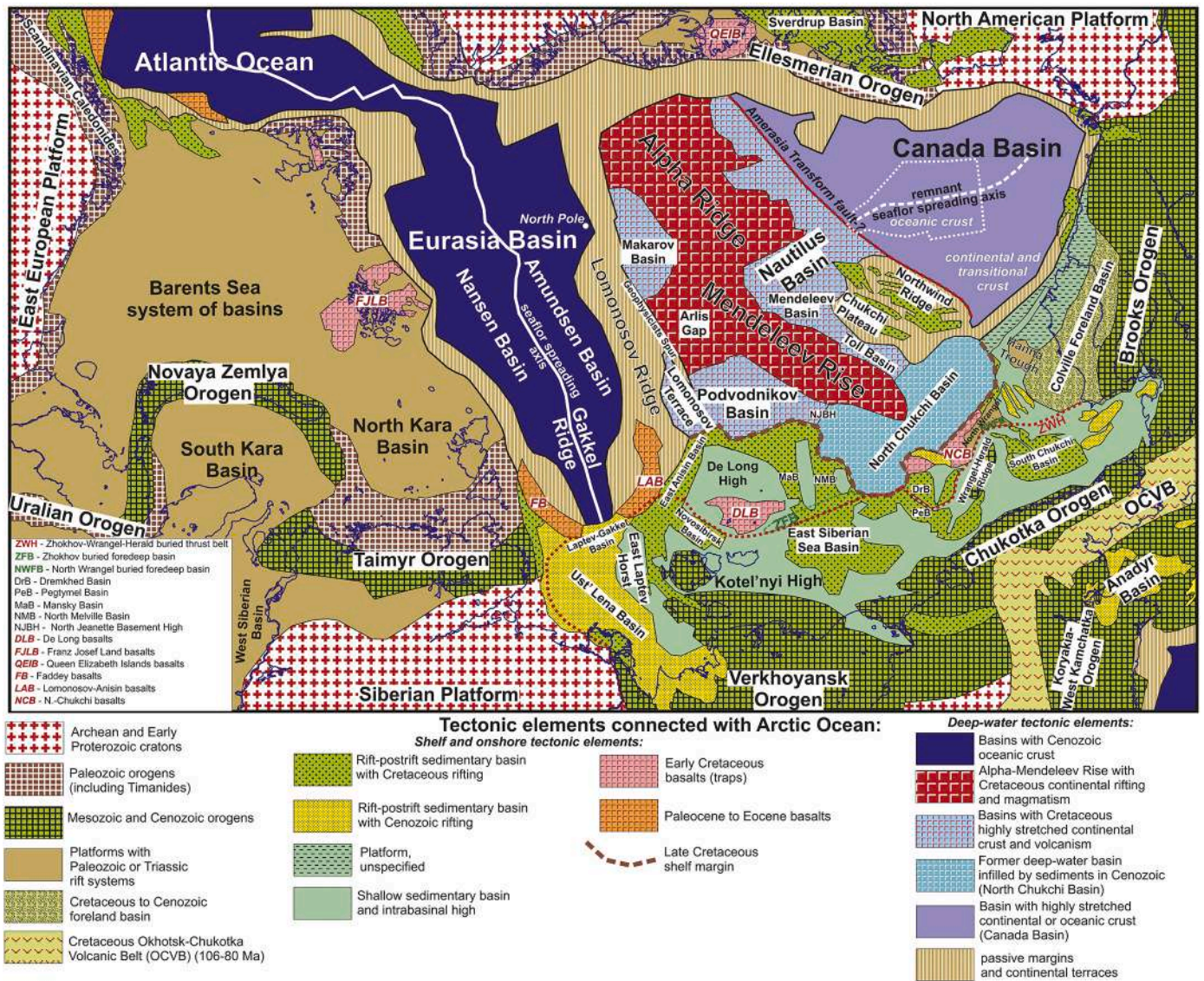


Fig. 2. Tectonic scheme of the Arctic Ocean region. New version, based on Nikishin et al. (2014, 2017, 2018) and new data. The Canada Basin structure has been resolved using data from Mosher et al. (2012) and Chian et al. (2016). For details and geography see Supplementary Fig. 1. Geographic base map is the Geological map of the Arctic (Harrison et al., 2011).

the Lomonosov Ridge: the Podvodnikov and the Makarov basins. In the area between the Alpha-Mendeleev Rise and the Canada Basin, the Nautilus, Mendeleev and the Chukchi Abyssal Plain basins (or Toll Basin) (Nikishin et al., 2017; Nikishin et al., 2014) are observed.

The Alpha-Mendeleev Rise crosses the Amerasia Basin and is located between the Russian East Siberian-Chukchi Sea shelves and the shelf associated with the islands of the Canadian Archipelago. The Alpha-Mendeleev Rise comprises a relative bathymetric high area with a relatively thickened crust up to 20-30 km thick (Alvey et al., 2008; Gaina et al., 2014; Jokat and Ickrath, 2015; Petrov et al., 2016; Lebedeva-Ivanova et al., 2019; Piskarev et al., 2019). Two main hypotheses concerning the crustal structure of this uplift exist (e.g., Gaina et al., 2014; Pease et al., 2014). Some authors propose that the uplifted zone comprises a Cretaceous oceanic plateau with a basaltic crust formed above a mantle plume (Jokat, 2003; Dove et al., 2010; Funck et al., 2011; Grantz et al., 2011; Bruvoll et al., 2012; Jokat and Ickrath, 2015). Other researchers suggest that this uplifted domain consists of a continental crust strongly thinned by rifting and within which Cretaceous plume volcanism manifested itself (Døssing et al., 2013; Miller and Verzhbitsky,

2009; Nikishin et al., 2017; Nikishin et al., 2014; Oakey and Saltus, 2016; Petrov et al., 2016; Vernikovskiy et al., 2014). The uplifted area is characterized by complex structure and associated significant seabed relief, and in general is expressed as an alternation of basins and ranges.

The crustal structure of the Makarov-Podvodnikov basin system has been a matter of debate (e.g., Evangelatos et al., 2017; Lebedeva-Ivanova et al., 2019). Some authors assume that this basin has an oceanic crust of an age that is not precisely known (Alvey et al., 2008; Grantz et al., 2011). Other authors believe that the basin has a continental crust thinned by rifting (Langinen et al., 2009; Glebovskiy et al., 2013; Kashubin et al., 2013; Laverov et al., 2013; Jokat and Ickrath, 2015; Nikishin et al., 2014, 2017; Petrov et al., 2016; Piskarev et al., 2019).

The Nautilus-Mendeleev-Toll basin system is situated between the Chukchi Plateau and the Mendeleev Rise. The structure of its crust is subject to debate. Some authors suggest that the basin's crust is oceanic (Grantz et al., 2011; Hegewald and Jokat, 2013). However, seismic data and gravity modeling suggest that the crust is likely characterized by continental crust strongly extended by rifting (Brumley, 2014; Nikishin et al., 2014, 2019).

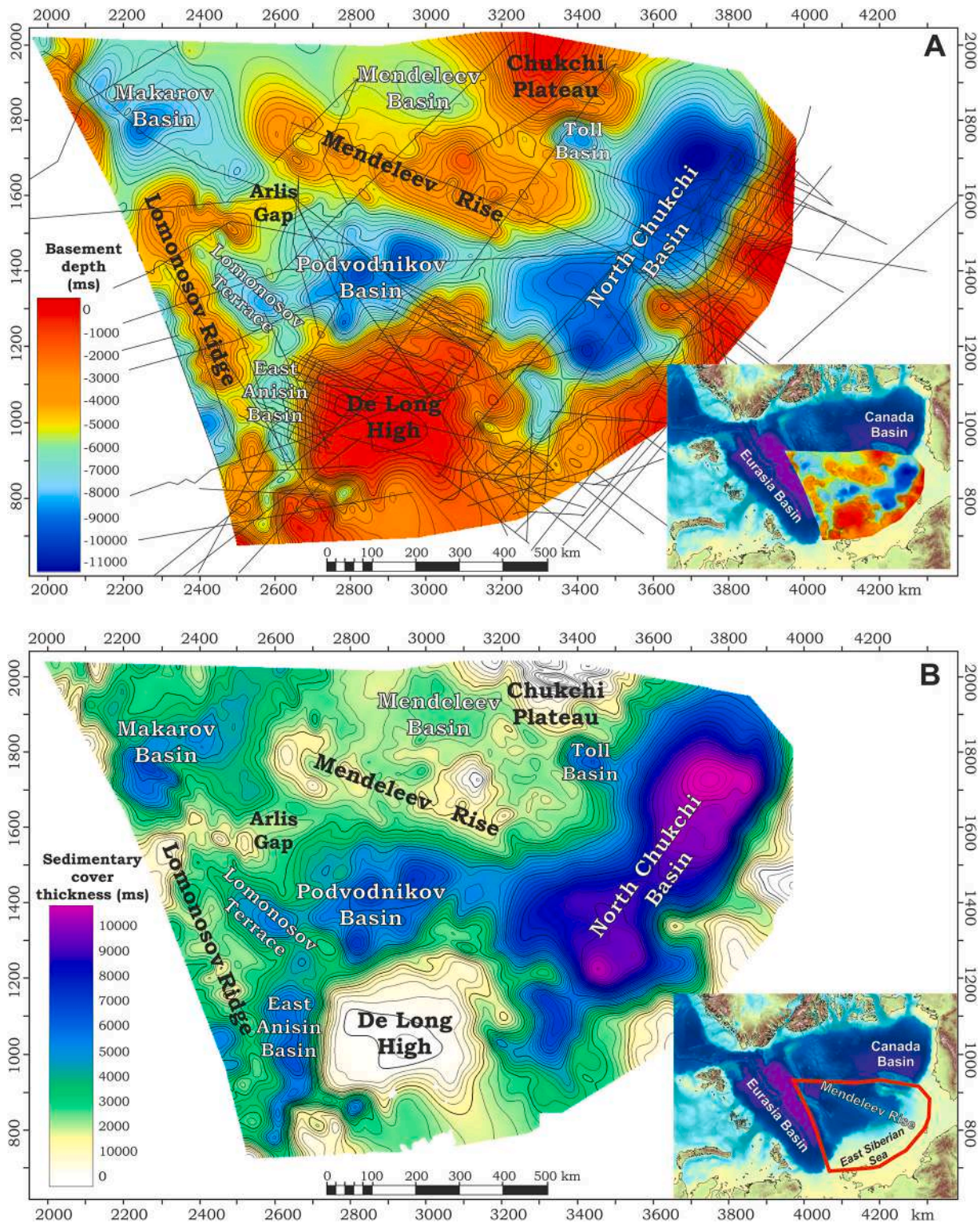


Fig. 3. A. Basement time depth map compiled using interpretation of 2D seismic lines (demonstrated as black solid lines). B. Sedimentary cover time thickness map (in msec) (for the southern margin of the North Chukchi Basin and to the south of the De Long High the maps were constructed using the base of Aptian sediments). The maps are for the Mendeleev Rise and North Chukchi Basin region (see map for location). The maps were compiled using Petrel software.

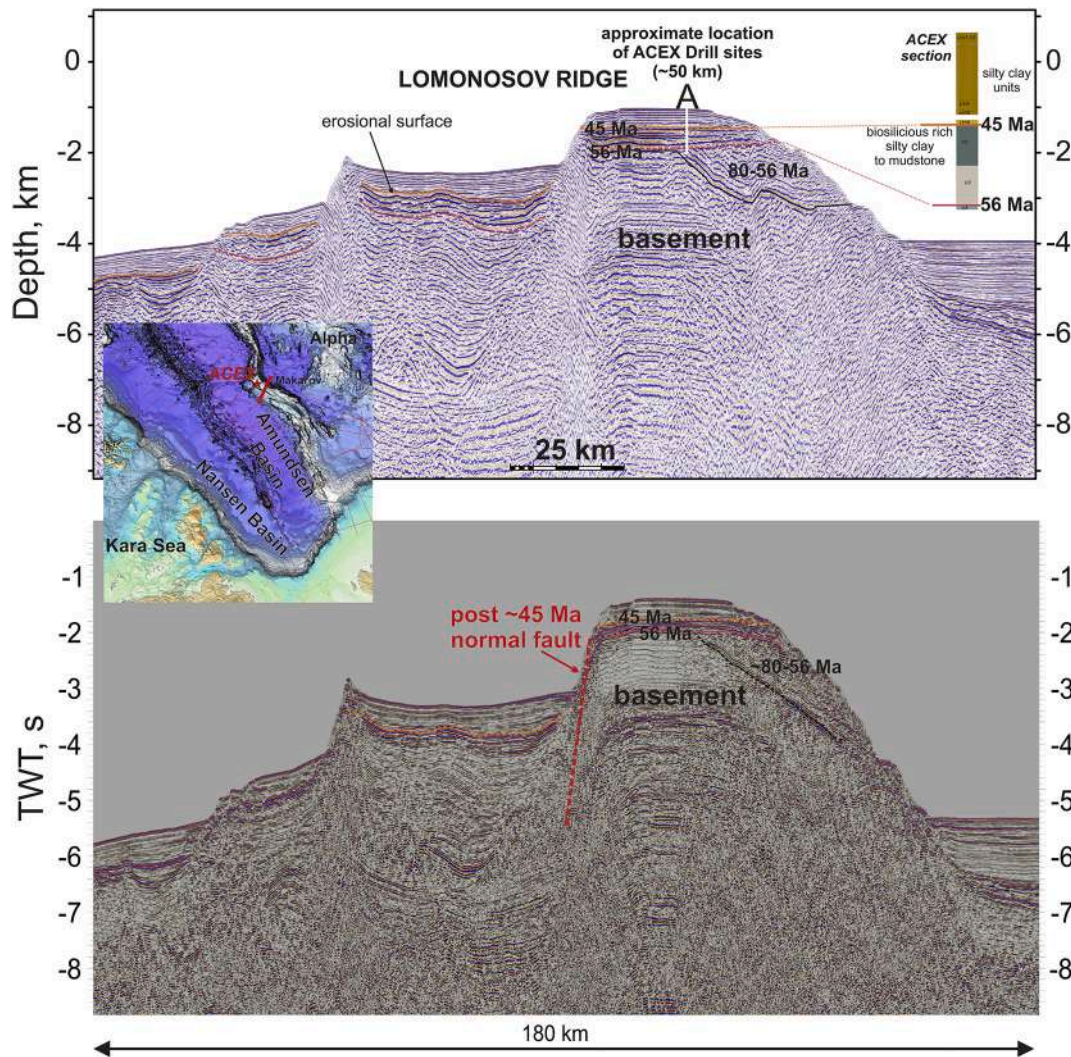


Fig. 4. Interpretation of a fragment of seismic profile ARC 14-07 for the Lomonosov Ridge area. The profile is located nearly 50 km from the ACEX drill sites. The profile is in time and depth scales. Depth-conversion methodology was discussed by Kashubin et al. (2018) and Nikishin et al. (2021a). Location of the profile is shown on the map. 56 Ma, 45 Ma are seismic horizons and their ages. Data for ACEX from Bruvoll et al. (2010).

The Chukchi Plateau is a zone of relatively shallow bathymetry associated with continental crust (Alvey et al., 2008; Kashubin et al., 2013; Gaina et al., 2014; Coakley et al., 2016; Ilhan and Coakley, 2018). Within the central part of the Chukchi Plateau, dredging revealed the presence of igneous rocks with an age of ca. 428 Ma, providing evidence of Early Paleozoic orogeny in this area of the plateau (Brumley et al., 2015). Consequently, it is likely that a crust of Early Paleozoic and older age exists there (Brumley et al., 2015).

The shelf seas of the Arctic Ocean display a broad range of geological structures. The Barents and Kara shelves and the shelf north of the Canadian Arctic Islands and Greenland are underlain by Paleozoic and Neoproterozoic basement. These shelves are characteristic of sedimentary basins with Paleozoic rifts (e.g., Nikishin et al., 2014; Pease et al., 2014). Jurassic and Cretaceous rifts are known for the area of the Sverdrup Basin (Harrison and Brent, 2005; Embry and Beauchamp, 2008; Hadlari et al., 2016).

The Alaskan Shelf is narrow with the Mesozoic and Cenozoic Brooks Orogen situated close to the shelf. On the Laptev, East Siberian and Chukchi shelves, numerous Cretaceous and Cenozoic rifts have been identified recently (Drachev et al., 2010, 2018; Franke, 2013; Nikishin et al., 2014, 2017, 2018, 2019; Ilhan and Coakley, 2018; Savin, 2020). These rifts extend to the continental margin of the deep-water Arctic

Basin, suggesting that the rifts and basins were formed within a single geodynamic environment. This issue is a prime focus in the present study, with an emphasis on the part of the Arctic Basin adjacent to Russia's territory.

3. Data and methods

In this paper, we will use data collected primarily by the Arktika-2011, Arktika-2012, and Arktika-2014 Projects. Characteristics of the seismic and other data are presented in Paper-1 (Nikishin et al., 2021a). In the present paper we use mainly 2D seismic data. We incorporated results of seismic sonobuoys published in some technical reports and papers (e.g., Poselov et al., 2012, 2019; Petrov, 2017; Butsenko et al., 2019), however we will not further discuss these data here as they will be fully reported in a separate paper.

For the Russian and American shelves, we utilized seismic lines acquired by the companies MAGE (Murmansk, Russia), DMNG (Yuzhno-Sakhalinsk, Russia), SMNG (Murmansk, Russia), ION-GXT (USA), and others. In addition, for the Russian part of the shelf we utilized all seismic lines available to the Ministry of Natural Resources and Environment of the Russian Federation. These data together formed the basis for the seismic stratigraphic framework presented here.

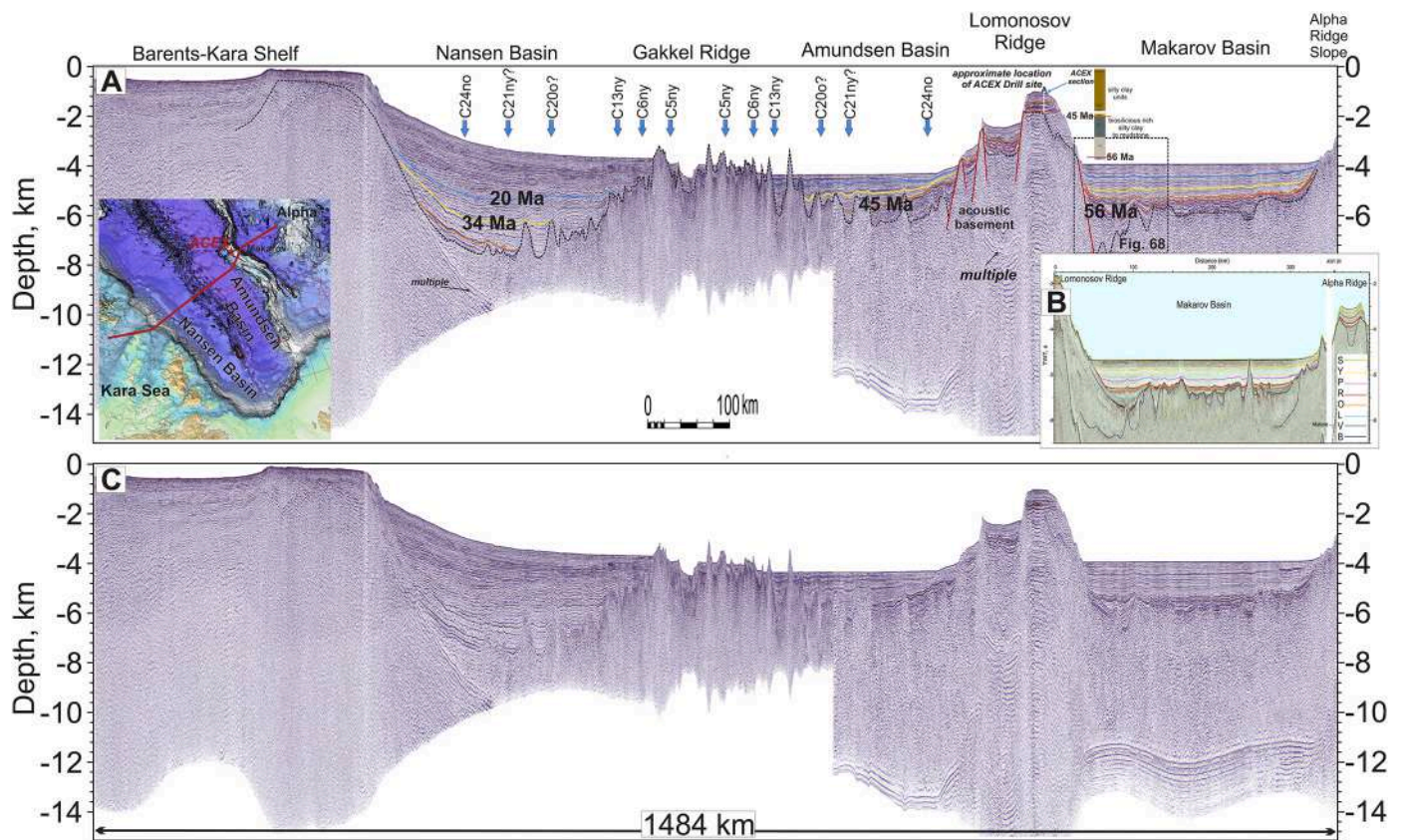


Fig. 5. A. Interpretation of regional seismic profile ARC 14-07. Location of the profile is shown on the map. 56 Ma, 45 Ma, 34 Ma, and 20 Ma are seismic horizons and their ages. Position of linear magnetic anomalies (C5ny and others) modified after Gaina et al. (2011). Data for ACEX from Bruvold et al. (2010). B. Seismic profile and its interpretation for the Makarov Basin from Evangelatos and Mosher (2016). This line is nearly parallel to our line. C. Seismic profile without interpretation. See also supplementary data, Fig. 5 (seismic profile without interpretation at high resolution). Depth-conversion methodology was discussed by Kashubin et al. (2018) and Nikishin et al. (2021a).

We used published and unpublished basement depth maps and structural maps for all Russian shelf basins based on all available data from the Ministry of Natural Resources and Environment of the Russian Federation as well as industry organizations. An example of our data is illustrated in Fig. 3.

4. Observations and interpretations of the stratigraphy of the Arctic Ocean area

The following data formed the basis for establishing the chronostratigraphic framework of the Arctic Ocean: (1) drilling data from the Lomonosov Ridge acquired within the ACEX Project (Moran et al., 2006; Backman et al., 2008), (2) age data of linear magnetic anomalies of the Eurasia Basin (Glebovsky et al., 2006; Gaina et al., 2011), (3) age data of the sedimentary cover of the Chukchi Sea Shelf based on well ties (Kumar et al., 2011; Hegewald and Jokat, 2013; Houseknecht and Wartes, 2013; Nikishin et al., 2014, 2017, 2019; Aleksandrova, 2016; Craddock and Houseknecht, 2016; Houseknecht et al., 2016; Ilhan and Coakley, 2018; Popova et al., 2018; Homza and Bergman, 2019; Houseknecht, 2019b; Houseknecht, 2019a; Skaryatin et al., 2020), (4) data on formation history of Mesozoic orogens on islands in the East Siberian and Chukchi Seas, (5) data on ages of De Long and Alpha-Mendeleev Rise basalts, which are a part of the Alpha-Mendeleev LIP or HALIP (Drachev and Saunders, 2006; Grantz et al., 2011; Morozov et al., 2013; Brumley, 2014; Coakley et al., 2016; Mukasa et al., 2020), (6) data on climate stratigraphy (Backman and Moran, 2009; Stein et al., 2015), and (7) other miscellaneous data.

4.1. Drilling data from the Lomonosov Ridge – the ACEX Project

Wells from the ACEX Project across the Lomonosov Ridge have been tied with seismic lines, which together formed the basis for the stratigraphic interpretation of that area (Jokat, 2005; Moran et al., 2006; Backman et al., 2008; Backman and Moran, 2009; Langinen et al., 2009; Bruvold et al., 2010; Poselov et al., 2012; Rekant and Gusev, 2012; Jokat et al., 2013; Weigelt et al., 2020). Two principal stratigraphic units with minimal structural dip are identified within the sedimentary cover: Miocene-Quaternary deposits (18.2-0 Ma) are separated from underlying Eocene deposits with an age of over 44.4 Ma, by an erosional surface. Within the Eocene deposits, a significant lithological boundary at 45.4 Ma lies between two stratigraphic units, U1/6 and U/2 (Backman et al., 2008; Bruvold et al., 2012). Below this boundary, mud-bearing bi-siliceous ooze is present, whereas above the boundary clays are dominant. This boundary corresponds to a climate transition from “green house” to “ice house” (Backman et al., 2008; Moran et al., 2006). In general, transparent seismic facies are observed above this boundary, whereas below this boundary a package with bright reflections is observed (Backman et al., 2008; Bruvold et al., 2010; Weigelt et al., 2014). According to ACEX Project drilling data, this boundary is characterized by a sharp change in rock density (Jakobsson et al., 2007). This surface corresponds precisely to the boundary which we date it as 45 Ma (Nikishin et al., 2014, 2017, 2018) and represents a regional stratigraphic boundary that is associated with a major change in the character of sedimentation and paleoclimate. In previous studies (Bruvold et al., 2010; Weigelt et al., 2014), this seismic boundary was tied to an erosional hiatus and was dated as a much younger intra-Early Miocene

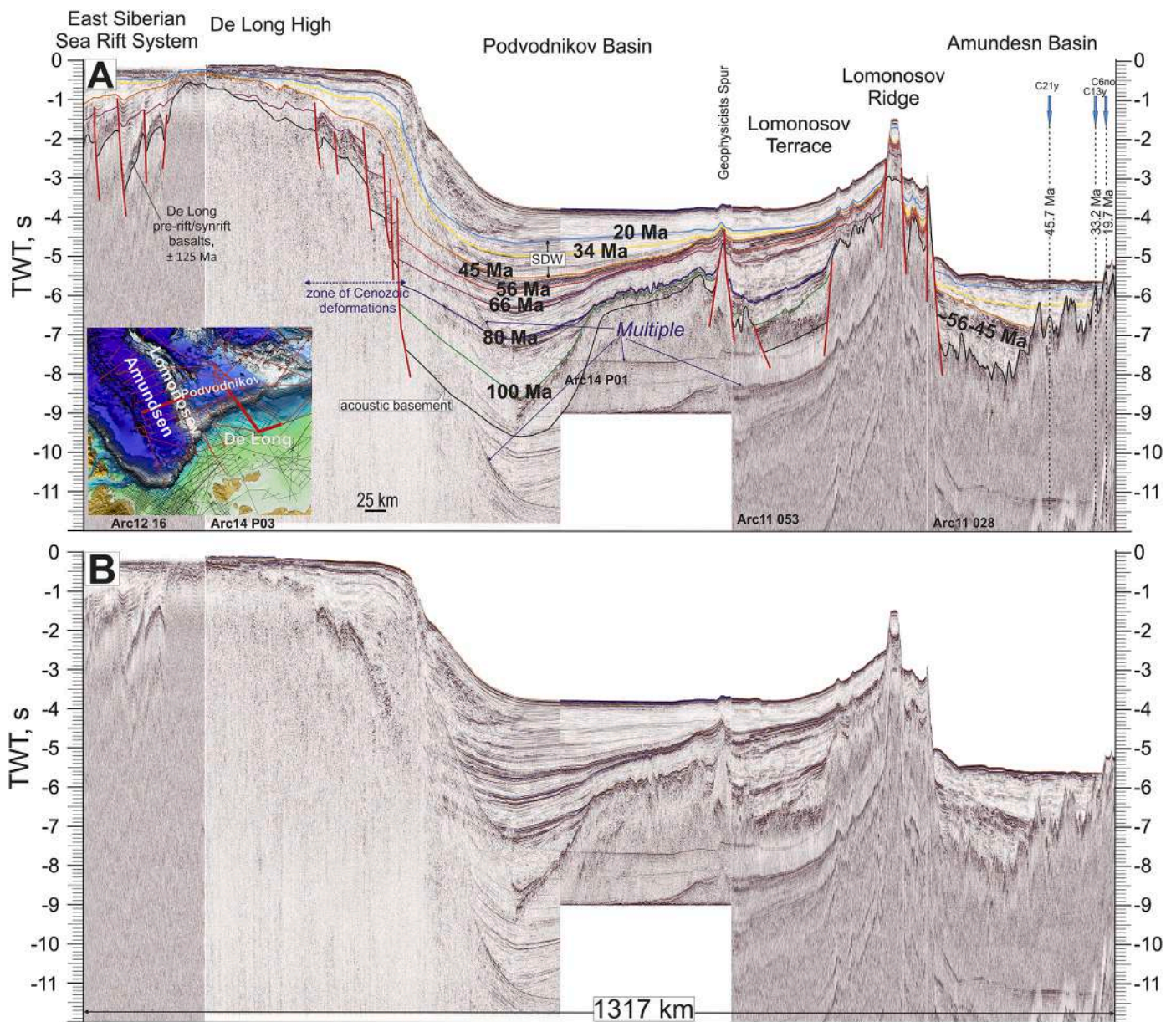


Fig. 6. A. Interpretation of composite seismic profile (lines ARC 12-06, ARC 14-03, ARC 11-53, and ARC 11-28) for the region from the East Siberian Shelf to Amundsen Basin and Gakkel Ridge. Location of the profile is shown on the map. Magnetic anomalies and their ages are after Gaina et al. (2011). Different color lines are seismic horizons and their ages. SDW – syntectonic depositional wedge. B. Seismic profile without interpretation. See also supplementary data, Fig. 6 (seismic profile without interpretation at high resolution).

surface.

Below the Eocene deposits, sediments in tilted fault blocks are observed, and are probably of Cretaceous age (the presence of Campanian deposits has been documented in previous studies) (Backman et al., 2008; Bruvoll et al., 2010). The Pre-Eocene unconformity may correspond to the onset of oceanic crust spreading in the Eurasia Basin (a breakup unconformity caused by the onset of oceanic crust spreading) (Backman et al., 2008; Bruvoll et al., 2010; Rekant and Gusev, 2012; Weigelt et al., 2014, 2020; Nikishin et al., 2014). We date this boundary on seismic lines as 56 Ma (Nikishin et al., 2018; Nikishin et al., 2017; Nikishin et al., 2014). The Russian seismic line Arktika 14-07 is located close the ACEX wells (Fig. 4), which allows correlation between borehole and seismic data and consequent inclusion of borehole data in the regional interpretation of the seismic data.

4.2. Magnetostratigraphy of the Eurasia Basin

The stratigraphy of the Eurasia Basin’s sedimentary cover is based on the correlation of linear magnetic anomalies with the age of the basement. Knowing the age of the basement, one can approximate the maximum age of the overlying sediments (Chernykh and Krylov, 2011; Rekant and Gusev, 2012). The linear magnetic anomalies are well known for the Eurasia Basin (Gaina et al., 2011; Glebovsky et al., 2006). We utilized these anomalies, each having its definite age, coupled with new seismic lines acquired in through the Arktika-2011 and Arktika-2014 Projects, as the basis for the chronostratigraphic framework. The least ambiguous pattern was observed on line ARC-028 (Nikishin et al., 2014, 2017, 2018). More regionally, analyses were carried out for the seismic line Arktika-2014-07, which crosses the entire Eurasia Basin (Fig. 5). The position of magnetic anomalies 21ny (45.7 Ma), 13ny

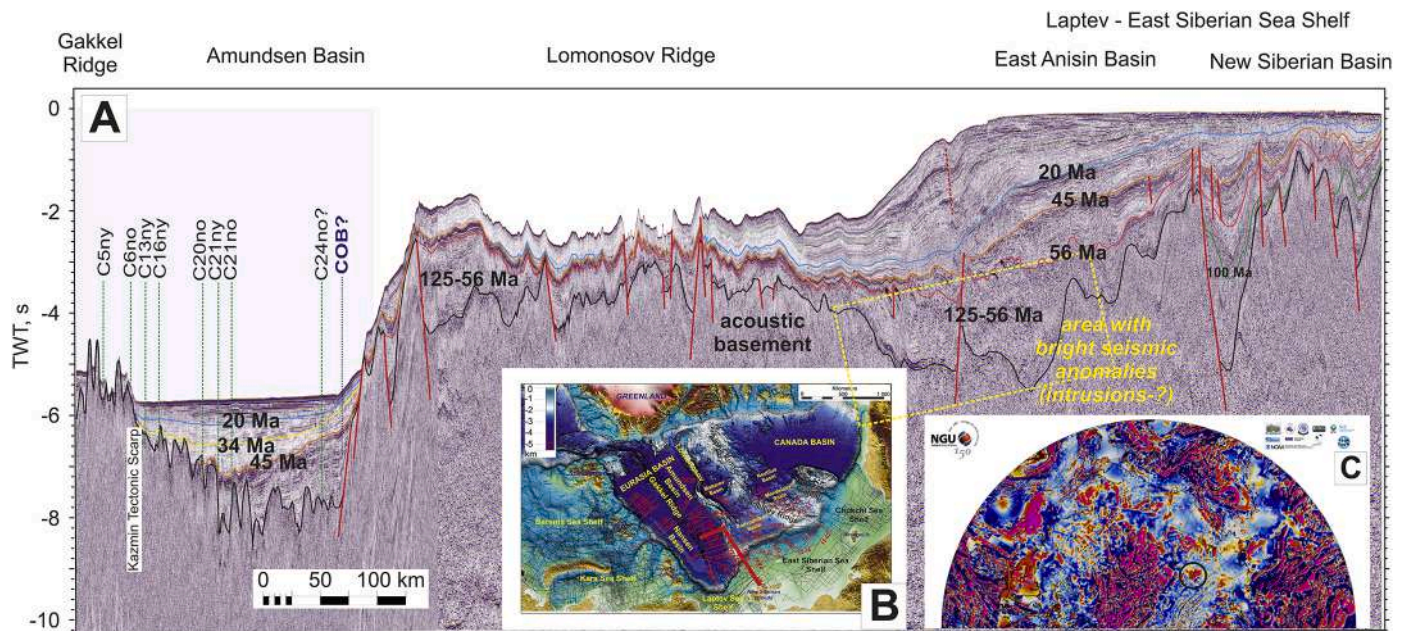


Fig. 7. A. Interpretation of composite seismic profile (lines ARC 11-A7 and ARC 11-29) for the region from the Laptev-East Siberian Sea Shelf and Lomonosov Ridge to Gakkel Ridge. Location of the profile is shown on the map (B). Magnetic anomalies and their ages are after Gaina et al. (2011). Different color lines are seismic horizons and their ages (Ma). C. Fragment of Arctic magnetic anomaly map (Gaina et al., 2011). Black circle shows a bright magnetic anomaly, which corresponds to a possible area with intrusions observed on the seismic profile. See also supplementary data, Fig. 7 (seismic profile without interpretation at high resolution).

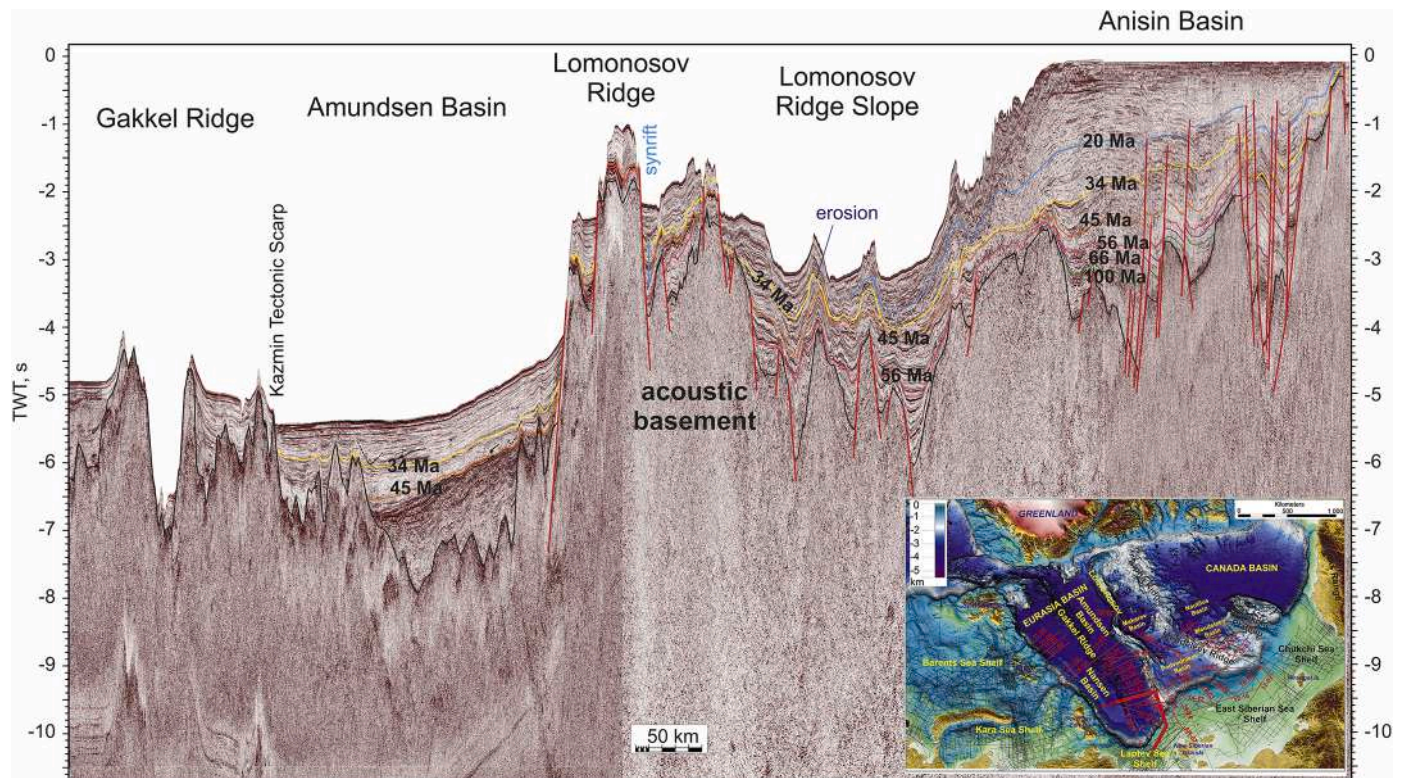


Fig. 8. Interpretation of composite seismic profile (lines ION11-4600, ARC 14-23, and ARC 14-05) for the region from the Laptev Sea Shelf and Lomonosov Ridge to Gakkel Ridge. Location of the profile is shown on the map. Different color lines are seismic horizons and corresponding ages (Ma). Kazmin Tectonic Scarp after Nikishin et al. (2018). See also supplementary data, Fig. 8 (seismic profile without interpretation at high resolution).

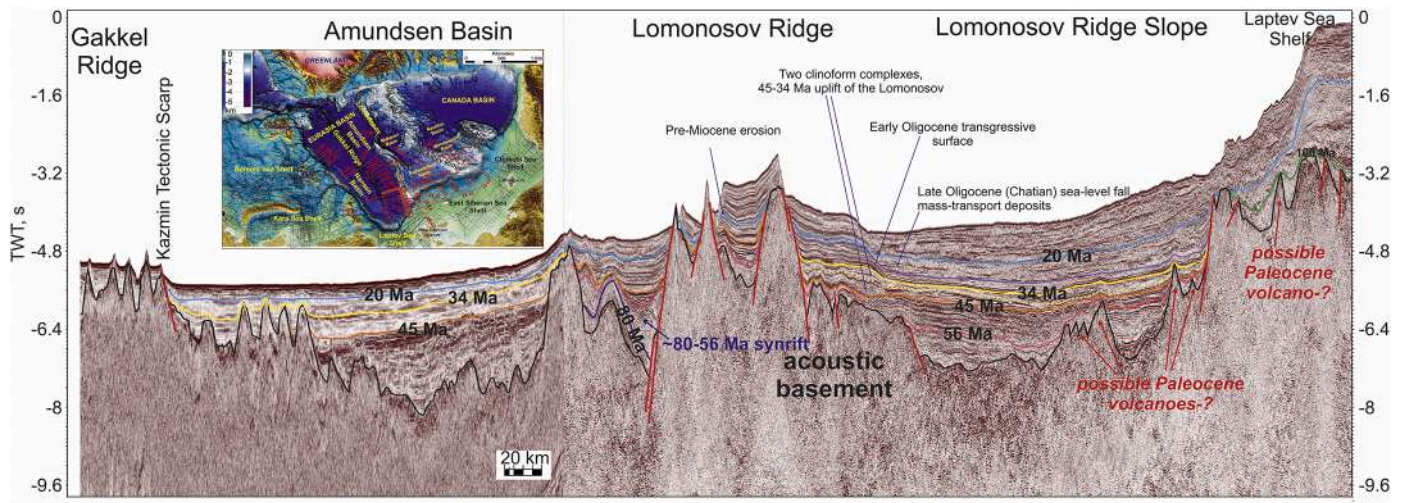


Fig. 9. Interpretation of composite seismic profile (lines ARC 14-22 and ARC 11-27) for the region from the Laptev Sea Shelf and along Lomonosov Ridge slope to Gakkel Ridge. Location of the profile is shown on the map. Different color lines are seismic horizons and corresponding ages (Ma). See also supplementary data, Fig. 9 (seismic profile without interpretation at high resolution).

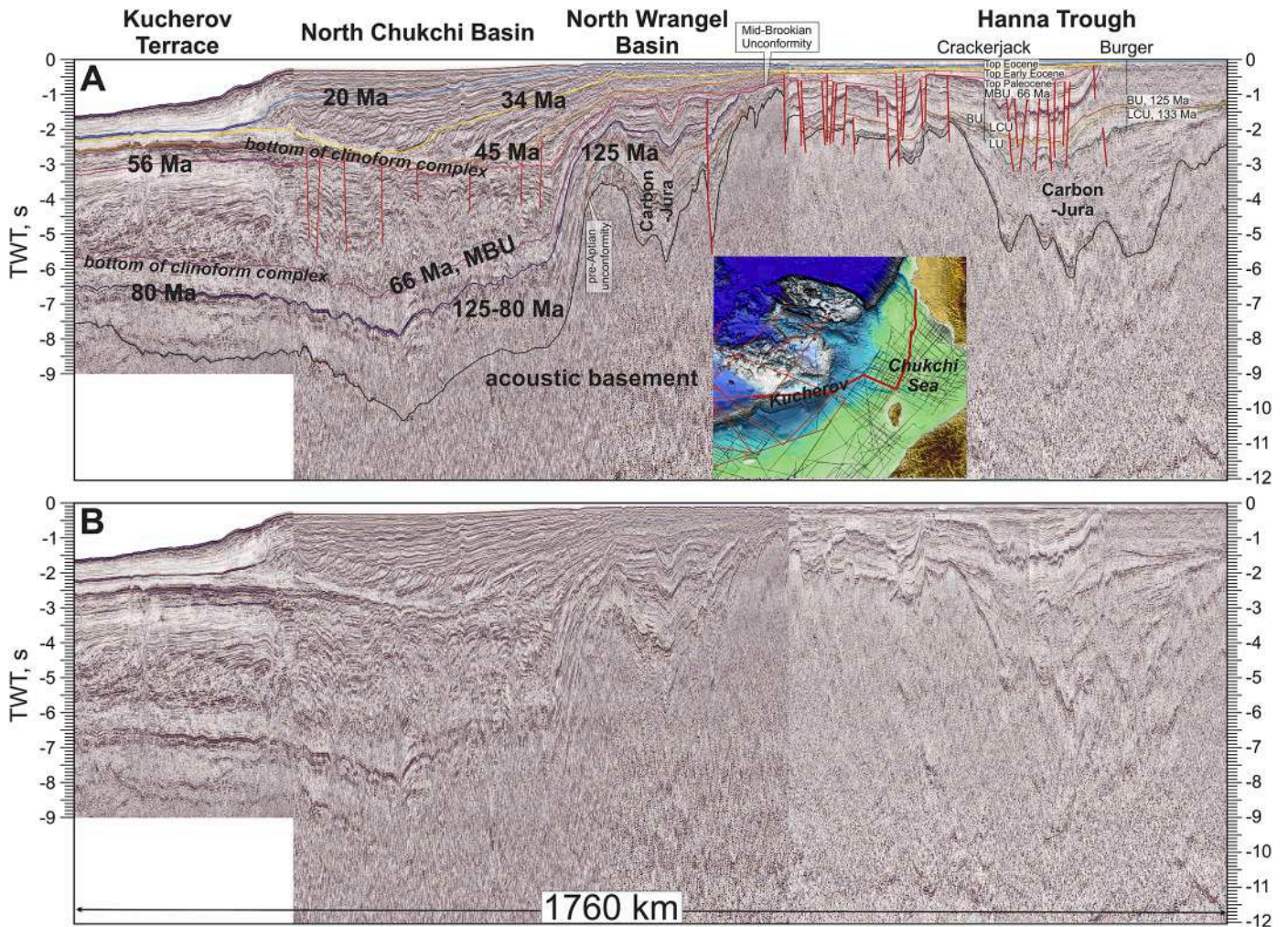


Fig. 10. A. Interpretation of composite seismic profile for the Chukchi Sea (fragments of lines ARC 14-01, ION 11-1400, ION 11-4200, ION 15-2000, CS1-11200, CS1-16100). Location of the profile is shown on the map. Location of boreholes is shown on the map and seismic profile in Fig. 11. Data are from Sherwood et al. (2002) and Kumar et al. (2011). Pre-Aptian (BU) and pre-Paleocene (MBU) unconformities can be traced from shelf areas toward the deep water Arctic Ocean. B. Seismic profile without interpretation. See also supplementary data, Fig. 10 (seismic profile without interpretation at high resolution).

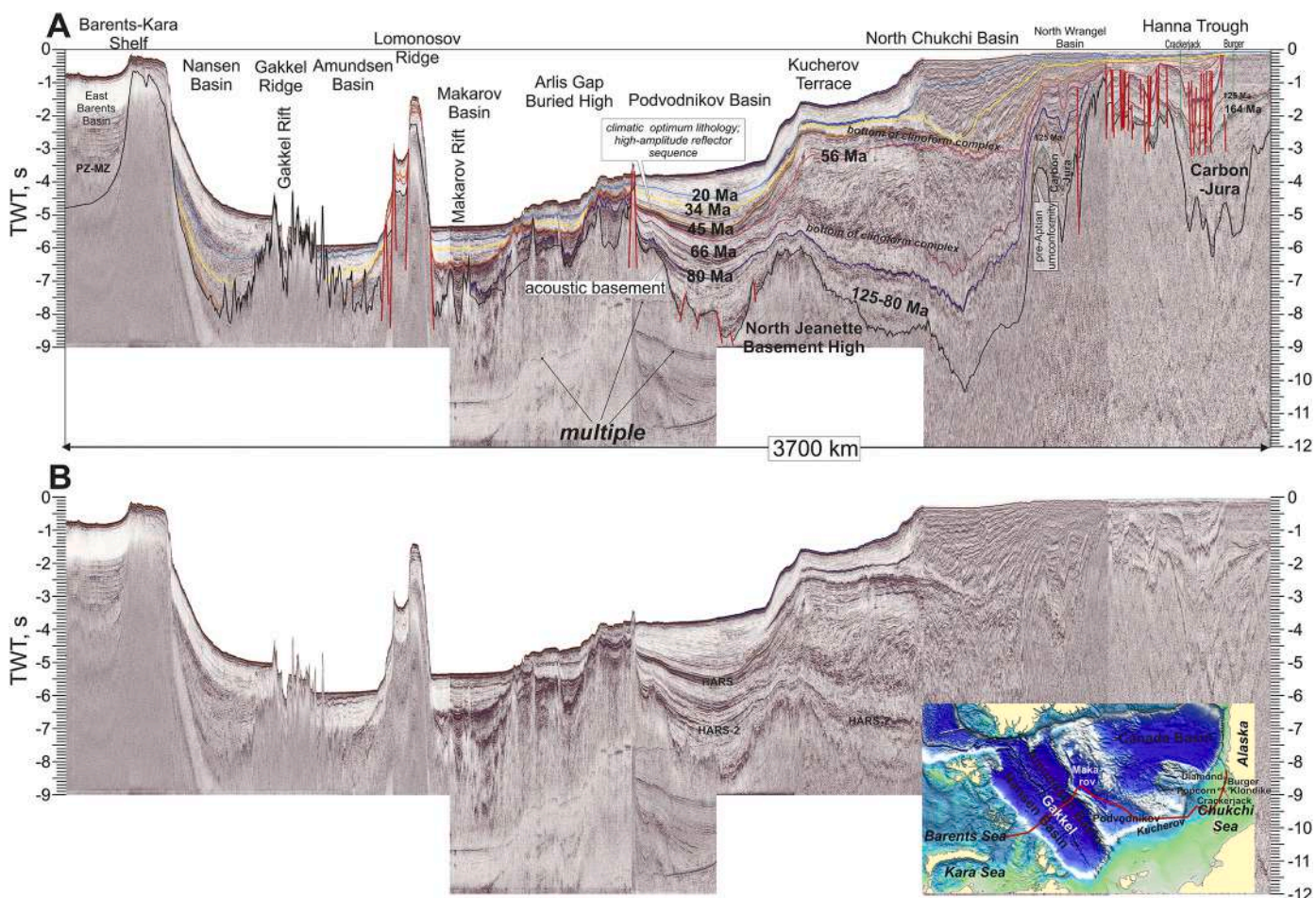


Fig. 11. A. Interpretation of composite seismic profile running from the Barents-Kara Seas shelf to Alaska Shelf (fragments of lines ARC 14-07, ARC 14-06, ARC 14-01, ION 11-1400, ION 11-1100, ION 11-1100, CS1-11200, CS1-16100). Location of the profile is shown on the map. The ages of seismic horizons were correlated with those of linear magnetic anomalies in the Eurasian Basin and data from Alaska Shelf boreholes. B. Seismic profile without interpretation. HARS - high-amplitude reflection sequence. See also supplementary data, Fig. 11 (seismic profile without interpretation at high resolution).

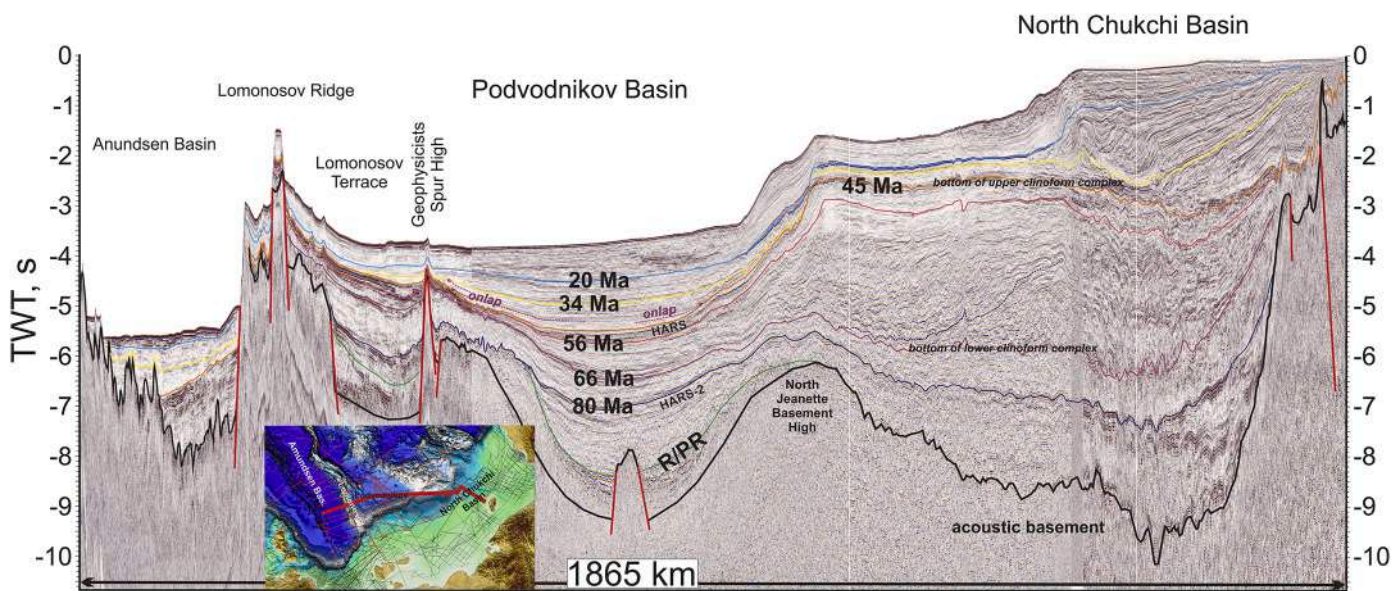


Fig. 12. Interpretation of composite seismic profile running from the Amundsen Basin to the North Chukchi Basin (fragments of lines ARC 11-28, ARC 14-01, ION 11-4300, and ION 11-1400). R/PR - rift/postrift boundary. Location of the profile is shown on the map. See also supplementary data, Fig. 12 (seismic profile without interpretation at high resolution).

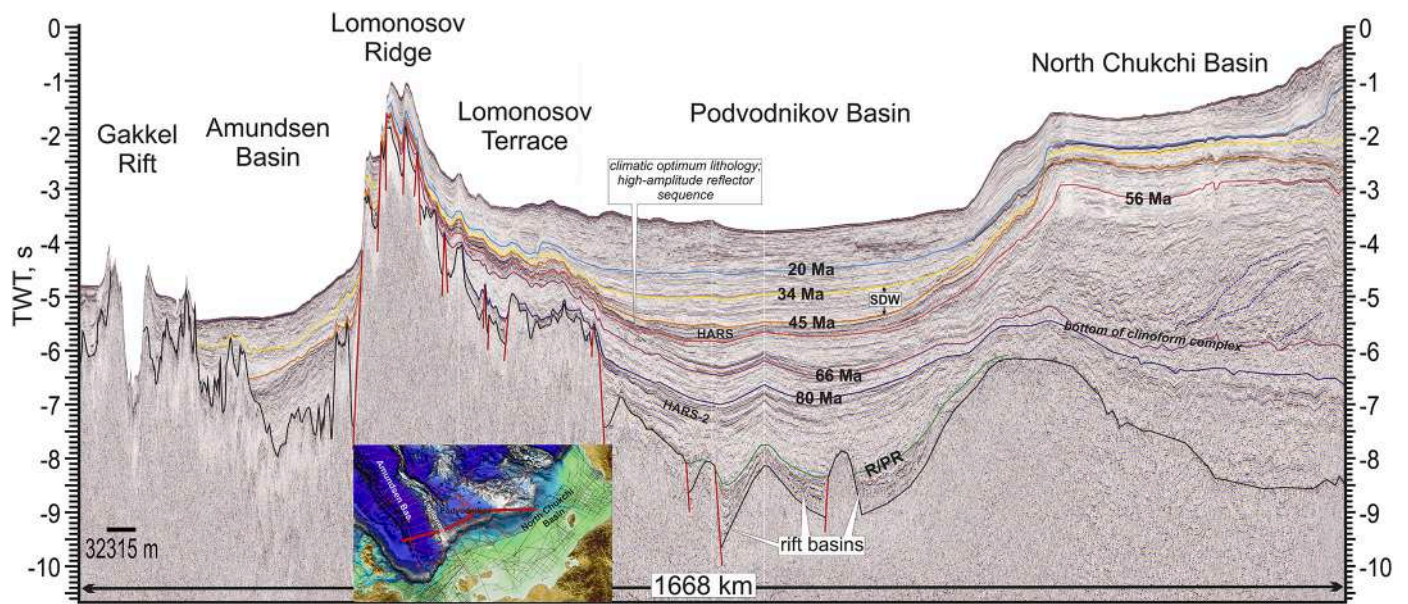


Fig. 13. Interpretation of composite seismic profile from the Gakkel Ridge to the North Chukchi Basin (fragments of lines ARC 14-05, ARC 14-13, ARC 14-03, and ARC 14-01). R/PR - rift/postrift boundary. Location of the profile is shown on the map. SDW – syntectonic depositional wedge. See also supplementary data, Fig. 13 (seismic profile without interpretation at high resolution).

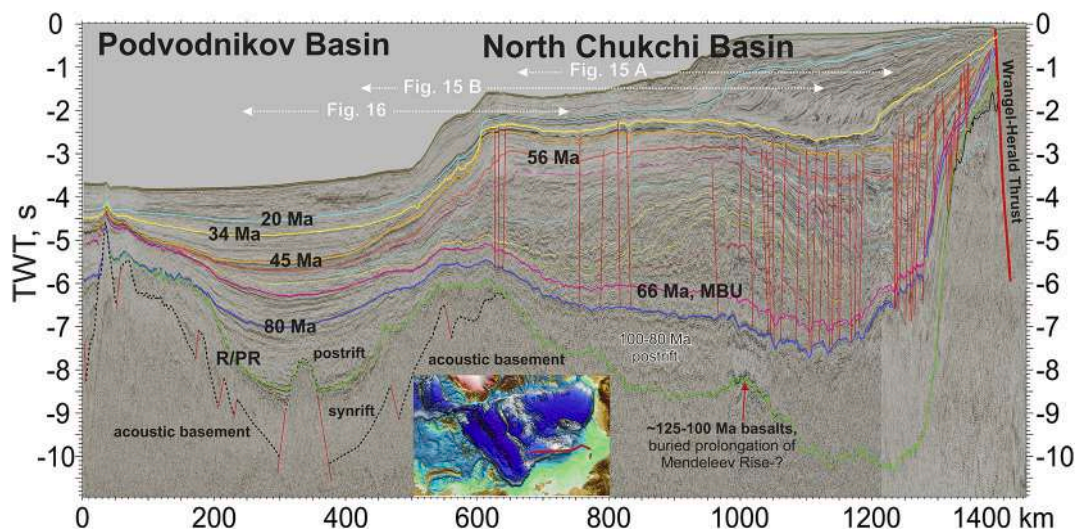


Fig. 14. Interpretation of composite seismic profile running from the Podvodnikov Basin to the North Chukchi Basin (fragments of lines ARC14_P01, ARS10F24, ION11_4200A). Location of the profile is shown on the map. See also supplementary data, Fig. 14 (seismic profile without interpretation at high resolution).

(33.16 Ma) and 6ny (19.7 Ma) is shown on the seismic profile. Sedimentary sequences with ages of 56-45.7 Ma, 45.7-33.16 Ma, 33.16-19.7 Ma and younger than 19.7 Ma, respectively, correspond to these magnetic anomalies ages.

The ages of magnetic anomalies do not coincide exactly with the ages of global sedimentary sequences (Gradstein et al., 2012). We also cannot exactly tie boundaries of seismically-identified sequences to ages of magnetic anomalies. Consequently, we assume that the boundary of sedimentary sequences with a magnetic age of 33.16 Ma likely correspond to the Eocene/Oligocene boundary (ca. 34 Ma). Similarly, the boundary with an age of 19.7 Ma may be close to the Oligocene/Miocene boundary (ca. 20 Ma) (Figs. 5, 6).

It should be noted that the 45.7 Ma boundary within the Eurasia Basin nearly coincides with the boundary of 45.4 Ma observed on the Lomonosov Ridge. The tops of the seismic sequences with these ages also

have similar attributes. Therefore, we interpret the 45 Ma boundary across the Eurasia Basin, in the Podvodnikov Basin, and on the Lomonosov Ridge with some confidence (Figs. 4, 5, 6). We also trace the 34 Ma boundary (approximately base of the Oligocene) across the Eurasia Basin and with high probability also into the Podvodnikov Basin (Figs. 5, 6). As sediments in the Eurasia Basin cannot be older than the basement, the oldest sediments, which correspond to the base of the sedimentary section and hence the age of basin formation, are 56 Ma (bottom of the Eocene). The base of these sediments correlates with the base of sediments on the Lomonosov Ridge (these sediments are present above an angular unconformity and the rift/postrift boundary).

In the Eurasia Basin and in the Podvodnikov Basin, the 45 Ma boundary separates the lower seismic facies characterized by high-amplitude reflections from the upper more transparent seismic facies. This is probably a regional lithological boundary (Figs. 5, 6). Note that

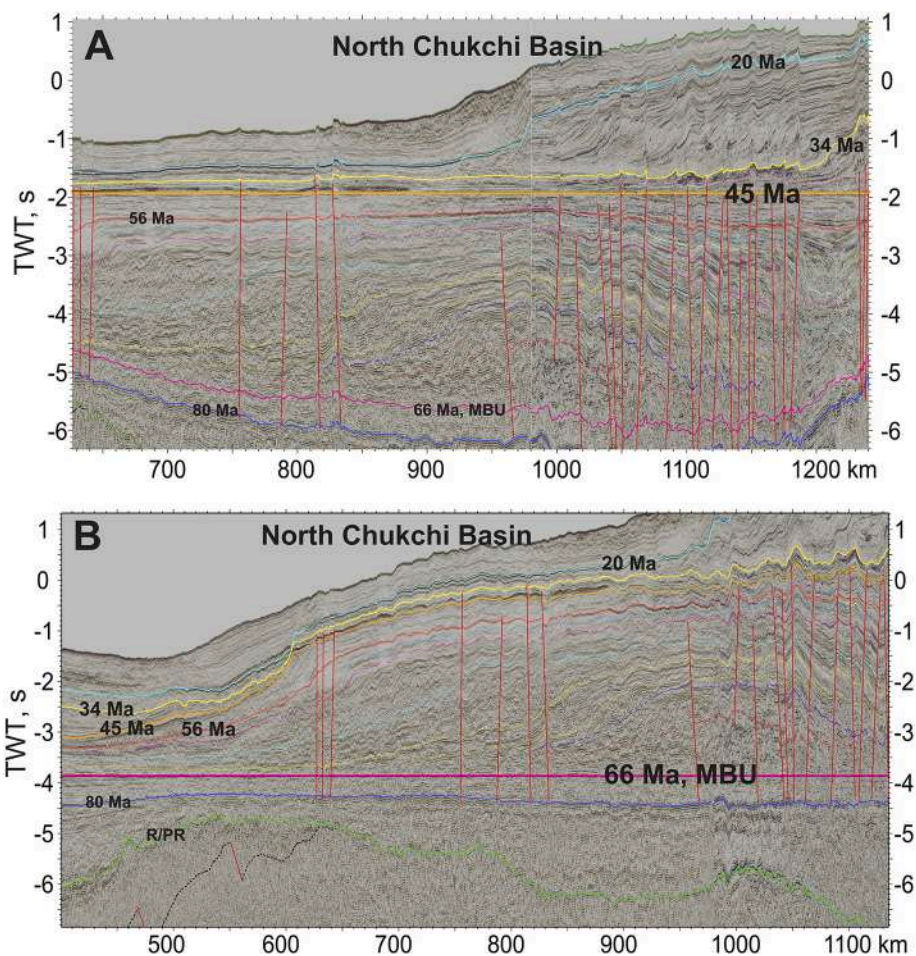


Fig. 15. Flattening on seismic horizons 45 Ma (A) and 66 Ma (B) for southern part of the seismic line shown in the Fig. 14. Large shelf clinoform complexes of the North Chukchi Basin with transition to deep-water deposits in the Podvodnikov Basin can be observed.

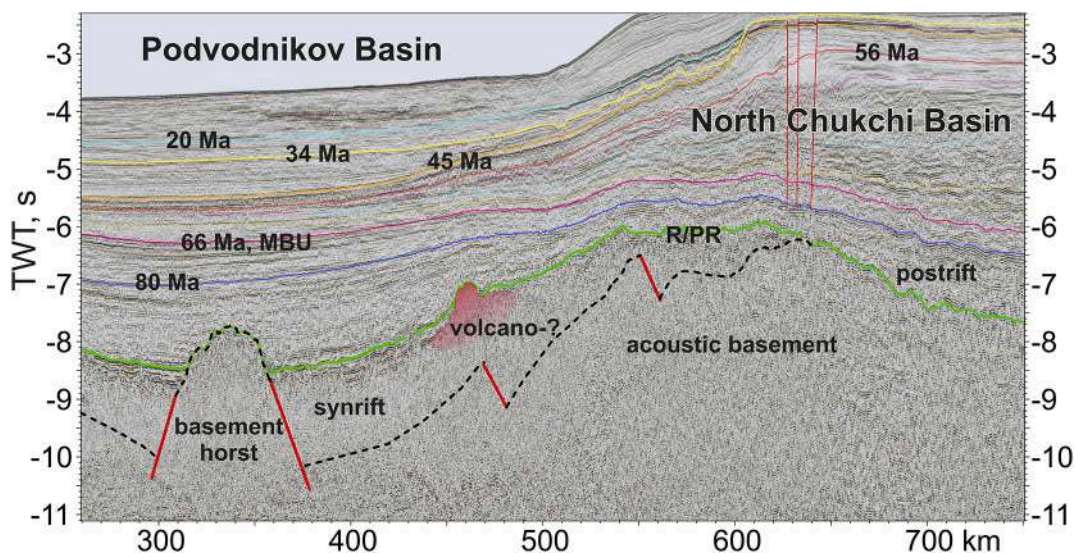


Fig. 16. Fragment of seismic profile presented on Fig. 14. Synrift and postrift complexes are observed in the Podvodnikov Basin. Rift/postrift (R/PR) boundary of the Podvodnikov Basin grades to a boundary between sedimentary cover and acoustic basement in the North Chukchi Basin. A volcano-like structure is observed on the top of synrift complex in the Podvodnikov Basin.

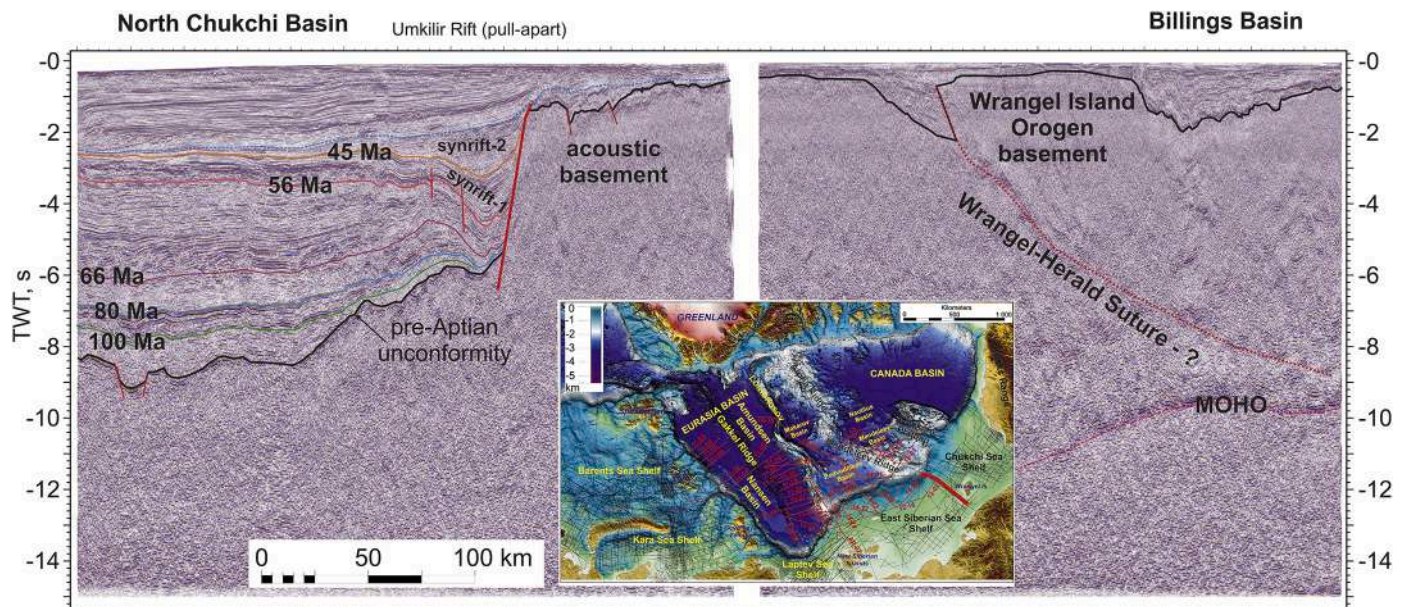


Fig. 17. Interpretation of regional seismic profile 5AR for the Chukchi Sea region. Location of the profile is shown on the map. Different color lines are seismic horizons and corresponding ages (Ma). See also supplementary data, Fig. 17 (seismic profile without interpretation at high resolution).

according to Moran et al. (2006) and Backman et al. (2008) ice-rafted sediments appear in Arctic deposits at ca. 44.8 Ma, as calibrated by the wells on the Lomonosov Ridge. Hence, a sharp climatic cooling likely started at approximately that time. Concurrently, this apparently was associated with a major change in the character of sedimentation. This boundary associated with linked lithological and climatic contrast has regional significance and can be mapped across the Arctic Ocean.

Examples of regional correlation of seismic stratigraphy between the Eurasia Basin, Lomonosov Ridge, and Laptev Sea Shelf are shown in Figs. 7, 8, 9. Our magnetostratigraphy of the Eurasia Basin (Nikishin et al., 2014, 2017, 2018) has been corroborated by new data presented by Weigelt et al. (2020). These authors recognize also seismic horizons 45 Ma, 34 Ma and 20 Ma in the Eurasia Basin.

4.3. Age data of the sedimentary cover of the Chukchi Sea Shelf

Several commercial wells (Popcorn, Crackerjack, Klondike, Burger, Diamond) have been drilled in the Arctic region in the American part of the Chukchi Sea (Sherwood et al., 2002; Kumar et al., 2011; Houseknecht and Wartes, 2013; Craddock and Houseknecht, 2016; Houseknecht et al., 2016; Ilhan and Coakley, 2018; Homza and Bergman, 2019). Based on data from these wells, a stratigraphic scheme has been developed for the Alaskan Shelf (Sherwood et al., 2002). We compiled composite seismic profiles linking the Russian seismic lines in the Arctic as well as some commercial seismic lines on the shelf and tied the stratigraphy to the Popcorn-1, Crackerjack-1, and Burger-1 wells. Figs. 10 and 11 show an example of this analysis. The Cretaceous/Paleogene boundary (the Mid-Brookian Unconformity, MBU) is traced rather robustly into the North Chukchi Basin and into the Amerasia Basin. On the Alaskan Shelf, this boundary commonly has an erosional character and an angular unconformity is observed (Sherwood et al., 2002; Kumar et al., 2011; Houseknecht et al., 2016; Ilhan and Coakley, 2018). In the North Chukchi Basin, the bottom of a thick clinoform sequence corresponds to this ca. 66 Ma boundary (Figs. 12–16). The Wrangel-Herald Ridge is located in the Russian part of the Chukchi Sea (e.g., Nikishin et al., 2015; Verzhbitsky et al., 2015; Verzhbitsky et al.,

2012) (Figs. 17, 18). Analysis of seismic and AFT data shows that a phase of thrust faulting in this uplift zone near the Cretaceous/Paleogene boundary with considerable uplift during the Maastrichtian-Paleocene occurred (Verzhbitsky et al., 2012, 2015; Nikishin et al., 2014). This event widely manifested itself in Alaska in the Brooks Orogen as well (O'Sullivan et al., 1997; Peters et al., 2011).

The most complete Cenozoic section, which includes Eocene deposits, is penetrated by the Popcorn-1 well (Sherwood et al., 2002; Ilhan and Coakley, 2018; Homza and Bergman, 2019; Houseknecht, 2019a, 2019b). The Eocene section is divided into three units: the Lower Eocene, the Middle Eocene and the Upper Eocene. The 45 Ma boundary can be traced into the North Chukchi Basin and into the deep-water part of the Arctic Ocean (Figs. 5–15), and in general can be traced all over the Arctic Ocean. In the North Chukchi Basin, this stratigraphic level corresponds to the bottom of a thick upper clinoform complex. The Paleocene/Eocene boundary (ca. 56 Ma) is also penetrated by the Popcorn-1 well and has been seismically mapped across the Arctic Ocean (Figs. 10–14). The Popcorn-1 well also penetrated Mesozoic deposits, though unequivocal seismic correlation of these deposits across the Arctic Ocean was not possible because of lack of definitive data. In general, at this stratigraphic level, seismic correlations with the wells on the Alaskan Shelf remain ambiguous.

Late Paleozoic to Jurassic sections were penetrated by several wells drilled in the American part of the Chukchi Sea and Alaska. (e.g., Homza and Bergman, 2019; Houseknecht, 2019a, 2019b; Sherwood et al., 2002). A Late Paleozoic to Jurassic stratigraphic framework was proposed for the southern part of the North Chukchi Basin using these borehole data (e.g., Drachev et al., 2010; Nikishin et al., 2014) (Fig. 10). Geoscientists from Rosneft Oil Company have carried out stratigraphic analyses of seismic data tied to American wells in the North Chukchi Basin (Fig. 19). They proposed the presence of a Carboniferous to Jurassic section below the Cretaceous section of the North Chukchi Basin. The key element proving the presence of a Paleozoic section is the presence of salt diapirs, as the salt can have only a Late Paleozoic age.

In the Russian part of the Chukchi Sea, one well, on the Ayon Island near the Chukchi Peninsula, is available (Aleksandrova, 2016). The well

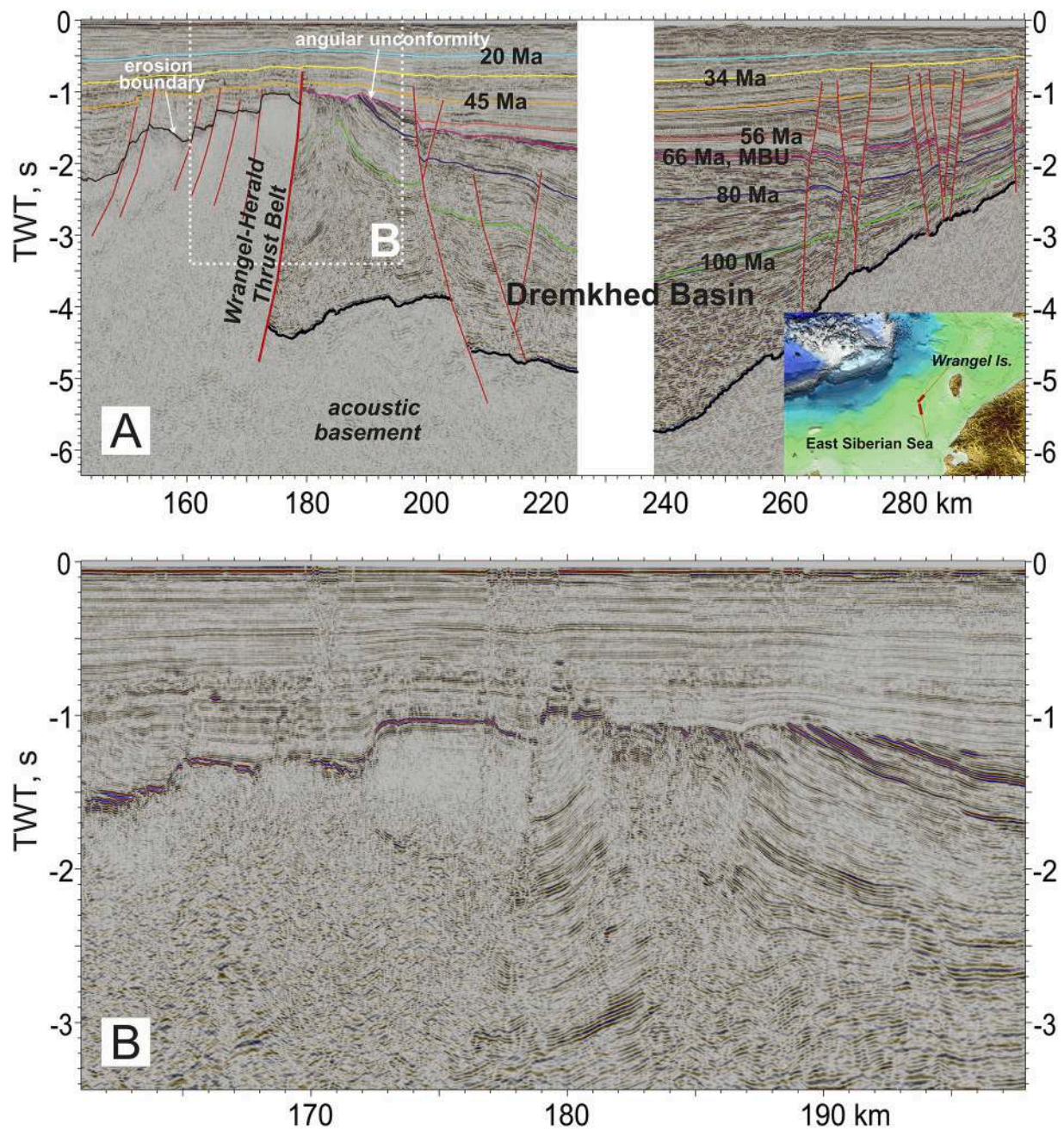


Fig. 18. A. Interpretation of composite seismic profile (DMNG_ES10Z05A, SC-90-20c). Location of the profile is shown on the map. Wrangel-Herald thrust belt is clearly observed. Thrusting started before 66 Ma. Orogenic collapse together with normal faulting took place before 45 Ma. B. Fragment of the seismic profile. Modified after Nikishin et al. (2019).

penetrated deposits from the Paleocene to the Quaternary (Supplementary Fig. 2) that are characterized by continental and shelf sediments. The principal hiatus is dated at 47-39 Ma, which generally coincides with the hiatus observed in the ACEX wells (44.4-18.2 Ma).

In Alaska two wells were drilled on the margin of the Hope Basin in the Chukchi Sea (Bird et al., 2017) and penetrate Neogene to Eocene deposits. Near the base of the well, Paleozoic carbonates are encountered. The Eocene sections contain volcanoclastic deposits and basalts. The basalts have isotopic ages of 42.3 ± 10 Ma and 40.7 ± 2 Ma. We use these data to calibrate the seismic stratigraphy of the Chukchi Sea.

4.4. Formation history of Mesozoic orogens on islands of the East Siberian and Chukchi Seas

An orogen of Mesozoic age is located in the Russian Far East in the area from the Verkhoyansk Range to the Chukchi Peninsula. The common name of this orogen is the Verkhoyansk-Chukotka Orogen (e.g., Puscharovsky, 1960) (Fig. 2). The main collisional event took place in the Early Cretaceous whereas the post-collision extension and intrusion of granites took place at ca. 118-100 Ma (Parfenov and Kuzmin, 2001; Sokolov et al., 2002; Miller et al., 2008, 2010, 2018a, 2018b);

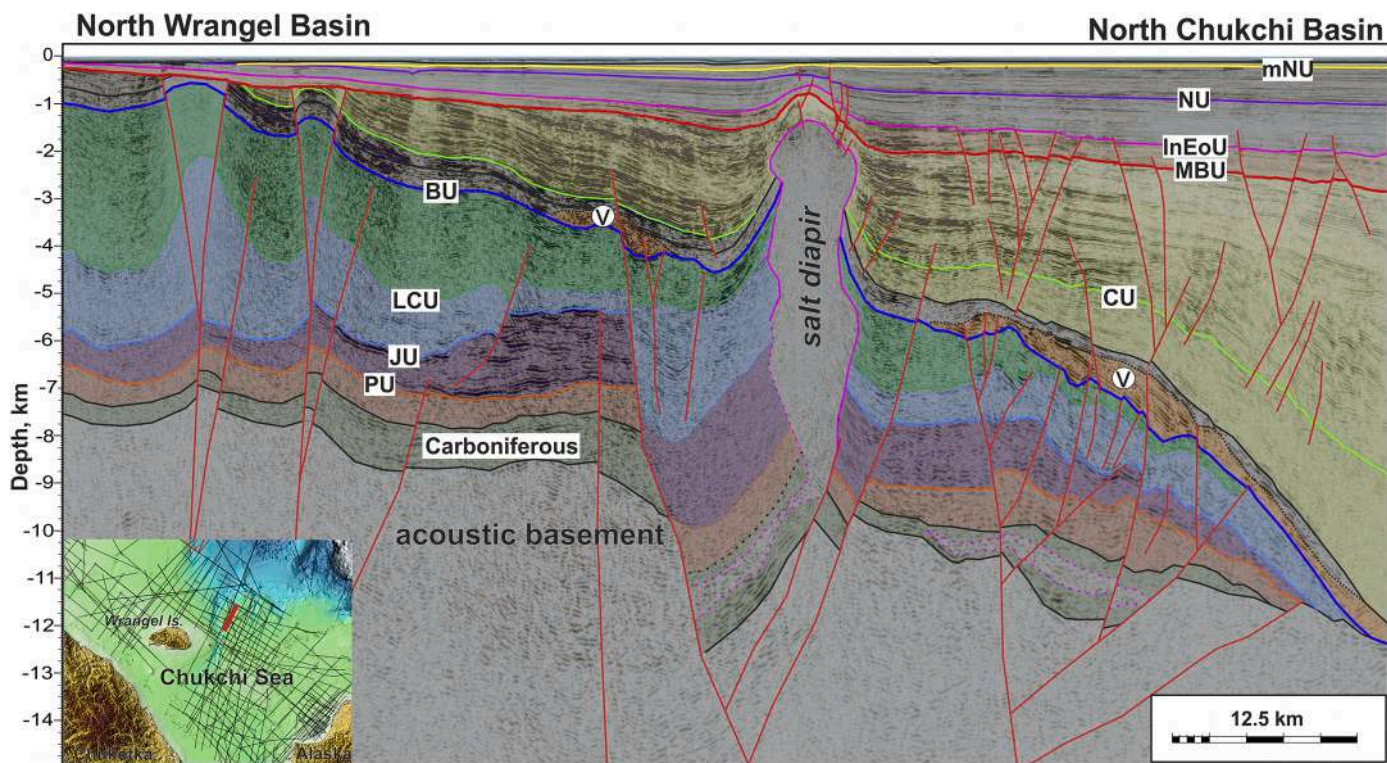


Fig. 19. Fragment of a seismic profile for the Chukchi Sea with geological interpretation. Location of the profile is shown on the map. Modified after Skaryatin et al. (2020). PU – Permian Unconformity, JU – Jurassic Unconformity, LCU – Lower Cretaceous Unconformity, BU – Brookian Unconformity, CU – Cenomanian Unconformity, MBU – Mid-Brookian Unconformity, InEoU – Intra-Eocene Unconformity, NU – Neogene Unconformity, mNU – Mid-Neogene Unconformity, v – unit with volcanics.

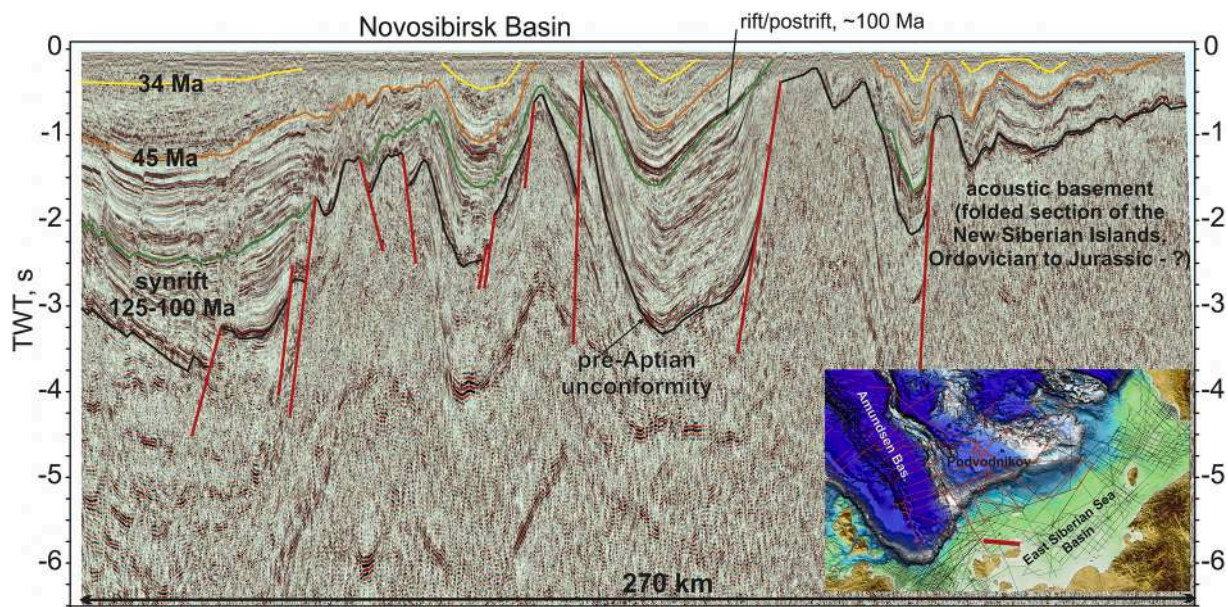


Fig. 20. Interpretation of seismic profile located to the north of the New Siberian Islands. Pre-Aptian or intra-Aptian angular unconformity is well documented for the New Siberian Islands (e.g. Kos'ko and Trufanov, 2002). Location of the profile is shown on the map. Data courtesy of the Ministry of Natural Resources, Russia.

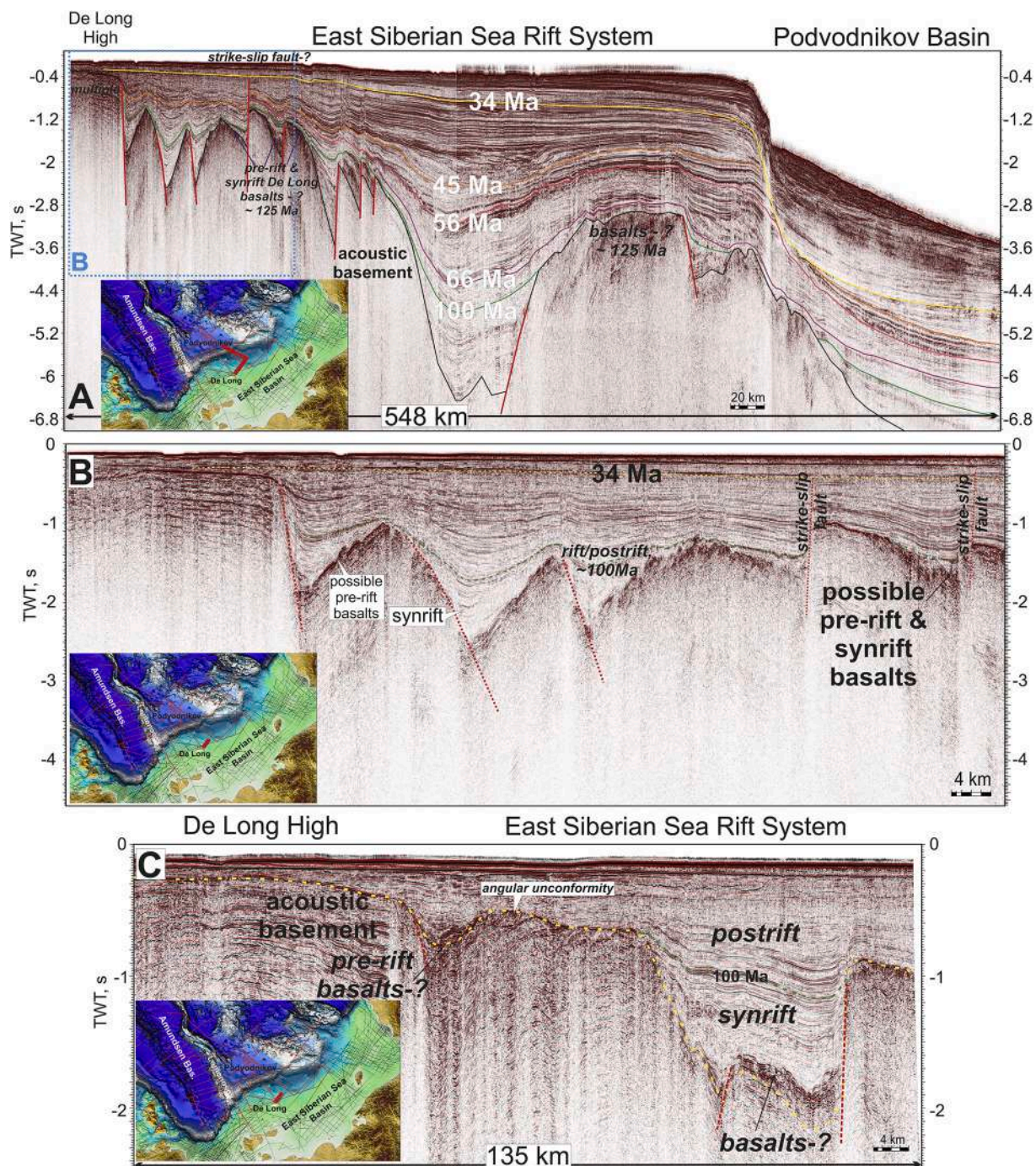


Fig. 21. Interpretation of seismic profiles for the East Siberian Sea Shelf (De Long High). A. Composite seismic profile from the East Siberian Sea Shelf (De Long High) to the Podvodnikov Basin (lines MAGE ESS1611 and MAGE ESS1601). B. Enlarged section of profile ESS1611. C. Seismic profile MAGE ESS1625. Location of the profiles is shown on the map. See also supplementary data, Fig. 21 (seismic profile without interpretation at high resolution).

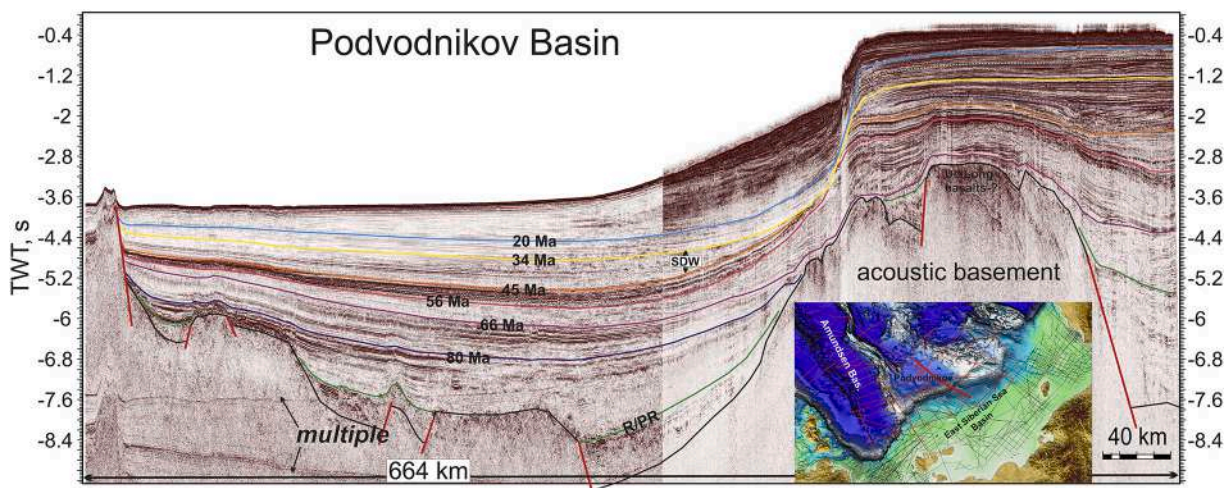


Fig. 22. Interpretation of composite seismic profile running from the East Siberian Sea Shelf to the Podvodnikov Basin (lines ARC 14-06 (fragment) and MAGE ESS1601). Location of the profile is shown on the map. R/PR – rift/postrift boundary. SDW – syntectonic depositional wedge. See also supplementary data, Fig. 22 (seismic profile without interpretation at high resolution).

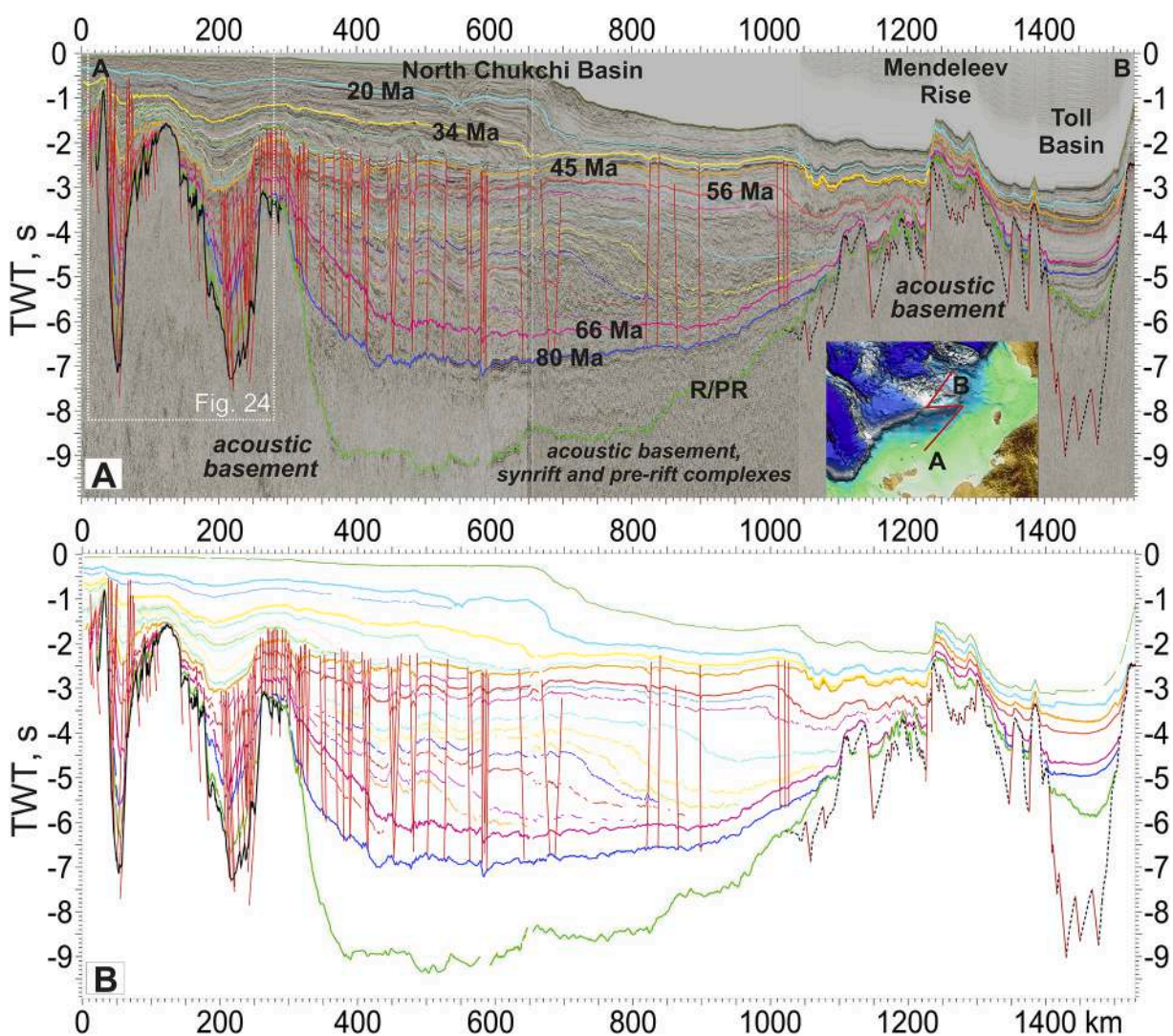


Fig. 23. A. Interpretation of composite seismic profile from the East Siberian Sea and Chukchi Sea Shelf to the Podvodnikov Basin, Mendeleev Rise and Toll Basin (lines ION12_1400, ION11_1400, 5AR, ARC14_P01, ARC12_03). Location of the profile is shown on the map. B. Interpretation without seismic imaging. See also supplementary data, Fig. 23 (seismic profile without interpretation at high resolution).

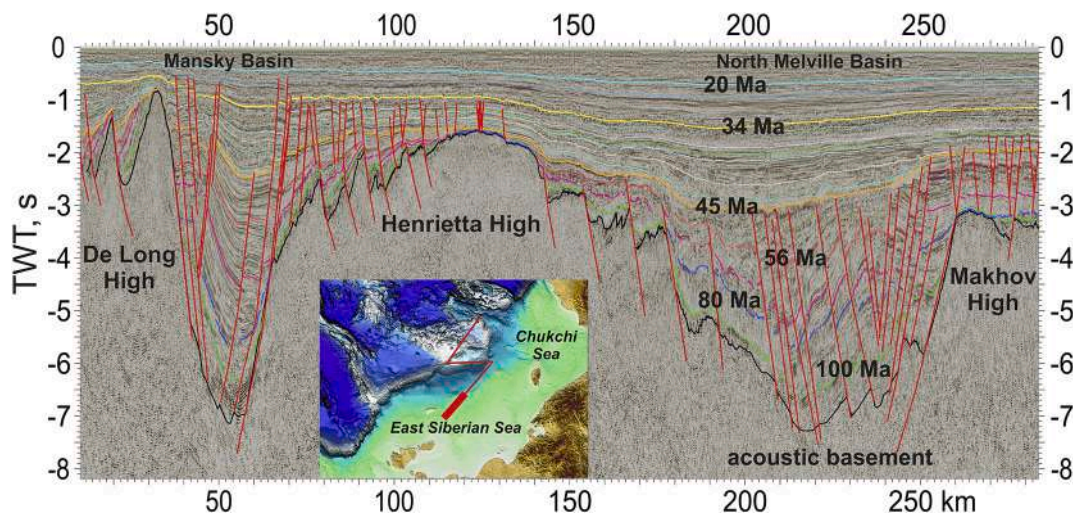


Fig. 24. Interpretation of a fragment of the composite seismic profile for the East Siberian Sea which is illustrated in Fig. 23 (white quadrangle) (line ION12_1400). A large continental rift system can be observed with a number of rift phases between 125 and 45 Ma and later. The correct timing of rifting is difficult to evaluate.

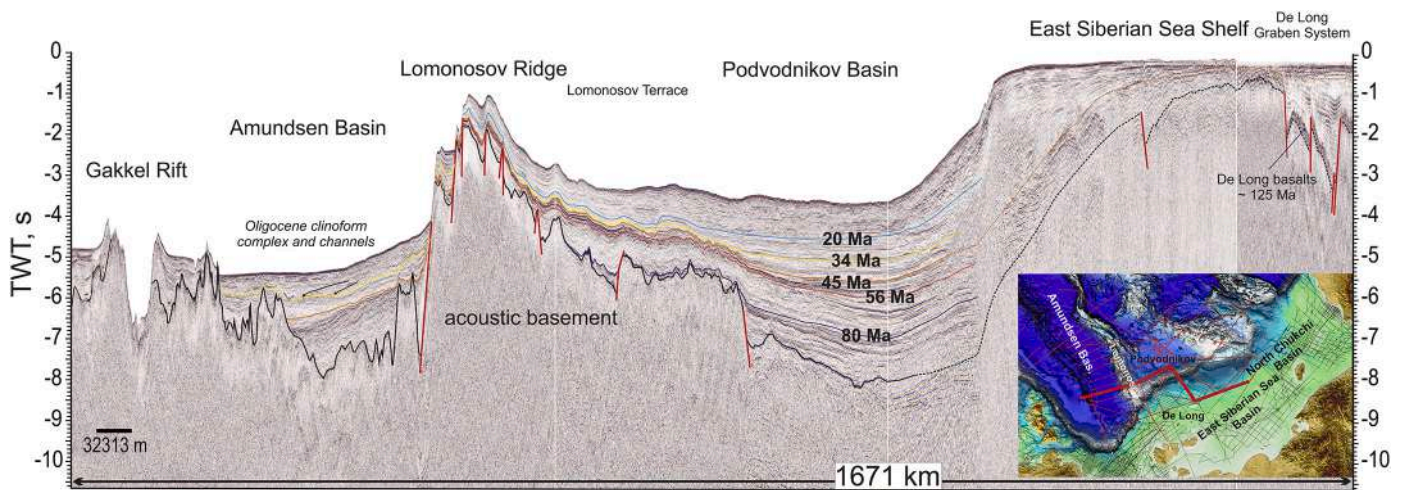


Fig. 25. Interpretation of composite seismic profile from the East Siberian Sea Shelf to the Gakkel Ridge (lines ARC 14-05, ARC 14-13, ARC 14-03, and ARC 12-16). Location of the profile is shown on the map. See also supplementary data, Fig. 25 (seismic profile without interpretation at high resolution).

Kuzmichev, 2009; Amato et al., 2015; Drachev, 2016; Toro et al., 2016; Petrov, 2017).

Mesozoic folding widely occurs on the New Siberian Islands and on the Wrangel Island in the Chukchi Sea. On the New Siberian Islands, the collisional orogeny ended before the Mid Aptian. Upper Aptian deposits unconformably overlie the Paleozoic-Lower Jurassic folded complex with the surface marked by angular discordance (Kos'ko and Trufanov, 2002; Kuzmichev et al., 2009, 2013; Kos'ko et al., 2013). This angular unconformity is well expressed on seismic profiles located in the area of the New Siberian Islands (Drachev et al., 2018; Nikishin et al., 2018; Nikishin et al., 2017; Nikishin et al., 2014) (Fig. 20). The following sedimentary sections have been identified on these islands (Kos'ko et al., 2013; Kuzmichev et al., 2013; Kuzmichev et al., 2009): the Late Aptian-Albian, Upper Cretaceous (Cenomanian-Coniacian), Eocene, and Quaternary. All deposits are represented predominantly by continental sandstones, siltstones and clays, intercalated with coal horizons. The presence of a Mesozoic pre-Aptian orogeny on the New Siberian Islands

coupled with considerable pre-Aptian erosion is indicative of the fact that sedimentary complexes of the East Siberian Sea system of rifts are not older than Aptian (Sekretov, 2001; Nikishin et al., 2017; Nikishin et al., 2014). The deposits of the East Siberian Sea rifts can be traced on seismic lines into the Podvodnikov and Makarov basins of the Arctic Ocean (Figs. 21-30).

On Wrangel Island, folded Silurian-Triassic deposits are observed (Kos'ko et al., 1993; Verzhbitsky et al., 2015; Sokolov et al., 2017). It is commonly assumed that the main folding took place in the Late Jurassic-Early Cretaceous ca. 150-120 Ma, whereas a major uplift phase took place at ca. 105-90 Ma and 72-64 Ma (Kos'ko et al., 1993; Miller et al., 2010, 2018a, 2018b.; Verzhbitsky et al., 2015, Verzhbitsky et al., 2012; Sokolov et al., 2017). Examination of seismic lines within the North Chukchi Basin, north of Wrangel Island, reveals that the sedimentary cover of the North Chukchi Basin probably overlies the folded structures exposed on Wrangel Island (Nikishin et al., 2014, 2017) (Figs. 10, 17). This suggests that the formation of the North Chukchi Basin is not older

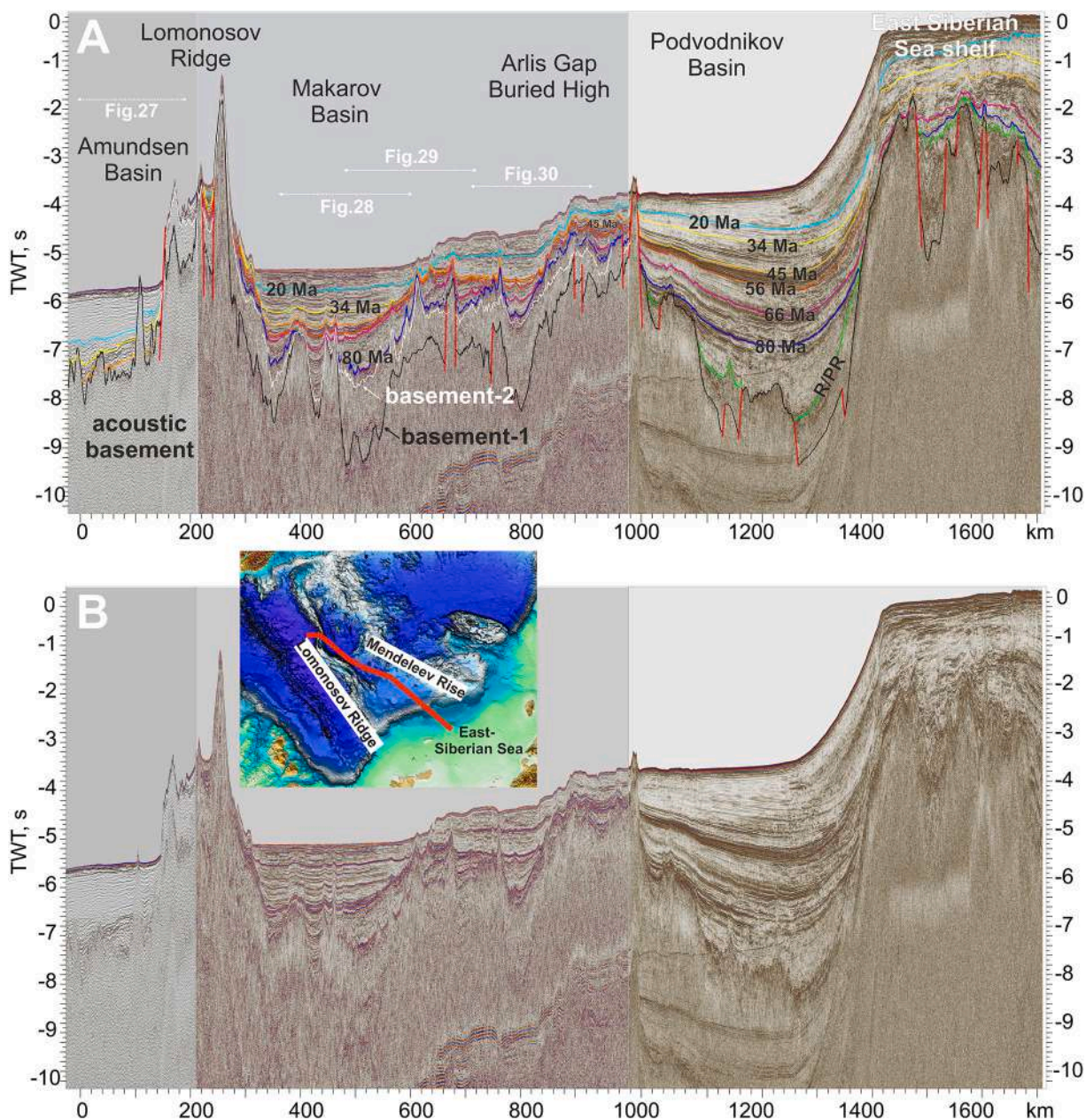


Fig. 26. A. Interpretation of composite seismic profile (lines ARC 14-39a, ARC 14-06, and ARC 14-02) for the region from the East Siberian Sea shelf to the Lomonosov Ridge and North Pole. Location of the profile is shown on the map. Different color lines are seismic horizons and corresponding ages (Ma). B. Seismic profile without interpretation. Basement-1 and basement-2 are two possible boundaries defining acoustic basement in the Arlis Gap-Makarov Basin region. An intermediate unit can be proposed between these boundaries. See also supplementary data, Fig. 26 (seismic profile without interpretation at high resolution).

than Aptian (Nikishin et al., 2014, 2017).

4.5. Formation history of Late Jurassic to Neocomian (pre-Aptian) foredeep basins in the East Siberian and Chukchi Seas

The Verkhoyansk-Chukotka Orogen has its possible northern boundary in the East Siberian and Chukchi seas and is expressed as a belt of syn-collisional foredeep basins (e.g., Puscharovsky, 1960; Miller and Verzhbitsky, 2009; Drachev et al., 2010, 2018; Nikishin et al., 2014, 2019; Bird et al., 2017; Popova et al., 2018). The basis of this hypothesis is that a Mesozoic orogeny was known for the New Siberian Islands and

Wrangel Island, however, the region of De Long Islands has Early Paleozoic and older crust. Drachev et al. (2010) presented geophysical data for location of this foredeep basin and Nikishin et al. (2014) identified this thrust belt on recent Russian seismic data. Popova et al. (2018) evaluated Rosneft Oil Company data and documented a pre-Aptian foredeep basin, which they named the Zhokhov Basin. Based on the number of recent seismic sections that cross this region (Fig. 31), we recognize a classical foredeep basin with thrusting towards the north. The two-way travel time thickness of the foredeep basin sedimentary fill is ca. 5 secs, with a width of nearly 50-100 km. The Mesozoic orogen together with its foredeep basin is covered by Cretaceous post-

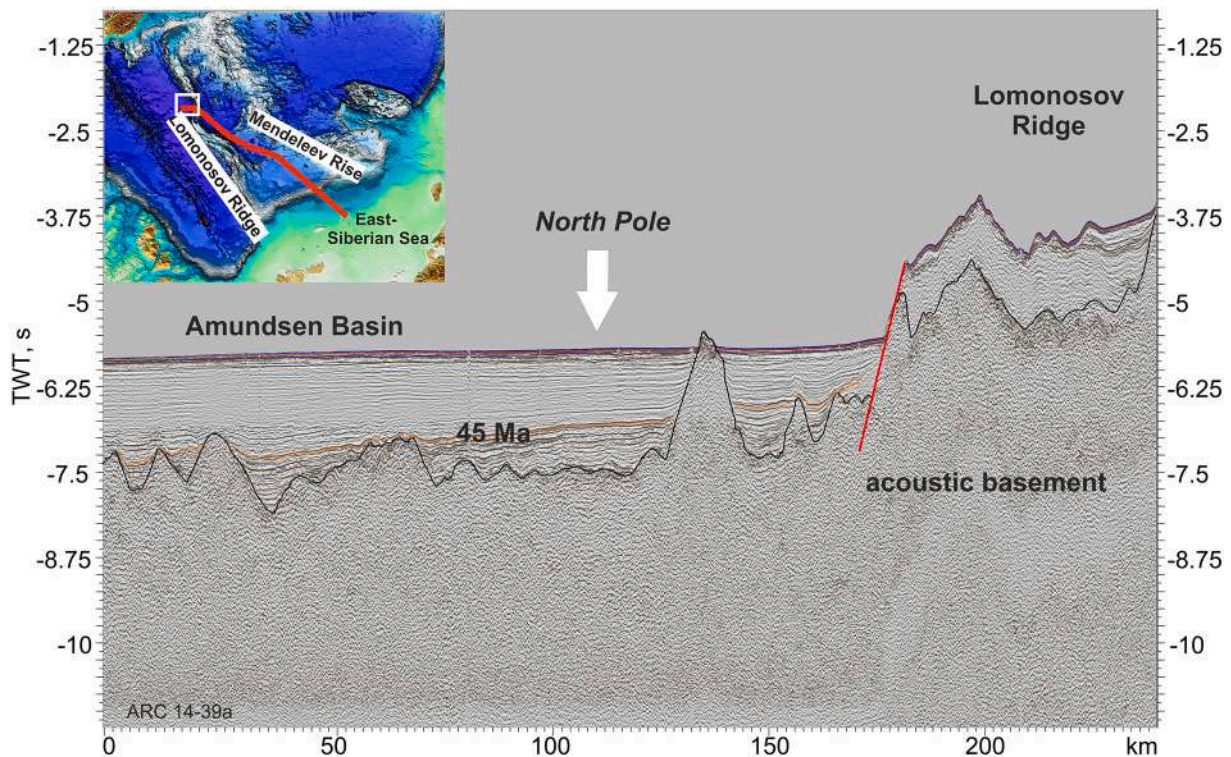


Fig. 27. Fragment of the profile shown in Fig. 26. This profile presents the first data illustrating the geological structure of the North Pole region. The North Pole is located in the Amundsen Basin and close to the Lomonosov Ridge. A key question concerns the position of the continental and oceanic crust boundary on this profile.

Barremian deposits. Some possible grabens can be recognized at the bottom of this Cretaceous section, the age of which is not older than the Aptian.

A pre-Aptian foredeep basin was proposed and documented north of Wrangel Island (Nikishin et al., 2014) and was named the North Wrangel Basin. Recent Rosneft Oil Company seismic data have supported this hypothesis (Skaryatin et al., 2020).

4.6. Formation history of the De Long plateau basalts and of the Alpha-Mendeleev Rise basalts

The De Long Islands are located in the northern part of the New Siberian Islands in the East Siberian Sea. On Bennett Island, one of the De Long Islands, Early Cretaceous plateau basalts are well known and overlie a Lower Paleozoic folded complex (Kos'ko et al., 2013). The age of the basalts is ca. 105-130 Ma (Drachev and Saunders, 2006; Kos'ko et al., 2013; Kuzmichev, personal communication). Below the basalts, Early Cretaceous sandstones with coals are observed (Kos'ko et al., 2013). A strong magnetic anomaly is associated with the De Long Islands, indicative of a possible widespread Early Cretaceous basaltic plateau (Drachev and Saunders, 2006; Drachev et al., 2010; Gaina et al., 2011; Saltus et al., 2011; Nikishin et al., 2014, 2017; Shipilov, 2016). The De Long Plateau forms an uplifted area and is transected by several seismic lines. Several grabens are located within the plateau (Drachev et al., 2010; Nikishin et al., 2014, 2017). At the base of some of the graben fills, packages of high-amplitude reflections are observed (Figs. 6, 21, 22). We assume that these high-amplitude reflections correspond to the De Long basalt complex interbedded with layers of sedimentary deposits (Nikishin et al., 2014, 2017; Shipilov, 2016). The most obvious example is in the Anisin Basin located just north-west of Kotelny Island of the New Siberian Islands where we recognize high-

amplitude reflections at the base of the graben and interpret as possible volcanics. In addition we see seismic reflection patterns indicative of the existence of numerous magmatic intrusions below the acoustic basement (Fig. 32). It follows from this hypothesis that the rifting in the East Siberian Sea started at the time of the basaltic volcanism, i.e., the start of the rifting took place not earlier than the Aptian (Nikishin et al., 2014, 2017).

Basalts were penetrated by shallow drilling on the slope of the Trukshin Seamount on the Mendeleev Rise yielding U-Pb ages of 127 Ma derived from zircon samples (Morozov et al., 2013) (see Paper-1, Nikishin et al., 2021a). Basalts of similar age are known in the Canadian Arctic Islands (e.g., Embry and Osadetz, 1989; Evenchick et al., 2015). On the seismic line across the Trukshin seamount these basalts are within the acoustic basement (Nikishin et al., 2014, 2017, 2021a). North of the Chukchi Plateau, basalts were recovered by dredging on slopes of bathymetric highs and have isotopic ages of 118-112 Ma, 105-100 Ma, and 90-70 Ma (Brumley, 2014; Mukasa et al., 2020). On the Mendeleev Rise they either are observed within the acoustic basement or are present as high-amplitude reflections in the cover (Brumley, 2014; Nikishin et al., 2014). These basalts are overlain by the Alpha-Mendeleev sedimentary cover. It should be noted that at the present time there is insufficient data on volcanic rocks of the Alpha-Mendeleev Rise, to allow for robust conclusions. The sedimentary cover possibly starts from the Middle-Upper Cretaceous and includes basalt deposits that form seismically-defined packages characterized by high-amplitude reflections (Nikishin et al., 2014; Rekant et al., 2015; Coakley et al., 2016) (Figs. 33-44).

In 2014 and 2016 rock samples were collected from four scarps on the Mendeleev Rise using a specially-equipped submarine (see Paper-1, Nikishin et al., 2021a). The samples were collected by Skolotnev et al. (2017, 2019,) and four sections were studied, composed mainly of

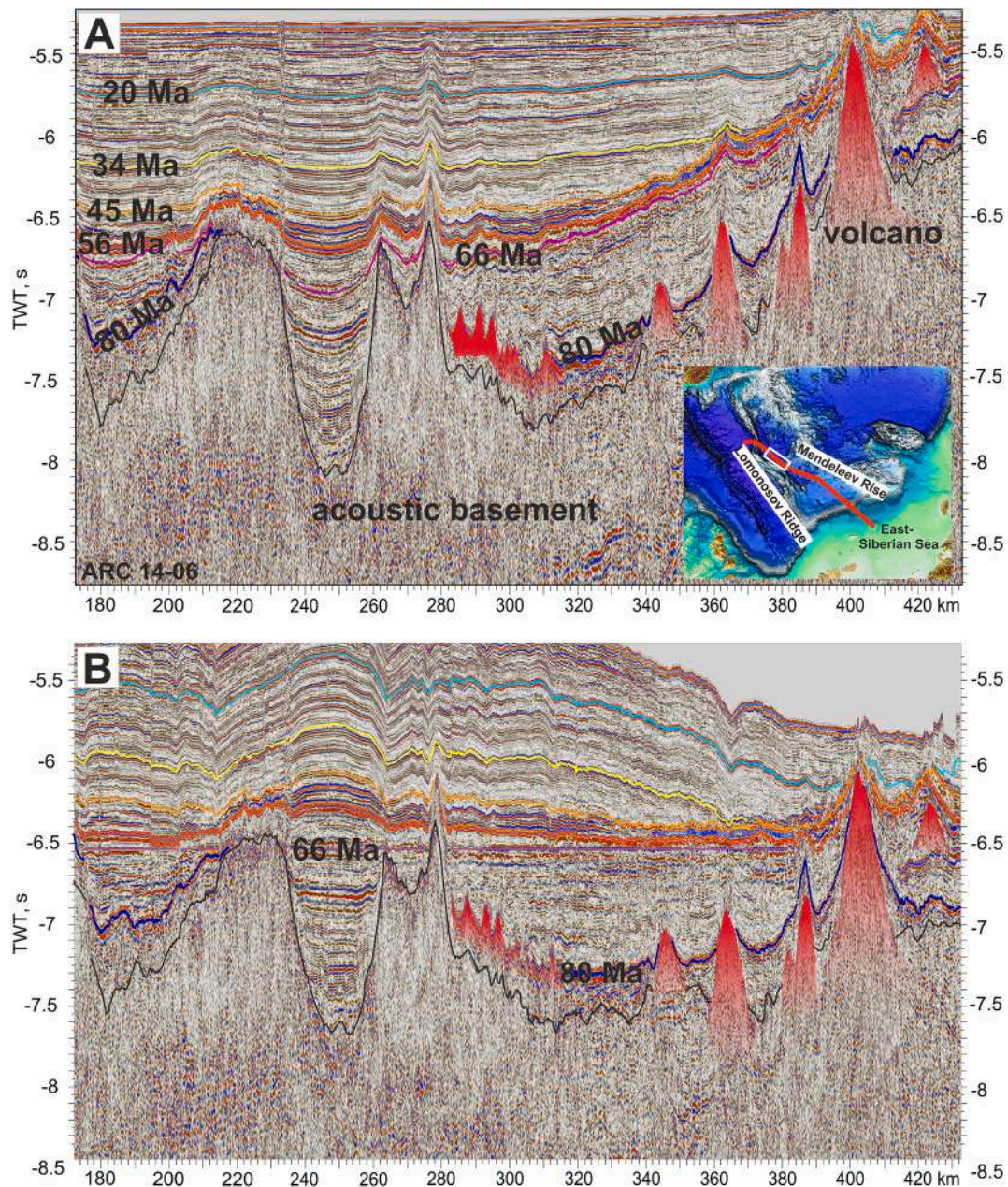


Fig. 28. Fragment of the profile shown in Fig. 26. This profile crosses the Makarov Basin and its southern margin. A. Interpretation of the profile. A V-shape trough is located in the central part of the basin, interpreted as a possible rift basin with a pre-66 Ma age. Possible volcanic structures with Cretaceous pre-80 Ma age are outlined by red lines. B. Section flattened on the 66 Ma horizon.

deformed sedimentary rocks with Ordovician to Devonian fauna (see Paper-1, Nikishin et al., 2021a). These sections are pierced by basalt dikes and sills of Early Cretaceous age (105-124 Ma) (Skolotnev et al., 2017, 2019; Skolotnev, unpublished data). The deformed Paleozoic deposits are unconformably covered by Aptian (or late Barremian to Aptian) sandstones in the Trukshin seamount, and basalts and basaltic tuffs with isotopic ages close to 112-124 Ma are observed (Petrov, 2017; Skolotnev et al., 2019; Skolotnev et al., 2017) (see Paper-1, Nikishin et al., 2021a). From these data it appears that the Mendeleev Rise comprises a continental terrane that has experienced strong extension and Cretaceous magmatism.

4.7. Formation history of rifting in the shelf basins of the East Siberian and Chukchi Seas

A large system of continental rifts is present within the shelves of the East Siberian and Chukchi Seas (Drachev et al., 2010; Nikishin et al., 2019; Nikishin et al., 2017; Nikishin et al., 2017; Popova et al., 2018) (see Paper-1, Nikishin et al., 2021a). As we pointed out in previous sections the most probable time of rift onset was the Aptian.

Numerous anomalies of apparent intrusive origin are observed on several seismic sections north of Wrangel Island in the Chukchi Sea (Figs. 45, 46). These anomalies, characterized by high-amplitude

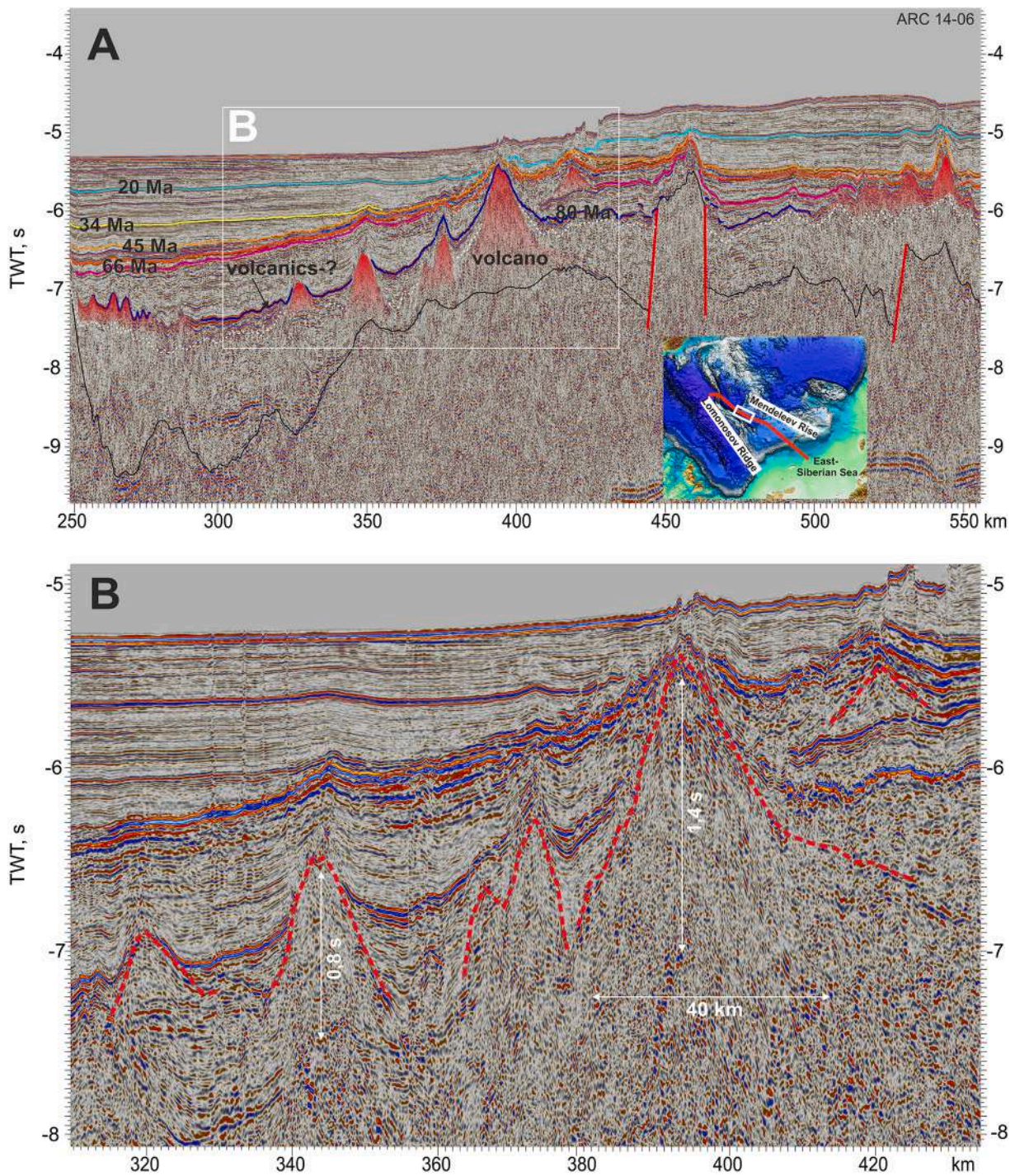


Fig. 29. A. Fragment of the profile shown in Figs. 26 and 28, and detailed fragment of Fig. 28. This profile is located in the region between Arlis Gap Buried Plateau and the Makarov Basin. A number of volcano-like features can be identified. Volcanoes have a Cretaceous pre-80 Ma age. B. Fragment of this profile. Dashed red lines outline possible volcanoes without evidence for subareal erosion, suggesting that these volcanoes originated as submarine structures.

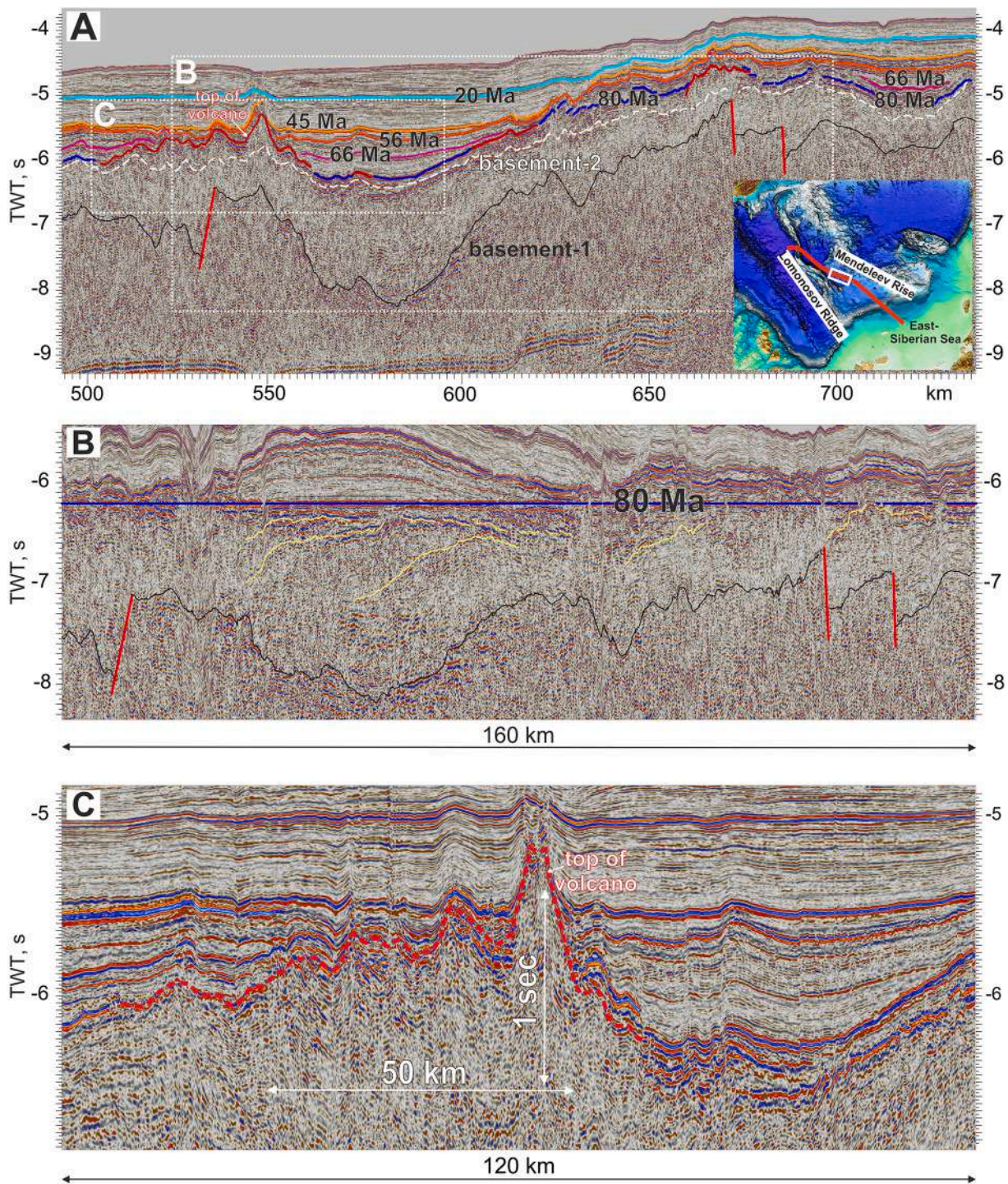


Fig. 30. A. Fragment of the profile shown in Fig. 26. This profile is located in the Arlis Gap Buried Plateau. Red lines are outlines of possible volcanoes. Onlapping of seismic horizons toward 80 Ma surface is observed, implying possible tectonic movements between 80 and 66 Ma and younger. B. Section flattened on the 80 Ma horizon. Possible synrift complex can be observed below 80 Ma horizon. C. Fragment of the seismic line with possible volcanic structures. These structures are of Cretaceous age (older than 80 Ma).

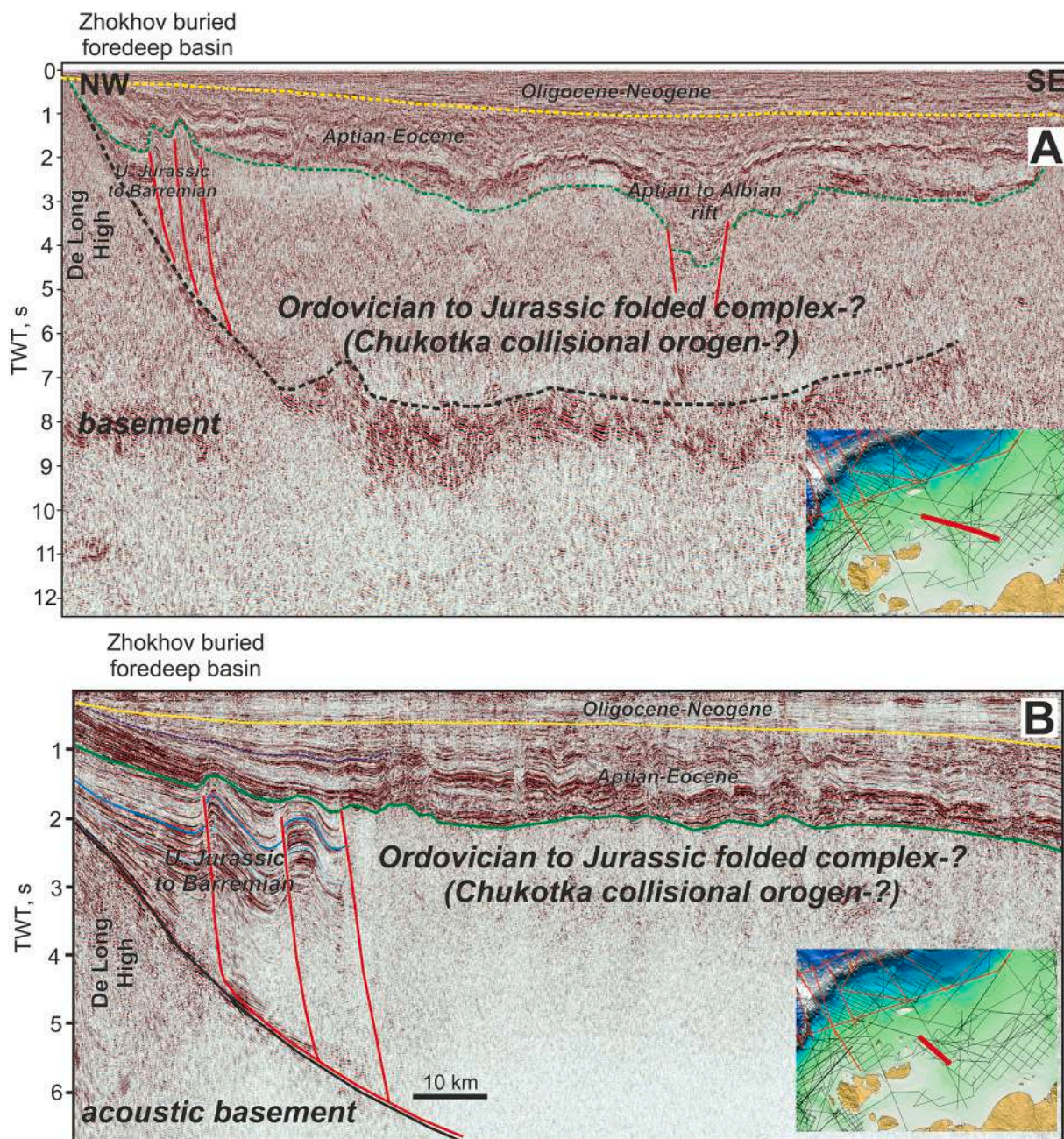


Fig. 31. Seismic profiles for the Zhokhov Foredeep Basin region. A. Modified after Nikishin et al. (2023). Fragment of the profile ES1_16ES21 (MAGE, Murmansk, data courtesy of the Ministry of Natural Resources, Russia).

reflections, all occur below the possible 125 Ma horizon (the base of the Aptian) and are similar to the numerous anomalies in the Barents Sea, which have been interpreted as Cretaceous intrusions (Corfu et al., 2013; Polteau et al., 2016; Minakov et al., 2018). In the North Chukchi Basin, high-amplitude reflections are present at the base of the stratigraphic section, and can be interpreted as alternating basalts and sedimentary rocks (Figs. 46, 47). This probable igneous province in the Chukchi Sea is distinctly identifiable on the magnetic anomaly map (Gaina et al., 2011) in the form of a strong positive anomaly. The age of the magmatism could be Aptian (or HALIP); in this case, the magmatism was approximately synchronous with the magmatism of the De Long

Plateau in the East Siberian Sea and with the magmatism on the Alpha-Mendelev Rise. We propose that at the onset of formation of the North Chukchi Basin, approximately in the Aptian, basaltic magmatism occurred.

Within the East Siberian and Chukchi Sea rifts, a rift/postrift boundary is seismically identified (Figs. 20–26, and 32) though its precise dating is difficult. Because an unconformity between the Albian and the Cenomanian exists on the New Siberian Islands, we propose as a hypothesis that this boundary corresponds to the rift/postrift boundary and we date it as 100 Ma. Miller et al. (2018b, 2018a) studied a normal fault event possibly related to rifting, on Wrangel Island using U-Pb and

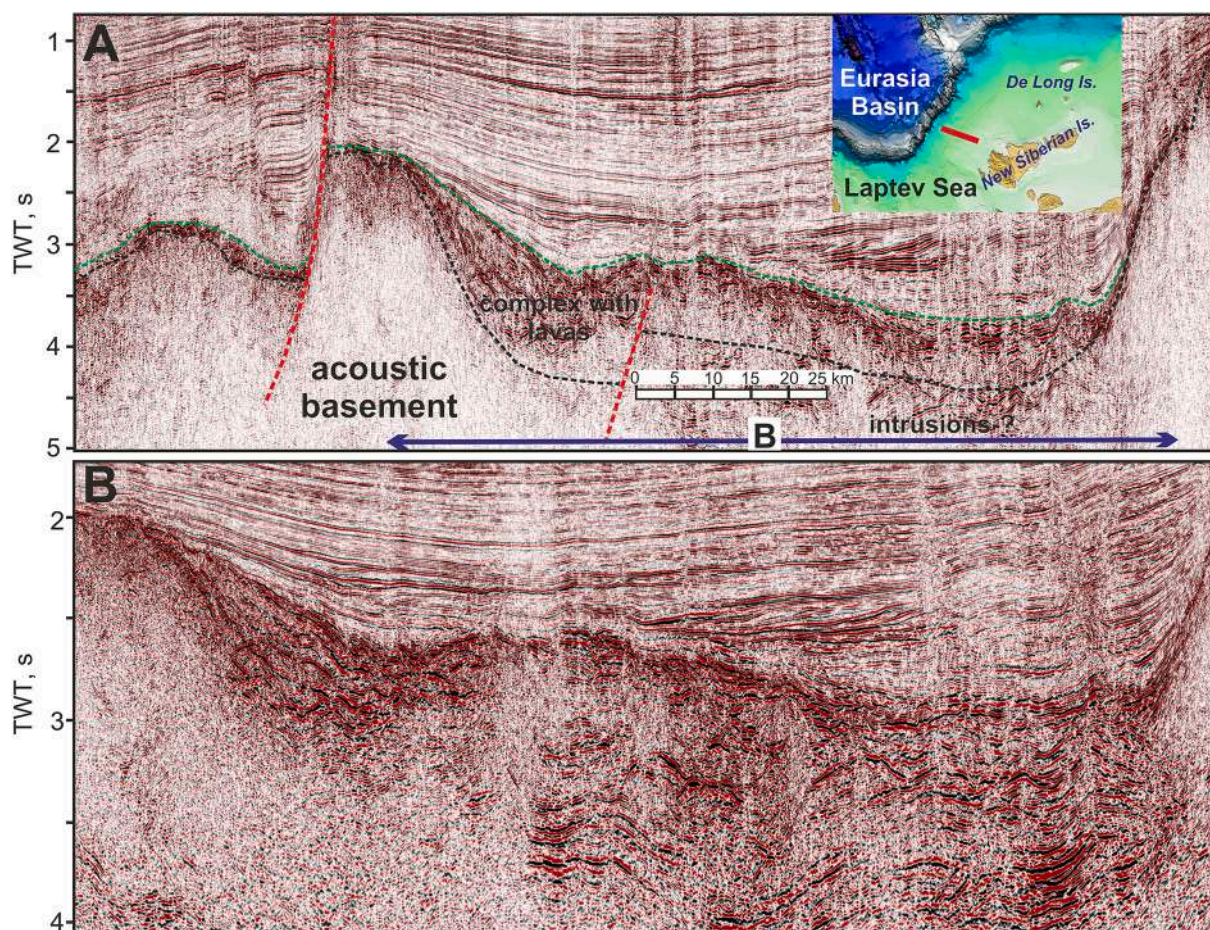


Fig. 32. A. Fragment of seismic profile across the Anisin Basin. Location of the profile is shown on a map. B. Fragment of profile A. Possible volcanic complex and intrusions can be observed. Volcanics are at the base of the rift basin. Data courtesy of the Ministry of Natural Resources, Russia.

AFT dating and concluded that the timing of fault motion was likely 105–100 to 95 Ma, with only a minor uplift after that. These data are consistent with our general model. This unconformity of Cenomanian or Early Cenomanian age also is well documented in the Beaufort-Mackenzie Basin (Embry and Dixon, 1994) and Arctic Alaska (Homza and Bergman, 2019; İlhan and Coakley, 2018).

New data on the New Siberian Islands history based on low-temperature thermochronology demonstrate that a cooling episode took place at 125–93 Ma (Prokopiev et al., 2018). We interpret this epoch as a rift shoulder uplift event. Our data do not support the hypothesis of Prokopiev et al. (2018) that it was a compressive event with thrusting.

4.8. A breakup unconformity on the Laptev Sea Shelf and on the Lomonosov Ridge

Retraction of the Lomonosov Ridge from the Barents-Kara Shelf is assumed to have occurred in the course of formation of the Eurasia Basin (e.g., Drachev et al., 2010); a breakup unconformity with an age of about 56 Ma corresponds to the time of onset of oceanic crustal spreading in the Eurasia Basin (Drachev et al., 2010; Franke, 2013; Nikishin et al., 2014; Weigelt et al., 2014). This boundary is observed in the Laptev Sea (Figs. 48, 49) and on the slopes of the Lomonosov Ridge (Figs. 7, 8, 9, 50), and can be correlated with boundaries of seismic sequences in the

Arctic Ocean.

New data on the New Siberian Islands history based on low-temperature thermochronology demonstrate that a cooling episode took place at ca. 53 Ma (Prokopiev et al., 2018). We interpret this epoch as a rift shoulder uplift event.

4.9. Seismic stratigraphy of the Laptev Sea Basin

The Laptev Sea basin is traditionally considered a single rift system (Drachev et al., 2010; Franke, 2013; Weigelt et al., 2014). Interpretation of the new grid of seismic lines shows that this is probably not correct (Nikishin et al., 2017, 2018). In the eastern part of the Laptev Sea in the area of the Anisin Basin, complex rifting probably started in the Aptian. There are two main constraints for this hypothesis: (1) At the base of the rift fill sections in the area of the De Long High, packages of high-amplitude reflections are observed, which are interpreted as basalts (Figs. 21, 32). These basalts are present on the nearby De Long Islands and have been dated at ca. 130–105 Ma (Barremian-Aptian) (Kos'ko and Trufanov, 2002; Drachev and Saunders, 2006; Kos'ko et al., 2013). (2) An angular unconformity at the base of the rift complex is observed on some seismic lines in the area of the De Long High (Nikishin et al., 2014). This unconformity probably corresponds to the known regional unconformity on the New Siberian Islands, which lies at the base of the Aptian and is substantiated in many studies (Kos'ko and Trufanov, 2002;

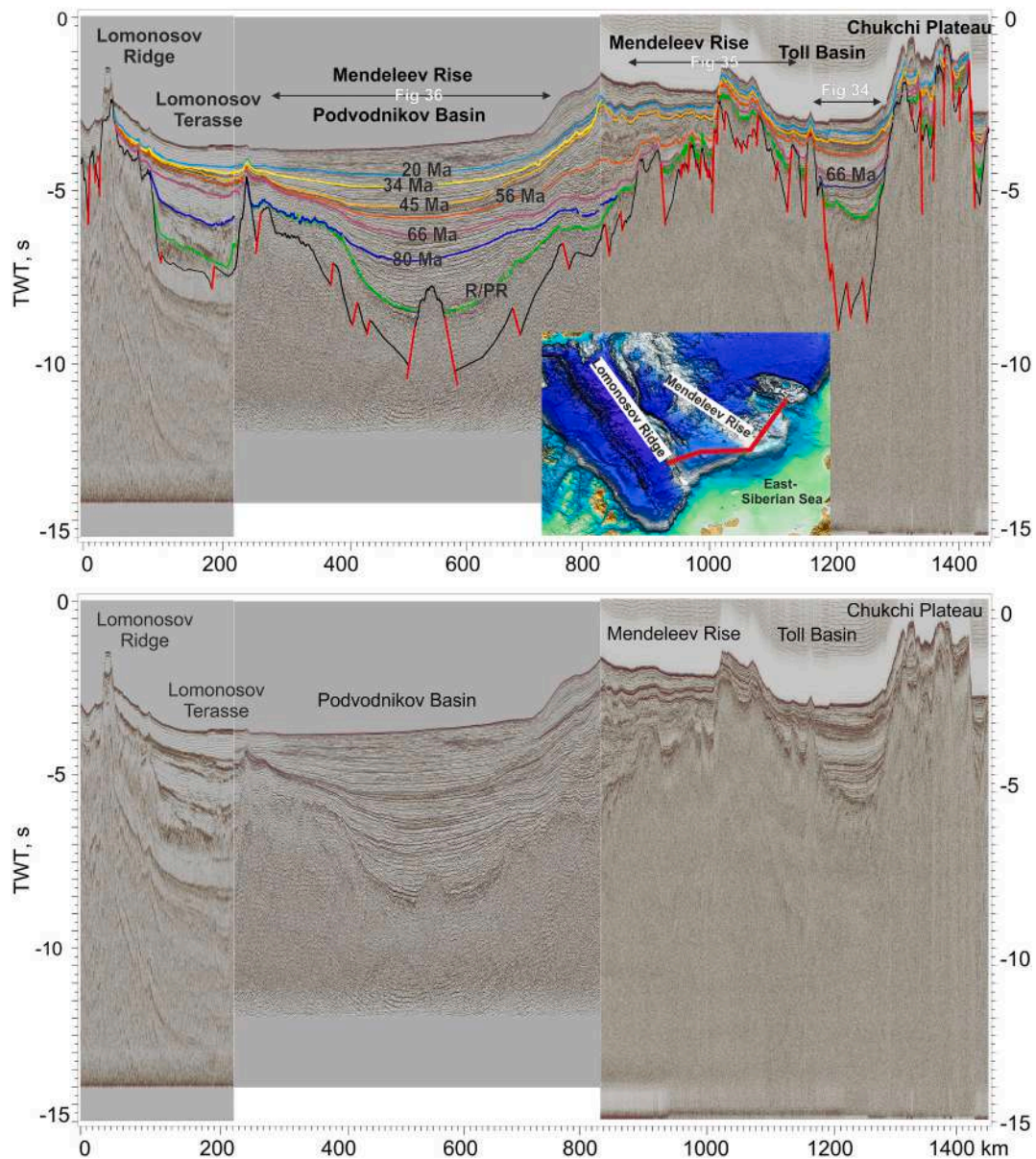


Fig. 33. Interpretation of composite seismic profile (lines ARC 12-03, ARC 14-01 and ARC 11-053) for the region from Lomonosov Ridge to Chukchi Plateau. Location of the profile is shown on the map. Different color lines are seismic horizons and corresponding ages (Ma), R/PR - rift/postrift boundary. See also supplementary data, Fig. 33 (seismic profile without interpretation at high resolution).

Kuzmichev et al., 2009, 2013; Kos'ko et al., 2013; Nikishin et al., 2017).

In the western part of the Laptev Sea Basin in the area of the Ust' Lena Basin, a breakup boundary is clearly observed, which is dated at 56 Ma (Fig. 48). Below this boundary, a synrift sediment complex is observed, which can be dated as Paleocene (or Cretaceous-Paleocene). That is, continental rifting in the Ust' Lena Basin took place in the Paleocene before the onset of the Eurasia Basin opening.

Numerous intrusive type anomalies associated with volcanic sills and dykes are observed in the western part of the Laptev Sea on some seismic sections (Fig. 48). These probable intrusions occur below the breakup boundary (56 Ma). High-amplitude reflections, which can be interpreted as volcanics, are identified below the Eocene section as well. The timing of magmatism is likely close to the Paleocene/Eocene boundary. The

presence of a likely igneous province is confirmed by the presence of a strong positive anomaly on the magnetic anomaly map (Gaina et al., 2011). It is likely that a period of basaltic magmatism took place before the onset of opening of the Eurasia Basin – we call this magmatic area the Faddey Magmatic Province. Based upon magnetics and seismic data, a very similar province with possible volcanoes is located on the other side of the Eurasia Basin at the transition between the Lomonosov Ridge and the shelf region (Figs. 7, 9). We name this magmatic area the Lomonosov-Anisin Magmatic Province.

New data show that in the eastern part of the Laptev Sea, the main rifting was in the Aptian-Albian. These rifts should be assigned to the system of rifts of the East Siberian and Chukchi Seas rifts and were connected with the Podvodnikov Basin (Nikishin et al., 2017). The Ust'

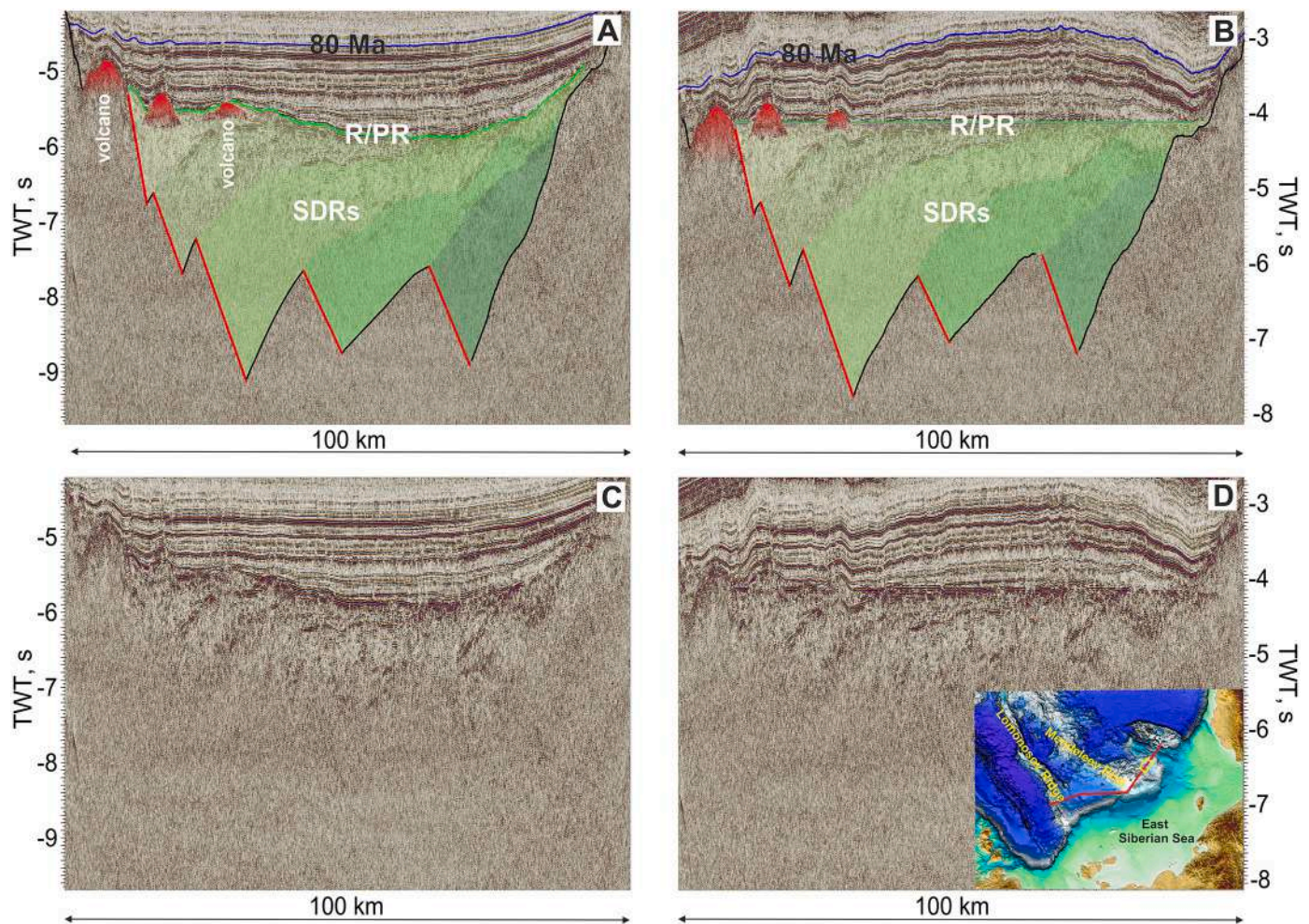


Fig. 34. A. Interpretation of a fragment of seismic profile (lines ARC 12-03) from the Toll Basin (Fig. 33). Location of the profile is shown on the map. Different color lines are seismic horizons and corresponding ages (Ma). SDR complexes and volcanoes on a top of SDRs are interpreted. B. Flattening on the rift/posrift boundary. C and D – profiles without interpretation.

Lena Rift in the western part of the Laptev Sea was associated with the subsequent opening of the Eurasia Basin.

Eocene-Quaternary normal faults are common in the Laptev Sea Basin (Figs. 51, 52). Their formation has traditionally been interpreted as the continuation of the Gakkel Mid-Oceanic Ridge (Drachev et al., 2010; Franke, 2013; Nikishin et al., 2018).

4.10. SDR complexes in the Mendeleev Rise and Podvodnikov and Toll basins

The Toll Basin is located between the Chukchi Plateau and the Mendeleev Rise. The Toll Basin has one significant feature in its lower part: there is a probable rift-posrift boundary below which packages of reflections dip uniformly towards the Mendeleev Rise (Nikishin et al., 2014) (Fig. 34). They are interpreted as possible Seaward Dipping Reflectors (SDRs) and are typical of volcanic passive continental margins (e.g., Geoffroy, 2005). Recently, American investigators published a profile that lies southward and almost parallel to our profile (Ilhan and Coakley, 2018). It clearly shows similar SDRs with the same polarity. SDRs are primarily composed of synrift basalts that are emplaced during continental rifting over mantle plumes (e.g., Geoffroy, 2005) (this is a

very specific topic which we will not discuss in detail here). Based upon our grid of seismic data, apparent SDR-like units are very common for the Mendeleev Rise (Figs. 34, 35, 36, 37, 38, 39, 40, and 41). They could be classical SDRs with basalts, though we cannot conclusively rule out the possibility that these reflections are indicative of sedimentary deposits within half grabens. The Mendeleev Rise appears to be divided into two parts, each of which characterized by a consistent and contrasting dip. Reflections dip toward the Toll Basin on the eastern slope of the Mendeleev Rise and toward the Podvodnikov Basin on its western slope. The presence of SDR-like units also is proposed for the Podvodnikov Basin. These units are observed along the eastern and western slopes of this basin (Figs. 33, 35, 36, 37). The rift/posrift boundary (or top of SDR complex) seems to be at nearly the same stratigraphic level in the regions of the Podvodnikov Basin, Mendeleev Rise, and Toll Basin (Figs. 33-42). Although this is not precisely determined, we cannot find evidence for moving this boundary to different stratigraphic levels. Our seismic data suggests that SDR-like units and/or half-grabens are characterized by strike that is approximately parallel to the Mendeleev Rise and Toll Basin (Figs. 33, 37). This implies that the orientation of extension was orthogonal to the Mendeleev Rise. We observe on 2D seismic sections volcano-like conical seismic structures at the top of the

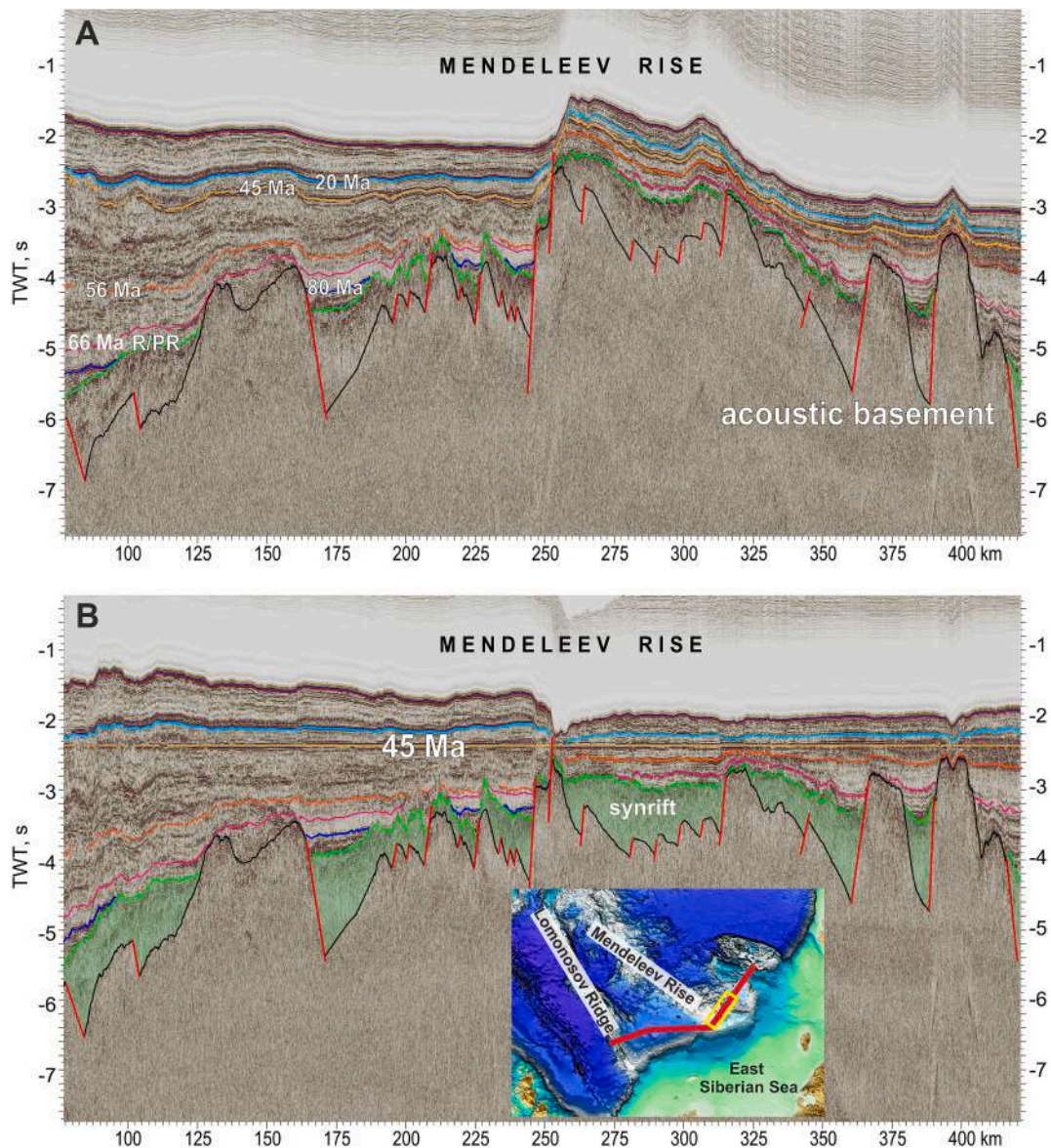


Fig. 35. A. Fragment of seismic profile shown in Fig. 33. The line ARC 12-03 for the Mendeleev Rise. Location of the profile is shown on the map. Different color lines are seismic horizons and corresponding ages (Ma). B. Profile flattened on the 45 Ma horizon. Horst/graben structure on the Mendeleev Rise acoustic basement can be observed.

SDR complexes along 2D seismic lines (Figs. 34, 36).

As discussed above, Skolotnev et al. (2017, 2019) studied samples collected on the Mendeleev Rise (see also Paper-1, Nikishin et al., 2021a). These authors documented the presence of Aptian (or Barremian-Aptian) shallow-marine sandstones, Cretaceous basalt lavas and Cretaceous tuffs. The Paleozoic section is associated with basaltic Cretaceous intrusions. Associated Cretaceous volcanic extrusives occurred in sub-aerial and shallow-marine conditions. The isotopic age of magmatism was close to 105-125 Ma (Skolotnev et al., 2019; Skolotnev et al., in preparation). Our seismic data together with the Skolotnev et al. (2019) data demonstrate that the Mendeleev Rise contains multiple half-grabens and/or SDR units. Half-grabens and/or SDRs are characterized by continental basement enriched with basalt intrusions.

A rift/postrift boundary is observed at nearly the same stratigraphic level in the region of the Podvodnikov Basin, Mendeleev Rise, and Toll

Basin as discussed above. We dated the rift/postrift boundary for shelf basins in the Laptev, East-Siberian Sea and Chukchi Sea as ca. 100 Ma. Although this is a speculative conclusion, it seems most reasonable to correlate this rift/postrift boundary on the shelf with the same boundary in the Mendeleev Rise region and dating to ca. 100 Ma, or younger.

4.11. Cretaceous seismic stratigraphy of the Laptev Sea-East Siberian Sea-North Chukchi Sea system shelf basins and Cretaceous seismic stratigraphy of adjacent deep-water Arctic basins and rises

Rift basins in the eastern part of the Laptev Sea and in the East-Siberian Sea and the North Chukchi Basin are characterized by a rift/postrift boundary at ca. 100 Ma (Figs. 6, 17, 18, 20, 21, 22, 23, 24, 26 and 32). Sediment thickness in the North Chukchi Basin is characterized by a TWT up to 9-11 secs (up to 20-22 km). The stratigraphic base of the

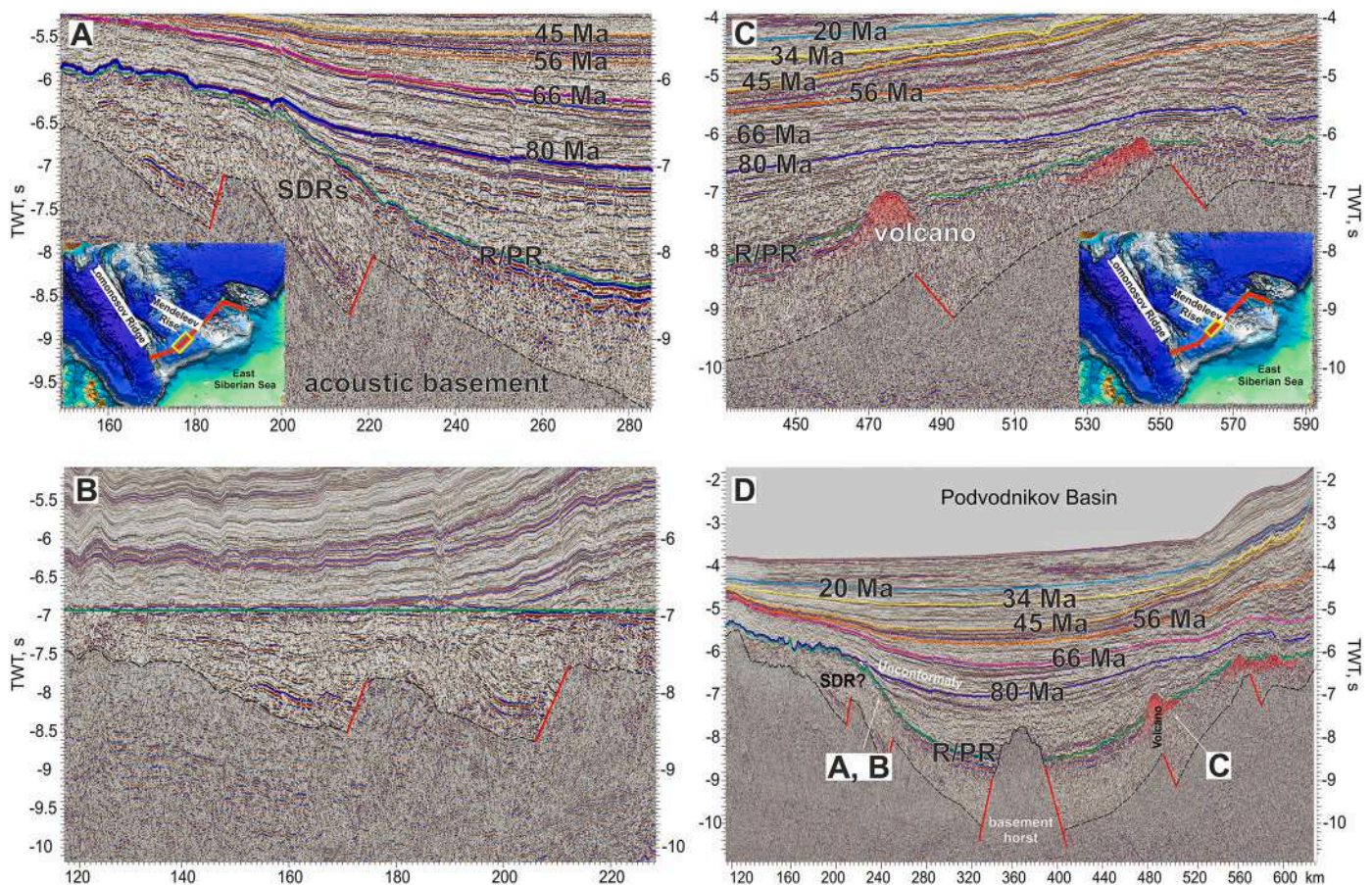


Fig. 36. Fragment of seismic profile shown in Fig. 33. Some details of the Podvodnikov Basin are shown. A. Western slope of the Podvodnikov Basin. SDR-complex can be observed below rift/postrift (R/PR) boundary. B. Profile flattened on the rift/postrift boundary. C. Possible volcanic structures at top of synrift complex in the south-eastern slope of the Podvodnikov Basin (top of volcanoes is outlined by red line). D. Fragment of seismic profile across the Podvodnikov Basin (Fig. 33)

North Chukchi Basin is relatively flat lying as was observed on a number of seismic profiles (Figs. 10, 11, 12, 13, 14, 23, and 53). We subsequently mapped that seismic horizon from the North Chukchi Basin into the Laptev and East Siberian Seas (Figs. 10, 12, 13, 14, 16, 23, and 53). We conclude that the stratigraphic base of the North Chukchi Basin comprises either a possible rift/postrift boundary or marks the top of SDR units for the Podvodnikov and Toll basins as well as for the Mendeleev Rise. We propose that synrift and pre-rift complexes are strongly stretched and represent the acoustic basement. Two possible explanations for these observations could be: (1) synrift hyperextension of a continental crust with possible exhumation of the lower crust, or (2) synrift exhumation of the mantle. Drachev et al. (2018) suggested the possibility of local mantle exhumation. However, we prefer hyperextension of the continental crust as a causal mechanism. Our interpretation is based on the calculated crustal structure of the North Chukchi Basin as presented by Poselov et al. (2019) and Savin (2020).

The rift/postrift (or top of SDRs) complex) boundary is at nearly the same stratigraphic level in the region of the Podvodnikov Basin, Mendeleev Rise, and Toll Basin as we discussed above. There are two important consequences of this observation: (1) the Podvodnikov and Toll basins together with the Mendeleev Rise have a nearly similar timing of development and originated as a single geodynamic system with extension orthogonal to the Mendeleev Rise; (2) the rift/postrift boundary for this system could be 100 Ma or younger; a younger age

could be proposed due to the general hypothesis that the end of rifting events in the shelf areas is typically older than the end of rifting in adjacent deep-water basins (the South China Sea is an example; e.g., Yang et al., 2018).

4.12. Climastratigraphy

Our correlations of seismic lines show that the boundary of ca. 45 Ma separates different seismic facies (Figs 5-16, 54). Above this boundary, weak seismic reflections prevail, while below this boundary high-amplitude reflections dominate (Weigelt et al., 2014; Nikishin et al., 2014). We associate this boundary with a sharp climatic cooling as has been proposed earlier (Backman et al., 2008; Moran et al., 2006).

The Paleocene-Eocene Thermal Maximum (PETM) is well substantiated for the Canadian Archipelago (West et al., 2015), Spitsbergen (Harding et al., 2011), and West Siberia (Akhmet'ev et al., 2010). Our boundary of 56 Ma in the Arctic Ocean probably corresponds to a phase of rapid warming. The Early Eocene is characterized by several phases of rapid warming (Cramer et al., 2009; Gradstein et al., 2012), which are observed for the Lomonosov Ridge as well (Stein et al., 2015). Deposition in the Arctic Ocean in general between 56-45 Ma is possibly associated with these rapid warming phases and expressed on seismic lines by the packages of high-amplitude reflections (Figs. 5-16).

A section characterized by high-amplitude reflections also is

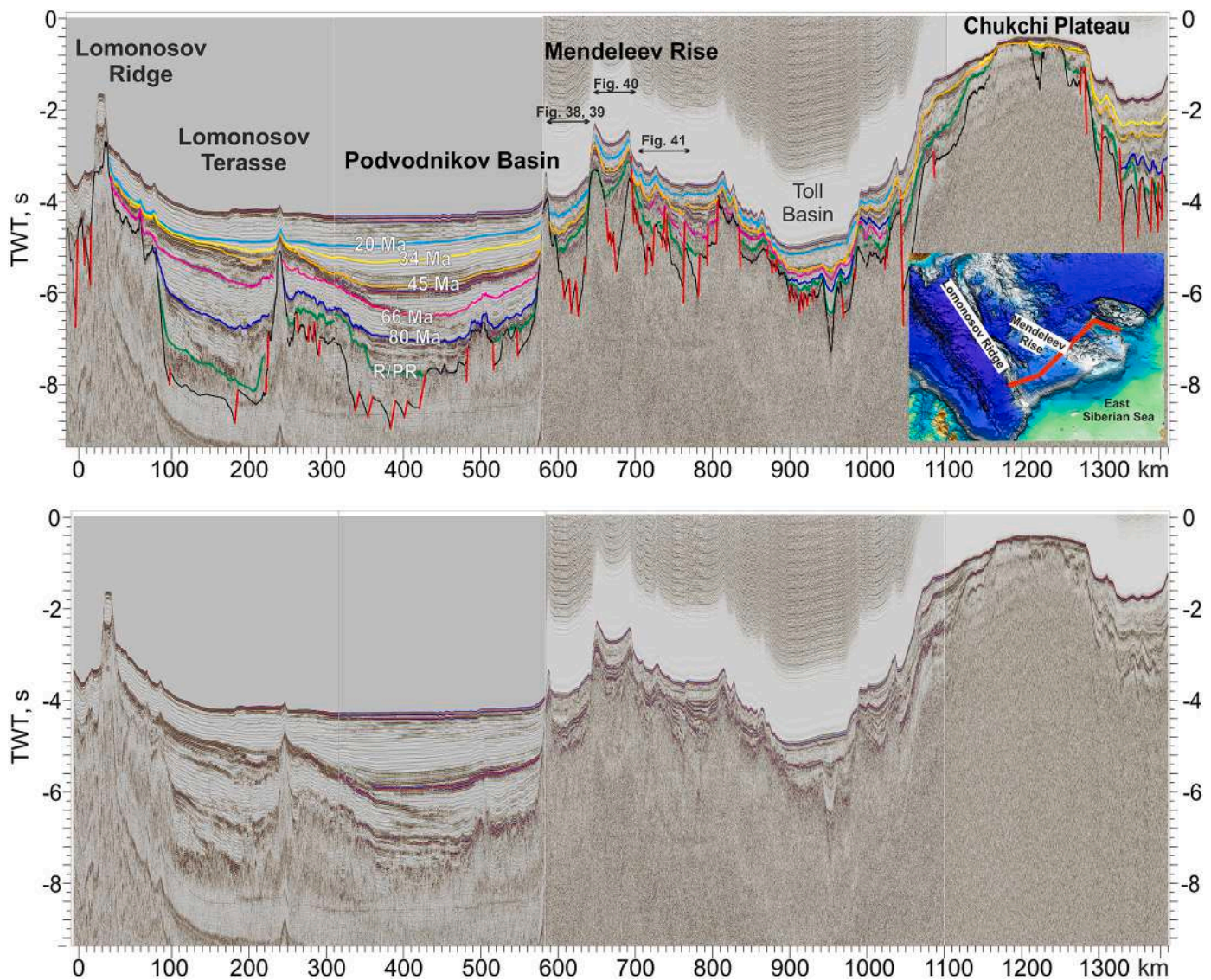


Fig. 37. Interpretation of composite seismic profile (lines ARC 11-53, ARC 12-04, ARC 11-65 and ARC 12-18) for the region from Lomonosov Ridge to Chukchi Plateau. Location of the profile is shown on the map. Different color lines are seismic horizons and corresponding ages (Ma). See also supplementary data, Fig. 37 (seismic profile without interpretation at high resolution).

observed below our proposed boundary of 80 Ma (Figs. 6, 10, 11, 12, 13, 14, 16, 22, 23, 25, 26, 33, 37, 44, and 53). We refer to this high-amplitude reflector sequence as HARS-2. This sequence has widespread distribution and can be mapped across the Podvodnikov Basin and in the North Chukchi Basin. We interpret the 80 Ma boundary to have specific climatic significance. Recently acquired paleontological and isotopic data show that during late Cretaceous time (close to 80-90 Ma) the Arctic climate was relatively warm with relative cooling close to Campanian time (Herman and Spicer, 1996; Jenkyns et al., 2004; Zakharov et al., 2011; Pugh et al., 2014; Schröder-Adams, 2014; Schröder-Adams et al., 2014; Herman et al., 2016). Other recent data show a relatively cool climate during early Cretaceous time with some short-lasting cooling events (Galloway et al., 2015; Herrle et al., 2015; Rogov et al., 2017). These data correlate with the record of global climatic history (O'Brien et al., 2017) (Fig. 55). We propose that our HARS-

2 sequence was formed during the late Cretaceous warm climate epoch. In any case, the climatic history of the Arctic region requires further investigations.

4.13. Identification of new igneous provinces on the shelf

We have found evidence for two new magmatic provinces in the region of the Laptev Sea (Figs. 7, 9, 48, 50). The age of the magmatism likely is close to the Paleocene-Eocene boundary. Additional evidence for the existence of volcanism associated with a rifted continental margin of the Eurasia Basin in the Laptev Sea is evidently needed. Our findings based on our newly acquired seismic data seem to contradict conventional assumptions concerning the formation dynamics of the Eurasia Basin (Drachev et al., 2010; Franke, 2013). A possible large magmatic province is identified for the southern part of the North

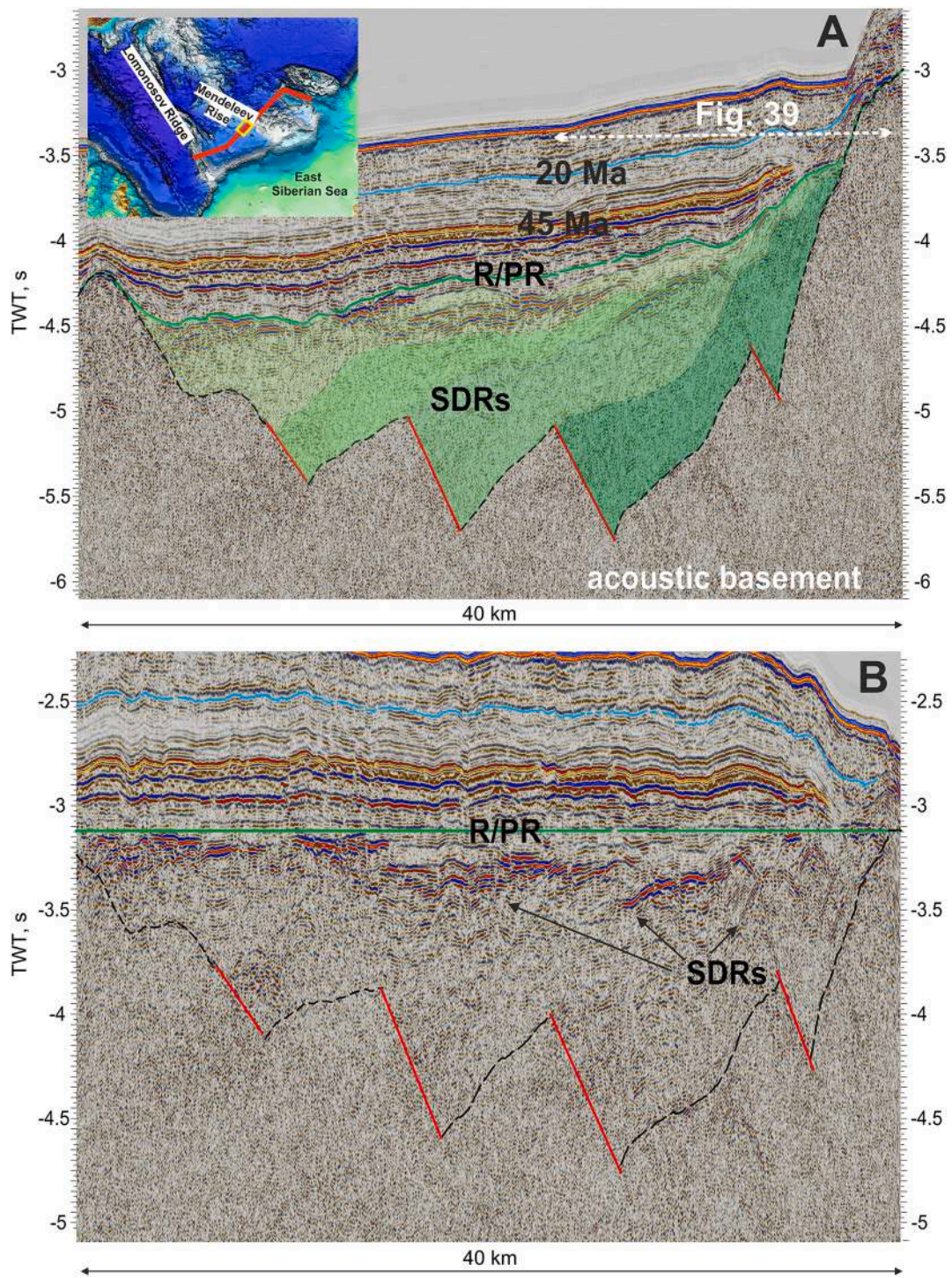


Fig. 38. A. Fragment of seismic profile shown in Fig. 37. Rift/posrift (R/PR) boundary and synrift SDR complex are interpreted. B. Profile flattened on the rift/posrift boundary.

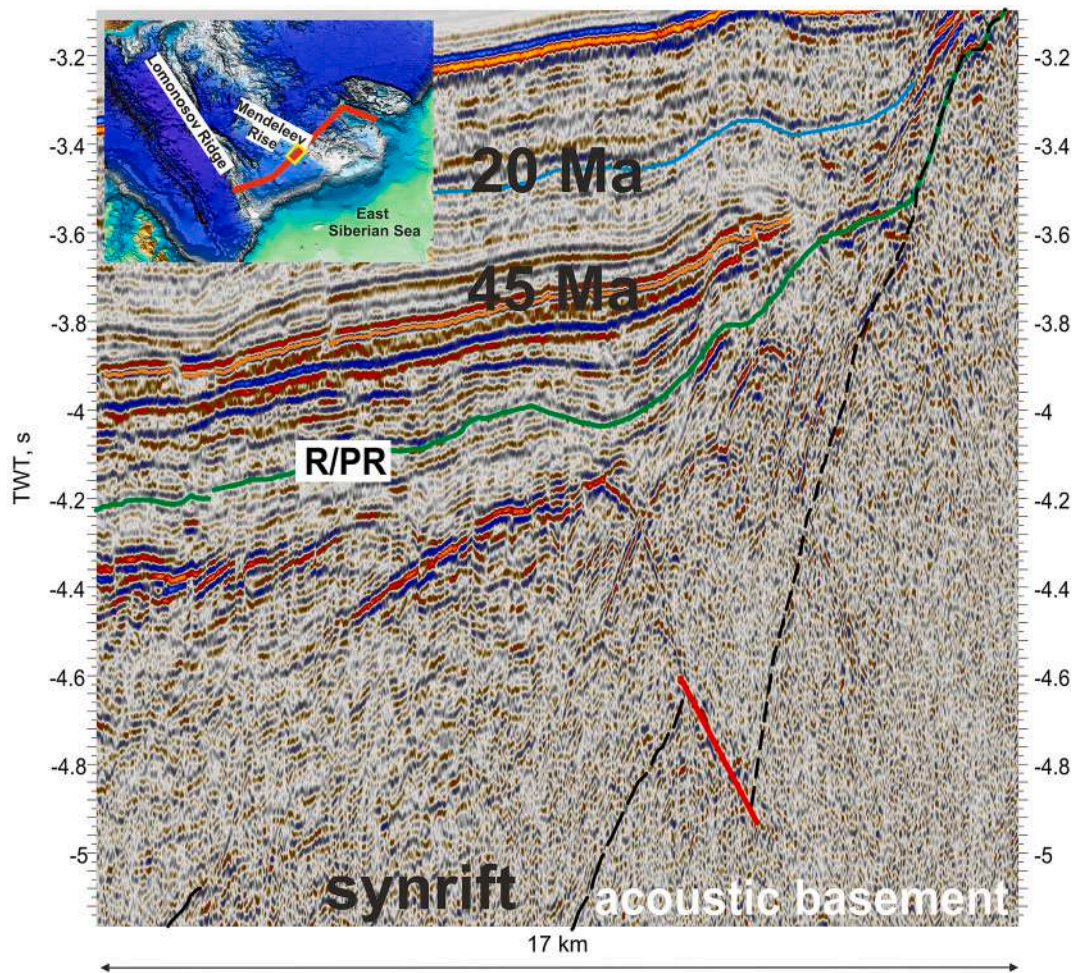


Fig. 39. Fragment of seismic profile shown in Fig. 37 and 38. Rift/postrift (R/PR) boundary and synrift complex are interpreted. A detailed image of possible SDR unit.

Chukchi Basin with a possible Aptian (or HALIP) age (Figs. 45, 46, 47). Further, our new seismic data demonstrate that the De Long magmatic province has a substantially larger size than proposed before (Figs. 6, 21, 25, and 32).

The occurrence of Cretaceous basalt magmatism is well known for the Barents Sea region. The magmatism has been studied for Franz Josef Land (e.g., Dobretsov et al., 2013) and has been dated to ca. 122-125 Ma (Corfu et al., 2013; Polteau et al., 2016). A key question is the correct age and extent of this magmatic province (e.g., Shipilov, 2016). South and southeast of Franz Josef Land, approximately at the base of the horizontally-layered Aptian sequence, a package with high-amplitude and chaotic reflections is observed (Fig. 56). Its typical thickness is ca. 50-100 msec. In our view, this package of high-amplitude reflections correlates with the basalt strata of Franz Josef Land. Based on borehole data tied to the 2D seismic grid our interpretation of the age of these reflections is close to the Barremian-Aptian boundary. Within the East Barents Megabasin a number of intrusions principally within Triassic shales have been observed (e.g., Dobretsov et al., 2013; Polteau et al., 2016; Shipilov, 2016). The precise age of the intrusions is not known but likely is the same as that of the lavas (Polteau et al., 2016). In association with the intrusions, we observe coeval forced folding (Fig. 56), implying that the intrusions occurred simultaneously with the basaltic volcanism

and structuration. Recently acquired regional data demonstrate that magmatism took place nearly simultaneously in the Barents Sea, East Siberian Sea and Chukchi Sea with a possible age close to 125 Ma.

4.14. Identification of regional seismic horizons

Based on the comprehensive data set reviewed here and in Nikishin et al. (2021a), we propose the following tectonostratigraphic model for the Arctic Ocean based on several key seismic horizons (Figs. 57, 58, 59):

1. The base of the stratigraphic section correlates with the onset of rifting on the shelves of the East Siberian and Chukchi Seas, which occurred during the Aptian-Albian. Consequently, we propose that the Podvodnikov Basin originated at this time (between ca. 100 Ma and 125 Ma). Any older deposits, if present, are included in the acoustic basement.
2. The rift/postrift boundary in the East Siberian Sea is tentatively dated as the boundary between the Upper and Lower Cretaceous (ca. 100 Ma). We can trace the rift/postrift boundary in the Podvodnikov Basin and in the area of the Lomonosov Ridge (Figs. 6, 20, 21, 22 and 26). We cannot date the age of the rift/postrift boundary in the deep-

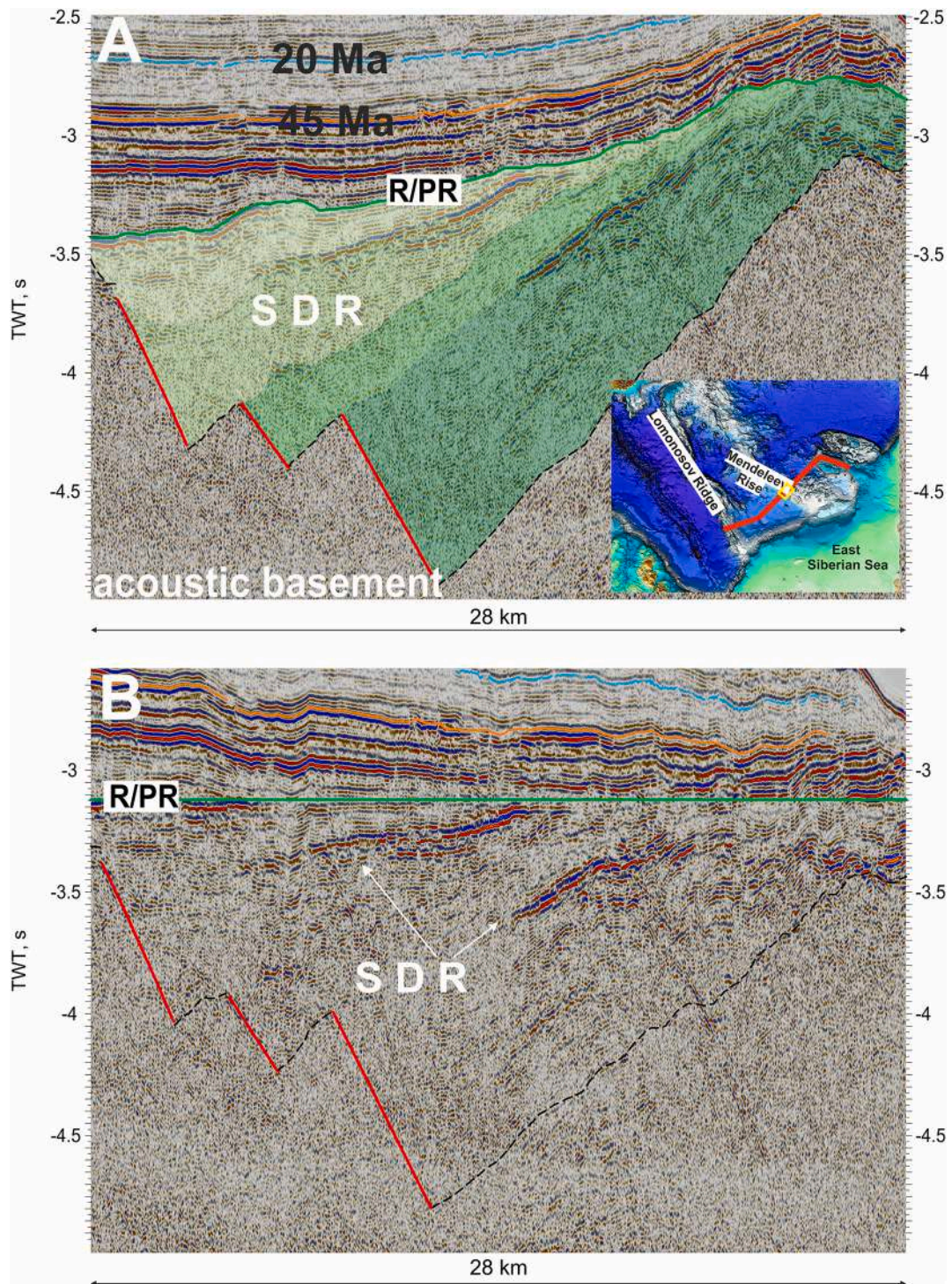


Fig. 40. A. Fragment of seismic profile shown in Fig. 37. Rift/postrift (R/PR) boundary and synfirth SDR complex are supposed. B. Profile flattened on the rift/postrift boundary.

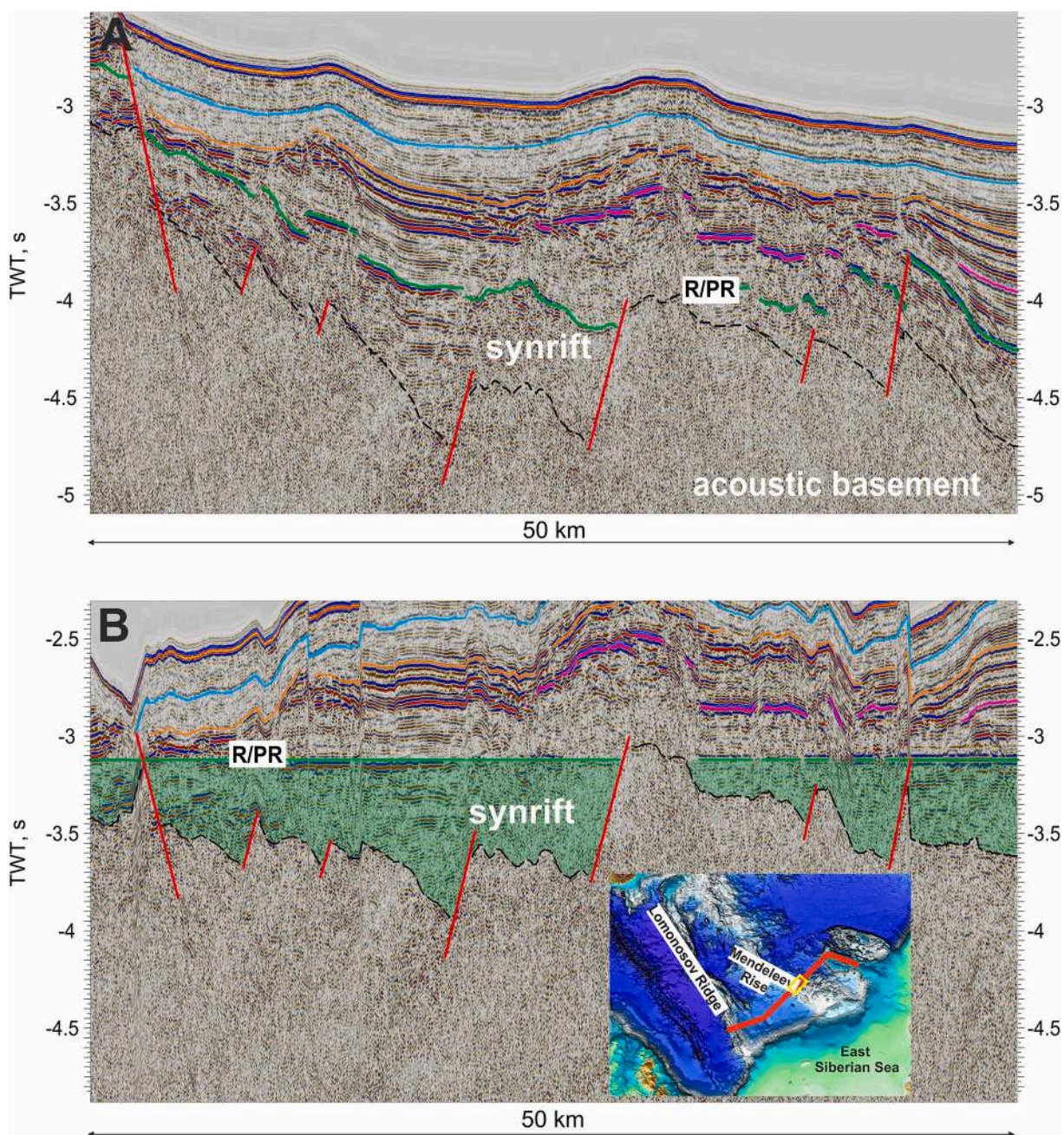


Fig. 41. A. Fragment of seismic profile shown in Fig. 37. Rift/postrift (R/PR) boundary and synrift complex are supposed. B. Profile Flattened on the rift/post-rift boundary.

water part of the Arctic Ocean. It could be 100 Ma or younger. The HARS-2 is readily traceable above this boundary (Figs. 6, 10, 11, 12, 13, 14, 16, 22, 23, 25, 26, 33, 37, 44, and 53).

3. Volcanism ended within the Mendeleev Rise approximately 80 Ma ago (Brumley, 2014; Coakley et al., 2016). This boundary approximately corresponds to the upper boundary of the seismic package associated with high-amplitude reflections (HARS-2). This 80 Ma horizon can be readily traced in the Mendeleev Rise and the Arlis Gap Buried High areas (Figs. 23, 26, 28, 29, 30, 33, 35, 37, and 44).

4. The 66 Ma boundary corresponds to the bottom of the clinoform complex observed in the North Chukchi Basin and to the MBU boundary on the Alaskan Shelf. This boundary was subsequently mapped into the deep-water part of the ocean (Figs. 10, 11, 12, 13, 14, 15, and 16).

5. The 56 Ma boundary corresponds to a breakup unconformity. It has the characteristics of a rift/postrift boundary on seismic sections. This boundary is clearly expressed on the slopes of the Eurasia Basin – in particular, on the Lomonosov Ridge and in the Laptev Sea (Figs. 7, 8, 9, 48, 49, 50, 51) and can be traced in most parts of the

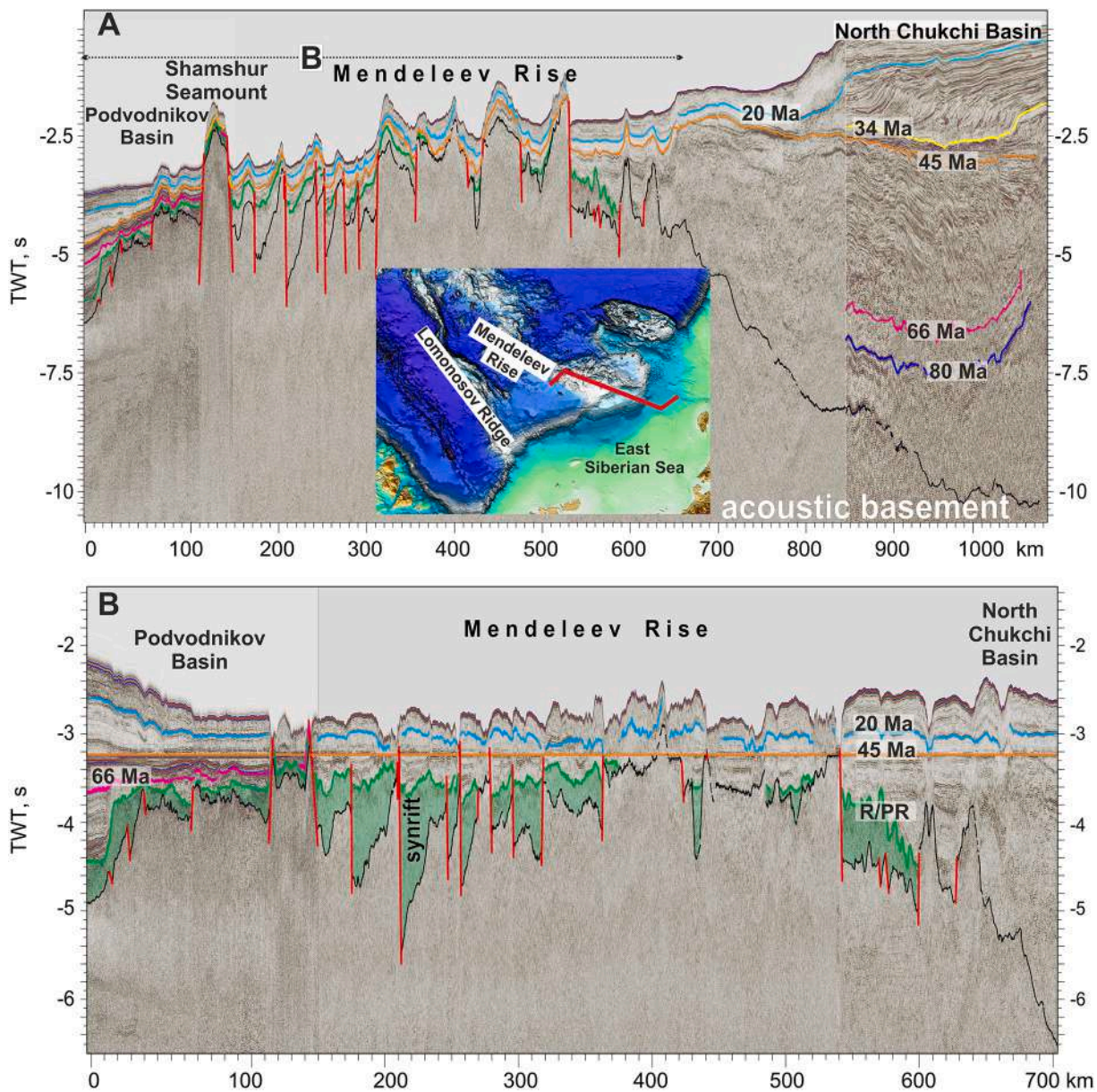


Fig. 42. A. Interpretation of composite seismic profile (lines ARC 12-17, ARC 12-01 and ARS 10F-24) for the region from the North Chukchi Basin and along the Mendeleev Rise.

Location of the profile is shown on the map. Different color lines are seismic horizons and corresponding ages (Ma). B. Profile flattened on the 45 Ma horizon. Horst/graben structure on the Mendeleev Rise acoustic basement can be observed. See also supplementary data, Fig. 42 (seismic profile without interpretation at high resolution).

Arctic Ocean along the base of the high-amplitude reflection sequence (HARS).

6. The 45 Ma boundary is primarily defined by the age of associated linear magnetic anomalies in the Eurasia Basin. It is also defined on the basis ACEX well borehole data (although different researchers disagree on age dating of the well sections that tie to this seismic horizon). This boundary corresponds to the top of the high-amplitude reflection sequence (HARS). We correlate this horizon with the timing of the onset of cooling and a concomitant sharp change in ocean sedimentation (the transition from more siliceous sediments to clays). The 56 Ma to 45 Ma section contains many high-

amplitude reflections. We associate this section with a warming epoch in the Eocene and hence – with an epoch of warmer-water sedimentation. The 45 Ma boundary corresponds to the base of the upper clinoform complex of the North Chukchi Basin. The 45 Ma seismic horizon is one of the most continuous reflections in the Arctic Ocean.

7. The 34 Ma boundary also is identified by age of associated linear magnetic anomalies in the Eurasia Basin. Clinoform complexes originating from the side of the Lomonosov Ridge are identified above this boundary in the Amundsen Basin (Fig. 25). On the East Siberian Sea and Chukchi Sea Shelf, activation of some thrust faults

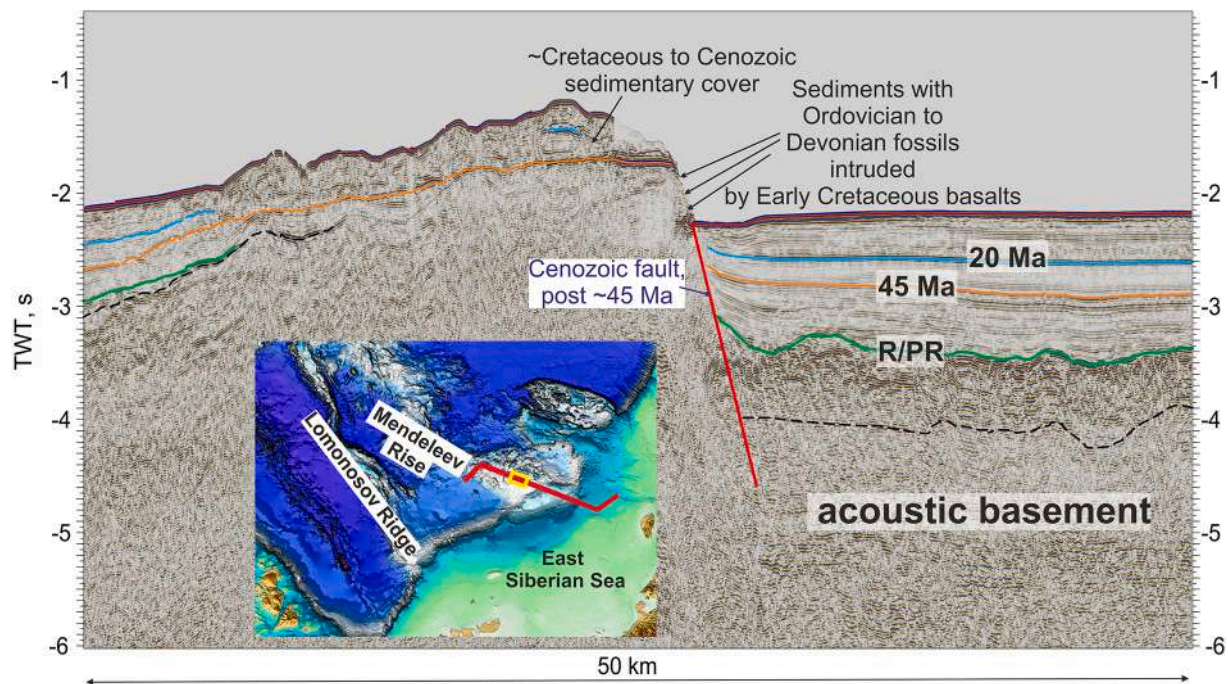


Fig. 43. Interpretation of a fragment of seismic profile (lines ARC 12-01) (Fig. 42) for the Mendeleev Rise region. Location of the profile is shown on the map. Different color lines are seismic horizons and corresponding ages (Ma). The escarpment was formed due to Cenozoic post-45 Ma extension. Samples were collected using special equipment on this scarp. Data from Skolotnev et al. (2019, 2017).

are approximately associated with this boundary (Nikishin et al., 2019; Nikishin et al., 2014) (Fig. 60).

8. The 20 Ma boundary is again mainly identified by age of associated magnetic anomalies in the Eurasia Basin. The erosional character, sometimes associated with responses to gravity tectonics (landslides, channels, and slope erosion), are commonly observed with this surface, which suggests that oceanic currents changed sharply in the Arctic Ocean at this time (Figs. 12, 13, 23, 53). Our data support an early Miocene onset of a ventilated circulation regime in the Arctic Ocean that was attributed to the opening of the Fram Strait as proposed by Jakobsson et al. (2007).

4.15. Vertical intraplate tectonic movements at 45-20 Ma

Our analysis of a grid of seismic lines shows that either syntectonic depositional wedges (SDW) or syntectonic deposition lenses with ages of 45-20 Ma are present in the Podvodnikov Basin and in the Makarov Basin (Figs. 6, 12, 13, 14, 25, 26, 28, 29, 30, 33, 37, and 61). These deposits progressively pinch out toward the Lomonosov Ridge from the side of the Podvodnikov Basin. This seismic sequence also pinches out toward the Arlis Gap Buried High from the side of the Makarov Basin and is absent in the ACEX wells on the Lomonosov Ridge.

In many instances, onlapping onto the 45 Ma surface is observed. It is likely that differential vertical movements started at 45 Ma. At that time, relative subsidence was initiated in the Podvodnikov and Makarov basins with the onset of relative uplift at the Lomonosov Ridge (this corresponds to the hiatus in the ACEX wells). A phase of relative uplift is also noted for the North Janette Basement High at the border of the North Chukchi and Podvodnikov basins (Figs. 11, 12, 14). On the East Siberian Sea-Chukchi Sea shelves and in the Amundsen Basin, a pronounced phase of low-amplitude normal faulting appears to have occurred around 45 Ma ago (Figs. 14, 15, 23, 24, 62) when activation of

normal faulting was established for the area of the Lomonosov Ridge (Figs. 4, 5, 6, 8, 11, 61). As a result of these vertical movements, the Makarov Basin became a separate basin. Phases of relative uplift possibly took place for the Mendeleev Rise as well at this time (Figs. 33, 37). A major normal fault between the Mendeleev Rise and the Podvodnikov Basin probably was activated between 45-20 Ma (Figs. 35, 37, 44). Further, we can unambiguously identify additional substantial vertical movements and phases of normal faulting between 45-20 Ma in this area. The principal driver behind these structural events can be explained by normal oceanic crustal spreading which then passed into ultra-slow spreading at ca. 45 Ma along the Gakkel Ridge (Glebovsky et al., 2006). The transition to ultra-slow spreading and the ultra-slow spreading itself probably occurred synchronously with the onset of super-regional intraplate. The cause of these processes is discussed in detail in Paper 3 (Nikishin et al., 2021b).

4.16. Comparison of different seismic stratigraphic frameworks

The seismic stratigraphic scheme for the area of the Podvodnikov Basin presented in Weigelt et al. (2014) is most widely accepted. This scheme is based on data from the ACEX wells as well as on correlation with major events in the Arctic. In general, our seismic stratigraphic scheme is similar that presented by Weigelt et al. (2014). However, one fundamental difference is that our 45 Ma boundary corresponds to their 23 Ma horizon. Weigelt et al. (2014) substantiated their age determination by arguing that a major regression took place at the end of Oligocene with which the hiatus in the ACEX wells is associated. In contrast, we argue that the correlation of the 45 Ma boundary with linear magnetic anomalies in the Eurasia Basin and with the clinofold complex in the Chukchi Sea places this boundary at 45 Ma. Another difference is that our boundary of 100 Ma, again based primarily on recognition of linear magnetic anomalies, compared with an age of 66

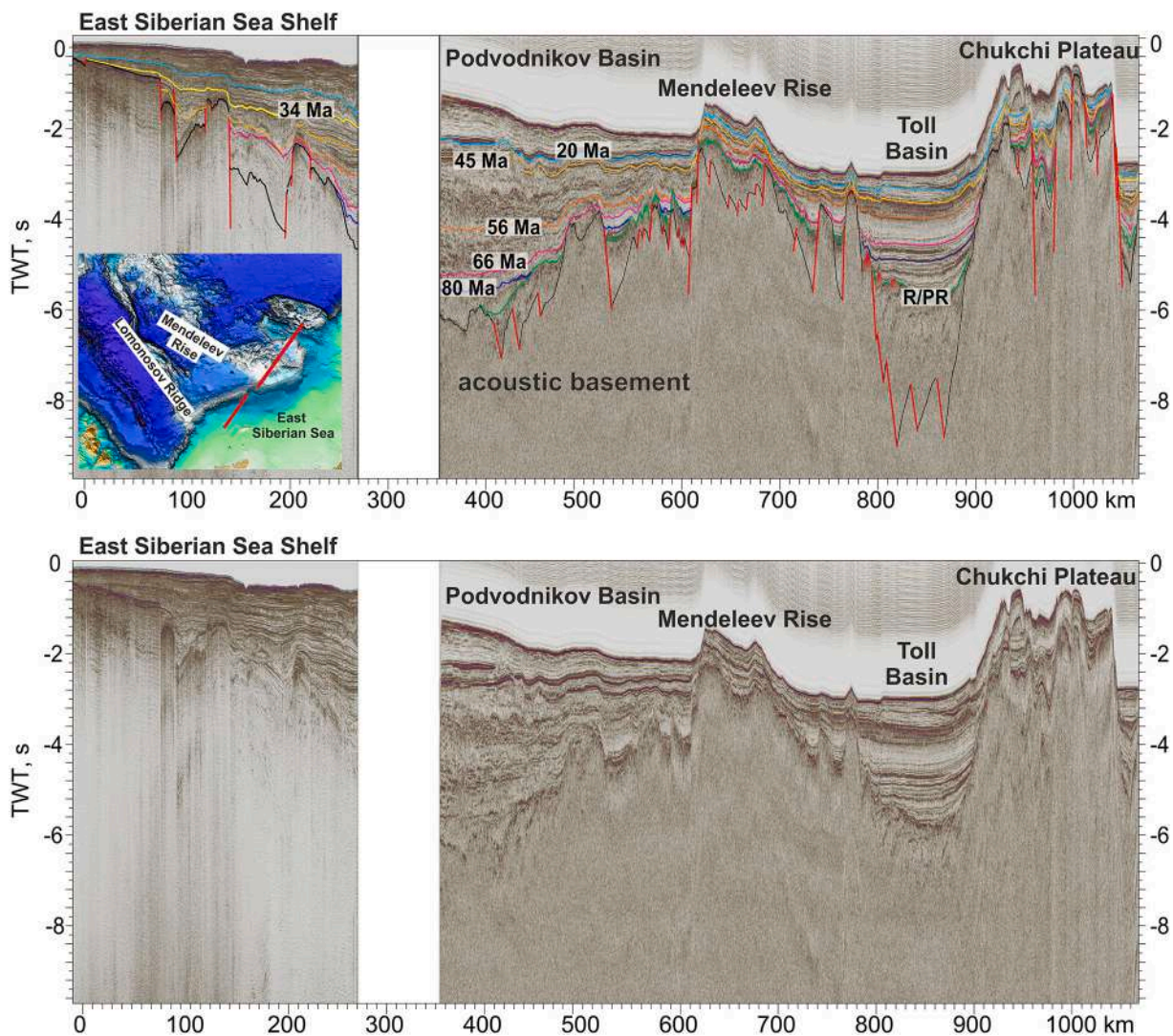


Fig. 44. Interpretation of composite seismic profile from the East Siberian Sea Shelf to the Chukchi Plateau (lines MAGE ESS1620 and ARC 12-03). Location of the profile is shown on the map. Rift systems of East Siberian Sea, Podvodnikov Basin, Mendeleev Rise, Toll Basin, and Chukchi Plateau possibly constitute a single geodynamic system with nearly synchronous history. See also supplementary data, Fig. 44 (seismic profile without interpretation at high resolution).

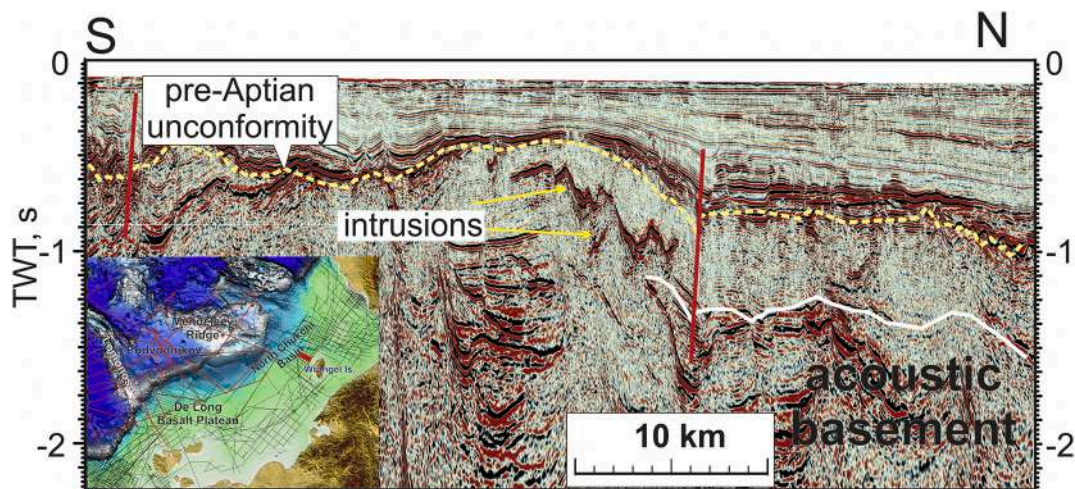


Fig. 45. Interpretation of a fragment of seismic profile. Location of the profile is shown on the map. A number of seismic anomalies can be interpreted as magmatic intrusions. All intrusions are located below horizon 125 Ma. Data courtesy of the Ministry of Natural Resources, Russia.

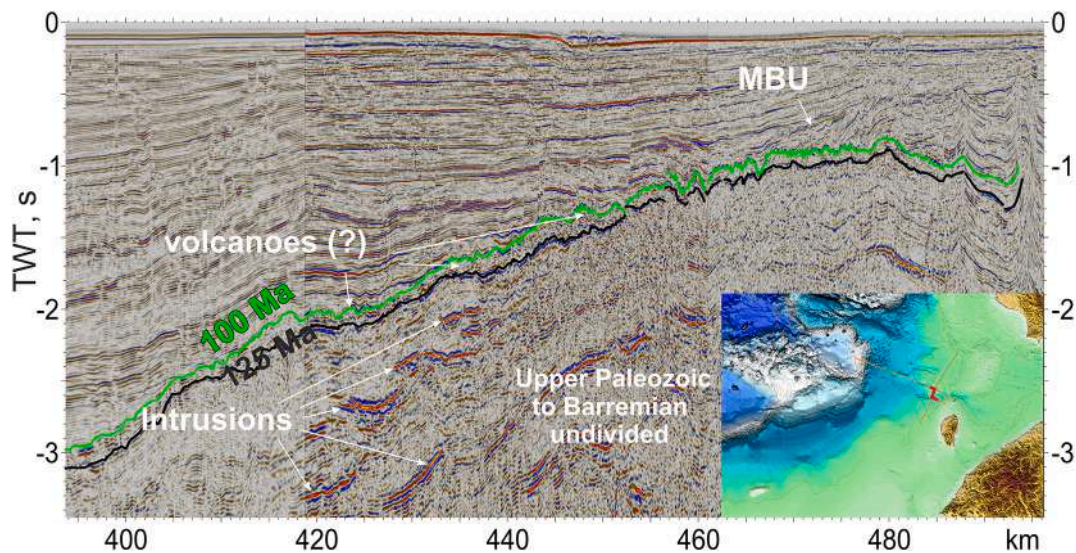


Fig. 46. Interpretation of a composite seismic profile (lines ION11_4200A, ION15_2000, ION15_4225). Location of the profile is shown on the map. A number of high-amplitude reflections below 125 Ma boundary can be identified. These can be magmatic intrusions within Paleozoic to Lower Cretaceous deposits. A chaotic seismic unit above 125 Ma can be a sequence containing volcanoes.

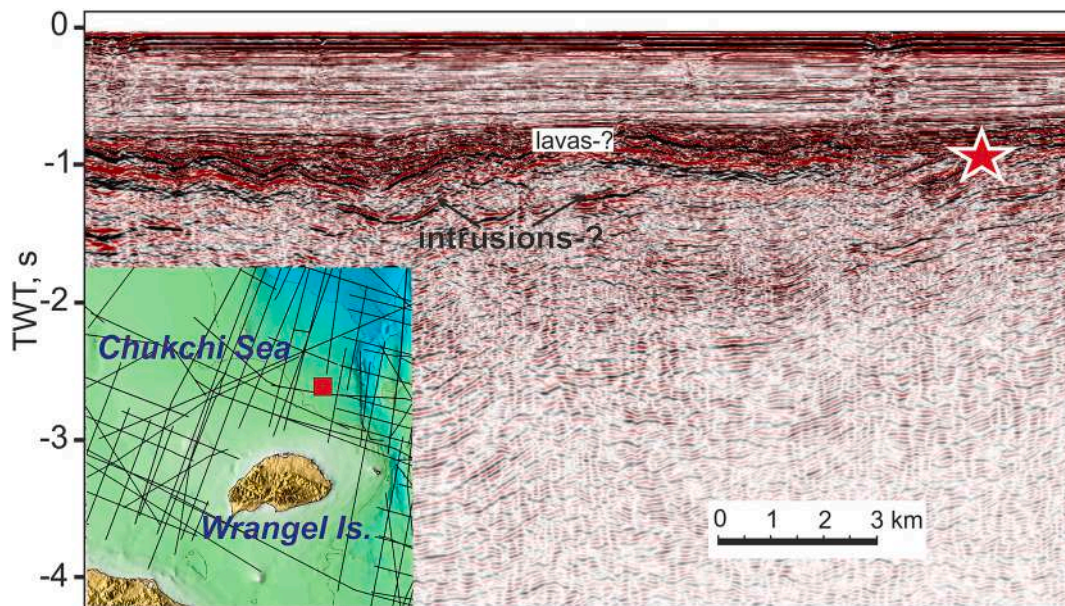


Fig. 47. Fragment of seismic profile for southern slope of the North Chukchi Basin. See map for location. Star shows a top of calculated magnetic bodies at depth close to 700 meters. A volcanic complex and intrusions can be recognized. Data courtesy of the Ministry of Natural Resources, Russia.

Ma (Base Tertiary) according to Weigelt et al. (2014) scale. Nonetheless it is noteworthy that irrespective of age differences, we have identified the same main seismic stratigraphic units.

For the Makarov Basin, the seismic stratigraphic framework in Evangelatos and Mosher (2016) in general coincides with our time scale. Nonetheless, differences are likely for interpretation of lower horizons.

A new seismic stratigraphic framework for the North Chukchi Basin has been proposed by Ilhan and Coakley (2018). Our stratigraphic schemes are very similar for the Aptian to Cenozoic deposits and we

reach similar conclusions (Nikishin et al., 2017; Nikishin et al., 2014). There is, however, one important difference is in the age of the lower synrift unit. Ilhan and Coakley (2018) recognized a synrift complex in the Toll Basin characterized by SDRs. They interpreted the rift/postrift boundary as a condensed section with an age approximately between Middle Jurassic and Neocomian (up to Barremian) with rifting having taken place during Jurassic time. We observe a similar situation in the Toll Basin with SDRs infilling a half graben (Nikishin et al., 2019, Nikishin et al., 2014) (Figs. 33, 34). We observe a number of SDR-like

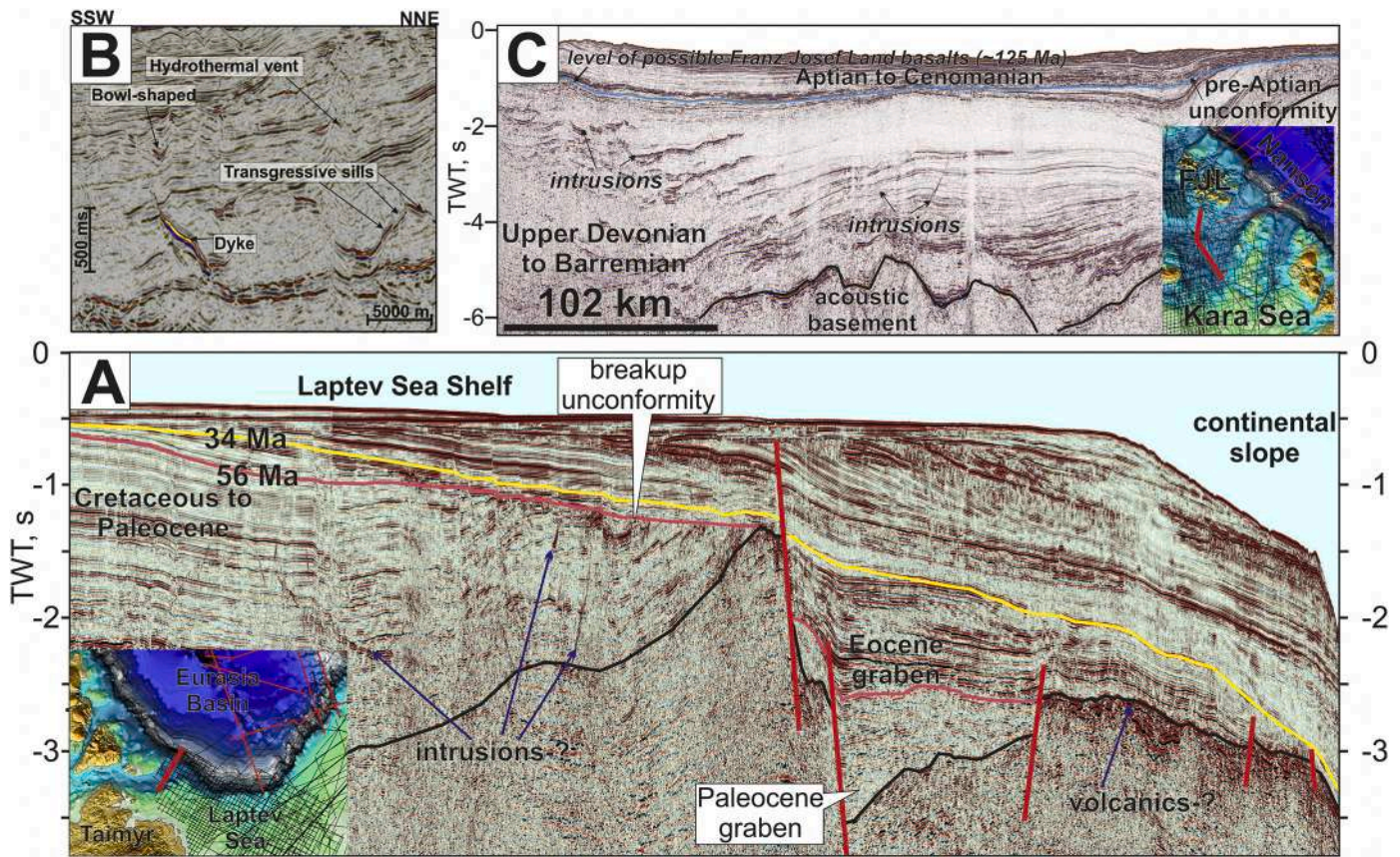


Fig. 48. A. Interpretation of seismic profile MAGE ESS1409. Location of the profile is shown on the map. Breakup unconformity is clearly observed (56 Ma). A number of seismic anomalies can be interpreted as magmatic intrusions. All intrusions are located below horizon 56 Ma. Bright reflection package at the basement could be interpreted as possible volcanics. B. Example of seismic expression of well documented intrusions in Stappen High, SW Barents Sea (Omosanya et al., 2016). Bowl-shaped sills are found above extrusive deposits. Dykes are vertical to sub-vertical positive impedance reflections, which acted as conduits for emplacement of other sills in this area. The extrusive rocks are parallel to sub-parallel to layered positive high amplitude anomalies. C. Fragment of seismic profile for the northern part of the Barents Sea. Intrusions are clearly observed. The profile is located close to Franz Josef Land where Early Cretaceous intrusions and basalt lavas are well documented.

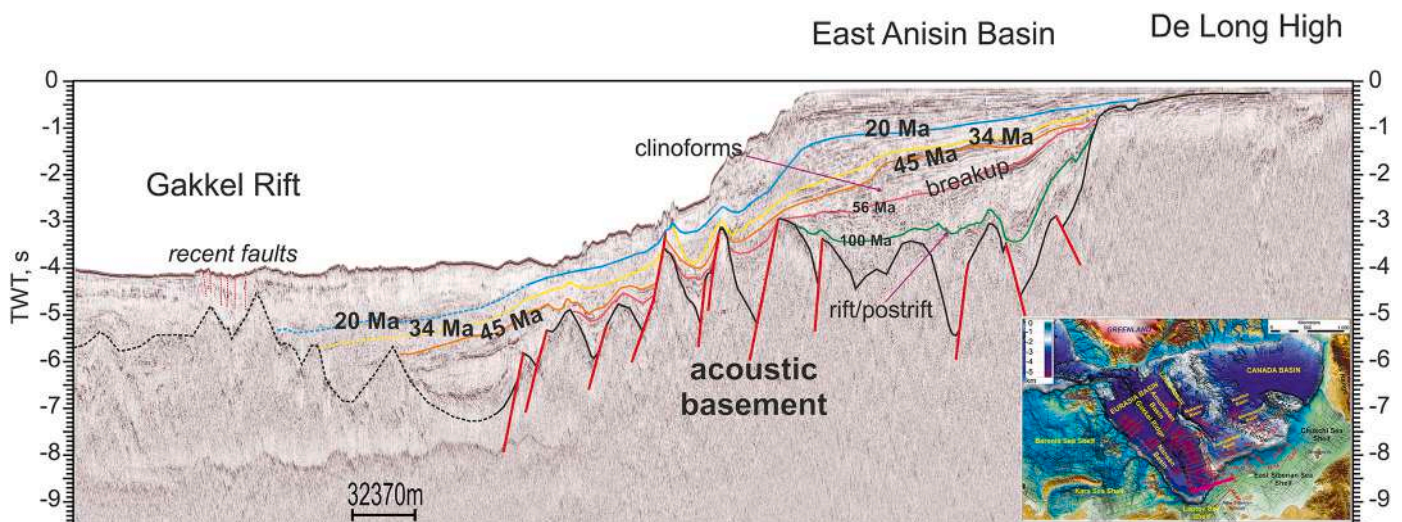


Fig. 49. Interpretation of seismic profile ARC-12-16 (western part) for area from the Laptev Sea Shelf to Eurasia Basin margin and Gakkel Rift (Nikishin et al., 2018, with additional interpretation). See also supplementary data, Fig. 49 (seismic profile without interpretation at high resolution).

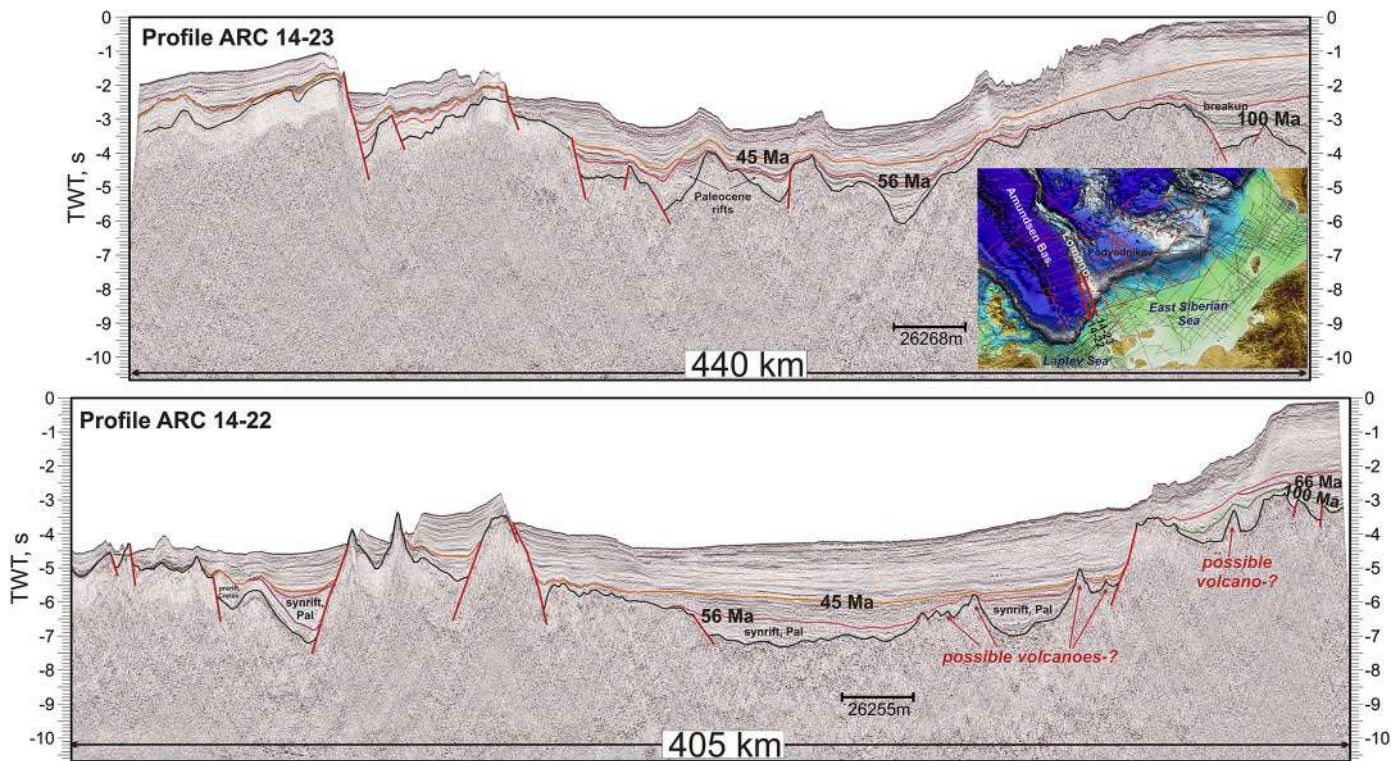


Fig. 50. Interpretation of seismic profiles ARC 14-23 and ARC 14-22 for the southern part of the Lomonosov Ridge and adjacent shelf area. See also supplementary data, Fig. 50 (seismic profile without interpretation at high resolution).

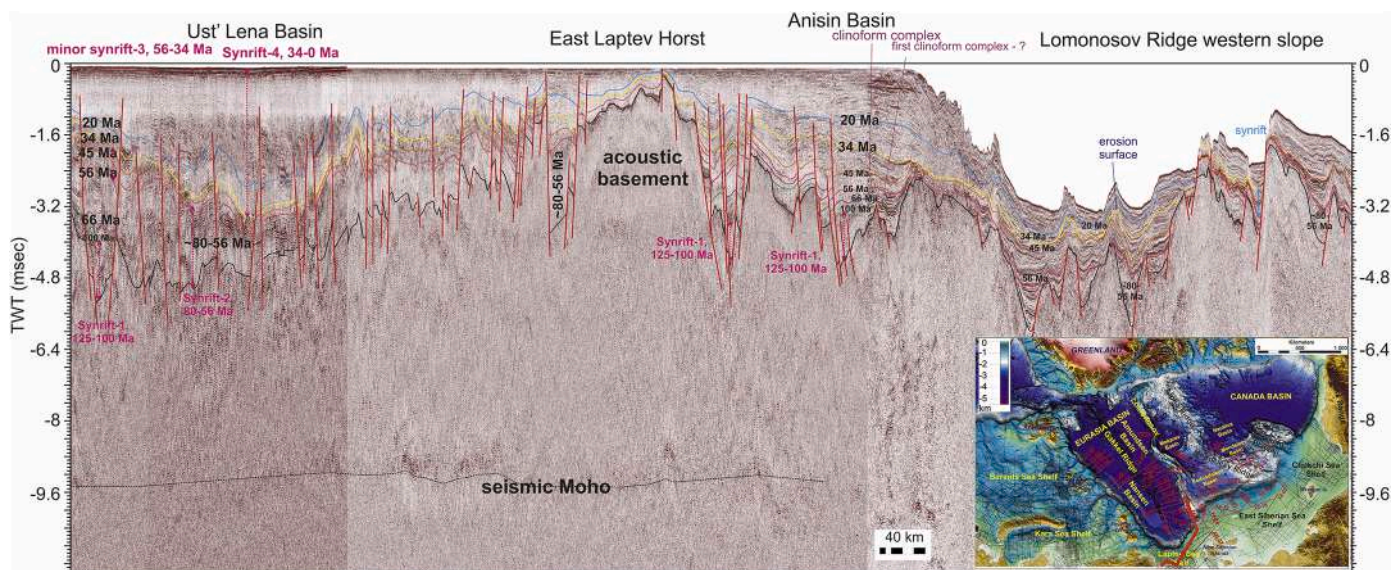


Fig. 51. Interpretation of composite seismic profile (lines ION11-1700, ION11-4600 and ARC 14-23) for the Laptev Sea Shelf and along the Lomonosov Ridge slope. Location of the profile is shown on the map. Different color lines are seismic horizons and corresponding ages (Ma). See also supplementary data, Fig. 51 (seismic profile without interpretation at high resolution).

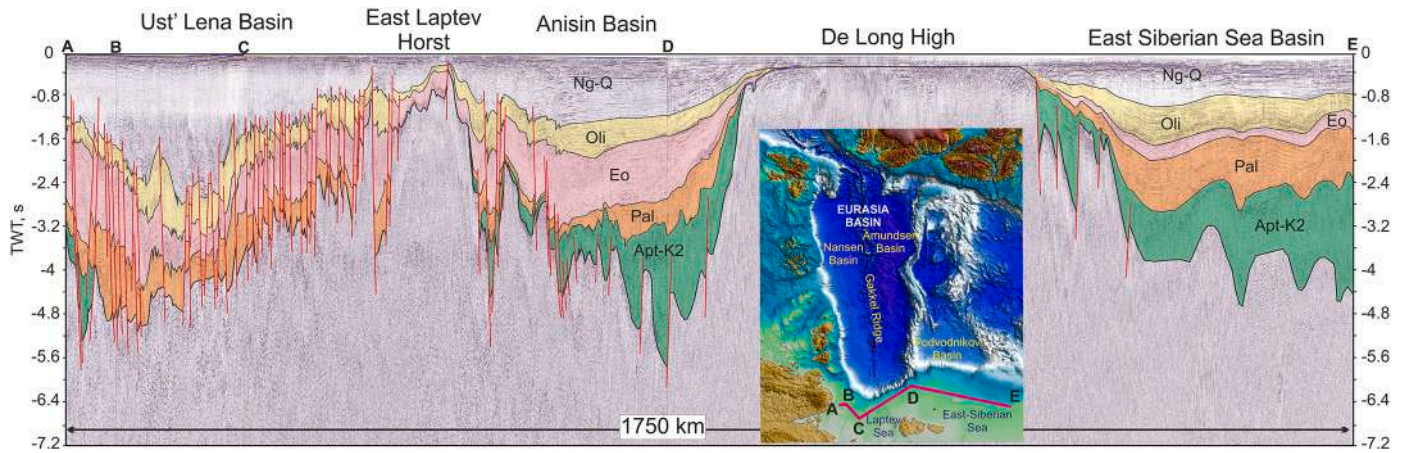


Fig. 52. Interpretation of composite seismic profile from the Laptev Sea Shelf to the East Siberian Sea Shelf (lines ION 11-1700, ION 11-4600 and ARC 12-16). Location of the profile is shown on the map. See also supplementary data, Fig. 52 (seismic profile without interpretation at high resolution).

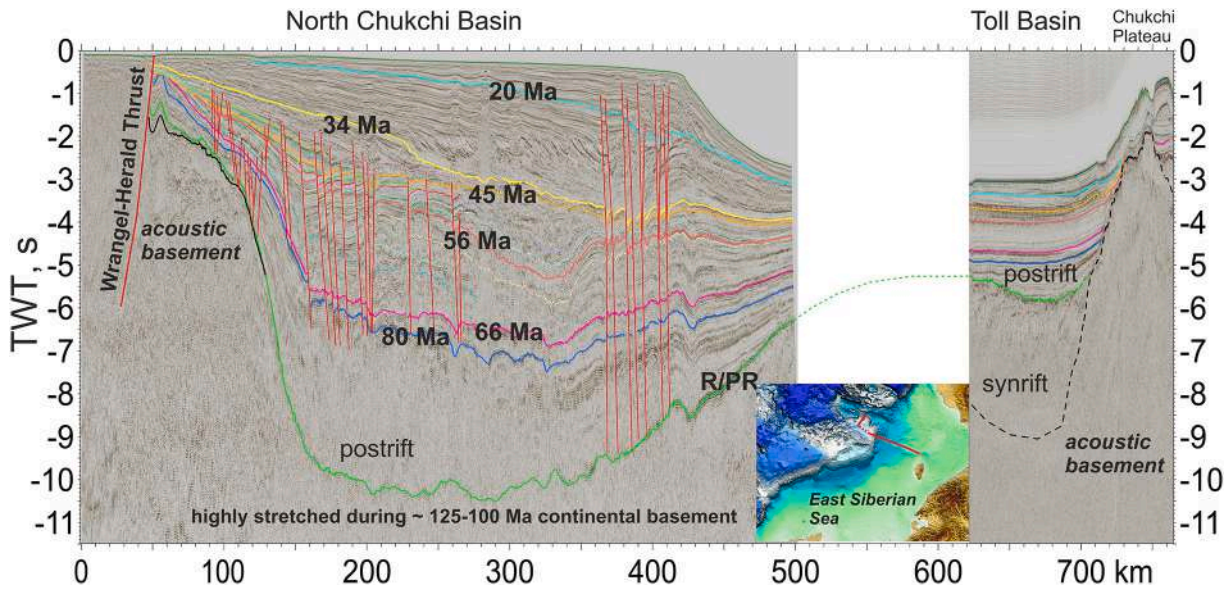


Fig. 53. Interpretation of composite seismic profile from the Chukchi Sea Shelf to the Toll Basin (lines ARC12_03, ION11_4200A). Location of the profile is shown on the map. Rift/postrift boundary in the Toll Basin possibly coincides with the base of sedimentary cover of the North Chukchi Basin, implying that the flattened bottom of the North Chukchi Basin is a rift/postrift boundary (green line). See also supplementary data, Fig. 53 (seismic profile without interpretation at high resolution).

units in the Mendeleev Rise region as well, but according to our interpretation Aptian or Aptian-Albian rifting was followed by late Cretaceous postrift subsidence with the rift/postrift boundary close to 100 Ma. We have no evidence for the presence of condensed sections between synrift and postrift complexes in the Podvodnikov-Mendeleev-Toll area (Figs. 33, 34, 35, 36, 37, 38, 39, 40 and 41). This rift/postrift boundary is very similar to well-known examples in other passive continental margins.

Hegewald and Jokat (2013) have prepared a seismic stratigraphy for the Chukchi Abyssal Plain (Toll Basin). In total, six horizons with ages between Barremian/Hauterivian and Top Miocene were identified. The age control on seismic data was based on five exploration wells located on the northwest coast of Alaska coupled with additional seismic reflection lines from the Chukchi Shelf. Their oldest horizon is the Lower

Cretaceous unconformity (Barremian-Hauterivian). In any case, they concluded that it was not possible to map each horizon through the entire new multi-channel seismic grid because of the presence of basement highs, faults, unconformities, and variations in sediment thickness. They interpret the Chukchi Abyssal Plain (Toll Basin) to have evolved in Jurassic to Early Cretaceous time during the opening of the Canada Basin. We have performed a similar study, correlating seismic horizons with exploration wells located on the northwest coast of Alaska. On the whole, correlations of our seismic lines with the wells on the Alaskan Shelf were ambiguous and as a result, unreliable. Five different teams from Moscow State University, Geological Survey of Russia, and Rosneft Oil Company suggested different correlations with different ages. Hegewald and Jokat (2013) and Ilhan and Coakley (2018) reported the same problem. The key driver in this conundrum lies in the selection of a

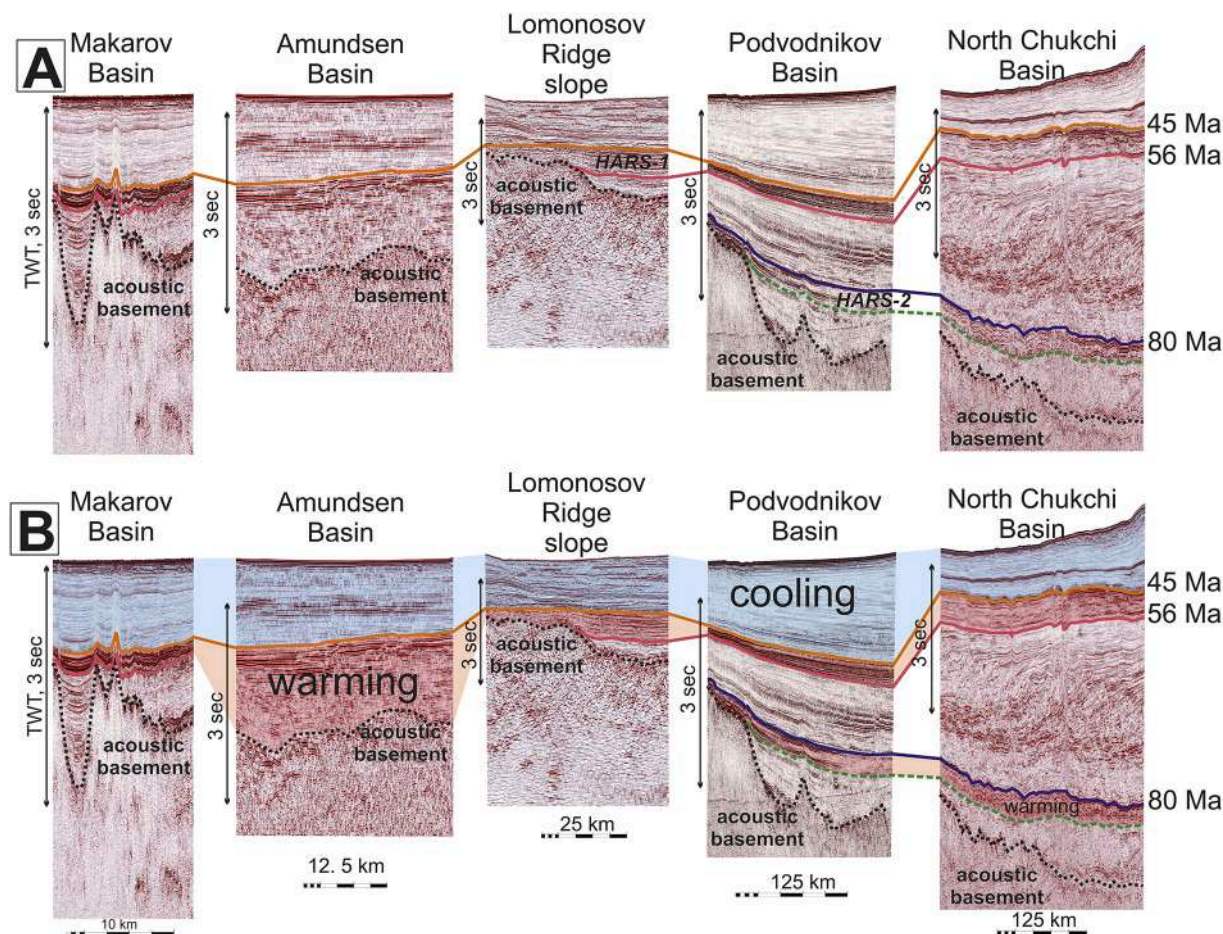


Fig. 54. Possible climatic seismic boundaries in different basins of the Arctic Ocean. A. Fragments of seismic profiles. B. Possible seismic units with anomalous climatic warming or cooling significance.

regional geodynamic model. Hegewald and Jokat (2013) and Ilhan and Coakley (2018) proposed that the Chukchi Abyssal Plain evolved during the opening of the Canada Basin. They used the well-known rotation model of the Amerasia Basin opening with simultaneous opening of the entire basin (e.g. Embry, 1990; Grantz et al., 2011; Grantz and Hart, 2012). According to our geodynamic model, however, the Toll Basin is not older than the rift system in the East Siberian and Chukchi Seas shelf. Hence, these rift systems are not older than Aptian. Nikishin et al. (2014) and Ilhan and Coakley (2018) recognized a synrift complex in the Toll Basin presented by SDRs. New data show that SDR-like units are common for the Mendeleev Rise and Podvodnikov Basin. According to our model, these SDRs have a HALIP age (not older than ± 130 Ma).

A number of geologists use the Arctic Alaska Basin stratigraphy for the North Chukchi Basin (e.g., Hegewald and Jokat, 2013; Ilhan and Coakley, 2018). They propose that the North Chukchi Basin has a Jurassic section and originated during Jurassic rifting. We constructed a geological section for the Arctic Alaska Basin and the North Chukchi Basin (Fig. 63). Clearly, the basins are not characterized by a similar stratigraphy. The Arctic Alaska Basin has a Beaufortian unit (Jurassic-Valanginian-?) with transport of clastic material from the North (Houseknecht, 2019a, 2019b). The North Chukchi Basin has no such unit at the base. The Arctic Alaska Basin has a condensed section between the Lower Cretaceous Unconformity (~intra-Valanginian) and GRZ (gamma-ray zone) (Aptian to Albian). The thickness of this unit is

minimal (Fig. 63) (Houseknecht, 2019a, 2019b) and the time of deposition is close to 10-20 million years. This unit is absent in the North Chukchi Basin. Consequently, our conclusion is that it is not reasonable to apply the timing of events in Arctic Alaska to those of the North Chukchi Basin.

Within our collective of co-authors, as is to be expected, different teams have used somewhat different stratigraphic boundaries for the shelf basins. These differences are not significant and discussions remain ongoing about precise ages of horizons within the Cretaceous and Cenozoic. Some variants of the stratigraphy were published by Popova et al. (2018) and Skaryatin et al. (2020). Evidently in the absence of wells, we have not yet seen the establishment of an unequivocal stratigraphic scheme for the Arctic Ocean at large.

5. Discussion

5.1. Correlation of major tectonic events in the geological history of the Arctic Ocean

Our new data allow for the refinement of existing hypotheses regarding the chronology of events in the history of the Arctic Ocean. Below we focus on the formation history of the major basins and uplifts.

The new data confirm many previously held assumptions concerning the history of the Eurasia Basin. Opening of the basin started at ca. 56 Ma

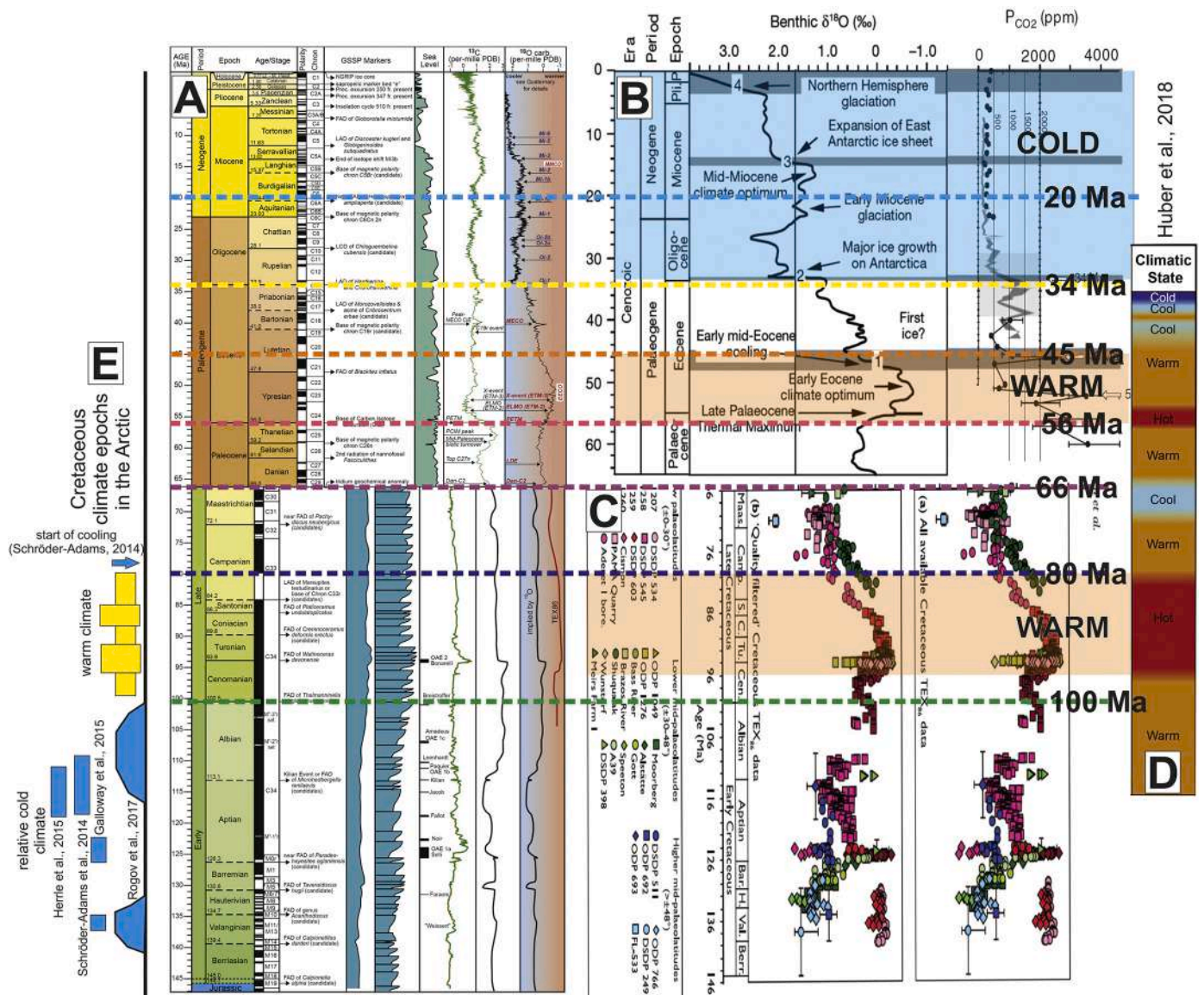


Fig. 55. Cretaceous to Cenozoic global climatic events and climatic stratigraphy of the Arctic Ocean. A. Global time scale (Ogg et al., 2016). B. Main climatic events in the Arctic Ocean in the Cenozoic (Stein, 2008). C. Main global Cretaceous climatic events (O'Brien et al., 2017). D. Global climatic stages (Huber et al., 2018). E. Cretaceous climatic epochs in the Arctic region (Schröder-Adams, 2014; Galloway et al., 2015; Herrle et al., 2015; Rogov et al., 2017). Horizontal colored dashed lines with ages represent seismic horizons.

(Glebovsky et al., 2006; Gaina et al., 2011; Pease et al., 2014; Coakley et al., 2016; Nikishin et al., 2017, 2018; Weigelt et al., 2020). Our data show that the opening of the Eurasia Basin was preceded by continental rifting in the western part of the Laptev Sea Basin (Figs. 48, 49) and on the western slopes of the Lomonosov Ridge (Figs. 7, 8, 9, 50, and 51). In the area of the Laptev Sea, basaltic magmatism probably preceded the opening of the Eurasia Basin (Fig. 48). If this is the case, the dynamics of Eurasia Basin opening is similar to the dynamics of the opening of the North Atlantic as proposed, for example, by Gaina et al. (2017), Wilkinson et al. (2017), and Foulger et al. (2020).

A remaining question concerns the model for the geological structure and history of the Amerasia Basin. Data presented in this paper demonstrate that the North Amerasia Domain (the Mendeleev Rise

together with adjacent deep-water basins) together with the Mesozoic rift system in the Laptev-East Siberian-Chukchi seas comprise a single geodynamic system and originated during the Aptian-Albian. The North Amerasia Domain is separated from the South Amerasia Domain (or Canada Basin Domain) by a proposed Amerasia transform fault (Fig. 2) (Nikishin et al., 2014). We include the Arctic Alaska Basin within the South Amerasia Domain comprising the margin of the Canada Basin. We propose here that the South Amerasia Domain had a different geodynamic history and timing of evolution than the North Amerasia Domain.

Regional seismic data without borehole control can lead to different interpretations with different models of proposed ages for different seismic horizons and units. Nonetheless, the seismic 2D grid

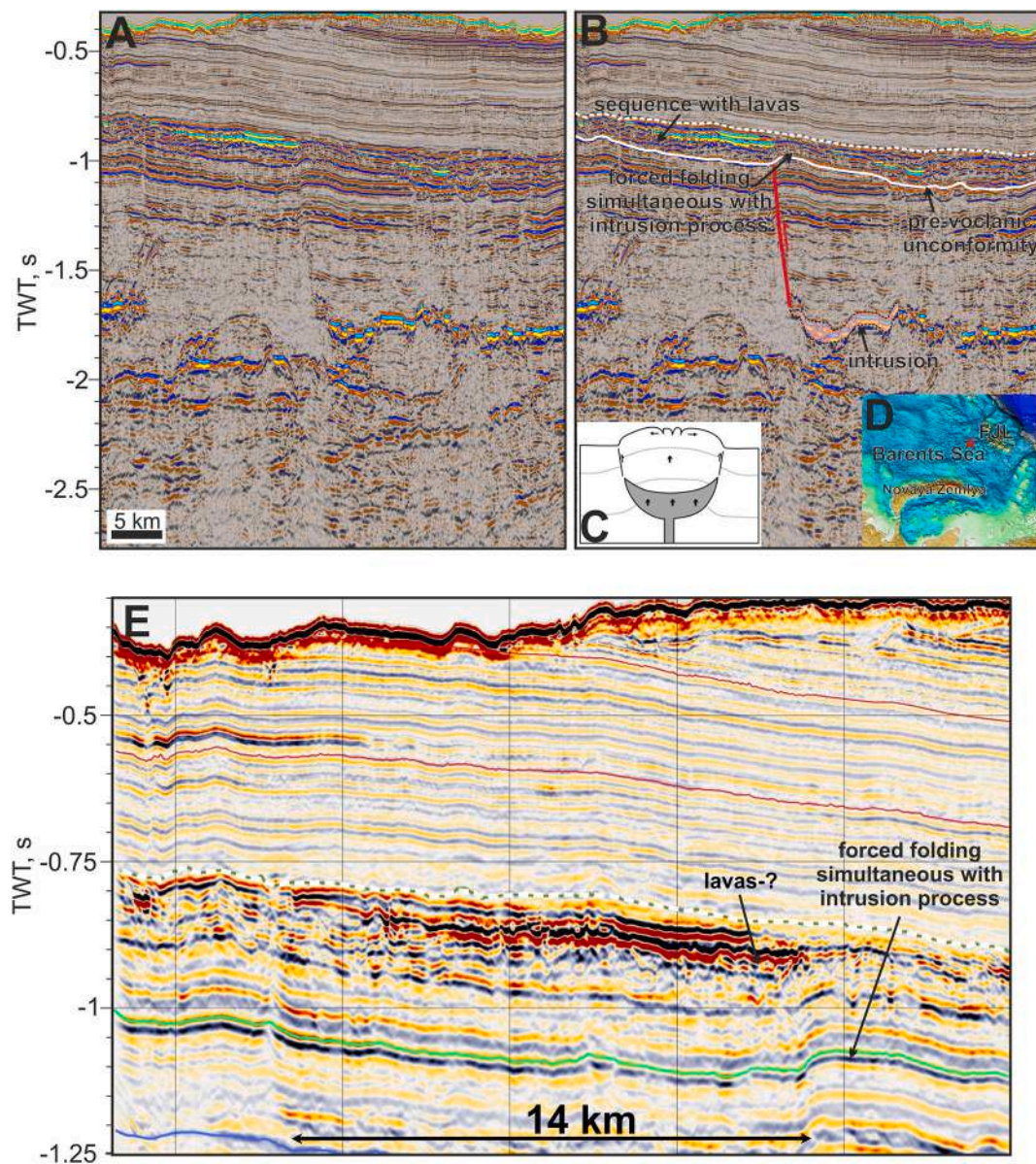


Fig. 56. A. Fragment of seismic profile for the Barents Sea. B. Interpretation of this seismic profile with possible lavas and intrusions. Correlations of seismic data with boreholes show that the age of lavas is close to the Barremian-Aptian boundary. C. Model of intrusion propagation and forced folding above the intrusion (Mathieu et al., 2008). D. Location of seismic profile (star). E. Fragment of the same profile with details. Data courtesy of the Ministry of Natural Resources, Russia.

demonstrates definitively a sequence if not the precise timing of geological events. We can recognize sequences of seismic complexes that originated within the context of uniform tectonic environments and can therefore be described as tectonostratigraphic units. Tectonostratigraphic units and their associated sequences form the basis of our tectonic restorations.

The first mega-tectonostratigraphic or seismic megasequence is the Paleozoic to Jurassic unit. It is located to the north of the Zhokhov-Wrangell-Herald-Brooks thrust belt. We do not further discuss this megasequence in detail here. This unit is documented in the Arctic Alaska Basin as Ellesmerian and Beaufortian (e.g., Homza and Bergman, 2019; Houseknecht, 2019a, 2019b). Our work suggests it as possible Ellesmerian and Beaufortian to the north of Wrangell Island (Figs. 10, 19).

The second proposed seismic megasequence is Late Jurassic to Neocomian in the North Amerasia Domain and Beaufortian in the South Amerasia Domain. We have mapped the distribution and characteristics of these seismic megasequences (Fig. 64), which are expressed as foredeep seismic megasequence in the Russian shelf. We can recognize a belt of foredeep basins north of the Zhokhov-Wrangell-Herald thrust belt (Figs. 2, 31). The Verkhoyansk-Chukotka Late Jurassic to Barremian collisional orogen was formed south of this thrust belt. These foredeep basins could be similar to the Verkhoyansk Foredeep Basin observed in Siberia. The age of the foredeep seismic megasequence likely is similar to the age of orogeny and close to Late Jurassic to Barremian.

The Arctic Alaska Basin is characterized by another type of seismic megasequence for this time interval (Fig. 64). A shelf basin existed in

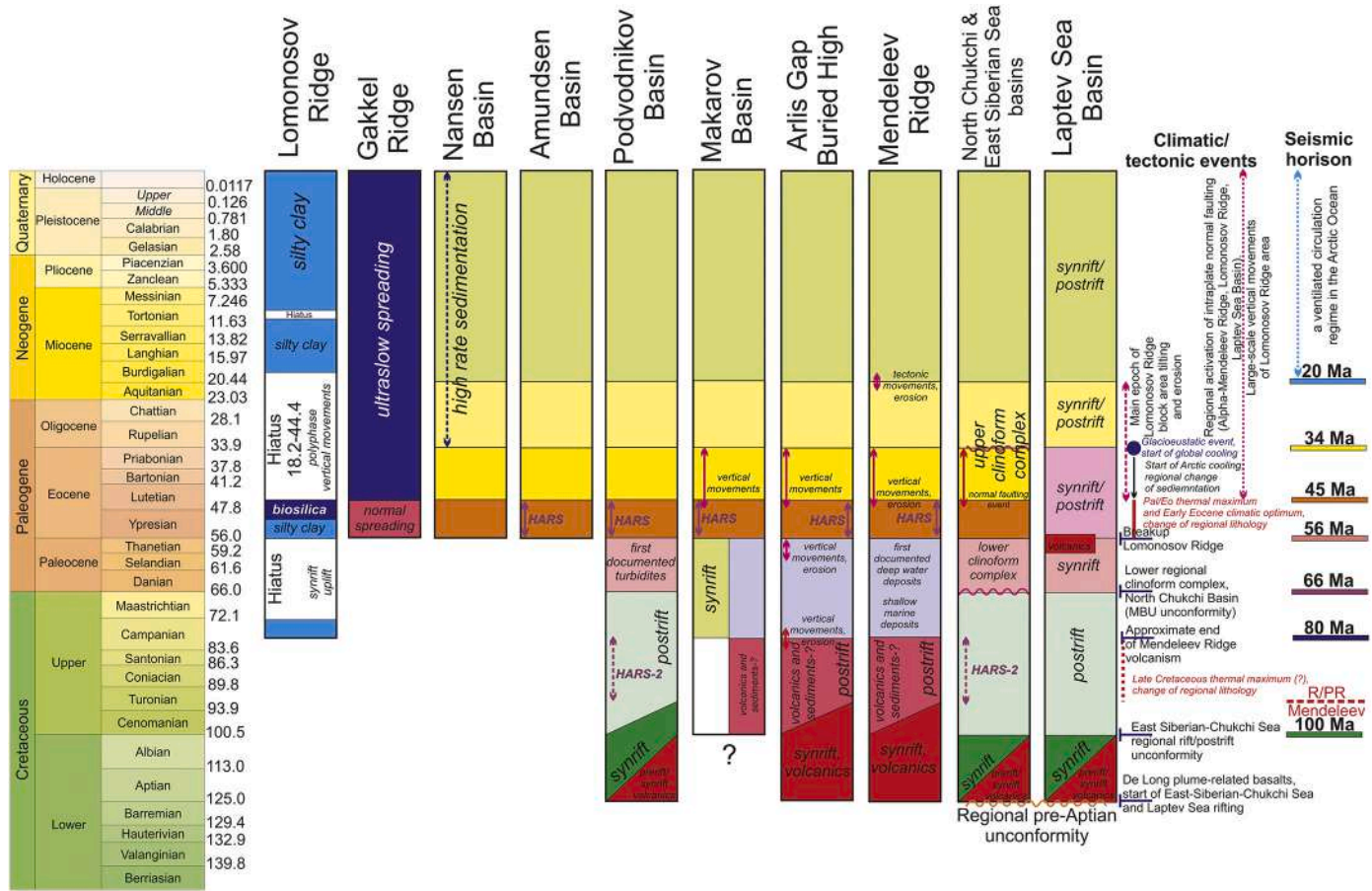


Fig. 57. Chronostratigraphic chart for the Arctic Ocean and Laptev Sea-Chukchi Sea Shelf. Lomonosov Ridge stratigraphy after Moran et al. (2006), Backman et al. (2008), Backman and Moran (2009). Gakkel Ridge spreading history after Glebovsky et al. (2006). Climatic events mainly from Moran et al. (2006), Backman et al. (2008), Stein (2008) and Stein et al. (2015). R/PR – possible rift/ postrift boundary for the Mendeleev Rise and Podvodnikov Basin.

this region during the time from Jurassic to Hauterivian with transport of clastic material from the north (possible Beaufort rift shoulder) (Houseknecht, 2019a, 2019b). Pre-Hauterivian (LCU) erosion took place in northern and western parts of the basin (Houseknecht, 2019a, 2019b). The uplift of the Beaufort High could be connected with rift shoulder uplift or a forebulge rise. The Colville Basin subsidence could be influenced by tectonic loading due to the start of Brookian orogenesis (e.g., Homza and Bergman, 2019; Houseknecht, 2019a, 2019b). The Lower Cretaceous Unconformity (LCU) was interpreted as being associated with continental break-up (Helwig et al., 2011) or as a result of flexural uplift related to Brookian orogenesis (Homza and Bergman, 2019).

We can observe a pronounced difference between the Russian and Alaskan parts of the basins for Late Jurassic to Neocomian time. We do not have any evidence for the existence of the North Chukchi Basin during this time and have proposed a strike-slip Neocomian fault between the South Amerasia and North Amerasia domains (Fig. 64) (Nikishin et al., 2014).

The third significant seismic megasequence is the package of proposed Aptian to Albian units. We have mapped the distribution and characteristics of these seismic megasequences (Fig. 65). Continental synrift and postrift seismic sequences, which spread from the Laptev Sea to the Chukchi Sea, are typical of the Russian shelf (Figs. 6, 10, 11, 20,

21, 22, 23, 24, 25, 26, 32, 44, and 52). The associated rift basins contain continental basalts. The De Long basalts have an isotopic age of ca. 105-130 Ma as we discussed above. We propose that the North Wrangel and Anisin basalts have a possible similar HALIP age. There are three key arguments for an Aptian-Albian age of continental rifting: (1) some rifts are located above the Neocomian collision orogen and could be interpreted as collapse structures; (2) seismic data demonstrate that synrift complexes overlap foredeep seismic megasequences with possible Late Jurassic to Barremian age (Fig. 31); (3) HALIP basalts lie at or near the base of a number of rifts (Figs. 21, 32). We can trace a rift/ postrift Cretaceous boundary at ca. 100 Ma from the shelf area toward the Podvodnikov and Toll basins and Mendeleev Rise (Figs. 6, 10, 11, 12, 13, 14, 16, 22, 23, 25, 26, 44, and 53). All rifts or half-grabens have nearly the same rift/ postrift boundary on the shelf and in deep-water areas. We discussed above that the age of this boundary could be younger in the deep-water area. Graben structures are typical for the Podvodnikov and Toll basins. SDR-like units are common features for these basins. The Mendeleev Rise has a typical structure of half-grabens and highs. Many half-grabens have SDR-like complexes. We recognized a number of possible volcanoes in the region of the Mendeleev Rise, Podvodnikov Basin and Arlis Gap (Figs. 16, 28, 29, 30, 34, and 36). The Mendeleev Rise has an axial line that separates SDRs or half-grabens with different polarity (Figs. 33, 34, 35, 36, 37, 38, 39, 40, 41, and 44). The Toll Basin

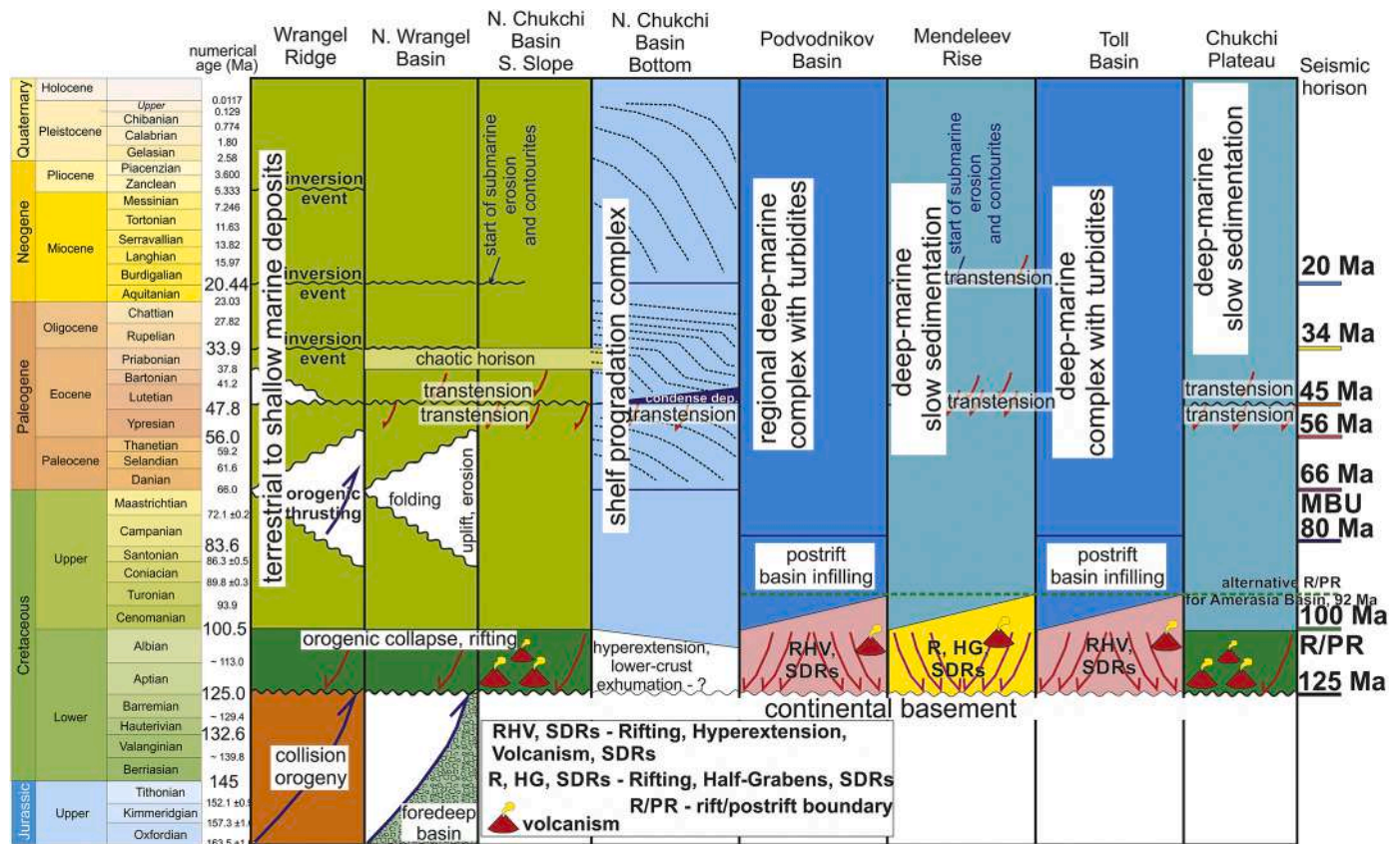


Fig. 58. Chronostratigraphy and main seismic complexes of the Chukchi Sea and adjacent region of the Arctic Ocean. Time scale is from <http://www.stratigraphy.org/index.php/ics-chart-timescale>.

has an axial rift or trough in the northern part (Figs. 65, 66, 67), which trends along the axial part of the basin. This trough directly coincides with a strong magnetic anomaly (see, e.g., Gaina et al., 2011). One possible explanation for this trough is that it represents an aborted start of lithospheric separation. Basalts close to 127-100 Ma in age are documented for the Mendeleev Rise. The Mendeleev Rise forms a single geodynamic system together with the Podvodnikov and Toll basins and originated due to extension orthogonal to the Mendeleev Rise as discussed above. The age of the basalts could be close to the age of rifting. As a consequence, we propose that the main rifting and extension took place close to the Aptian-Albian time. We do not exclude the possibility that rifting in the deep-water part of the Arctic Ocean could have continued after the termination of rifting in the shelf region. A possible age of the rift/postrift boundary could be from 100 Ma and up to 90-80 Ma. Our key conclusion is that rift systems in the shelf region originated together and nearly simultaneous with the systems of the Mendeleev Rise and adjacent Podvodnikov and Toll basins.

Multiple depositional environments can be recognized for the Arctic Alaska Basin (Fig. 65). The Aptian to Albian is represented by the Torok and Nanushuk stratigraphic units (e.g., Homza and Bergman, 2019; Houseknecht, 2019a, 2019b). Condensed deposits are located at the base of this sequence (Houseknecht, 2019a, 2019b) (Fig. 63). Clinoform complexes within the Torok unit are common and well known (e.g., Houseknecht, 2019a, 2019b) with transport of clastic sediments from the Chukotka region and the Brooks Orogen (Fig. 65) toward the Canada deep-water basin, which possibly existed at that time.

A major difference in tectonic environment during the Aptian-Albian for South Amerasia and North Amerasia domains can be recognized. In

this context, we propose the hypothesis that the Canada Basin originated before the Aptian time as a deep-water basin.

A significant tectonic event took place close to 80 Ma in the North Amerasia Domain. Sediments with an age younger than 80 Ma commonly have uniform thicknesses in the Podvodnikov and Toll basins region and commonly cover all highs (Figs. 6, 11, 12, 13, 14, 16, 22, 23, 25, 26, 33, 36, 37, 44, 53, and 61). This suggests that the formation of the Amerasia Basin occurred close to 80 Ma and regional uniform thermal subsidence proceeded afterwards.

The seismic stratigraphy of the Podvodnikov Basin as a whole is similar with that of the North Chukchi Basin and the East Siberian Sea Basin (Figs. 6, 10, 11, 12, 13, 14, 21, 22, 23, 25, 26, 44, 53, and 61). Isolated rifts can be observed at the base of the basin (Figs. 12, 13, 14, 16, 22, 33, 36, 37, and 44). Synrift sedimentary wedges, which are typical for continental rifting, can be identified in these rifts. Therefore, it is likely that the Podvodnikov Basin has a strongly extended continental crust (Nikishin et al., 2017; Nikishin et al., 2014; Petrov et al., 2016). Similar conclusions were presented by Weigelt et al. (2014), Jokat and Ickrath (2015), and Lebedeva-Ivanova et al., 2019, Lebedeva-Ivanova et al., 2011.

The seismic stratigraphy of the Lomonosov Ridge is characteristic of numerous rifts in the region. On the eastern slope of the Lomonosov Ridge, a rift system forms the Lomonosov Terrace (Figs. 6, 33, 37). This zone is typical of continental rifts that have an Early Cretaceous, Aptian-Albian age according to our scheme (older than 100 Ma at least). On the western slope of the Lomonosov Ridge, synrift deposits are observed below the 56 Ma boundary (Figs. 7, 8, 9, 50, 51), probably corresponding to Paleocene rifts. This rifting preceded the onset of opening of

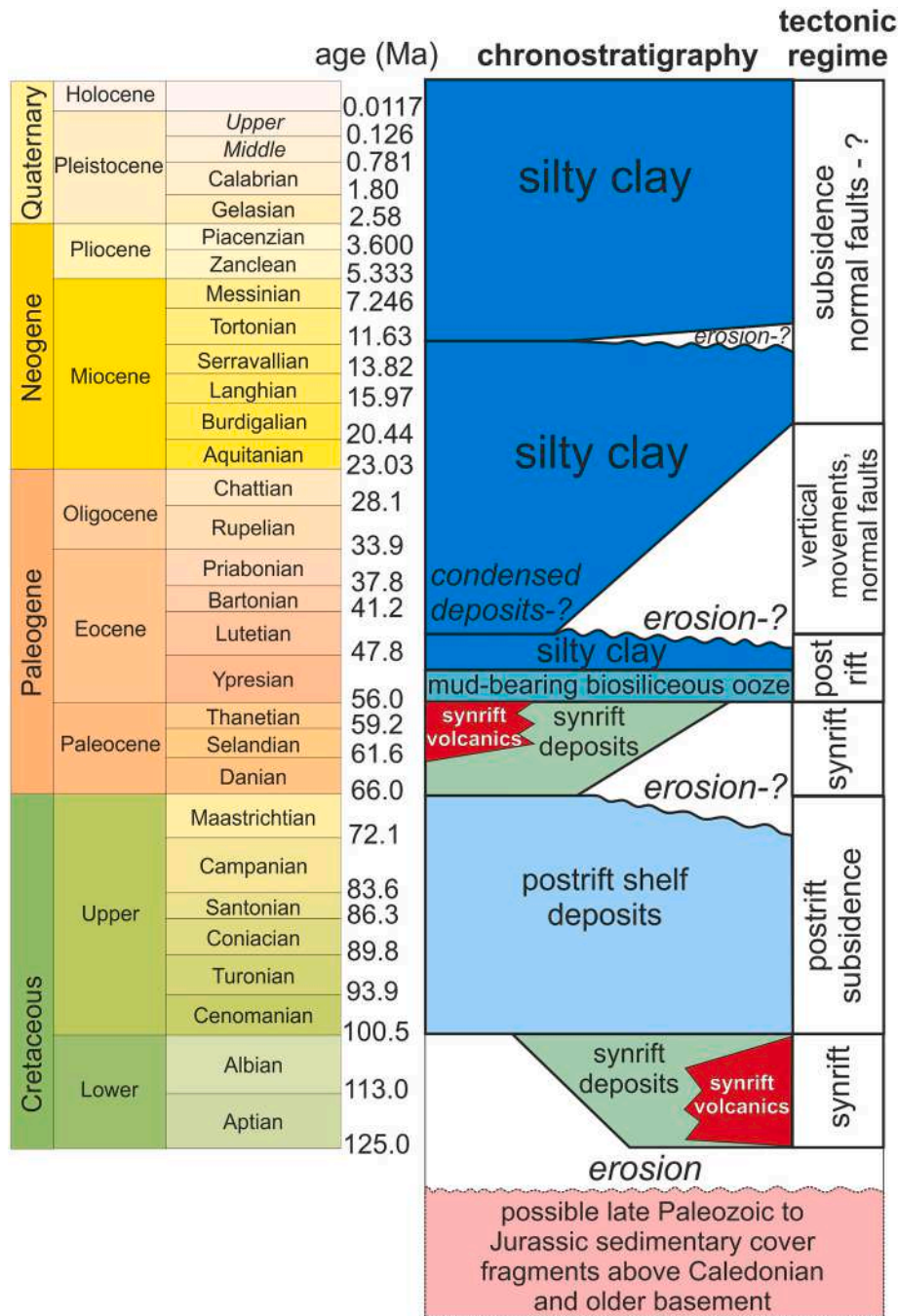


Fig. 59. Tectonostratigraphy for the Lomonosov Ridge.

the Eurasia Basin.

The new seismic data across the Mendeleev Rise (Figs. 33, 35, 37, 42, 44) reveals that structure of the Mendeleev Rise is almost identical to the structure of the Alpha Ridge as reported by Brumley (2014) and Evangelatos et al. (2017). Jokat and Ickrath (2015) noted that the Mendeleev Rise does not seem to be associated with horst-graben basement structure. However, in contrast, our seismic lines, which run across and along the Mendeleev Rise (Figs. 33, 35, 37, 42, 44) clearly indicate the presence of basement grabens and horsts.

A key question remains with regard to how the irregular basement

relief should be interpreted. We interpret this irregular relief as apparent horsts and grabens punctuating the acoustic basement surface of the Mendeleev Rise. It is likely that the interpreted horsts are not volcanic edifices and that they do, in fact, constitute horst-and-graben topography associated with rifting. We flattened the 45 Ma horizon on seismic lines (Figs. 35, 42). With this procedure, post-depositional structure is removed, and original topography is restored, thus affording an ambiguous view of the paleo-geography. Whereas alternative interpretations are possible, we lean toward the horst-and-graben model of Brumley (2014) and Nikishin et al. (2014).

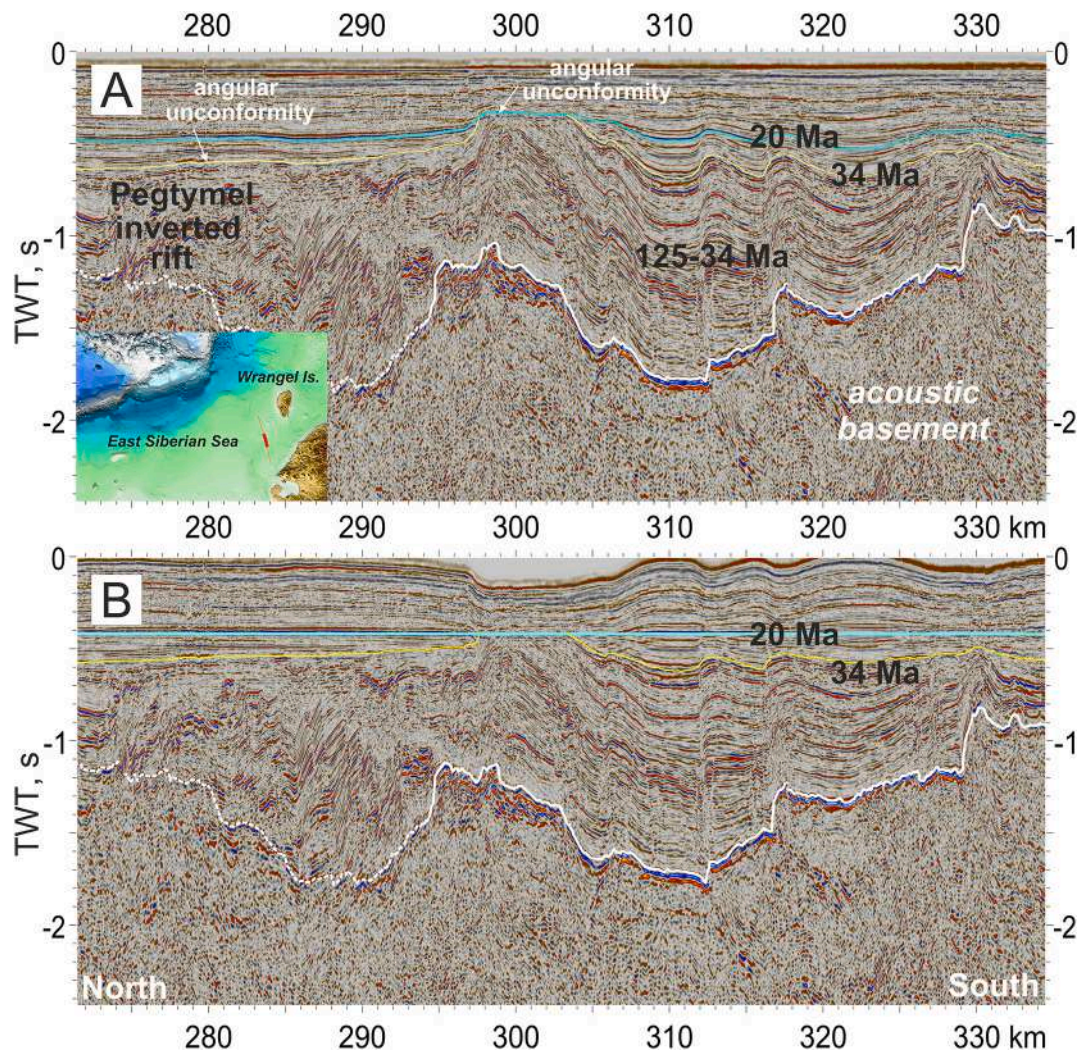


Fig. 60. A. Interpretation of fragment of seismic profile ION15_4410 via Pegtymel Basin, located to the south of Zhokhov-Wrangel-Herald Thrust Belt (Fig. 2 and supplementary data, Fig. 1). The rift basin originated not earlier than the Aptian as it has pre-Aptian orogenic basement. B. Profile flattened on horizon 20 Ma. The rift basin was inverted with main events prior to 34 Ma and 20 Ma. As seismic stratigraphy for this region is badly constrained, ages of inversion could be younger. Modified after Nikishin et al. (2019).

We identified the Arlis Gap Buried High, which separates the Podvodnikov and Makarov basins, on seismic lines (Figs. 11, 26, 30). With respect to the acoustic basement relief, the Arlis Gap Buried High looks similar to the Mendeleev Rise. Consequently, we consider this high to be a continuation of the Mendeleev Rise structure. The magnetic anomalies, which characterize the Mendeleev Rise, generally are analogous to the anomalies of this high (Gaina et al., 2011; Oakey and Saltus, 2016). The lower seismic stratigraphic unit contains many high-amplitude reflections and extends into the Makarov Basin as described by Evangelatos and Mosher (2016) and Evangelatos et al. (2017). This unit can be interpreted as interbedded volcanic and sedimentary deposits formed at the end of a volcanic epoch in the area of the Alpha-Mendeleev Rise (Evangelatos and Mosher, 2016). We interpret several possible volcanic structures as expressed on 2D seismic profiles (Figs. 26, 28, 29, 30). The 80 Ma horizon boundary, characterized by reflection onlap terminations and a small angular unconformity, is observed in the area of this high (Figs. 26, 28, 30). This suggests that just after deposition at 80 Ma,

vertical movements took place, ending at ca. 56 Ma. The 80-56 Ma seismic stratigraphic unit is characterized by variable thickness (Fig. 30), which is indicative of tectonic movement during the time of its deposition.

In the Makarov Basin, two domains, the West Makarov Basin and the East Makarov Basin, can be identified on the basis of acoustic basement characteristics. This is consistent with the interpretation of Evangelatos and Mosher (2016) and Evangelatos et al. (2017). Two of our seismic lines cross the East Makarov Basin, one from the side of the Alpha Ridge and one from the side of the Arlis Gap Buried High (Figs 5, 68, 26 and 28). The acoustic basement relief there is strikingly similar to that of the Alpha-Mendeleev Rise. The lower seismic stratigraphic unit contains high-amplitude reflections and can be mapped from the Makarov basin onto the Arlis Gap Buried High and probably onto the Alpha Ridge as well. This is confirmed by Evangelatos and Mosher (2016) who mapped along another seismic line that crossed the Makarov Basin and the Alpha Ridge. This high-amplitude reflection package probably corresponds to

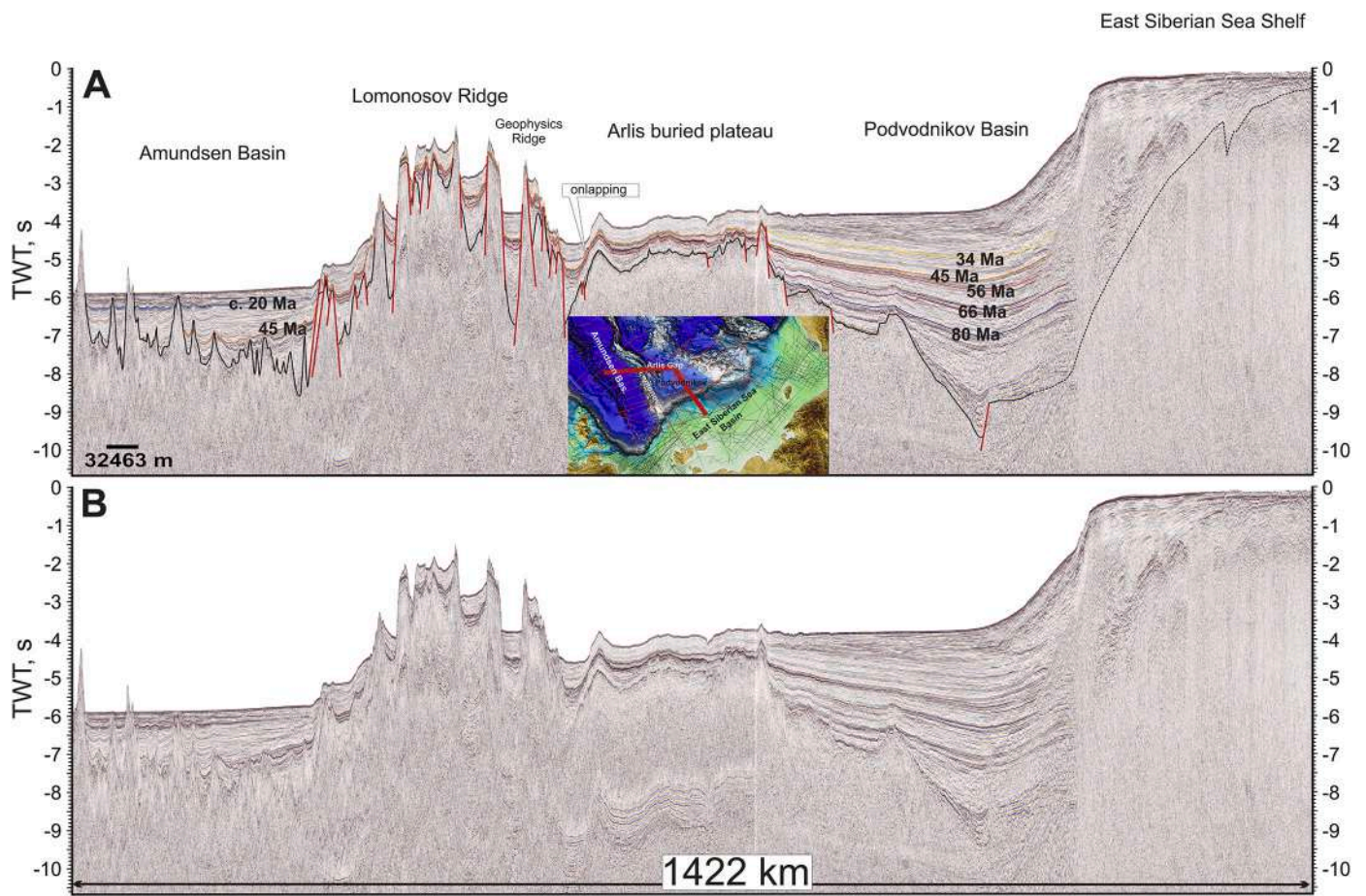


Fig. 61. A. Interpretation of composite seismic profile from the Amundsen Basin to the East Siberian Sea Shelf (lines ARC 14-09 and ARC 14-03). Location of the profile is shown on the map. The trough/ridge topography of the Lomonosov Ridge could be due to Cenozoic normal faulting. B. Seismic profile without interpretation. See also supplementary data, Fig. 61 (seismic profile without interpretation at high resolution).

a succession of volcanic and sedimentary deposits with an age greater than 80 Ma. We propose that the East Makarov Basin is a more subsided part of the Alpha-Mendeleev Rise. The West Makarov Basin has pronounced grabens at the base of the section (Figs. 28, 68 and Evangelatos and Mosher, 2016). Unfortunately, with a loose 2D seismic grid, we have no reliable data regarding the trend of these grabens. A small angular unconformity, which can be interpreted as a rift/posrift unconformity, was observed near the 66 Ma boundary (Figs. 28, 68). It follows from this that rifting in the West Makarov Basin took place just before the Paleocene. Our seismic stratigraphic correlations indicate no clear base to the rift basin fill. Consequently, the best we can surmise is that the rifting occurred sometime during the Late Cretaceous-Paleocene. The key conclusion is that this rift event is nonetheless younger than the Aptian to Albian rifting in the East Siberian and Chukchi seas shelf and Podvodnikov Basin.

We have noted the presence of evidence for likely vertical movement dating to 80-56 Ma in the area of the Arlis Gap Buried High. These vertical movements probably were synchronous with the rifting that occurred in the West Makarov Basin. The main rifting probably took place within the confines of the Lomonosov Ridge slope and was probably associated with strike-slip faults. Probably the West Makarov Basin was formed at 80-66 (or 80-56) Ma as a pull-apart basin. This hypothesis was discussed by us earlier in preliminary form (Nikishin et al., 2014,

2017). Our interpretation likewise is consistent with the conclusion of Evangelatos and Mosher (2016) that the West Makarov Basin was formed as a pull-apart structure, though these authors argue that the basin was formed earlier than 80 Ma.

5.2. 2D seismic data and crustal structure of some basins and rises

The crustal structure of the Arctic Ocean is the subject of much debate. A number of reviews have been presented (see, e.g., Pease et al., 2014, Lebedeva-Ivanova et al., 2019). The North Chukchi Basin is a prominent example of a super-deep sedimentary basin. It has a sedimentary fill thickness of up to 20-22 km. We document evidence of super-stretching of its basement but an open question remains concerning the type of the basin's basement. According to our model and the recent calculated model of Savin (2020), this could be hyper-extended continental crust. At present, however, we lack the data to unequivocally establish the crustal structure. Hopefully, future numerical modelling can potentially offer greater insight.

The Ust' Lena Basin of the Laptev Sea has a sedimentary cover thickness of the up to 7.5 secs TWT (nearly 15 km). The seismically-identified Moho is elevated to approximately 28 km calculated depth. Seismic data suggest that the Moho is for the most part flattened (see Paper-1, Nikishin et al., 2021a). Drachev et al. (2018) proposed mantle

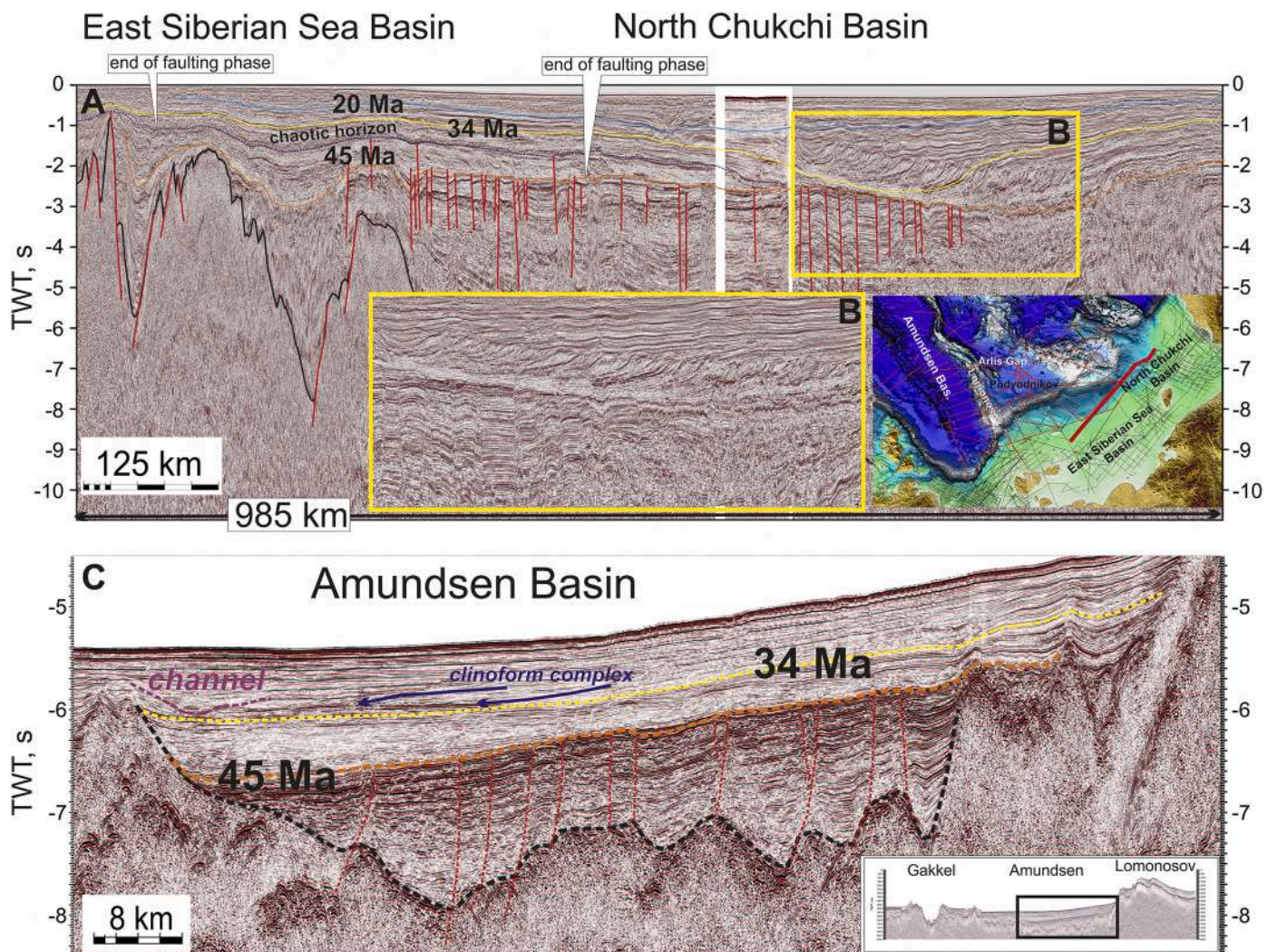


Fig. 62. A. Interpretation of composite seismic profile for the East Siberian Sea and the Chukchi Sea Shelf (lines ION 12-1440 – Arc 14-01 – ION 11-1400). B. Enlarged section of seismic profile without interpretation. C. Interpretation of fragment of seismic profile ARC 14-05 for the Amundsen Basin (see Fig. 25 for location). Two profiles show observed faulting with an age close to 45 Ma.

exhumation below the sedimentary cover in this basin, however, our grid of seismic lines does not show any unusual features. Consequently, our data and new calculations of the crustal structure of the Laptev Sea (Savin, 2020) do not support the hypothesis by Drachev et al. (2018).

Drachev et al. (2018) proposed mantle exhumation below the sedimentary cover in the East Anisin Basin, located between the continental shelf and the Lomonosov Ridge (Fig. 2). We present a few seismic lines for this area (Figs. 7, 8, 9, 22, 49, 50, and 51) and observe that the thickness of the sedimentary cover is less than 5 secs TWT. We conclude that there is no seismic evidence for the Khatanga-Lomonosov fault as an important active structure (Figs. 7, 8, 9, 22, 49, 50, and 51). We refer the reader to Nikishin et al. (2018) for further discussion of Drachev et al. (2018) hypothesis.

We present new data and a novel geological model for the Mendeleev Rise. The key element is the presence of SDR-like units and half-grabens. Basalts are well documented there as well. We propose that the Mendeleev Rise has a stretched continental crust enriched with basalt intrusions. A similar model was proposed for the mid-Norwegian volcanic

continental margin (e.g., Abdelmalak et al., 2016). Skolotnev et al., 2019, Skolotnev et al., 2017 studied four scarps in the Mendeleev Rise, and for every scarp Paleozoic samples were collected. Basalts and dolerites were collected at stations close to the Paleozoic outcrops. As a consequence, they surmise that the total relative volume of intrusions could be up to 10-30% of the pre-Cretaceous basement. This clearly represents an intriguing case of a combination of extension, volcanism, rifting and intrusive magmatism.

The southern part of the Toll Basin is characterized by SDR complexes within half-grabens (Figs. 33, 34). This is typical for inner SDRs of volcanic passive continental margins with continental basement (e.g., Foulger et al., 2020). The northern part of the Toll Basin (or Mendeleev Basin) has a narrow axial rift or trough (Figs. 66, 67). We propose that this trough could be explained as a failed start of lithospheric separation. The Toll Basin could be a good example of aborted oceanic spreading.

The Podvodnikov Basin has a highly stretched continental crust. The key evidence is the presence of half-grabens and SDR-like units, typical of continental crustal extension.

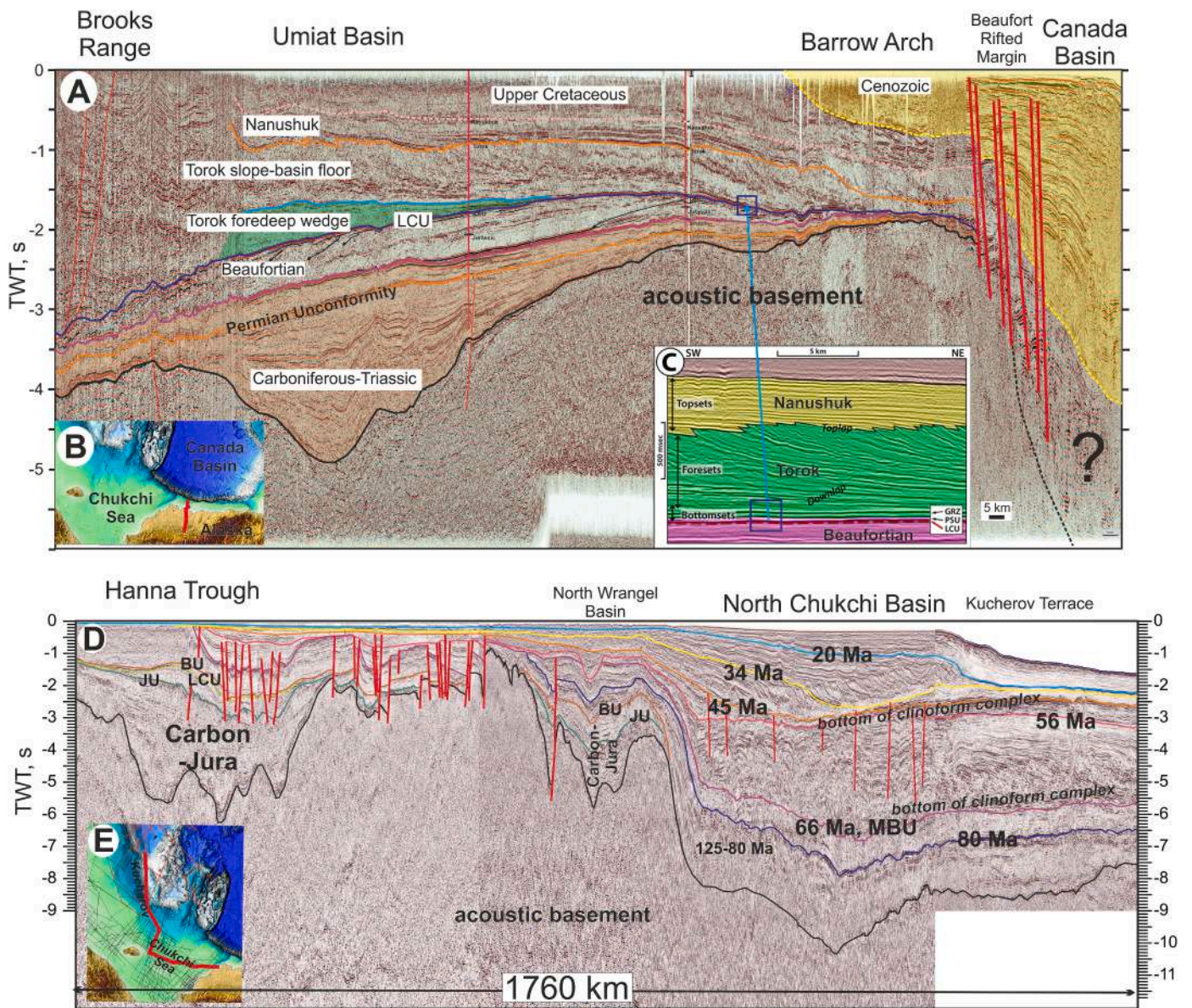


Fig. 63. A. Composite seismic profile for the Arctic Alaska Basin (lines usgs-r-8, usgs-6-74, usgs-6D-74, usgs-4-74, usgs-GM-5S, usgs-GM-5D, usgs-GM-4D, usgs_HW81-24, usgs_HW81-11, usgs_WB-558, and usgs-71GSG-G-88). Seismic data from U.S. Geological Survey. Data of Houseknecht (2019a, 2019b) were used for interpretation. B. Location of the profile. C. Detail of seismic image with approximate position on line A (Houseknecht, 2019b). LCU – Lower Cretaceous Unconformity, PSU – Pebble Shale Unit, GRZ – Gamma-Ray Zone; condensed sections are between LCU and GRZ. D. Composite seismic profile for the North Chukchi Basin (Fig. 10). E. Location of the profile.

Additional data are required to better understand the crustal structure of the Arctic Ocean. Examples of crustal structural modelling using seismic data were presented in a number of publications (e.g., Jokat and Ickrath, 2015; Chian et al., 2016; Oakey and Saltus, 2016; Evangelatos et al., 2017; Kashubin et al., 2018; Lebedeva-Ivanova et al., 2019; Poselov et al., 2019; Savin, 2020). A new generation of such models could integrate data on the geological evolution and basin structure and architecture with constraints from geophysical observations of the crust and lithosphere.

5.3. Proposed model of the Arctic Ocean history

Many reconstructions of the formation history of the Arctic Ocean presently exist (e.g., Alvey et al., 2008; Amato et al., 2015; Grantz et al., 2011; Grantz and Hart, 2012; Hutchinson et al., 2017; Lawver et al., 2015; Mosher et al., 2012; Shephard et al., 2013). It is clear that models of different authors differ significantly (Paper-1, Nikishin et al., 2021a). We propose as a hypothesis that the Arctic Ocean probably was formed during four phases with different kinematics. The key tectonostratigraphic phases are: 133-125 Ma, 125-80 Ma, 80-56 Ma, and 56-0 Ma.

The boundaries of the first phase correspond to two regional

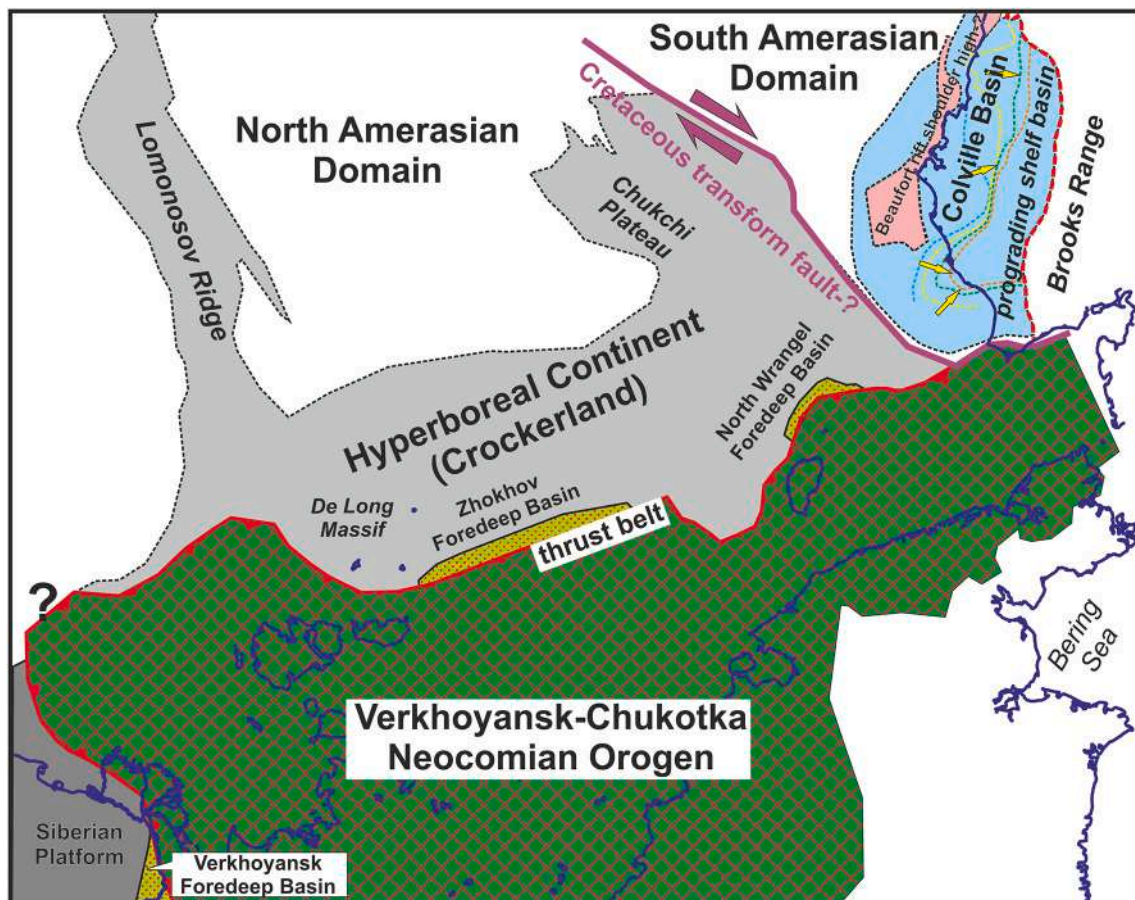


Fig. 64. Types of Late Jurassic to Neocomian seismic sequences and some paleogeographic elements on a modern geographic basis. Data for the Alaska region are from Houseknecht (2019a, 2019b).

unconformities observed on the Alaskan Arctic Shelf: 133 Ma – the Lower Cretaceous Unconformity (LCU) and 125 Ma – the Brookian Unconformity (BU) (Sherwood et al., 2002). According to our model, the LCU corresponds to the onset of opening of the Canada Basin, and the BU to the end of formation of the Canada Basin. The duration of Canada Basin formation is approximately 8 Ma. Such a rapid formation time is typical of back-arc basins of the type observed in the Sea of Japan and the South China Sea (see Ziegler and Cloetingh, 2004 for a review). Their widths have similar values (about 600-700 km) as to what is observed in the Arctic region.

The timing of the cessation of Canada Basin formation probably coincides with the onset of the large-scale collapse of the Verkhoyansk-Chukotka Orogen and onset of continental rifting in the East Siberian Sea and in the Russian part of the Chukchi Sea (Miller and Verzhbitsky, 2009; Nikishin et al., 2014, 2017). A major rearrangement of lithospheric plate kinematics occurred at ca. 125 Ma. The collapse of the Verkhoyansk-Chukotka Orogen and onset of the impact of the HALIP superplume corresponded to this rearrangement. A similar situation occurred approximately at the Permian/Triassic boundary in West Siberia where plume magmatism (e.g. the Siberian Platform, Taimyr) and large-scale rifting took place simultaneously in different places (e.g., Nikishin et al., 2002). In the Arctic, these processes led to formation of the deep-water rifted Podvodnikov and the Toll-Mendelev-Nautilus basins and the volcanic edifice of the Alpha-Mendelev Rise on

continental crust strongly thinned by rifting. These processes lasted approximately till 80 Ma.

80 Ma is the approximate time of the end of subduction-related volcanism in the Okhotsk-Chukotka volcanic belt (Fig. 2) (Akinin, 2012). After that, formation of the Koryakia-West Kamchatka accretional orogen began (Soloviev, 2008; Akinin, 2012) whose formation ended at ca. 50-45 Ma (Soloviev, 2008). The end of subduction-related volcanism in the Okhotsk-Chukotka volcanic belt may correspond to the time of significant plate kinematic rearrangement and end of Alpha-Mendelev Rise formation.

During the 80 Ma-66 (56) Ma time interval, large-scale slip fault deformation possibly occurred and resulted in the formation of the West Makarov and other rift basins. These slip fault deformations probably controlled the plate kinematics in the Atlantic and Pacific Regions.

From 56 Ma (or earlier) onward the formation history of the Arctic Ocean was associated with opening of the Atlantic Ocean and the Eurasia Basin was formed.

6. Conclusions

In this study, a new seismic stratigraphic framework is proposed for much of the Arctic Ocean. We identified and traced extensively a number of boundaries with ages of 100 Ma, 80 Ma, 66 Ma, 56 Ma, 34 Ma and 20 Ma. The new seismic stratigraphic framework led to a new model

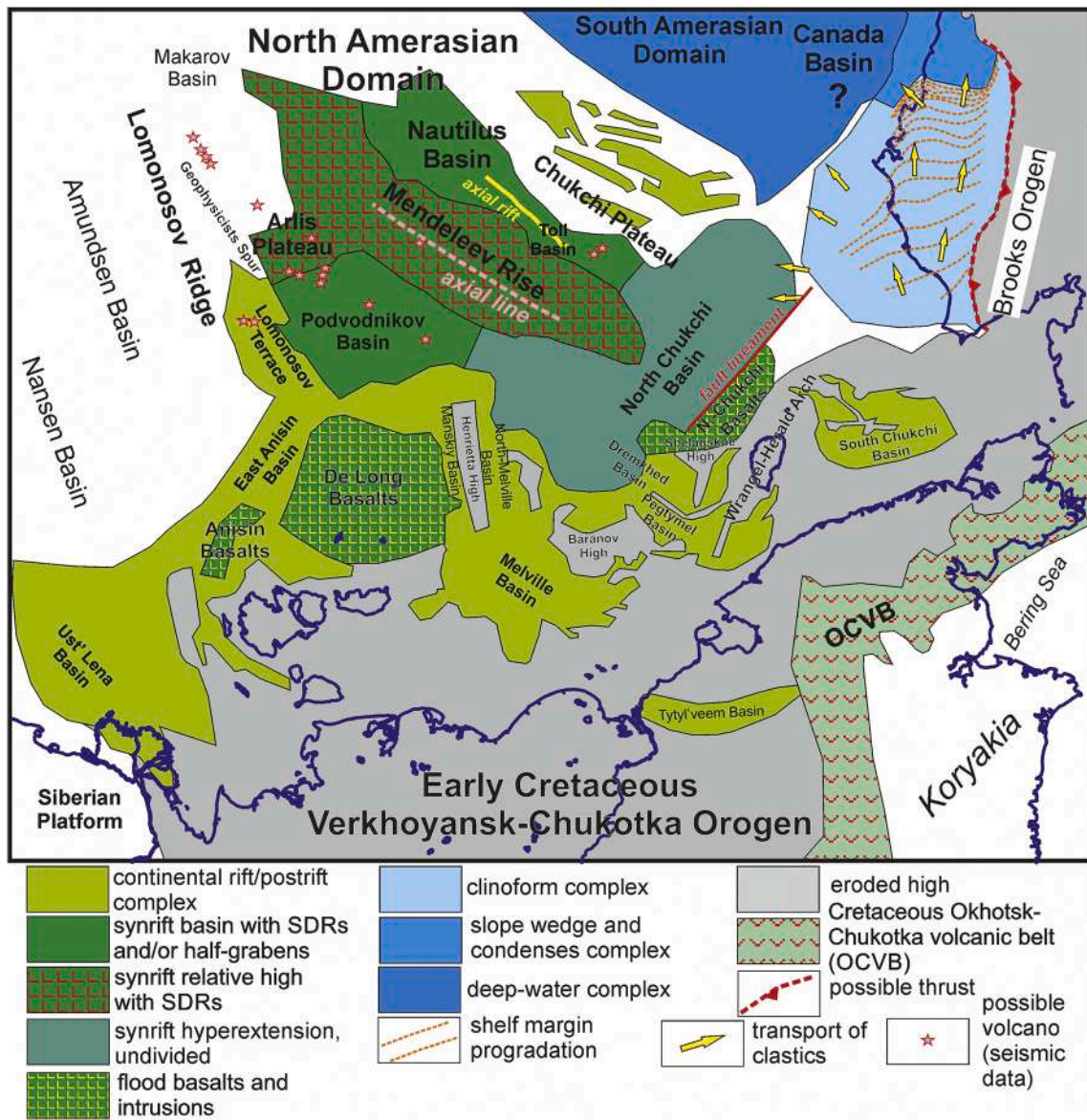


Fig. 65. Types of the Aptian-Albian seismic sequences and some paleogeographic elements on a modern geographic basis. Data for the Alaska region are from Houseknecht (2019a, 2019b).

for the geological history of the Arctic Ocean (it should be noted, however, that we specifically did not include the Canada Basin).

On the shelves of the Laptev, East Siberian and Chukchi Seas, large-scale continental rifting took place in the Aptian-Albian. The Podvodnikov Basin and probably the Toll Basin started to form not earlier than the Aptian; the rifting processes were completed by ca. 100-90 Ma.

We propose the existence of a new Aptian igneous province north of Wrangel Island. The Alpha-Mendeleev Igneous Province was surrounded on all sides (except the area of the Canada Basin) by Early Cretaceous igneous provinces. An approximately simultaneous onset of magmatism at 130-125 Ma is likely to have occurred within a vast area. Analysis of seismic data shows that the Arlis Gap Buried High is a continuation of the structure underlying the Mendeleev Rise. Our data also show that most of the Makarov Basin basement constitutes a continuation of the Alpha Ridge structure. Summing up these data, it appears that the

Alpha-Mendeleev Igneous Province started to form at the eastern margin of the Lomonosov Ridge. That is, the Alpha-Mendeleev Igneous Province started to form at ca. 125 Ma as a volcanic rifted continental margin. The Arctic superplume HALIP probably did not result in the opening of a new ocean. No data are available to conclusively prove that a large-scale formation of oceanic crust was taking place in the Late Cretaceous and origin of the Alpha-Mendeleev Rise area. The problem of structure and origin of the Alpha-Mendeleev Rise will require further analysis. A key novel finding is the presence of SDR-like units in the Mendeleev Rise and Podvodnikov and Toll basins.

The time interval of about 80-66 (56) Ma is characteristic of strike-slip fault tectonics. The West Makarov Basin was formed in this time likely as a pull-apart basin. During the Late Cretaceous-Paleocene (ca. 80-56 Ma), continental rifting widely manifested itself in the western part of the Laptev Sea and on the western slope of the Lomonosov Ridge.

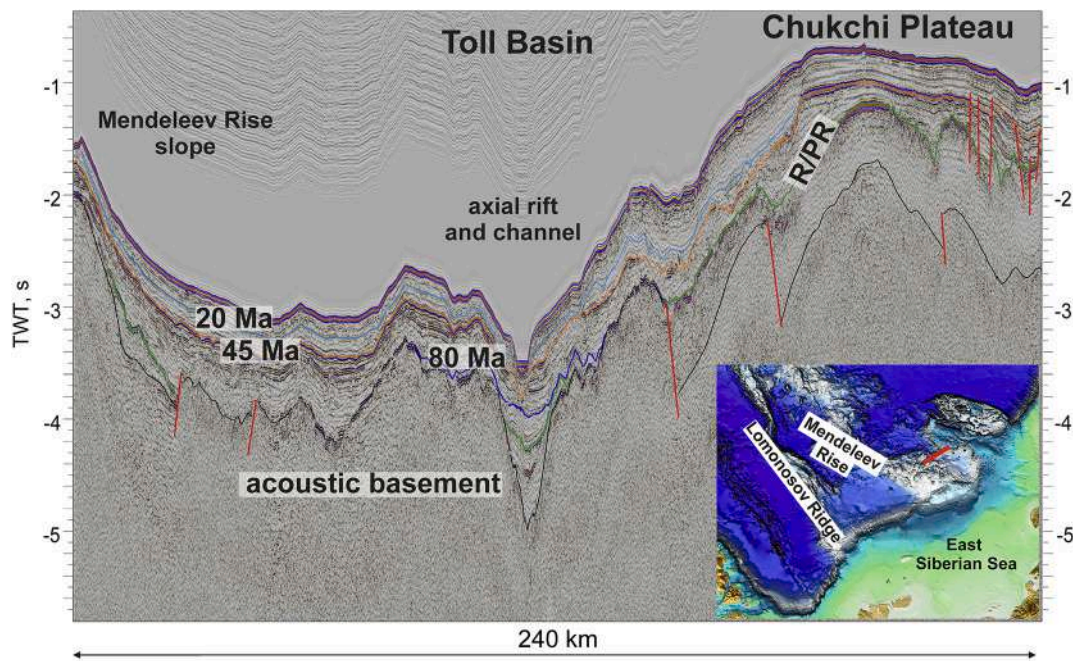


Fig. 66. Interpretation of western part of seismic profile ARC12_19. Location of the profile is shown on the map. The Toll Basin is located between Mendeleev Rise and Chukchi Plateau. The basin is characterized by axial V-shape paleorift of the Cretaceous age. The rift strikes along the basin (Fig. 65). Mendeleev Rise and Chukchi Plateau have systems of half-grabens along slopes of the Toll Basin. R/PR – rift/posrift boundary.

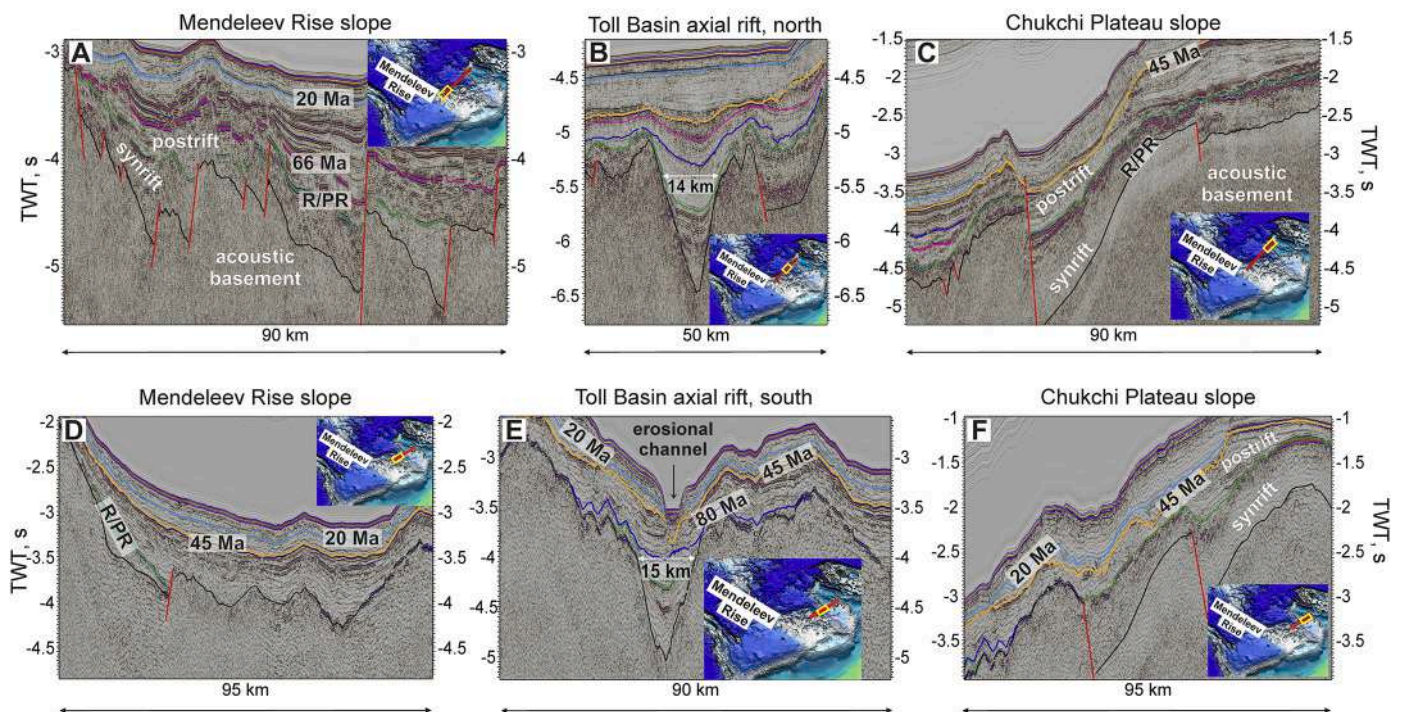


Fig. 67. Interpretation of seismic data for the Toll Basin Axial Rift region. A, B, C. Fragments of seismic profile ARC12_04 from Mendeleev Rise toward Chukchi Plateau. D, E, F. Fragments of seismic profile ARC12_19 from Mendeleev Rise toward Chukchi Plateau (Fig. 66). The profiles are parallel to each other. Slopes of Mendeleev Rise and Chukchi Plateau have similar and symmetric horst and half-graben structure. Axial zone of the Toll Basin is characterized by buried Cretaceous trough-like rift with V-shape. Width of this rift is close to 14-15 km. This trough could be explained as a failed start of lithospheric separation.

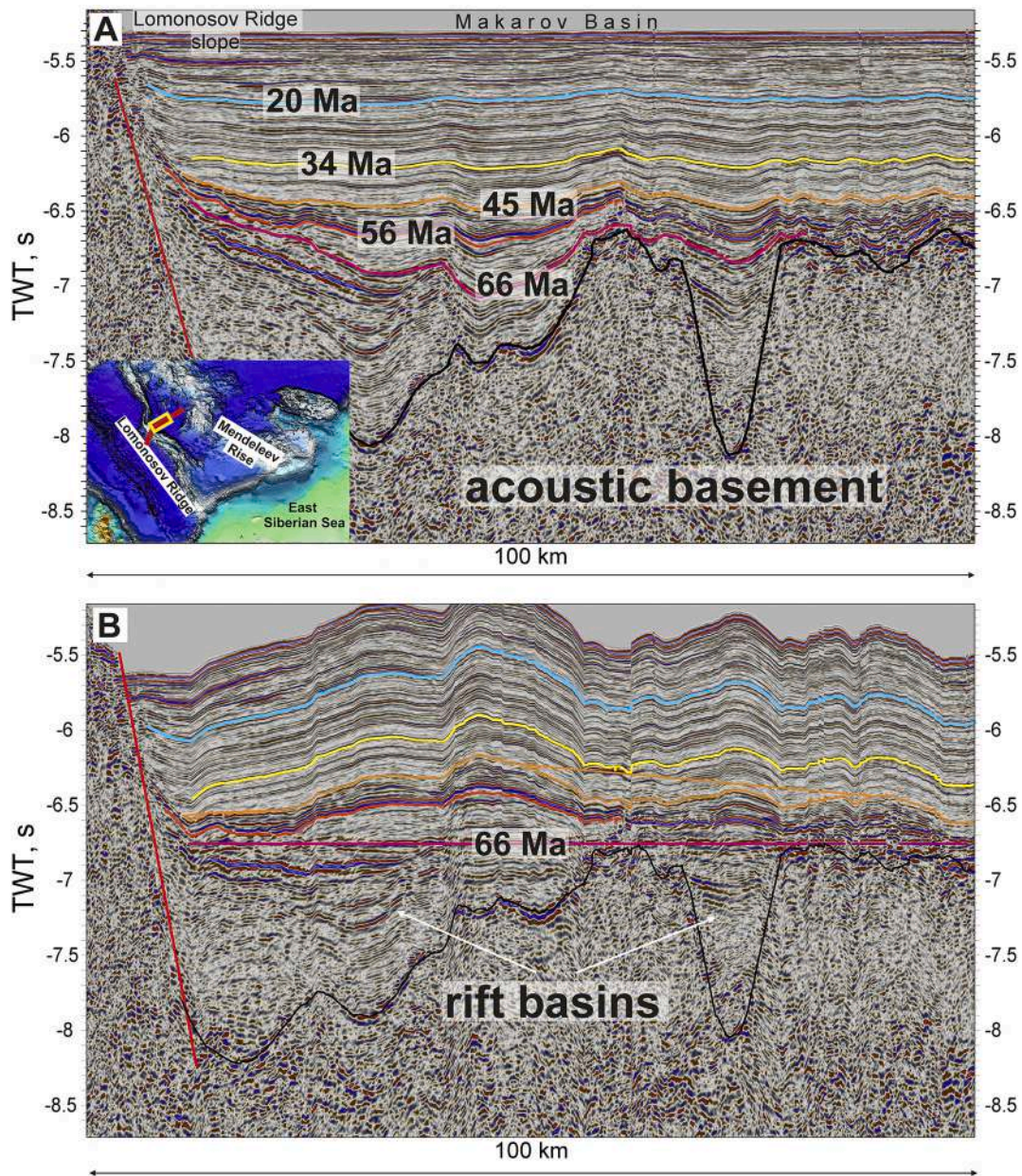


Fig. 68. A. Interpretation of fragment of profile ARC_14-07 shown in Fig. 5. The profile crosses the Makarov Basin and the Lomonosov Ridge slope. This profile is nearly orthogonal to the profile on Fig. 28. V-shape trough is observed in the central part of the Makarov Basin. This trough, a rift basin, is possibly the same as shown in Fig. 28. Another rift basin is located between the Lomonosov Ridge and Makarov Basin. B. Profile flattened on the 66 Ma horizon. We assume a pre-66 Ma age of rifting.

This rifting preceded the opening of the Eurasia Basin. In the western part of the Laptev Sea, an igneous province was identified using seismic data. The possible age of volcanism is ca. 56 Ma. This magmatism preceded the opening of the Eurasia Basin.

The 45-34 Ma (or 45-20 Ma) time interval constitutes a period of large-scale vertical intraplate movements in the Arctic Ocean. At that time, relative highs commonly experienced uplift, while relative lows experienced subsidence. Synchronously with vertical movements, activation of normal faulting took place on the Lomonosov Ridge and Mendeleev Rise. The present-day bathymetry of the Arctic Ocean was formed at this time with processes of vertical movement and normal faulting continuing up until the present time. The transition from normal

spreading to ultra-slow spreading on the Gakkel Ridge happened at 45 Ma. Synchronously with this event, intraplate vertical movements started and a phase of super-regional, low-amplitude normal faulting took place. Normal faults of this age are detected in widespread regions ranging from the Amundsen Basin up to the shelves of the East Siberian and Chukchi Seas.

Climatic events are recorded in the sedimentary cover of the Arctic Ocean. During the 56-45 Ma time interval, as constrained by analysis of seismic facies, a marked period of global warming occurred in the Arctic region. An abrupt cooling that began at 45 Ma was caused by a sharp change in paleogeography that occurred in response to an acceleration of uplift around the ocean.

Declaration of Competing Interest

We have no conflict of interest.

Acknowledgements

The authors are grateful to the Ministry of Natural Resources and Ecology of Russia for the opportunity to publish this paper. Discussions with C. Gaina, E. Miller, V. Pease, W. Jokat, D. Hutchinson, J.I. Faleide, S. Drachev, R. Stephenson, D. Franke, A. Escalona, I. Norton, N. Lebedeva-Ivanova, E. Lundin, A. Doré, E. Weigelt, D. Mosher, and D. Zastrozhnov stimulated our work. We are thankful to many Russian geologists from different scientific organizations with whom we conducted numerous discussions: L.I. Lobkovsky, V.A. Vernikovskiy, S.D. Sokolov, S.G. Skolotnev, A.K. Khudoley, A.V. Prokopiev, O.V. Petrov, E. V. Shipilov, A.V. Stoupakova, E.A. Gusev, P.V. Rekant, V.A. Poselov, S. N. Kashubin, V.V. Akinin, A.S. Alekseev, G.N. Aleksandrova, A.B. Herman, V.A. Savin, and others. In the course of studying the Arctic, we had the opportunity to conduct scientific discussions with geologists from different companies: Rosneft, Total, ExxonMobil, Statoil, BP, Gazprom Neft, Gazprom. We thank companies MAGE, DMNG and ION-GXT for the use of their seismic data. E. Bulgakova, A. Popova, M. Skaryatin, A. Fedechkina, I. Mazaeva, O. Makhova, S. Zaytseva, N. Kulyukina, and D. Igtisamov (Rosneft) provided constructive feedback for our seismic data interpretation. The work of AMN, SIF, KFS, and NNZ was supported by RFBR grants (18-05-70011 and 18-05-00495). We thank François Roue and anonymous reviewers for generous, detailed, and constructive criticism. We express many thanks to Tim Horscroft and Gillian Foulger as editors for this paper.

Appendix A. Supplementary data

Supplementary data (mainly regional seismic profiles without interpretation) are presented in: https://yadi.sk/d/yZ1N6crs_eFBeA. Supplementary data to this article can be found online at <https://doi.org/10.1016/j.earscirev.2021.103581>.

References

- Abdelmalak, M.M., Meyer, R., Planke, S., Faleide, J.I., Gernigon, L., Frieling, J., Sluijs, A., Reichart, G.-J., Zastrozhnov, D., Theissen-Krah, S., Said, A., Myklebust, R., 2016. Pre-breakup magmatism on the Vøring Margin: Insight from new sub-basalt imaging and results from Ocean Drilling Program Hole 642E. *Tectonophysics* 675, 258–274. <https://doi.org/10.1016/j.tecto.2016.02.037>.
- Akhmet'ev, M.A., Zaporozhets, N.I., Yakovleva, A.I., Aleksandrova, G.N., Beniamovskiy, V.N., Oreshkina, T.V., Gnibidenko, Z.N., Dolya, Z.A., 2010. Comparative analysis of marine paleogene sections and biota from West Siberia and the Arctic Region. *Stratigr. Geol. Correl.* 18, 635–659. <https://doi.org/10.1134/S0869593810060043>.
- Akinin, V.V., 2012. Late Mesozoic and Cenozoic magmatism and lower crust modifications in the northern framing of Pacific. IGEM RAS, Moscow.
- Aleksandrova, G.N., 2016. Geological evolution of Chauna depression (North-Eastern Russia) during Paleogene and Neogene. 1. Paleogene. (in Russian). *Bull. Moscow Soc. Nat. Geol. Ser.* 91, 148–164 (in Russian).
- Alvey, A., Gaina, C., Kuszniir, N.J., Torsvik, T.H., 2008. Integrated crustal thickness mapping and plate reconstructions for the high Arctic. *Earth Planet. Sci. Lett.* 274, 310–321. <https://doi.org/10.1016/j.epsl.2008.07.036>.
- Amato, J.M., Toro, J., Akinin, V.V., Hampton, B.A., Salnikov, A.S., Tuckkova, M.I., 2015. Tectonic evolution of the Mesozoic South Anyui suture zone, eastern Russia: A critical component of paleogeographic reconstructions of the Arctic region. *Geosphere* 11, 1530–1564. <https://doi.org/10.1130/GES01165.1>.
- Backman, J., Moran, K., 2009. Expanding the cenozoic paleoceanographic record in the central arctic ocean: IODP expedition 302 synthesis. *Open Geosci.* 1 <https://doi.org/10.2478/v10085-009-0015-6>.
- Backman, J., Jakobsson, M., Frank, M., Sangiorgi, F., Brinkhuis, H., Stickley, C., O'Regan, M., Lovlie, R., Pälke, H., Spofforth, D., Gattacecca, J., Moran, K., King, J., Heil, C., 2008. Age model and core-seismic integration for the Cenozoic Arctic Coring Expedition sediments from the Lomonosov Ridge. *Paleoceanography* 23. <https://doi.org/10.1029/2007PA001476>.
- Bird, K.J., Houseknecht, D.W., Pitman, J.K., 2017. Geology and assessment of undiscovered oil and gas resources of the Hope Basin Province, 2008. In: Moore, T. E., Gautier, D.L. (Eds.), *The 2008 Circum-Arctic Resource Appraisal*. U.S. Geological Survey Professional Paper 1824, Reston, Virginia, pp. 1–9. <https://doi.org/10.3133/pp1824d>.
- Brinkhuis, H., Schouten, S., Collinson, M.E., Sluijs, A., Damsté, J.S.S., Dickens, G.R., Huber, M., Cronin, T.M., Onodera, J., Takahashi, K., Bujak, J.P., Stein, R., van der Burgh, J., Eldrett, J.S., Harding, I.C., Lotter, A.F., Sangiorgi, F., van Cittert, H.K., de Leeuw, J.W., Matthiessen, J., Backman, J., Moran, K., 2006. Episodic fresh surface waters in the Eocene Arctic Ocean. *Nature* 441, 606–609. <https://doi.org/10.1038/nature04692>.
- Brumley, K., 2014. Geologic history of the Chukchi Borderland, Arctic Ocean. A dissertation submitted to the department of geology and environmental sciences and the committee on graduate studies of Stanford university in partial fulfillment of the requirements for the degree of Doctor of philosophy. <http://purl.stanford.edu/hz857zk1405>.
- Brumley, K., Miller, E.L., Konstantinou, A., Grove, M., Meisling, K.E., Mayer, L.A., 2015. First bedrock samples dredged from submarine outcrops in the Chukchi Borderland, Arctic Ocean. *Geosphere* 11, 76–92. <https://doi.org/10.1130/GES01044.1>.
- Bruvold, V., Kristoffersen, Y., Coakley, B.J., Hopper, J.R., 2010. Hemipelagic deposits on the Mendeleev and northwestern Alpha submarine Ridges in the Arctic Ocean: acoustic stratigraphy, depositional environment and an inter-ridge correlation calibrated by the ACEX results. *Mar. Geophys. Res.* 31, 149–171. <https://doi.org/10.1007/s11001-010-9094-9>.
- Bruvold, V., Kristoffersen, Y., Coakley, B.J., Hopper, J.R., Planke, S., Kandilarov, A., 2012. The nature of the acoustic basement on Mendeleev and northwestern Alpha ridges, Arctic Ocean. *Tectonophysics* 514–517, 123–145. <https://doi.org/10.1016/j.tecto.2011.10.015>.
- Butsenko, V.V., Poselov, V.A., Zholondz, S.M., Smirnov, O.E., 2019. Seismic attributes of the Podvodnikov Basin basement. *Dokl. Earth Sci.* 488, 1182–1185. <https://doi.org/10.1134/S1028334X19100015>.
- Chernykh, A.A., Krylov, A.A., 2011. Sedimentogenesis in the Amundsen Basin from geophysical data and drilling results on the Lomonosov Ridge. *Dokl. Earth Sci.* 440, 1372–1376. <https://doi.org/10.1134/S1028334X11100011>.
- Chian, D., Jackson, H.R., Hutchinson, D.R., Shimeld, J.W., Oakey, G.N., Lebedeva-Ivanova, N., Li, Q., Saltus, R.W., Mosher, D.C., 2016. Distribution of crustal types in Canada Basin, Arctic Ocean. *Tectonophysics* 691, 8–30. <https://doi.org/10.1016/j.tecto.2016.01.038>.
- Coakley, B., Brumley, K., Lebedeva-Ivanova, N., Mosher, D., 2016. Exploring the geology of the central Arctic Ocean; understanding the basin features in place and time. *J. Geol. Soc. Lond.* 173, 967–987. <https://doi.org/10.1144/jgs2016-082>.
- Corfu, F., Polteau, S., Planke, S., Faleide, J.I., Svensen, H., Zayoncheck, A., Stolbov, N., 2013. U–Pb geochronology of Cretaceous magmatism on Svalbard and Franz Josef Land, Barents Sea Large Igneous Province. *Geol. Mag.* 150, 1127–1135. <https://doi.org/10.1017/S0016756813000162>.
- Craddock, W.H., Houseknecht, D.W., 2016. Cretaceous–Cenozoic burial and exhumation history of the Chukchi shelf, offshore Arctic Alaska. *Am. Assoc. Pet. Geol. Bull.* 100, 63–100. <https://doi.org/10.1306/09291515010>.
- Cramer, B.S., Toggweiler, J.R., Wright, J.D., Katz, M.E., Miller, K.G., 2009. Ocean overturning since the Late Cretaceous: inferences from a new benthic foraminiferal isotope compilation. *Paleoceanography* 24. <https://doi.org/10.1029/2008PA001683>.
- Dick, H.J.B., Lin, J., Schouten, H., 2003. An ultraslow-spreading class of ocean ridge. *Nature* 426, 405–412. <https://doi.org/10.1038/nature02128>.
- Dobretsov, N.L., Vernikovskiy, V.A., Karyakin, Y.V., Korago, E.A., Simonov, V.A., 2013. Mesozoic–Cenozoic volcanism and geodynamic events in the Central and Eastern Arctic. *Russ. Geol. Geophys.* 54, 874–887. <https://doi.org/10.1016/j.rgg.2013.07.008>.
- Døssing, A., Jackson, H.R., Matzka, J., Einarsson, I., Rasmussen, T.M., Olesen, A.V., Brozena, J.M., 2013. On the origin of the Amerasia Basin and the High Arctic Large Igneous Province—Results of new aeromagnetic data. *Earth Planet. Sci. Lett.* 363, 219–230. <https://doi.org/10.1016/j.epsl.2012.12.013>.
- Dove, D., Coakley, B., Hopper, J., Kristoffersen, Y., Team, H.G., 2010. Bathymetry, controlled source seismic and gravity observations of the Mendeleev ridge; implications for ridge structure, origin, and regional tectonics. *Geophys. J. Int.* 183, 481–502. <https://doi.org/10.1111/j.1365-246X.2010.04746.x>.
- Drachev, S., Saunders, A., 2006. The Early Cretaceous Arctic LIP: its geodynamic setting and implications for Canada Basin opening. In: Scott, R.A., Thurston, D.K. (Eds.), *Proceedings of the Fourth International Conference on Arctic Margins*. US Department of the Interior MMS, Dartmouth, Nova Scotia, Canada, pp. 216–223.
- Drachev, S.S., 2016. Fold belts and sedimentary basins of the Eurasian Arctic. *Arktos* 2, 21. <https://doi.org/10.1007/s41063-015-0014-8>.
- Drachev, S.S., Malyshev, N.A., Nikishin, A.M., 2010. Tectonic history and petroleum geology of the Russian Arctic Shelves: an overview. *Geol. Soc. Lond. Pet. Geol. Conf. Ser.* 7, 591–619. <https://doi.org/10.1144/0070591>.
- Drachev, S.S., Mazur, S., Campbell, S., Green, C., Tishchenko, A., 2018. Crustal architecture of the East Siberian Arctic Shelf and adjacent Arctic Ocean constrained by seismic data and gravity modeling results. *J. Geodyn.* 119, 123–148. <https://doi.org/10.1016/j.jog.2018.03.005>.
- Ehlers, B.-M., Jokat, W., 2013. Paleo-bathymetry of the northern North Atlantic and consequences for the opening of the Fram Strait. *Mar. Geophys. Res.* 34, 25–43. <https://doi.org/10.1007/s11001-013-9165-9>.
- Embry, A., Beauchamp, B., 2008. Chapter 13, Sverdrup Basin. In: *Sedimentary Basins of the World*, pp. 451–471. [https://doi.org/10.1016/S1874-5997\(08\)00013-0](https://doi.org/10.1016/S1874-5997(08)00013-0).
- Embry, A., Dixon, J., 1994. The age of the Amerasia Basin. In: Fujita, K., Thurston, D.K. (Eds.), *Proceedings of the 1992 International Conference on Arctic Margins*. U.S. Dept. of the Interior Minerals Management Service, OCS Study, Anchorage, pp. 289–294.
- Embry, A.F., 1990. Geological and geophysical evidence in support of the hypothesis of anticlockwise rotation of northern Alaska. *Mar. Geol.* 93, 317–329. [https://doi.org/10.1016/0025-3227\(90\)90090-7](https://doi.org/10.1016/0025-3227(90)90090-7).

- Embry, A.F., Osadetz, K.G., 1989. Stratigraphy and tectonic significance of Cretaceous volcanism in the Queen Elizabeth Islands. *Canad. Arctic Archipelago: Reply. Can. J. Earth Sci.* 26, 2740–2741. <https://doi.org/10.1139/e89-236>.
- Evangelatos, J., Mosher, D.C., 2016. Seismic stratigraphy, structure and morphology of Makarov Basin and surrounding regions: tectonic implications. *Mar. Geol.* 374, 1–13. <https://doi.org/10.1016/j.margeo.2016.01.013>.
- Evangelatos, J., Funck, T., Mosher, D.C., 2017. The sedimentary and crustal velocity structure of Makarov Basin and adjacent Alpha Ridge. *Tectonophysics* 696–697, 99–114. <https://doi.org/10.1016/j.tecto.2016.12.026>.
- Evenchick, C.A., Davis, W.J., Bédard, J.H., Hayward, N., Friedman, R.M., 2015. Evidence for protracted High Arctic large igneous province magmatism in the central Sverdrup Basin from stratigraphy, geochronology, and paleodepths of saucer-shaped sills. *Geol. Soc. Am. Bull.* 127, 1366–1390. <https://doi.org/10.1130/B31190.1>.
- Foulger, G.R., Doré, T., Emeleus, C.H., Franke, D., Geoffroy, L., Gernigon, L., Hey, R., Holdsworth, R.E., Hole, M., Höskuldsson, A., Julian, B., Kuszniir, N., Martinez, F., McCaffrey, K.J.W., Natland, J.H., Pearce, A., Petersen, K., Schiffer, C., Stephenson, R., Stoker, M., 2020. A continental Greenland-Iceland-Faroe Ridge. *Earth-Sci. Rev.* 102926 <https://doi.org/10.1016/j.earscirev.2019.102926>.
- Franke, D., 2013. Rifting, lithosphere breakup and volcanism: Comparison of magma-poor and volcanic rifted margins. *Mar. Pet. Geol.* 43, 63–87. <https://doi.org/10.1016/j.marpetgeo.2012.11.003>.
- Funck, T., Jackson, H.R., Shimeld, J., 2011. The crustal structure of the Alpha Ridge at the transition to the Canadian Polar Margin: Results from a seismic refraction experiment. *J. Geophys. Res.* 116, B12101 <https://doi.org/10.1029/2011JB008411>.
- Gaina, C., Werner, S.C., Saltus, R., Maus, S., 2011. Chapter 3 Circum-Arctic mapping project: new magnetic and gravity anomaly maps of the Arctic. *Geol. Soc. Lond. Mem.* 35, 39–48. <https://doi.org/10.1144/M35.3>.
- Gaina, C., Medvedev, S., Torsvik, T.H., Koulakov, I., Werner, S.C., 2014. 4D Arctic: A glimpse into the structure and evolution of the arctic in the light of new geophysical maps, plate tectonics and tomographic models. *Surv. Geophys.* 35, 1095–1122. <https://doi.org/10.1007/s10712-013-9254-y>.
- Gaina, C., Nasuti, A., Kimbell, G.S., Blischke, A., 2017. Break-up and seafloor spreading domains in the NE Atlantic. *Geol. Soc. Lond. Spec. Publ.* 447, 393–417. <https://doi.org/10.1144/SP447.12>.
- Galloway, J.M., Tullius, D.N., Evenchick, C.A., Swindles, G.T., Hadlari, T., Embry, A., 2015. Early Cretaceous vegetation and climate change at high latitude: Palynological evidence from Isachsen Formation, Arctic Canada. *Cretac. Res.* 56, 399–420. <https://doi.org/10.1016/j.cretres.2015.04.002>.
- Geoffroy, L., 2005. Volcanic passive margins. *Compt. Rendus Geosci.* 337, 1395–1408. <https://doi.org/10.1016/j.crte.2005.10.006>.
- Glebovsky, V.Y., Kaminsky, V.D., Minakov, A.N., Merkur'ev, S.A., Childers, V.A., Brozina, J.M., 2006. Formation of the Eurasia Basin in the Arctic Ocean as inferred from geohistorical analysis of the anomalous magnetic field. *Geotectonics* 40, 263–281. <https://doi.org/10.1134/S0016852106040029>.
- Glebovsky, V.Y., Astafurova, E.G., Chernykh, A.A., Korneva, M.A., Kaminsky, V.D., Poselov, V.A., 2013. Thickness of the Earth's crust in the deep Arctic Ocean: Results of a 3D gravity modeling. *Russ. Geol. Geophys.* 54, 247–262. <https://doi.org/10.1016/j.rgg.2013.02.001>.
- Gradstein, F.M., Ogg, J.G., Schmitz, M.D., Ogg, G.M. (Eds.), 2012. *The Geologic Time Scale*. Elsevier. <https://doi.org/10.1016/C2011-1-08249-8>.
- Grantz, A., Hart, P.E., 2012. Petroleum prospectivity of the Canada Basin, Arctic Ocean. *Mar. Pet. Geol.* 30, 126–143. <https://doi.org/10.1016/j.marpetgeo.2011.11.001>.
- Grantz, A., Scott, R.A., Drachev, S.S., Moore, T.E., Valin, Z.C., 2011. Chapter 2 Sedimentary successions of the Arctic Region (58–64° to 90°N) that may be prospective for hydrocarbons. *Geol. Soc. Lond. Mem.* 35, 17–37. <https://doi.org/10.1144/M35.2>.
- Hadlari, T., Midwinter, D., Galloway, J.M., Dewing, K., Durban, A.M., 2016. Mesozoic rift to post-rift tectonostratigraphy of the Sverdrup Basin, Canadian Arctic. *Mar. Pet. Geol.* 76, 148–158. <https://doi.org/10.1016/j.marpetgeo.2016.05.008>.
- Harding, I.C., Charles, A.J., Marshall, J.E.A., Pällike, H., Roberts, A.P., Wilson, P.A., Jarvis, E., Thorne, R., Morris, E., Moremon, R., Pearce, R.B., Akbari, S., 2011. Sea-level and salinity fluctuations during the Paleocene–Eocene thermal maximum in Arctic Spitsbergen. *Earth Planet. Sci. Lett.* 303, 97–107. <https://doi.org/10.1016/j.epsl.2010.12.043>.
- Harrison, J.C., Brent, T.A., 2005. Basins and fold belts of Prince Patrick Island and adjacent area. *Can. Arctic Islands*. <https://doi.org/10.4095/220345>.
- Harrison, J.C., St-Onge, M.R., Petrov, O.V., Strel'nikov, S.I., Lopatin, B.G., Wilson, F.H., Tella, S., Paul, D., Lynds, T., Shokalsky, S.P., Hults, C.K., Bergman, S., Jepsen, H.F., Solli, A., 2011. *Geological map of the Arctic; Geological Survey of Canada, Map 2159A, scale 1:5 000 000*.
- Hegewald, A., Jokat, W., 2013. Tectonic and sedimentary structures in the northern Chukchi region, Arctic Ocean. *J. Geophys. Res. Solid Earth* 118, 3285–3296. <https://doi.org/10.1002/jgrb.50282>.
- Helwig, J., Kumar, N., Emmet, P., Dinkelman, M.G., 2011. Chapter 35 Regional seismic interpretation of crustal framework, Canadian Arctic passive margin, Beaufort Sea, with comments on petroleum potential. *Geol. Soc. Lond. Mem.* 35, 527–543. <https://doi.org/10.1144/M35.35>.
- Herman, A.B., Spicer, R.A., 1996. Palaeobotanical evidence for a warm Cretaceous Arctic Ocean. *Nature* 380, 330–333. <https://doi.org/10.1038/380330a0>.
- Herman, A.B., Spicer, R.A., Spicer, T.E.V., 2016. Environmental constraints on terrestrial vertebrate behaviour and reproduction in the high Arctic of the Late Cretaceous. *Palaeogeogr. Palaeoclimatol. Palaeoecol.* 441, 317–338. <https://doi.org/10.1016/j.palaeo.2015.09.041>.
- Herrle, J.O., Schröder-Adams, C.J., Davis, W., Pugh, A.T., Galloway, J.M., Fath, J., 2015. Mid-Cretaceous high arctic stratigraphy, climate, and oceanic anoxic events. *Geology* 43, 403–406. <https://doi.org/10.1130/G36439.1>.
- Homza, T.X., Bergman, S.C., 2019. *A Geologic Interpretation of the Chukchi Sea Petroleum Province: Offshore Alaska, USA*. The American Association of Petroleum Geologists. <https://doi.org/10.1306/AAPG119>.
- Houseknecht, D.W., 2019a. Evolution of the Arctic Alaska Sedimentary Basin. In: *The Sedimentary Basins of the United States and Canada*. Elsevier, pp. 719–745. <https://doi.org/10.1016/B978-0-444-63895-3.00018-8>.
- Houseknecht, D.W., 2019b. Petroleum systems framework of significant new oil discoveries in a giant Cretaceous (Aptian–Cenomanian) clinothem in Arctic Alaska. *Am. Assoc. Pet. Geol. Bull.* 103, 619–652. <https://doi.org/10.1306/08151817281>.
- Houseknecht, D.W., Bird, K.J., 2011. Chapter 34 Geology and petroleum potential of the rifted margins of the Canada Basin. *Geol. Soc. Lond. Mem.* 35, 509–526. <https://doi.org/10.1144/M35.34>.
- Houseknecht, D.W., Wartes, M.A., 2013. Clinoform deposition across a boundary between orogenic front and foredeep - an example from the Lower Cretaceous in Arctic Alaska. *Terra Nova* 25, 206–211. <https://doi.org/10.1111/ter.12024>.
- Houseknecht, D.W., Craddock, W.H., Lease, R.O., 2016. Upper Cretaceous and Lower Jurassic strata in shallow cores on the Chukchi Shelf, Arctic Alaska. In: *USGS Prof. Pap.* 1814, p. 37. <https://doi.org/10.3133/pp1814C>.
- Huber, B.T., MacLeod, K.G., Watkins, D.K., Coffin, M.F., 2018. The rise and fall of the Cretaceous Hot Greenhouse climate. *Glob. Planet. Chang.* 167, 1–23. <https://doi.org/10.1016/j.gloplacha.2018.04.004>.
- Hutchinson, D.R., Jackson, H.R., Houseknecht, D.W., Li, Q., Shimeld, J.W., Mosher, D.C., Chian, D., Saltus, R.W., Oakey, G.N., 2017. Significance of Northeast-trending features in Canada Basin, Arctic Ocean. *Geochem. Geophys. Geosyst.* 18, 4156–4178. <https://doi.org/10.1002/2017GC007099>.
- Ilhan, I., Coakley, B.J., 2018. Meso–Cenozoic evolution of the southwestern Chukchi Borderland, Arctic Ocean. *Mar. Pet. Geol.* 95, 100–109. <https://doi.org/10.1016/j.marpetgeo.2018.04.014>.
- Jakobsson, M., Backman, J., Rudels, B., Nycander, J., Frank, M., Mayer, L., Jokat, W., Sangiorgi, F., O'Regan, M., Brinkhuis, H., King, J., Moran, K., 2007. The early Miocene onset of a ventilated circulation regime in the Arctic Ocean. *Nature* 447, 986–990. <https://doi.org/10.1038/nature05924>.
- Jakobsson, M., Mayer, L., Coakley, B., Dowdeswell, J.A., Forbes, S., Fridman, B., Hodnesdal, H., Noormets, R., Pedersen, R., Rebesco, M., Schenke, H.W., Zarayskaya, Y., Accettella, D., Armstrong, A., Anderson, R.M., Bienhoff, P., Camerlenghi, A., Church, I., Edwards, M., Gardner, J.V., Hall, J.K., Hell, B., Hestvik, O., Kristoffersen, Y., Marcussen, C., Mohammad, R., Mosher, D., Nghiem, S. V., Pedrosa, M.T., Travaglini, P.G., Weatherall, P., 2012. The International Bathymetric chart of the Arctic Ocean (IBCAO) Version 3.0. *Geophys. Res. Lett.* 39 <https://doi.org/10.1029/2012GL052219>.
- Jakobsson, M., Mayer, L.A., Bringenspar, C., et al., 2020. The International Bathymetric Chart of the Arctic Ocean Version 4.0. *Sci Data* 7, 176. <https://doi.org/10.1038/s41597-020-0520-9>.
- Jenkyns, H.C., Forster, A., Schouten, S., Sinninghe Damsté, J.S., 2004. High temperatures in the Late Cretaceous Arctic Ocean. *Nature* 432, 888–892. <https://doi.org/10.1038/nature03143>.
- Jokat, W., 2003. Seismic investigations along the western sector of Alpha Ridge, Central Arctic Ocean. *Geophys. J. Int.* 152, 185–201. <https://doi.org/10.1046/j.1365-246X.2003.01839.x>.
- Jokat, W., 2005. The sedimentary structure of the Lomonosov Ridge between 88°N and 80°N. *Geophys. J. Int.* 163, 698–726. <https://doi.org/10.1111/j.1365-246X.2005.02786.x>.
- Jokat, W., Ickrath, M., 2015. Structure of ridges and basins off East Siberia along 81°N, Arctic Ocean. *Mar. Pet. Geol.* 64, 222–232. <https://doi.org/10.1016/j.marpetgeo.2015.02.047>.
- Jokat, W., Ickrath, M., O'Connor, J., 2013. Seismic transect across the Lomonosov and Mendeleev Ridges: Constraints on the geological evolution of the Amerasia Basin, Arctic Ocean. *Geophys. Res. Lett.* 40, 5047–5051. <https://doi.org/10.1002/grl.50975>.
- Kashubin, S.N., Pavlenkova, N.I., Petrov, O.V., Mil'shteyn, E.D., Shokalsky, S.P., Erinchek, Y.M., 2013. *Earth crust types of the Circum-Polar Arctics*. *Reg. Geol. I Metallog.* 55, 5–20 (in Russian).
- Kashubin, S.N., Petrov, O.V., Artemieva, I.M., Morozov, A.F., Vyatkina, D.V., Golysheva, Y.S., Kashubina, T.V., Milshtein, E.D., Rybalka, A.V., Erinchek, Y.M., Sakulina, T.S., Krupnova, N.A., Shulgin, A.A., 2018. Crustal structure of the Mendeleev Rise and the Chukchi Plateau (Arctic Ocean) along the Russian wide-angle and multichannel seismic reflection experiment “Arctic-2012”. *J. Geodyn.* 119, 107–122. <https://doi.org/10.1016/j.jog.2018.03.006>.
- Knudsen, C., Hopper, J.R., Bierman, P.R., Bjerager, M., Funck, T., Green, P.F., Ineson, J. R., Japsen, P., Marcussen, C., Sherlock, S.C., Thomsen, T.B., 2018. Samples from the Lomonosov Ridge place new constraints on the geological evolution of the Arctic Ocean. *Geol. Soc. Lond. Spec. Publ.* 460, 397–418. <https://doi.org/10.1144/SP460.17>.
- Kos'ko, M.K., Trufanov, G.V., 2002. Middle Cretaceous to Eo-pleistocene sequences on the New Siberian Islands: an approach to interpret offshore seismic. *Mar. Pet. Geol.* 19, 901–919.
- Kos'ko, M.K., Cecile, M.P., Harrison, J.C., Ganelin, V.G., Khandoshko, N.V., Lopatin, B. G., 1993. *Geology of Wrangel Island, between Chukchi and East Siberian seas, northeastern Russia*. *Geol. Surv. Canada Bull.* 461, 101.
- Kos'ko, M.K., Sobolev, N.N., Korago, E.A., Proskurnin, V.F., Stolbov, N.M., 2013. *Geology of Novosibirskian Islands – a basis for interpretation of geophysical data on the Eastern Arctic shelf of Russia*. *Neftegazov. Geol. Teor. I Prakt.* 8. https://doi.org/10.17353/2070-5379/17_2013.
- Kumar, N., Granath, J.W., Emmet, P.A., Helwig, J.A., Dinkelman, M.G., 2011. Chapter 33 Stratigraphic and tectonic framework of the US Chukchi Shelf: exploration insights

- from a new regional deep-seismic reflection survey. *Geol. Soc. Lond. Mem.* 35, 501–508. <https://doi.org/10.1144/M35.33>.
- Kuzmichev, A.B., 2009. Where does the South Anyui suture go in the New Siberian islands and Laptev Sea? Implications for the Amerasia basin origin. *Tectonophysics* 463, 86–108. <https://doi.org/10.1016/j.tecto.2008.09.017>.
- Kuzmichev, A.B., Aleksandrova, G.N., Herman, A.B., 2009. Aptian-Albian coaliferous sediments of Kotel'nyi Island (New Siberian Islands): new data on the section structure and ignimbrite volcanism. *Stratigr. Geol. Correl.* 17, 519–543. <https://doi.org/10.1134/S0869593809050050>.
- Kuzmichev, A.B., Aleksandrova, G.N., Herman, A.B., Danukalova, M.K., Simakova, A.N., 2013. Paleogene-Neogene sediments of Bel'kov Island (New Siberian Islands): characteristics of sedimentary cover in the eastern Laptev shelf. *Stratigr. Geol. Correl.* 21, 421–444. <https://doi.org/10.1134/S0869593813040059>.
- Langinen, A.E., Lebedeva-Ivanova, N.N., Gee, D.G., Zamansky, Y.Y., 2009. Correlations between the Lomonosov Ridge, Marvin Spur and adjacent basins of the Arctic Ocean based on seismic data. *Tectonophysics* 472, 309–322. <https://doi.org/10.1016/j.tecto.2008.05.029>.
- Laverov, N.P., Lobkovsky, L.I., Kononov, M.V., Dobretsov, N.L., Vernikovskiy, V.A., Sokolov, S.D., Shipilov, E.V., 2013. A geodynamic model of the evolution of the Arctic basin and adjacent territories in the Mesozoic and Cenozoic and the outer limit of the Russian Continental Shelf. *Geotectonics* 47, 1–30. <https://doi.org/10.1134/S0016852113010044>.
- Lawver, L., Norton, I., Garagan, L., 2015. The bigger picture: A need for the whole earth plate tectonic setting when reconstructing Greenland. In: *3P Arctic. The Polar Petroleum Potential. Conference & Exhibition. Abstract Book. Stavanger*, p. 61.
- Lebedeva-Ivanova, N., Gaina, C., Minakov, A., Kashubin, S., 2019. ArcCRUST: arctic crustal thickness from 3-D gravity inversion. *Geochem. Geophys. Geosyst.* <https://doi.org/10.1029/2018GC008098>, 2018GC008098.
- Lebedeva-Ivanova, N.N., Gee, D.G., Sergeyev, M.B., 2011. Chapter 26 Crustal structure of the East Siberian continental margin, Podvodnikov and Makarov basins, based on refraction seismic data (TransArctic 1989–1991). *Geol. Soc. Lond. Mem.* 35, 395–411. <https://doi.org/10.1144/M35.26>.
- Lobkovsky, L.I., 2016. Deformable plate tectonics and regional geodynamic model of the Arctic region and Northeastern Asia. *Russ. Geol. Geophys.* 57, 371–386. <https://doi.org/10.1016/j.rgg.2016.03.002>.
- Mathieu, L., van Wyk de Vries, B., Holohan, E.P., Troll, V.R., 2008. Dykes, cups, saucers and sills: analogue experiments on magma intrusion into brittle rocks. *Earth Planet. Sci. Lett.* 271, 1–13. <https://doi.org/10.1016/j.epsl.2008.02.020>.
- Miller, E.L., Verzhbitskiy, V.E., 2009. Structural studies near Pevek, Russia: implications for formation of the East Siberian Shelf and Makarov Basin of the Arctic Ocean. *Stephan Mueller Spec. Publ. Ser.* 4, 223–241. <https://doi.org/10.5194/smeps-4-223-2009>.
- Miller, E.L., Soloviev, A., Kuzmichev, A., Gehrels, G.E., Toro, J., Tsuchkova, M., 2008. Jura-Cretaceous foreland basin deposits of the Russian Arctic: Separated by birth of Makarov Basin?, in: *Nor. J. Geol.* 201–226.
- Miller, E.L., Gehrels, G.E., Pease, V., Sokolov, S., 2010. Paleozoic and Mesozoic stratigraphy and U–Pb detrital zircon geochronology of Wrangel Island, Russia: constraints on paleogeography and paleocontinental reconstructions of the Arctic. *Am. Assoc. Pet. Geol. Bull.* 94, 665–692.
- Miller, E.L., Akinin, V.V., Dumitru, T.A., Gottlieb, E.S., Grove, M., Meisling, K., Seward, G., 2018a. Deformational history and thermochronology of Wrangel Island, East Siberian Shelf and coastal Chukotka, Arctic Russia. *Geol. Soc. Lond. Spec. Publ.* 460, 207–238. <https://doi.org/10.1144/SP460.7>.
- Miller, E.L., Meisling, K.E., Akinin, V.V., Brumley, K., Coakley, B.J., Gottlieb, E.S., Hoiland, C.W., O'Brien, T.M., Soboleva, A., Toro, J., 2018b. Circum-Arctic Lithosphere Evolution (CALE) Transect C: displacement of the Arctic Alaska–Chukotka microplate towards the Pacific during opening of the Amerasia Basin of the Arctic. *Geol. Soc. Lond. Spec. Publ.* 460, 57–120. <https://doi.org/10.1144/SP460.9>.
- Minakov, A., Yarushina, V., Faleide, J.I., Krupnova, N., Sakoulina, T., Dergunov, N., Glebovskiy, V., 2018. Dyke emplacement and crustal structure within a continental large igneous province, northern Barents Sea. *Geol. Soc. Lond. Spec. Publ.* 460, 371–395. <https://doi.org/10.1144/SP460.4>.
- Moran, K., Backman, J., Brinkhuis, H., Clemens, S.C., Cronin, T., Dickens, G.R., Eynaud, F., Gattacceca, J., Jakobsson, M., Jordan, R.W., Kaminski, M., King, J., Koc, N., Krylov, A., Martinez, N., Matthiessen, J., McInroy, D., Moore, T.C., Onodera, J., O'Regan, M., Pälike, H., Rea, B., Rio, D., Sakamoto, T., Smith, D.C., Stein, R., St John, K., Suto, I., Suzuki, N., Takahashi, K., Watanabe, M., Yamamoto, M., Farrell, J., Frank, M., Kubik, P., Jokat, W., Kristoffersen, Y., 2006. The Cenozoic palaeoenvironment of the Arctic Ocean. *Nature* 441, 601–605. <https://doi.org/10.1038/nature04800>.
- Morozov, A.F., Petrov, O.V., S.P. S., Kashubin, S.N., Kremenetskiy, A.A., Shkatov, M.Y., Kaminsky, V.D., Gusev, E.A., Grikurov, G.E., Rekant, P.V., Shevchenko, S.S., Sergeev, S.A., Shtatov, V.V., 2013. New geological data substantiating continental nature of region of Central-Arctic rises. *Reg. Geol. I Metallog.* 55, 34–55.
- Mosher, D.C., Shimeld, J., Hutchinson, D., Chian, D., Lebedeva-Ivanova, N., Jackson, R., 2012. Canada Basin revealed. In: *Society of Petroleum Engineers - Arctic Technology Conference 2012*, pp. 805–815.
- Mukasa, S.B., Andronikov, A., Brumley, K., Mayer, L.A., Armstrong, A., 2020. Basalts from the Chukchi Borderland: 40Ar/39Ar Ages and Geochemistry of submarine intraplate lavas dredged from the western Arctic Ocean. *Am. Geophys. Union.* <https://doi.org/10.1029/2019JB017604>.
- Nikishin, A.M., Ziegler, P., Abbott, D., Brunet, M.-F., Cloetingh, S., 2002. Permo–Triassic intraplate magmatism and rifting in Eurasia: implications for mantle plumes and mantle dynamics. *Tectonophysics* 351, 3–39. [https://doi.org/10.1016/S0040-1951\(02\)00123-3](https://doi.org/10.1016/S0040-1951(02)00123-3).
- Nikishin, A.M., Petrov, E.I., Malyshev, N.A., 2014. Geological Structure and History of the Arctic Ocean. EAGE Publications bv. <https://doi.org/10.3997/9789462821880>.
- Nikishin, A.M., Petrov, E.I., Malyshev, N.A., Ershova, V.P., 2017. Rift systems of the Russian Eastern Arctic shelf and Arctic deep water basins: Link between geological history and geodynamics. *Geodyn. Tectonophysics* 8, 11–43. <https://doi.org/10.5800/GT-2017-8-1-0231>.
- Nikishin, A.M., Gaina, C., Petrov, E.I., Malyshev, N.A., Freiman, S.I., 2018. Eurasia Basin and Gakkel Ridge, Arctic Ocean: Crustal asymmetry, ultra-slow spreading and continental rifting revealed by new seismic data. *Tectonophysics* 746, 64–82. <https://doi.org/10.1016/j.tecto.2017.09.006>.
- Nikishin, A.M., Startseva, K.F., Verzhbitskiy, V.E., Cloetingh, S., Malyshev, N.A., Petrov, E.I., Posamentier, H., Freiman, S.I., Lineva, M.D., Zhukov, N.N., 2019. Sedimentary Basins of the East Siberian Sea and the Chukchi Sea and the adjacent area of the Amerasia Basin: Seismic stratigraphy and stages of geological history. *Geotectonics* 53, 635–657. <https://doi.org/10.1134/S0016852119060104>.
- Nikishin, A.M., Petrov, E.I., Cloetingh, S., Korniyuchuk, A.V., Morozov, A.F., Petrov, O.V., Poselov, V.A., Beziyakov, A.V., Skolotnev, S.G., Malyshev, N.A., Verzhbitskiy, V.E., Posamentier, H.W., Freiman, S.I., Rodina, E.A., Startseva, K.F., Zhukov, N.N., 2021a. Arctic ocean mega project: Paper 1 - Data collection. *Earth-Sci. Rev.* <https://doi.org/10.1016/j.earscirev.2021.103559>.
- Nikishin, A.V., Petrov, E.I., Cloetingh, S., Freiman, S.I., Malyshev, N.A., Morozov, A.F., Posamentier, H.W., Verzhbitskiy, V.E., Zhukov, N.N., 2021b. Arctic Ocean Mega-project: Paper 3 – Mesozoic to Cenozoic geological evolution. *Earth Sci. Rev.* <https://doi.org/10.1016/j.earscirev.2019.103034>.
- O'Brien, C.L., Robinson, S.A., Pancost, R.D., Sinninghe Damsté, J.S., Schouten, S., Lunt, D.J., Alsenz, H., Bornemann, A., Bottini, C., Brassell, S.C., Farnsworth, A., Forster, A., Huber, B.T., Inglis, G.N., Jenkens, H.C., Linnert, C., Littler, K., Markwick, P., McAnena, A., Mutterlose, J., Naafs, B.D.A., Püttmann, W., Sluijs, A., van Helmond, N.A.G.M., Vellekoop, J., Wagner, T., Wrobel, N.E., 2017. Cretaceous sea-surface temperature evolution: constraints from TEX 86 and planktonic foraminiferal oxygen isotopes. *Earth-Sci. Rev.* 172, 224–247. <https://doi.org/10.1016/j.earscirev.2017.07.012>.
- O'Regan, M., Moran, K., Baxter, C.D.P., Cartwright, J., Vogt, C., Kölling, M., 2010. Towards ground truthing exploration in the central Arctic Ocean: a Cenozoic compaction history from the Lomonosov Ridge. *Basin Res.* 22, 215–235. <https://doi.org/10.1111/j.1365-2117.2009.00403.x>.
- O'Sullivan, P.B., Murphy, J.M., Blythe, A.E., 1997. Late Mesozoic and Cenozoic thermotectonic evolution of the central Brooks Range and adjacent North Slope foreland basin, Alaska: Including fission track results from the Trans-Alaska Crustal Transect (TACT). *J. Geophys. Res. Solid Earth* 102, 20821–20845. <https://doi.org/10.1029/96JB03411>.
- Oakey, G.N., Saltus, R.W., 2016. Geophysical analysis of the Alpha–Mendeleev ridge complex: characterization of the high arctic large Igneous Province. *Tectonophysics* 691, 65–84. <https://doi.org/10.1016/j.tecto.2016.08.005>.
- Ogg, J.G., Ogg, G.M., Gradstein, F.M., 2016. *A Concise Geologic TimeScale*. Elsevier.
- Omosanya, K.O., Johansen, S.E., Abrahamson, P., 2016. Magmatic activity during the breakup of Greenland–Eurasia and fluid-flow in Stappen High, SW Barents Sea. *Mar. Pet. Geol.* 76, 397–411. <https://doi.org/10.1016/j.marpetgeo.2016.05.017>.
- Parfenov, L.M., Kuzmin, M.I. (Eds.), 2001. *Tectonics, Geodynamics and Metallogeny of the Territory of the Sakha Republic (Yakutia)*. MAIK “Nauka/Interperiodika,” Moscow.
- Pease, V., Drachev, S., Stephenson, R., Zhang, X., 2014. Arctic lithosphere — A review. *Tectonophysics* 628, 1–25. <https://doi.org/10.1016/j.tecto.2014.05.033>.
- Peters, K., Schenk, O., Bird, K., 2011. Timing of petroleum system events controls accumulations on the North Slope, Alaska. In: *AAPG Memoir*.
- Petrov, O., Morozov, A., Shokalskiy, S., Kashubin, S., Artemieva, I.M., Sobolev, N., Petrov, E., Ernst, R.E., Sergeev, S., Smelov, M., 2016. Crustal structure and tectonic model of the Arctic region. *Earth-Sci. Rev.* 154, 29–71. <https://doi.org/10.1016/j.earscirev.2015.11.013>.
- Petrov, O.V., 2017. *Tectonic map of the Arctic*. VSEGEI Publishing House, St. Petersburg.
- Piskarev, A., Poselov, V., Kaminsky, V. (Eds.), 2019. *Geologic Structures of the Arctic Basin*. Springer International Publishing, Cham. <https://doi.org/10.1007/978-3-319-7742-9>.
- Polteau, S., Hendriks, B.W.H., Planke, S., Ganerød, M., Corfu, F., Faleide, J.I., Midtkandal, I., Svensen, H.S., Mykkelbust, R., 2016. The early cretaceous barents Sea Sill Complex: distribution, 40Ar/39Ar geochronology, and implications for carbon gas formation. *Palaeogeogr. Palaeoclimatol. Palaeoecol.* 441, 83–95. <https://doi.org/10.1016/j.palaeo.2015.07.007>.
- Popova, A.B., Makhova, O.S., Malyshev, N.A., Verzhbitskiy, V.E., Obmetko, V.V., Borodulin, A.A., 2018. Construction of an integrated seismic-geological model of the East Siberian Sea shelf. *Neft. Khozyaystvo - Oil Ind.* 30–34. <https://doi.org/10.24887/0028-2448-2018-4-30-34>.
- Poselov, V.A., Avetisov, G.P., Butsenko, V.V., Zholondz, S.M., Kaminsky, V.D., Pavlov, S.P., 2012. The Lomonosov Ridge as a natural extension of the Eurasian continental margin into the Arctic Basin. *Russ. Geol. Geophys.* 53, 1276–1290. <https://doi.org/10.1016/j.rgg.2012.10.002>.
- Poselov, V.A., Verba, V.V., Zholondz, S.M., Butsenko, V.V., 2019. The rises of the Amerasia basin, arctic ocean, and possible equivalents in the Atlantic ocean. *Океанология* 59, 810–825. <https://doi.org/10.31857/S0030-1574595810-825>.
- Prokopyev, A.V., Ershova, V.B., Anfinsen, O., Stockli, D., Powell, J., Khudoley, A.K., Vasiliev, D.A., Sobolev, N.N., Petrov, E.O., 2018. Tectonics of the New Siberian Islands archipelago: Structural styles and low-temperature thermochronology. *J. Geodyn.* 121, 155–184. <https://doi.org/10.1016/j.jog.2018.09.001>.
- Pugh, A.T., Schröder-Adams, C.J., Carter, E.S., Herrle, J.O., Galloway, J., Haggart, J.W., Andrews, J.L., Hatsukano, K., 2014. Cenomanian to Santonian radiolarian biostratigraphy, carbon isotope stratigraphy and paleoenvironments of the Sverdrup

- Basin, Ellef Ringnes Island, Nunavut, Canada. *Palaeogeogr. Palaeoclimatol. Palaeoecol.* 413, 101–122. <https://doi.org/10.1016/j.palaeo.2014.06.010>.
- Puscharovskiy, Y.M., 1960. Some general problems of the Arctic tectonics. *Reports Acad. Sci. USSR* 9, 15–28 (in Russian).
- Rekant, P., Sobolev, N., Portnov, A., Belyatsky, B., Dipre, G., Pakhalko, A., Kaban'kov, V., Andreeva, I., 2019. Basement segmentation and tectonic structure of the Lomonosov Ridge, arctic Ocean: insights from bedrock geochronology. *J. Geodyn.* 128, 38–54. <https://doi.org/10.1016/j.jog.2019.05.001>.
- Rekant, P.V., Gusev, E.A., 2012. Seismic geologic structure model for the sedimentary cover of the Laptev Sea part of the Lomonosov Ridge and adjacent parts of the Amundsen Plain and Podvodnikov Basin. *Russ. Geol. Geophys.* 53, 1150–1162. <https://doi.org/10.1016/j.rgg.2012.09.003>.
- Rekant, P.V., Petrov, O.V., Kashubin, S.N., Rybalka, A.V., Shokalsky, S.P., Petrov, E.O., Vinokurov, I.Y., Gusev, E.A., 2015. Geological history of sedimentary cover of deep-water part of the Arctic Basin according to seismic data. *Reg. Geol. I Metallog.* 55, 34–55 (in Russian).
- Rogov, M.A., Ershova, V.B., Shchepetova, E.V., Zakharov, V.A., Pokrovsky, B.G., Khudoley, A.K., 2017. Earliest cretaceous (late Berriasian) glendonites from Northeast Siberia revise the timing of initiation of transient early cretaceous cooling in the high latitudes. *Cretac. Res.* 71, 102–112. <https://doi.org/10.1016/j.cretres.2016.11.011>.
- Saltus, R.W., Miller, E.L., Gaina, C., Brown, P.J., 2011. Chapter 4 Regional magnetic domains of the Circum-Arctic: a framework for geodynamic interpretation. *Geol. Soc. Lond. Mem.* 35, 49–60. <https://doi.org/10.1144/M35.4>.
- Savin, V.A., 2020. Earth crust structure of sedimentary basins of the Laptev and East Siberian seas based on geophysical modelling. In: VNIIOkeangeologia, p. 128. PhD Thesis. (in Russian). <http://www.ipgg.sbras.ru/ru/education/commettee/savin2019>.
- Schröder-Adams, C., 2014. The Cretaceous Polar and Western Interior seas: paleoenvironmental history and paleoceanographic linkages. *Sediment. Geol.* 301, 26–40. <https://doi.org/10.1016/j.sedgeo.2013.12.003>.
- Schröder-Adams, C.J., Herrle, J.O., Embry, A.F., Haggart, J.W., Galloway, J.M., Pugh, A.T., Harwood, D.M., 2014. Aptian to Santonian foraminiferal biostratigraphy and paleoenvironmental change in the Sverdrup Basin as revealed at Glacier Fiord, Axel Heiberg Island, Canadian Arctic Archipelago. *Palaeogeogr. Palaeoclimatol. Palaeoecol.* 413, 81–100. <https://doi.org/10.1016/j.palaeo.2014.03.010>.
- Sekretov, S.B., 2001. Northwestern margin of the East Siberian Sea, Russian Arctic: seismic stratigraphy, structure of the sedimentary cover and some remarks on the tectonic history. *Tectonophysics* 339, 353–371. [https://doi.org/10.1016/S0040-1951\(01\)00108-1](https://doi.org/10.1016/S0040-1951(01)00108-1).
- Shephard, G.E., Müller, R.D., Seton, M., 2013. The tectonic evolution of the Arctic since Pangea breakup: Integrating constraints from surface geology and geophysics with mantle structure. *Earth-Sci. Rev.* 124, 148–183. <https://doi.org/10.1016/j.earscirev.2013.05.012>.
- Sherwood, K.W., Johnson, P.P., Craig, J.D., Zerwick, S.A., Lothamer, R.T., Thurston, D.K., Hurlbert, S.B., 2002. Structure and stratigraphy of the Hanna Trough, U.S. Chukchi Shelf, Alaska. In: Miller, E.L., Grantz, A., Klemperer, S.L. (Eds.), *Special Paper 360: Tectonic Evolution of the Bering Shelf-Chukchi Sea-Artic Margin and Adjacent Landmasses*. Geological Society of America, Boulder, Colorado, pp. 39–66. <https://doi.org/10.1130/0-8137-2360-4.39>.
- Shipilov, E.V., 2016. Basaltic magmatism and strike-slip tectonics in the Arctic margin of Eurasia: evidence for the early stage of geodynamic evolution of the Amerasia Basin. *Russ. Geol. Geophys.* 57, 1668–1687. <https://doi.org/10.1016/j.rgg.2016.04.007>.
- Skaryatin, M.V., Batalova, A.A., Vorgacheva, E.Y., Bulgakova, E.A., Zaytseva, S.A., Igtisamov, D.V., Moiseeva, R.K., Verzhbitskiy, V.E., Malyshev, N.A., Obmetko, V.V., Borodulin, A.A., 2020. Salt tectonics and petroleum prospectivity of the Russian Chukchi Sea. *Neft. khozyaystvo - Oil Ind.* 2, 12–17. <https://doi.org/10.24887/0028-2448-2020-2-12-17>.
- Skolotnev, S., Aleksandrova, G., Isakova, T., Tolmacheva, T., Kurilenko, A., Raevskaya, E., Rozhnov, S., Petrov, E., Korniyuchuk, A., 2019. Fossils from seabed bedrocks: Implications for the nature of the acoustic basement of the Mendeleev Rise (Arctic Ocean). *Mar. Geol.* 407, 148–163. <https://doi.org/10.1016/j.margeo.2018.11.002>.
- Skolotnev, S.G., Fedonkin, M.A., Korniyuchuk, A.V., 2017. New data on the geological structure of the southwestern Mendeleev Rise. *Arctic Ocean. Dokl. Earth Sci.* 476, 1001–1006. <https://doi.org/10.1134/S1028334X17090173>.
- Sokolov, S.D., Bondarenko, G.Y., Morozov, O.L., Shekhovtsov, V.A., Glotov, S.P., Ganelin, A.V., Kravchenko-Berezhnoy, I.R., 2002. South Anyui suture, northeast Arctic Russia: Facts and problems. In: Miller, E.L., Grantz, A., Klemperer, S. (Eds.), *Special Paper 360: Tectonic Evolution of the Bering Shelf-Chukchi Sea-Artic Margin and Adjacent Landmasses*. Geological Society of America, Boulder, Colorado, pp. 209–224. <https://doi.org/10.1130/0-8137-2360-4.209>.
- Sokolov, S.D., Tuchkova, M.I., Moiseev, A.V., Verzhbitskiy, V.E., Malyshev, N.A., Gushchina, M.Yu., 2017. Tectonic Zoning of Wrangel Island, Arctic Region. *Geotectonics*, 2017 51 (1), 3–16. <https://doi.org/10.1134/S0016852117010083>.
- Soloviev, A.V., 2008. Investigation of the Tectonic Processes of the Convergent Setting of Lithosphere Plates: Fission-Track Dating and Structural Analysis. *Nauka, Moscow*.
- Stein, R., 2008. *Arctic Ocean Sediments: Processes, Proxies, and Paleoenvironment*, 1st ed. Elsevier Science.
- Stein, R., Jokat, W., Niessen, F., Weigelt, E., 2015. Exploring the long-term Cenozoic Arctic Ocean climate history: a challenge within the International Ocean Discovery Program (IODP). *Arktos* 1, 3. <https://doi.org/10.1007/s41063-015-0012-x>.
- Thorarinsson, S.B., Söderlund, U., Døssing, A., Holm, P.M., Ernst, R.E., Tegner, C., 2015. Rift magmatism on the Eurasia basin margin: U–Pb baddeleyite ages of alkaline dyke swarms in North Greenland. *J. Geol. Soc. Lond.* 172, 721–726. <https://doi.org/10.1144/jgs2015-049>.
- Toro, J., Miller, E.L., Prokopyev, A.V., Zhang, X., Veselovskiy, R., 2016. Mesozoic orogens of the Arctic from Novaya Zemlya to Alaska. *J. Geol. Soc. Lond.* 173, 989–1006. <https://doi.org/10.1144/jgs2016-083>.
- Vernikovskiy, V.A., Dobretsov, N.L., Metelkin, D.V., Matushkin, N.Y., Koulakov, I.Y., 2013. Concerning tectonics and the tectonic evolution of the Arctic. *Russ. Geol. Geophys.* 54, 838–858. <https://doi.org/10.1016/j.rgg.2013.07.006>.
- Vernikovskiy, V.A., Morozov, A.F., Petrov, O.V., Travin, A.V., Kashubin, S.N., Shokal'sky, S.P., Shevchenko, S.S., Petrov, E.O., 2014. New data on the age of dolerites and basalts of Mendeleev Rise (Arctic Ocean). *Dokl. Earth Sci.* 454, 97–101. <https://doi.org/10.1134/S1028334X1402007X>.
- Verzhbitskiy, V.E., Sokolov, S.D., Tuchkova, M.I., Frantzen, E.M., Little, A., Lobkovskiy, L.I., 2012. The South Chukchi Sedimentary Basin (Chukchi Sea, Russian Arctic), in: *Tectonics and Sedimentation*. American Association of Petroleum Geologists, Tulsa, Oklahoma, pp. 267–290. <https://doi.org/10.1306/13351557M1003534>.
- Verzhbitskiy, V.E., Sokolov, S.D., Tuchkova, M.I., 2015. Present-day structure and stages of tectonic evolution of Wrangel Island, Russian eastern Arctic Region. *Geotectonics* 49, 165–192. <https://doi.org/10.1134/S001685211503005X>.
- Weigelt, E., Jokat, W., Franke, D., 2014. Seismostratigraphy of the Siberian Sector of the Arctic Ocean and adjacent Laptev Sea Shelf. *J. Geophys. Res. Solid Earth* 119, 5275–5289. <https://doi.org/10.1002/2013JB010727>.
- Weigelt, E., Jokat, W., Eisermann, H., 2020. Deposition history and paleo-current activity on the southeastern Lomonosov Ridge and its Eurasian flank based on seismic data. *Geochem. Geophys. Geosyst.* 21, e2020GC009133 <https://doi.org/10.1029/2020GC009133>.
- West, C.K., Greenwood, D.R., Basinger, J.F., 2015. Was the Arctic Eocene 'rainforest' monsoonal? Estimates of seasonal precipitation from early Eocene megaflores from Ellesmere Island, Nunavut. *Earth Planet. Sci. Lett.* 427, 18–30. <https://doi.org/10.1016/j.epsl.2015.06.036>.
- Wilkinson, C.M., Ganerod, M., Hendriks, B.W.H., Eide, E.A., 2017. Compilation and appraisal of geochronological data from the North Atlantic Igneous Province (NAIP). *Geol. Soc. Lond. Spec. Publ.* 447, 69–103. <https://doi.org/10.1144/SP447.10>.
- Yang, L., Ren, J., McIntosh, K., Pang, X., Lei, C., Zhao, Y., 2018. The structure and evolution of deepwater basins in the distal margin of the northern South China Sea and their implications for the formation of the continental margin. *Mar. Pet. Geol.* 92, 234–254. <https://doi.org/10.1016/j.marpetgeo.2018.02.032>.
- Zakharov, Y.D., Shigeta, Y., Popov, A.M., Velivetskaya, T.A., Afanasyeva, T.B., 2011. Cretaceous climatic oscillations in the Bering area (Alaska and Koryak Upland): Isotopic and palaeontological evidence. *Sediment. Geol.* 235, 122–131. <https://doi.org/10.1016/j.sedgeo.2010.03.012>.
- Ziegler, P.A., 1988. *Evolution of the Arctic-North Atlantic and the Western Tethys*. *Am. Assoc. Pet. Geol. Mem.* 43, 1–198.
- Ziegler, P.A., Cloetingh, S., 2004. Dynamic processes controlling evolution of rifted basins. *Earth-Sci. Rev.* 64, 1–50. [https://doi.org/10.1016/S0012-8252\(03\)00041-2](https://doi.org/10.1016/S0012-8252(03)00041-2).



Arctic Ocean Mega Project: Paper 3 - Mesozoic to Cenozoic geological evolution

Anatoly M. Nikishin^{a,*}, Eugene I. Petrov^b, Sierd Cloetingh^c, Sergey I. Freiman^a, Nikolay A. Malyshev^d, Andrey F. Morozov^b, Henry W. Posamentier^e, Vladimir E. Verzhbitsky^d, Nikolay N. Zhukov^a, Ksenia Startseva^a

^a Geological Faculty, Moscow State University, Moscow, Russia

^b Ministry of Natural Resources and Environment of the Russian Federation, Moscow, Russia

^c Utrecht University, Utrecht, the Netherlands

^d Rosneft, Moscow, Russia

^e Consultant, 25 Topside Row Drive, the Woodlands, TX 77380, USA

ARTICLE INFO

Keywords:

Arctic
Lomonosov Ridge
Amundsen Basin
Nansen Basin
Podvodnikov Basin
North Chukchi Basin
Mendelev Ridge
Laptev Sea Basin
East Siberian Sea Basin
Gakkel Ridge

ABSTRACT

We present an atlas of paleogeographic and paleotectonic maps which documents major events in the Arctic for 0–157 Ma. We demonstrate that the Mendeleev Ridge has a continental basement. The following chronology of events in the history of the Arctic Ocean is proposed: (1) Jurassic: continental rifting in the area of the Sverdrup-Banks basins and in the area of the present-day Canada Basin; a system of continental-margin volcanic belts formed in the region of Chukotka and the Verkhoyansk-Omolon; (2) Berriasian-Barremian: formation of the continental-margin Verkhoyansk-Chukotka Orogen; fast opening of Canada Basin (~133–125 Ma); (3) Aptian-Albian: formation of continental igneous provinces, rifting and magmatism in the area of the Alpha-Mendelev ridges; rifting in the Ust'-Lena, Anisin, North-Chukchi, Podvodnikov and Toll basins; (4) Cenomanian-Campanian: intraplate magmatism in the area of the Alpha-Mendelev ridges; (5) Campanian-Maastrichtian: a likely start of compressional deformations in the area of the Chukchi Sea; (6) Paleocene: formation of the continental-margin orogen; continental rifting along the present-day Eurasia Basin and the Ust'-Lena Basin; (7) Early-Middle Eocene: onset of opening of the Eurasia Basin started; (8) Middle-Late Eocene: a major restructuring of paleogeography of the Arctic took place at ca. 45 Ma with subaerial emergence of the Barents and Kara Sea shelves and onset of ultra-slow spreading of the Gakkel Ridge, and start of the epoch of formation of normal and strike-slip faults on the Lomonosov and Alpha-Mendelev ridges and on the shelves of the Chukchi and East Siberian seas. Paleoclimate is discussed in connection with changes in the paleogeography.

1. Introduction

Key information on concepts of the geological and tectonic history of the Arctic is presented in many studies (e.g., [Grantz et al., 2011b, 2011a](#); [Piskarev et al., 2019](#); [Stein, 2008](#)). Our objective is to analyze the onshore and offshore records within these time intervals and to develop paleogeographical and paleotectonic maps for different intervals of the geological history of the entire Arctic. Similar efforts have been made by many authors (e.g., [Alvey et al., 2008](#); [Hutchinson et al., 2017](#); [Jokat and Ickrath, 2015](#); [Kuzmichev, 2009](#); [Laverov et al., 2013](#); [Lawver et al., 2015, 2011](#); [Lobkovsky, 2016](#); [Metelkin et al., 2016](#); [Miller et al., 2018b, 2018a](#); [Miller and Verzhbitsky, 2009](#); [Nikishin et al., 2017a, 2017b,](#)

[2015](#); [Petrov et al., 2016](#); [Petrov, 2017](#); [Piskarev et al., 2019](#); [Shephard et al., 2013](#); [Shipilov, 2016](#); [Sømme et al., 2018](#); [Vernikovskiy et al., 2013](#); [Weigelt et al., 2014](#); [Ziegler, 1989, 1988](#)). The main challenge to develop these models resides in the lack of understanding of the structure of the Amerasia Basin. Two main groups of models for the tectonic history of the Amerasia Basin exist. The first group of models considers a rotational hypothesis in which the Amerasia Basin opened as an integral structure with a pole of rotation in the south and a transform segment along the Lomonosov Ridge ([Evangelatos and Mosher, 2016](#); [Grantz et al., 2011b, 2011a](#); [Shephard et al., 2013](#)). The South Anyui Ocean closed concurrently with formation of the accretionary-collisional Verkhoyansk-Chukotka orogen ([Grantz et al., 2011b, 2011a](#); [Piepjohn et al.,](#)

* Corresponding author.

E-mail address: nikishin@geol.msu.ru (A.M. Nikishin).

2018). The second group of models assumes that Canada Basin formed independently, while the region of the Alpha-Mendelev ridges and the Podvodnikov Basin formed in a separate tectonic environment and at a different time than Canada Basin (Alvey et al., 2008; Doré et al., 2016; Hutchinson et al., 2017; Lobkovsky, 2016; Miller and Verzhbitsky, 2009; Nikishin et al., 2017a, 2017b; Nikishin et al., 2015; Shipilov, 2016). The models within each group may also differ significantly.

We refrain here from a discussion of the structure and geological history of Canada Basin. The new data have been well documented (Chian et al., 2016; Chian and Lebedeva-Ivanova, 2015; Coakley et al., 2016; Coakley and Ilhan, 2012; Hutchinson et al., 2017; Mosher et al., 2012). The formation time of Canada Basin is debatable and different models for the formation of this basin from Early Jurassic to Late Cretaceous have been proposed (Coakley et al., 2016; Dixon et al., 2019; Grantz et al., 2011a, 2011b; Houseknecht, 2019; Hutchinson et al., 2017; Miller et al., 2018b, 2018a; Mosher et al., 2012; Pease et al., 2014; Toro et al., 2016). In accordance with the model of Helwig et al. (2011), the breakup unconformity has an age ca. 133 Ma (the Valanginian/Hauterivian boundary) and oceanic crust was formed prior to mid-Aptian (ca. 117 Ma). This model is based on the notion that the rift/postrift boundary in the Sverdrup Basin has an age of about 135–130 Ma, while this boundary should correspond to the breakup unconformity in Canada Basin (Hadlari et al., 2016). New data for Canada Basin (Chian et al., 2016; Coakley et al., 2016; Hutchinson et al., 2017; Mosher et al., 2012) show that its opening took place under cool mantle conditions.

A key challenge in the geological history of the Arctic Ocean is the issue of the basement of the Alpha-Mendelev ridges (see Paper 2). In all models ridges are volcanic edifices, though the type of crust unambiguously identified upon which this volcanism did take place has not yet been identified (Brumley, 2014; Bruvoll et al., 2012, 2010; Kashubin et al., 2018, 2013). Our new data are indicative of a continental nature of the Alpha-Mendelev terrane. Just after the completion of the Verkhoyansk-Chukotka Orogeny at ca. 125 Ma, formation of basaltic igneous provinces started throughout the Arctic. Basaltic provinces are well known on the Ellesmere Island, on Svalbard, on Franz Josef Land, and on the De Long Islands (Corfu et al., 2013; Drachev and Saunders, 2006). We identified a new hypothetical igneous province north of Wrangel Island (see Paper 2). These data show that the Alpha-Mendelev Igneous Province was surrounded by igneous provinces on all sides (except the area of Canada Basin). The available data show that volcanism in the Alpha-Mendelev Province also started at ca. 127–110 Ma. This implies that within the framework of the available data, an approximately synchronous onset of volcanism in a large area can be assumed. Our analyses of seismic lines show that the Arlis Gap Buried High is a continuation of the structure of the Mendelev Ridge (see Paper 2). Our data also show that most part of the Makarov Basin's basement is a continuation of the structure of the Alpha Ridge. A similar conclusion is presented in Evangelatos and Mosher (2016). Summing up these data, it appears that the Alpha-Mendelev Igneous Province started to form at the eastern margin of the Lomonosov Ridge. That is, the Alpha-Mendelev Igneous Province started to form at ca. 125 Ma as a volcanic continental margin. This hypothesis is in good agreement with inferences from analysis of gravity and magnetic anomalies (Gaina et al., 2011; Oakey and Saltus, 2016). This hypothesis was mentioned in Dove et al. (2010) as one of the probable concepts. The Alpha-Mendelev Igneous Province can be compared with the Kerguelen Plateau (Bénard et al., 2010; Borissova et al., 2003) in the Indian Ocean (Nikishin et al., 2015; Oakey and Saltus, 2016) or with the Vøring Plateau on the continental margin of Norway in the North Atlantic (see also Abdelmalak et al. (2016) and Omosanya et al. (2016)).

In 2014 and 2016, rock samples were taken with the use of a specially equipped submarine on three scarps on the Mendelev Ridge (Skolotnev et al., 2019, 2017). As a result, three sections were studied, which are composed mainly of sedimentary rocks with Paleozoic fauna. These sections are pierced by basalt dykes and sills of Early Cretaceous

age (110–115 Ma) (Petrov, 2017; Skolotnev et al., 2019, 2017). These data suggest that the Mendelev Ridge is a continental terrane that experienced a strong extension and magmatism. Most recent geometrical reconstructions of the Arctic Ocean history with synchronous opening of the Amerasia Basin and closure of the South Anyui Ocean are probably not correct due to existence of a large-size continental Alpha-Mendelev terrane which does not comply with such a model.

2. Data and methods

The bulk of our new data is presented in Papers 1 and 2. This applies in particular to the revised seismostratigraphy and tectonostratigraphy of the Arctic Ocean. In this paper, we aim to provide a synthesis of all our and published tectonostratigraphy data of the ocean jointly with the paleogeographic and paleotectonic history of the onshore regions surrounding the ocean with the objective to create a model for the geological history of the area of the Arctic Ocean in the Mesozoic and Cenozoic. We will also utilize published data on the geology of the onshore. We used all published data on detrital zircon ages from samples from different places to reconstruct a paleogeography (our zircon age data include also a number of unpublished results and data in industrial reports (Nikishin et al., in preparation)). We used G-Plates technology for paleotectonic restorations. By doing so, we are presenting a new atlas of the geological history of the Arctic Ocean.

3. Paleogeographic and paleotectonic history of the Arctic Ocean in the Mesozoic and Cenozoic

3.1. Geometrical reconstructions of the Arctic region

Many kinematic reconstructions of the geography of the Arctic Ocean exist. Global reconstructions with a focus on the Arctic region are widely known (e.g., Alvey et al., 2008; Golonka, 2011; Lawver et al., 2015, 2011; Shephard et al., 2013). We made kinematic reconstructions of the Arctic region taking into consideration that the Alpha-Mendelev Terrane has a continental crust and was of great importance in the opening of the ocean (Freiman et al., 2018; Nikishin et al., 2015, 2017a, 2017b).

3.2. Structure and age of the Pre Mesozoic basement of the region of the Arctic Ocean

We constructed a map of basement age of the Arctic on a reconstruction for the Permian/Triassic boundary (Fig. 1). An area with Neoproterozoic-Cambrian basement (ca. 650–520 Ma) is wide-spread. These areas are usually named Timanides (Gee et al., 2006; Hoiland et al., 2018; Kuznetsov et al., 2010; Miller et al., 2018b, 2018a; Nikishin et al., 2015). Recent data show areas with a Timanian basement including Timan-Pechora Basin (Gee et al., 2006; Kuznetsov et al., 2010), Novaya Zemlya (Gee et al., 2006; Kuznetsov et al., 2010; Pease and Scott, 2009), the Severnaya Zemlya and Izvestiy Tsik Islands (the North Kara Sea region) (Gee et al., 2006; Nikishin et al., 2017b), the Zhokhov Island of the New Siberian Island (Akinin et al., 2015), the Wrangel Island in the Chukchi Sea (Gorodinsky, 1999a; Gottlieb et al., 2018; Kos'ko et al., 1993; Luchitskaya et al., 2017), the northern part of Chukotka (Gottlieb et al., 2018), and Seward Terrane on Alaska (Hoiland et al., 2018). A large number of detrital zircons with ages of ca. 650–520 Ma are encountered in Paleozoic sediments of the Arctic (e.g., Ershova et al., 2018, 2016a, 2016b, 2015b, 2015a; Gottlieb et al., 2014; Miller et al., 2018b, 2018a; V. A. Nikishin et al., 2017; Pease et al., 2014). It follows from this information that a large-size composite terrane did have a crust with an age of about 650–520 Ma (Kuznetsov et al., 2010; Miller et al., 2018b, 2018a; Nikishin et al., 2015; Pease et al., 2014). Existence of such a continental landmass was assumed by N. Shatskiy (Shatskiy, 1935) who named it the Hyperboreal Continent. This idea was developed by L. Zonenshain who named this continent

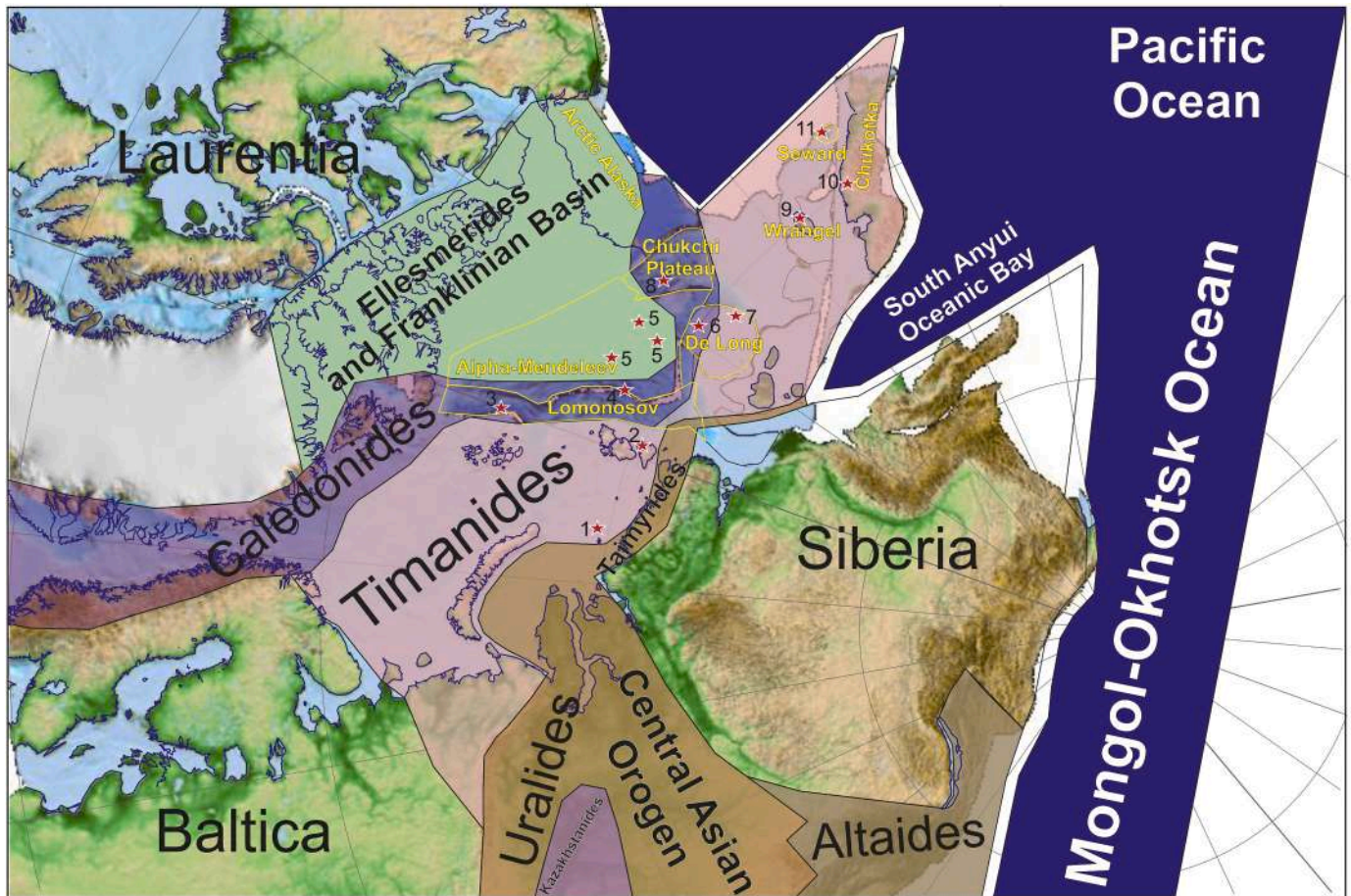


Fig. 1. Main basement provinces of the Arctic region compiled using kinematic restoration for Permian/Triassic transition (~250 Ma). Some key references: 1 - V. A. Nikishin et al., 2017; 2 - V. A. Nikishin et al., 2017; 3 - Knudsen et al., 2018; 4 - Rekant et al., 2019; 5 - Skolotnev et al., 2019; 6 - Ershova et al., 2016a; Prokopiev et al., 2018; 7 - Akinin et al., 2015; 8 - Brumley et al., 2015; O'Brien et al., 2016; 9 - Gottlieb et al., 2018; Luchitskaya et al., 2017; 10 - Gottlieb et al., 2018; 11 - Hoiland et al., 2018.

Arctica (Laverov et al., 2013; Zonenshain et al., 1990). A. Embry (e.g., 2011) called approximately this continental landmass Crockerland.

The classical belt of the Caledonides is known in the North Atlantic region. The Caledonides of Scandinavia, East Greenland and Svalbard belong to them (Gee et al., 2006; Lawver et al., 2011; Ziegler, 1989, 1988). The Caledonian Pearya Terrane on the Ellesmere Island is also well-known (Estrada et al., 2018; Gee et al., 2006). All these Caledonian terranes composed previously a single collisional belt (Ziegler, 1989, 1988). In recent years, rock samples were taken from subsea scarps of the Lomonosov Ridge (Knudsen et al., 2018; Rekant et al., 2019) and of the Chukchi Plateau (Brumley et al., 2015; O'Brien et al., 2016). It is assumed that these samples are indicative of the Caledonian basement. On the Henrietta and Jeanette Islands at the north of the New Siberian Islands, an Early Paleozoic volcanic arc is described and presence of Caledonides is assumed (Chernova et al., 2017; Ershova et al., 2016a, 2016b; Prokopiev et al., 2018). Caledonides are possible on Alaska (Hoiland et al., 2018). It has been assumed that a belt of Caledonides crossed the Arctic from the North Atlantic to Alaska, though accurate geometry of this orogen is not clear yet (Brumley et al., 2015; Gee et al., 2006; Miller et al., 2018b, 2018a; Nikishin et al., 2015; O'Brien et al., 2016; Ziegler, 1989, 1988).

The Ellesmere Orogen is well known for the northern part of the Canadian islands. The main collisional processes took place at the end of the Devonian and beginning of the Carboniferous (Colpron and Nelson, 2011; Golonka, 2011; Hadlari et al., 2014; Kumar et al., 2011; Lane, 2007; Piepjohn et al., 2015; Rippinton et al., 2010; Ziegler, 1989, 1988).

The Ellesmere Orogen is composed mainly of Neoproterozoic-Devonian or Cambrian-Devonian sedimentary deposits (Hadlari et al., 2014; Kumar et al., 2011; Morrell, 1995). The so-called Franklinian Basin previously existed in its place (Embry et al., 2018; Harrison and Brent, 2005; Kumar et al., 2011; Morrell, 1995). This basin probably formed at the edge of the American continent (Cocks and Torsvik, 2011; Hadlari et al., 2014). After completion of the Ellesmere Orogeny, major rift basins of the type of Sverdrup Basin and Hanna Trough formed in the Early Carboniferous (e.g., Galloway et al., 2018; Kumar et al., 2011).

Rock samples were taken on three slopes of the Mendeleev Ridge (Skolotnev et al., 2019, 2017). The slopes samples are composed mainly of shallow-water carbonates and sandstones which form a folded structure. Late Ordovician-Silurian and Middle-Late Devonian fauna are found in the rocks. The Franklinian Basin probably was also situated within the Mendeleev Ridge in the Paleozoic. In this case, we assume that the continental margin of the American (Laurentia) continent forms the basement of the Mendeleev Ridge.

On Taimyr, the Paleozoic Taimyr Orogen is situated (Vernikovskiy, 1996). In recent years many new data were obtained on the basis of studying the Paleozoic orogen itself (Ershova et al., 2016a, 2016b; Gee et al., 2006; Khudoley et al., 2018; Makariev, 2013; Pease, 2011; Pease and Scott, 2009; Proskurnin et al., 2014; Vernikovskiy and Vernikovskaya, 2001; Zhang et al., 2013, 2016) and its Taimyr Foredeep in the South Taimyr zone (Afanasenkov et al., 2016; Khudoley et al., 2018; Pogrebitsky, 1971; Zhang et al., 2016, 2013). New data also were presented for the synorogenic molasse basins on islands of the Novaya

Zemlya Archipelago (Ershova et al., 2015b, 2015a; V. A. Nikishin et al., 2017). New seismic lines have been acquired for the shelf of the North Kara Basin on which the northern boundary of the Taimyr Orogen is observed (Malyshev et al., 2012; Nikishin et al., 2015). Many new seismic lines have also been acquired for the Yenisei-Khatanga Basin that is situated south of the Taimyr Orogen (Afanasenkov et al., 2016). Some seismic lines cross the South Taimyr zone (Late Paleozoic foredeep basin) (Afanasenkov et al., 2016). These data were synthesized by Nikishin et al. (2015, 2010) and Afanasenkov et al. (2016). Syncollisional granite intrusions in the northern part of Taimyr have an age ranging from 344 to 275 Ma (from the Visean to the end of Early Permian) (Khudoley et al., 2018; Pease, 2011; Vernikovskiy, 1996). The Late Carboniferous – Early Permian Akhmatov Formation of the Bolshevik Island (the island of the Severnaya Zemlya Archipelago) forms a synorogenic molasse basin. Detrital zircons in sandstones have peak ages in the range of about 350–306 Ma (V. A. Nikishin et al., 2017). Carboniferous sandstones of the Novaya Zemlya islands have peak ages of detrital sandstones ca. 323 Ma (Nikishin et al., 2016). The possible provenance of these sandstones involved the Taimyr Orogen. Within the North Kara Basin, a distinct angular unconformity is observed on seismic lines which is dated as approximately the Devonian/Carboniferous boundary (Malyshev et al., 2012; Nikishin et al., 2015; Nikishin, 2013). On seismic lines for the South Taimyr zone, an angular unconformity is observed that is situated approximately within the Early Carboniferous. This unconformity corresponds to the onset of formation of the Taimyr Foredeep Basin (Afanasenkov et al., 2016). The age spectra of detrital zircons for Carboniferous deposits of the Taimyr Foredeep Basin (Zhang et al., 2013) and for the Carboniferous of Novaya Zemlya practically coincide, providing evidence for a single provenance of detrital material. In the area of the northern part of the Barents Megabasin, clinoforms and turbidite complexes are detected at the level of the Early Carboniferous with material transport from the side of the North Kara Basin and Taimyr (Nikishin et al., 2016; Startseva, 2018). As early as the Early Carboniferous, sediment transport from the Taimyr Orogen took place both to the north of the orogen (the area of the Barents Megabasin) and to the south of it (the area of the Taimyr Foredeep Basin). The main collision in the area of Taimyr may be thought to start at approximately the Devonian/Carboniferous boundary and in the Early Carboniferous (Nikishin et al., 2015). Collisional deformations continued until the end of the Early Permian (Khudoley et al., 2018). The main collision on Taimyr was in the Early Permian (Cocks and Torsvik, 2011) or in the Carboniferous (Ershova et al., 2016a, 2016b).

In the west, the Taimyr Orogen is overlain by the sedimentary cover of the South Kara Basin. No data are available for its structure and age. Data from commercial drilling demonstrated that the Lower Jurassic sedimentary cover overlies the basement. On the Novaya Zemlya islands, the change of carbonate sedimentation for clays and clastics took place at the Carboniferous/Permian boundary (Korago et al., 1992). In the Permian, the Novaya Zemlya area probably experiences subsidence as a foredeep basin. Upper Permian deposits are represented by alluvial and deltaic complexes. Our data on ages of Upper Permian detrital sandstones show that ages within the range of 280 Ma to 360 Ma dominate (Nikishin et al., in preparation). Transport of sediments in the Permian took place from the side of the South Kara Basin. Hence it follows that a collisional orogen was formed at the site of the South Kara Basin in the Permian. It merged the Central Asian Orogen (the Uralides) and the Taimyr Orogen into a single belt. We named the Late Paleozoic orogen in the area of the present-day South Kara Basin the Baydaratskiy Orogen (Nikishin et al., 2015).

In the east, the Taimyr Orogen is buried under shelf complexes of the Laptev Sea and it is unknown where its eastern continuation is situated. The Taimyr Orogen was probably situated on the Laptev Sea Shelf in the form of the Belkovsky collisional orogen; while further eastward it transited into the South Chukotka active continental margin of the Pacific Ocean (Nikishin et al., 2015). Over recent years, many data were collected on ages of detrital zircons for different islands of the Arctic, for

Taimyr, and for Chukotka (Danukalova and Kuzmichev, 2018; Ershova et al., 2015b, 2015a; V. A. Nikishin et al., 2017). In the Late Devonian, Carboniferous and Early Permian, a deep trough was formed at the western edge of the New Siberian Islands (Danukalova et al., 2017, 2014; Ershova et al., 2015b, 2015a). Analysis of ages of detrital zircons in Devonian deposits of the New Siberian Islands, Severnaya Zemlya islands and Wrangel Island demonstrates that they have a similar character and had a single provenance in the form of the Laurentia-Baltica (Laurussia) paleocontinent (Ershova et al., 2015b, 2015a). A similar situation occurred in the Early Carboniferous as well (at least, in the Tournaisian). A sharp change in the source area of clastic material on the Belkovsky Island took place in the Permian with zircons ages ca. 284–298 Ma became strongly prevalent (Danukalova et al., 2017; Ershova et al., 2015b, 2015a; Pease et al., 2014). It is assumed that the Taimyr Orogen became the source area of clastic material (Danukalova et al., 2017; Ershova et al., 2015b, 2015a; Pease et al., 2014). In the Devonian, a hypothetical ocean existed in the place of the Paleozoic Taimyr Orogen (Khudoley et al., 2018; Pease, 2011; Vernikovskiy, 1996). Hence, the areas of the New Siberian Islands and the Severnaya Zemlya Archipelago were situated north of this ocean (in the present-day coordinates). The Siberian continent was situated south of the mentioned ocean. It is conceivable that the collision of the Siberian continent with the Laurentia-Baltica (Laurussia) continent started approximately at the Devonian/Carboniferous boundary and was completed in the Permian. At that time, a marginal flexural basin was forming in the area of the Belkovsky Island for the Belkovsky collisional orogen in the Late Paleozoic. This foredeep was situated north-east of the orogen in present-day coordinates.

On Chukotka, Early Carboniferous subduction-related granites with ages of 352–359 Ma are established at different places (Luchitskaya et al., 2015). They could form a continental-marginal igneous belt of an active continental margin. It should also be noted that a large number of detrital zircons of Carboniferous and Permian age are encountered in Late Jurassic and Early Cretaceous sandstones of Chukotka (Vatrushkina, 2018). It is likely that the Taimyr Orogen transformed in the east into the active continental margin of Chukotka in the Late Paleozoic.

Summing up the data on probable ages of basement in the Arctic region, the following preliminary conclusions can be made: (1) basement is formed by orogens of Timanian, Caledonian and Late Paleozoic ages; (2) in the Cambrian, the Timanides became a part of the Baltica paleocontinent (Gee et al., 2006; Hoiland et al., 2018; Kuznetsov et al., 2010; Miller et al., 2018b, 2018a; Nikishin et al., 2015, 1996); (3) the Caledonian orogen was formed during the collision of Laurentia and Baltica (together with the Timanides); (4) the belt of Taimyrides together with the Ural Orogen and the Central Asian Orogen were formed during the collision of the Siberian paleocontinent and the Laurentia-Baltica (Laurussia) continent starting approximately from the Devonian/Carboniferous boundary (Nikishin et al., 2015); (5) the nature of the Ellesmere Orogeny is unclear; it was probably synchronous with the Taimyr Orogeny and was caused by the collision of the Siberian paleocontinent and the Laurentia-Baltica (Laurussia) continent.

3.3. Late Jurassic history of the Arctic

According to our model, the history of formation of the Arctic Ocean started from the Jurassic. That is why we will begin our discussion of this process from this time onward. At first we compiled a paleogeographical map of the Arctic for the Late Jurassic on the present-day geographic framework (Fig. 2). For the Russian part of the Arctic Ocean, we utilized our interpretation of federal and commercial seismic lines. Seismostratigraphy was tied to all available offshore boreholes. These data have been presented in the form of PhD theses (Mordasova, 2018; Nikishin, 2013; Startseva, 2018; Suslova, 2013). For the Norwegian Barents Sea, published data were utilized (e.g., Smelror et al., 2009; Torsvik et al., 2002; Torsvik and Cocks, 2017; Ziegler, 1988) along with our results of seismic data interpretation. For the European onshore and Siberia, the

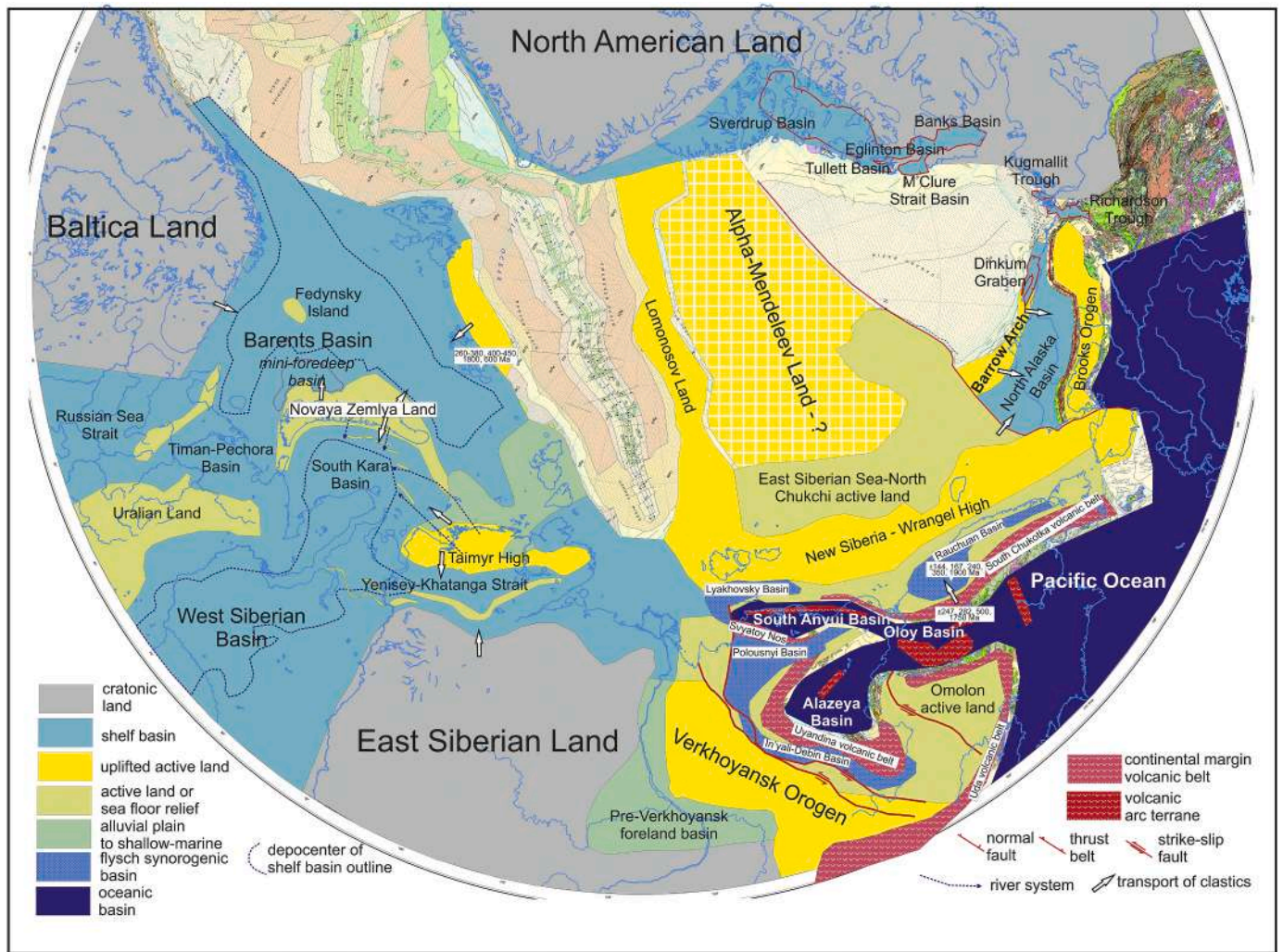


Fig. 2. Paleogeographic map of the Arctic for the Late Jurassic, Kimmeridgian to Tithonian (157–145 Ma), on the present-day geographic framework. Geographic base map is Geological map of the Arctic (Harrison et al., 2011). Ages in the white boxes – ages of peaks of detrital zircons (our data).

basis was the study of Vinogradov (1968) and numerous recent publications (e.g., Kontorovich et al., 2013). For North America, published data were utilized (e.g., Embry and Beauchamp, 2008; Houseknecht, 2019). For islands of the Russian Arctic, data of our field work were used also.

In the Late Jurassic, a single shelf basin existed which included the Barents Sea Basin, Timan-Pechora Basin, South Kara Basin, North Kara Basin, West Siberian Basin, Yenisey-Khatanga Basin, and Russian Sea Strait (Fig. 2). A system of uplifts was forming in this shelf sea. Interpretation of seismic data shows that transport of clastic material took place periodically from Novaya Zemlya toward the Barents and South Kara Basins (Nikishin, 2013; Suslova, 2013). Material was transported from the side of Taimyr in the South Kara Basin. In Upper Jurassic rocks of Franz Josef Land, peaks of detrital zircon ages have the following values: 260–380 Ma, 400–450 Ma, 1800 Ma, 600 Ma (Nikishin et al., in preparation). The abundance of zircons of the “Uralian” and “Caledonian” ages is indicative of the fact that an onshore landmass composed of Paleozoic orogens existed north of Franz Josef Land (in the present-day coordinates).

A system of inversion anticlines is present above Permo-Triassic rifts in the Yenisey-Khatanga Basin (e.g., Afanasev et al., 2016; Kontorovich et al., 2013; Unger et al., 2017). These anticlines were formed slowly in a compressional environment from the Callovian to the Aptian

(Unger et al., 2017). Similar anticlinal folds were formed from the Callovian to the Aptian in the South Kara Basin (Nikishin et al., 2015; Nikishin, 2013) and in the West Siberian Basin (Kontorovich et al., 2013). In the Barents Sea, periodic uplift of the Fedynsky High took place (our seismic data). It is assumed that uplift of the Urals (Kontorovich et al., 2013) and Timan (Vinogradov, 1968) took place. It should be noted that from the Callovian until the Aptian, the main phase of folding and collision in the Verkhoyansk-Chukotka region of the Russian Far East took place (Parfenov, 1991, 1984; Parfenov and Kuzmin, 2001). The formation of compressional anticlines in the area of the Barents and Kara Seas and in West Siberia was probably associated with the Verkhoyansk-Chukotka Orogeny.

The Late Jurassic paleogeography and paleotectonics of the Russian Far East is a highly debatable issue (e.g., Amato et al., 2015; Didenko et al., 2002; Drachev, 2016; Kuzmichev, 2009; Miller et al., 2018a, 2018b, 2002; Parfenov, 1991, 1984; Parfenov and Natal'in, 1986; Sokolov et al., 2015; Toro et al., 2016). Our main hypothesis is that in the Late Jurassic, a subduction continental-marginal volcanic belt between Asia and the Pacific Ocean existed along the entire Far Eastern margin of Russia. Individual fragments of this belt have been known for a long time. In the south, the Uda (or Uda-Murgal) Late Jurassic – Neocomian volcanic belt is identified under the Okhotsk-Chukotka Cretaceous volcanic belt (Akinin, 2012; Miller et al., 2002; Parfenov,

1984; Tikhomirov, 2018; Toro et al., 2016). In the north, the Uda volcanic belt transits into the Oloy volcanic belt that is superimposed onto the edge of the Omolon Massif (Tikhomirov, 2018; Toro et al., 2016). On the northwestern continuation of the Oloy belt, the well-known Uyandina-Yasachnaya volcanic belt of Late Jurassic age is situated (Natapov and Surmilova, 1992; Parfenov and Kuzmin, 2001; Toro et al., 2016). New data show that the Uyandina-Yasachnaya volcanic belt is synchronous in age with the Main (Kolyma) granitoid belt of the Chersky Range and that it was a single continental-marginal igneous belt with subduction directed under the Asian continent (Didenko et al., 2002; Toro et al., 2016; Zonenshain et al., 1990; Prokopiev, personal communications). In the South of Chukotka, Tikhomirov (2018) identified the South Chukotka subduction-related volcanic belt with isotopic ages of volcanites at ca. 150–130 Ma, and with Tithonian-Berriasian paleontological ages (Tikhomirov, 2018; Vatrushkina, 2018). New data show that volcanic material (including pebbles) is present in Upper Jurassic – Berriasian sandstones of Chukotka for the Rauchuan Basin (Vatrushkina, 2018). Ages of detrital zircons have maxima in the intervals of 130–152 Ma and 152–190 Ma whereas the zircons are of igneous origin (Vatrushkina, 2018). The data for ages of detrital zircons demonstrate that a continental-marginal volcanic belt was situated along the southern edge of Chukotka in the Middle-Late Jurassic. This conclusion expressed in Tikhomirov (2018) contradicts the earlier concepts that a passive continental margin existed in the south of Chukotka in the Jurassic (e.g., Sokolov et al., 2015).

Along the southern edge in the west of the South Anyui Suture Zone described in Kuzmichev (2009), Sokolov et al. (2015), Amato et al. (2015), Toro et al. (2016), the Svyatoy Nos Zone is identified, which is considered as a Late Jurassic, Tithonian volcanic arc (Natapov and Surmilova, 1992). We assume that the Svyatoy Nos volcanic belt is a continuation of the continental-marginal Uyandina-Yasachnaya volcanic belt.

In the Late Jurassic, a system of sedimentary basins with accumulation of deep-water sediments, including turbidites, was formed between continental-marginal volcanic belts and the continent of Asia. Such basins include the In'yali-Debin Basin in the eastern part of the Verkhoyansk Orogen (Parfenov and Kuzmin, 2001; Vinogradov, 1968), the Polousnyi Basin south of the South Anyui Orogen (Kuzmichev, 2009; Natapov and Surmilova, 1992; Toro et al., 2016; Vinogradov, 1968), the Lyakhovskiy Basin north of the South Anyuy Orogen (Kuzmichev, 2009; Nikishin et al., 2015), and the Rauchuan Basin on Chukotka (Gorodinsky, 1999b, 1999a; Miller and Verzhbitsky, 2009; Vatrushkina, 2018; Vinogradov, 1968). These troughs are usually considered as foreland basins (Kuzmichev, 2009), although they are poorly studied. In any of the models, these basins were considered as having a syntectonic origin.

The time of the onset of orogeny in the Verkhoyansk Orogen is not known exactly and is believed to start approximately in the Middle-Late Jurassic (Vinogradov, 1968). From this time on, the Verkhoyansk Foredeep Basin started to form, though its Late Jurassic subsidence was limited (Vinogradov, 1968).

The Upper Jurassic is absent in the area of the New Siberian Islands and Wrangel Island (Kuzmichev, 2009; Nikitenko et al., 2017; Sokolov et al., 2017; Vinogradov, 1968). This territory is considered to have experienced *syn*-compressional uplift (Kuzmichev, 2009; Miller et al., 2018b, 2018a; Sokolov et al., 2017; Verzhbitsky et al., 2012).

For the north of Canada and Alaska, the best known Jurassic basin is the Sverdrup Basin and its coeval analogs (Embry, 2011; Embry and Beauchamp, 2008; Hadlari et al., 2016; Houseknecht and Bird, 2011; Torsvik and Cocks, 2017; Ziegler, 1988). Examination of well data showed that synrift deposits have ages from Early Jurassic (Pliensbachian) to Early Cretaceous (Valanginian) (Hadlari et al., 2016). The Valanginian/Hauterivian boundary or a boundary within the Hauterivian is interpreted as a rift/postrift boundary. In regional context, it is considered as a breakup unconformity, which corresponds to the onset of opening of the Canada Basin ca. 135–130 Ma (Hadlari et al., 2016).

This conclusion is in agreement with data on the structure of Canada Basin's continental margin (Helwig et al., 2011). Jurassic-Early Cretaceous rifts are known along the entire strip of the Canada Basin's continental margin. The Tullet Basin, Eglinton Basin, Banks Basin, M'Clure Basin, Kugmallit Basin, Richardson Trough, Dinkum Graben belong to them (Harrison and Brent, 2005; Houseknecht, 2019; Houseknecht and Connors, 2016; Hutchinson et al., 2017). They are blanketed by a sedimentary cover and are poorly studied yet. An important inference is that their development preceded opening time of the Canada Basin.

In the north of Alaska, the Kingak Shale shelf formation was formed in Jurassic times (Houseknecht and Bird, 2011).

A land mass was probably preserved in the Late Jurassic at the location of the Lomonosov Ridge. The fact that transport of sedimentary matter in the Barents Basin was from the north is evidential of this. A land mass was probably preserved at the location of the Alpha-Mendelev ridges as well. This is evidenced by the fact that in the section of the Trukshin Seamount (Mendelev Ridge) Paleozoic deposits are overlain by Aptian or Barremian-Aptian deposits with an angular unconformity (Skolotnev et al., 2019).

We developed kinematic tectonic reconstructions of the history of the Arctic for the Mesozoic and Cenozoic within the framework of the GPlates software (Freiman et al., 2018; Nikishin et al., 2015). The reconstruction for the Late Jurassic (150 Ma) is presented in Fig. 3. We superimposed data of our paleogeography onto the geometric reconstruction. In the present-day tectonic setting of the Verkhoyansk-Chukotka region, there are two major oroclines: the Kolyma and South Anyui. The first of them – the Kolyma Loop was identified by Zonenshain et al. (1990). The South Anyui Orocline was characterized in Kuzmichev (2009). Following Kuzmichev (2009), we straightened these two oroclines for the time of formation of volcanic belts. In contrast to the Kuzmichev model, we believe that these volcanic belts were continental-margin arcs and not intraoceanic volcanic arcs. It appears that in the Late Jurassic the entire area of the Russian Far East was in the rear of an active continental margin and experienced compression from the Verkhoyansk Orogen and Chukotka Orogen to the area of the Barents-Kara Sea and Taimyr. At that time, in the north of North America, extension took place and continental rifts were formed (Embry and Beauchamp, 2008; Houseknecht, 2019; Hutchinson et al., 2017). Continental rifting occurred probably at the site of the Canada Basin as well.

3.4. Berriasian-Barremian (Neocomian) history of the Arctic

Fig. 4 presents our paleogeographical map of the Arctic for the Neocomian on the present-day geological framework. For the Barents and Kara Seas, we utilized results of our interpretation of seismic lines and of drilling data. For the Barents Sea, data of the LoCrA (Grundvåg et al., 2017; Kairanov et al., 2018; Mordasova, 2018) were also extensively used along with other data (e.g., Nikishin, 2013; Smelror et al., 2009; Startseva, 2018; Torsvik et al., 2002; Torsvik and Cocks, 2017; Ziegler, 1988). For the South Kara Basin and for West Siberia, data in Borodkin and Kurchikov (2010), Kurchikov and Borodkin (2011), Kontorovich et al. (2014) and Nikishin (2013) were used. For the European onshore and for Siberia, the basis was the study of Vinogradov (1968) along with numerous recent publications. For North America, published data were utilized (e.g., Embry and Beauchamp, 2008; Houseknecht, 2019). For islands of the Russian Arctic, data of our field work were used also.

In the Neocomian, clinoform sedimentation with progradation of the shelf edge toward the residual shelf seas prevailed in the Barents-West Siberian region (Borodkin and Kurchikov, 2010; Grundvåg et al., 2017; Kontorovich et al., 2014). We identify two major megabasins: the Barents Basin and the West Siberian Basin (together with the South Kara and Yenisey-Khatanga basins). These two megabasins were separated by the Ural-Novaya Zemlya-Taimyr belt of uplifts. Clinoforms and their strikes are well observed on seismic lines. In the Barents Megabasin, the main transport of material took place from the north and northeast (in

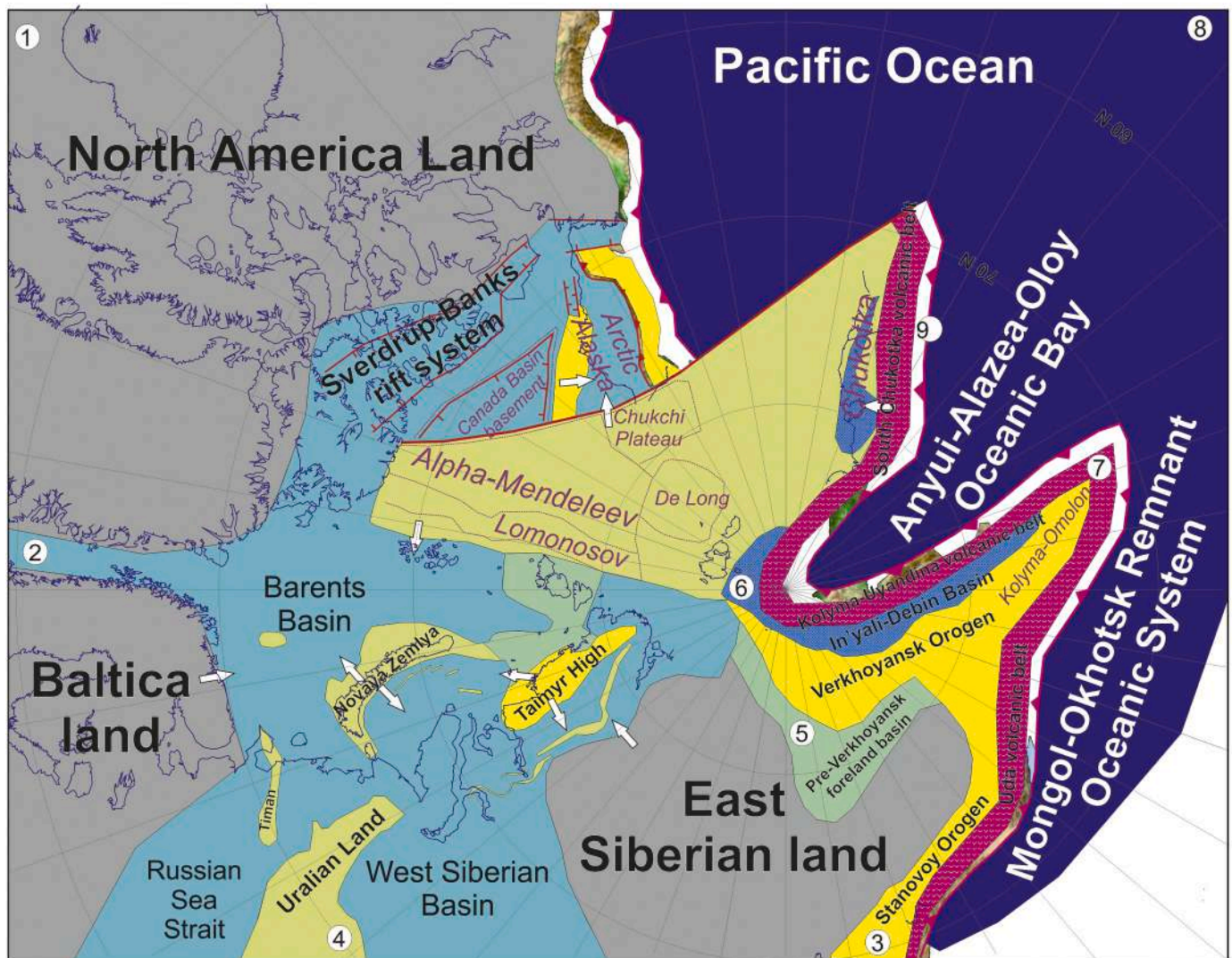


Fig. 3. Tectonic restoration of the Arctic region for the Late Jurassic, Kimmeridgian to Tithonian (157–145 Ma). Kinematic restoration for the 150 Ma. Restoration was performed using GPlates programme. Legend is similar to Fig. 2. 1 – cratonic land, 2 – shelf basin, 3 – uplifted active land, 4 – active land or sea floor relief, 5 – alluvial plain to shallow-marine, 6 – flysch synorogenic basin, 7 – continental margin volcanic belt, 8 – oceanic basin, 9 – subduction zone. Violet outlines and letters mark position of some terranes and their names. (For interpretation of the references to colour in this figure legend, the reader is referred to the web version of this article.)

present-day coordinates). Sediments were partly transported from the Novaya Zemlya High. This finding is in agreement with the data in Grundvåg et al. (2017) and Mordasova (2018). Interpretation of seismic lines shows that in the Barents Megabasin, in the West Siberian, South Kara and Yenisey-Khatanga basins, many anticlinal highs are presumed with *syn*-tectonic sedimentation (Kairanov et al., 2018; Kontorovich et al., 2014; Mordasova, 2018; Nikishin et al., 2015). Where good seismic data are available, it appears that swells grew approximately from the Callovian until the end-Barremian. The examples are the Fedynsky High and Shtokman High in the Barents Sea (our seismic and drilling data, and data in Mordasova (2018)), Storbanken, Persey and Pinegin highs in the Norwegian Barents Sea (Kairanov et al., 2018), Universitetskaya High in the South Kara Basin (Nikishin, 2013), system of swells in the Yenisey-Khatanga Basin (Afanasenkov et al., 2016; Unger et al., 2017) and West Siberian Basin (Kontorovich et al., 2014). The time of development of these *syn*-compressional anticlinal highs coincides with the period of the main collision in the Verkhoyansk-Chukotka region. Therefore, we consider these two synchronous processes as related phenomena.

The Verkhoyansk-Chukotka Orogen was formed in the Neocomian in the Russian Far East (Amato et al., 2015; Didenko et al., 2002; Parfenov and Kuzmin, 2001; Puscharovsky, 1960; Shatskiy, 1935; Sokolov, 2010; Toro et al., 2016; Vinogradov, 1968; Zonenshain et al., 1990). The following two major problems exist within its boundaries: (1) a possible western continuation of the South Anyui accretional-collisional orogen (e.g., Kuzmichev, 2009; Piepjohn et al., 2018); (2) interrelationship of the Chukotka Orogen and Alaska (Amato et al., 2015; Miller et al., 2018b, 2018a).

A probable thrust front can be observed on seismic lines in the Laptev Sea and in the East Siberian Sea in the acoustic basement. The thrust front appears north of the New Siberian Islands and transits in the east into the known Zhokhov-Wrangell-Herald Thrust Belt (Drachev et al., 2010; Nikishin et al., 2017a, 2017b; Nikishin et al., 2015). No seismic data are available that would indicate that the South Anyui Suture proceeds northward into the Arctic. Our model is close to the study of Kuzmichev (2009). The conventional line of the Khatanga-Lomonosov fault inherits the northern boundary of the Early Cretaceous orogen. According to our data, we do not interpret Arctic Alaska as a part of the

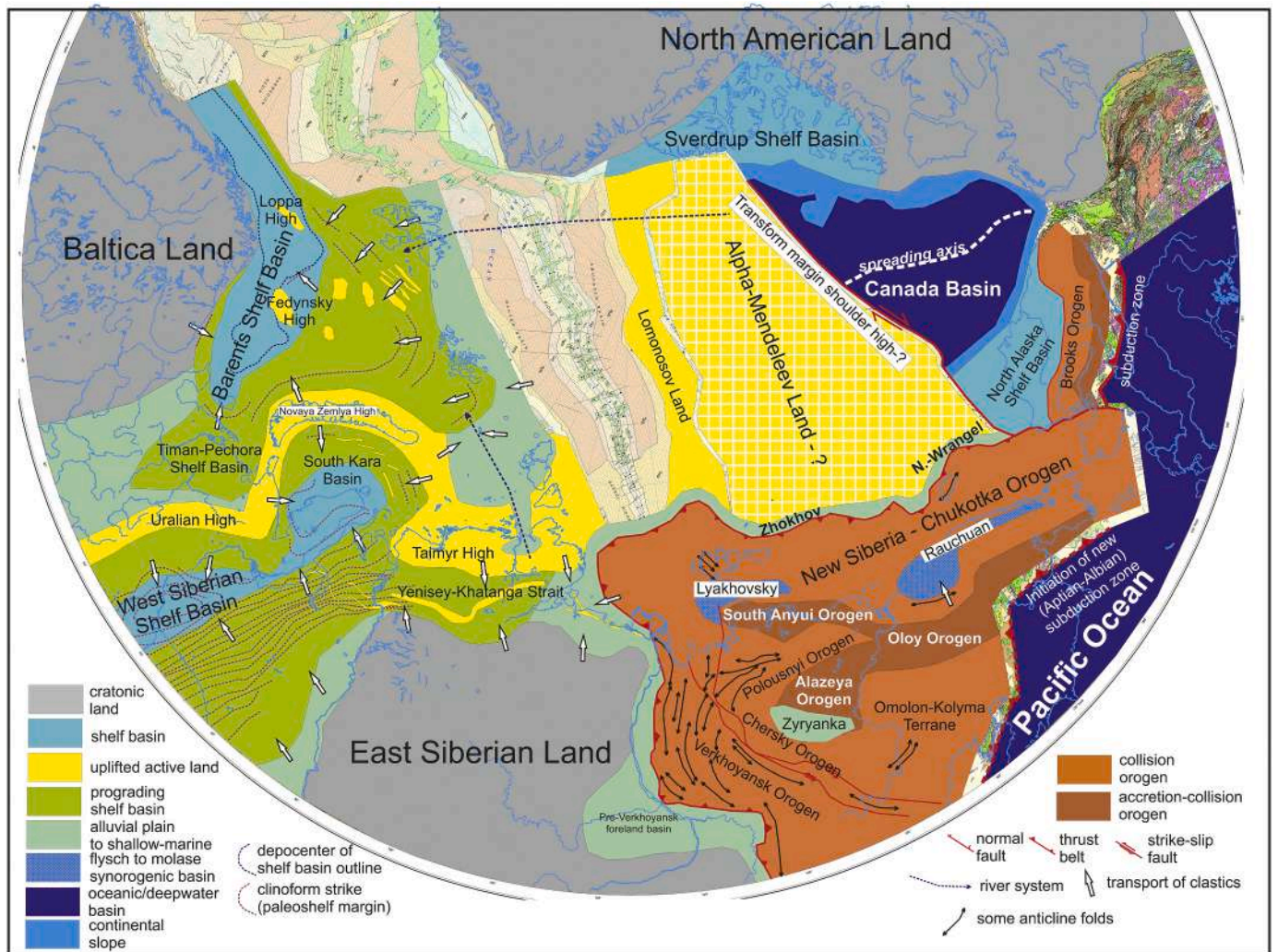


Fig. 4. Paleogeographic map of the Arctic for the Early Cretaceous, Berriasian to Barremian (145–125 Ma), on the present-day geographic framework. Geographic base map is Geological map of the Arctic (Harrison et al., 2011).

integrated Arctic Alaska-Chukotka Microplate. In our model, Alaska and Chukotka are separated by a major strike-slip zone (Nikishin et al., 2017a, 2017b; Nikishin et al., 2015).

The western boundary of the Verkhoyansk Orogen takes course along the Verkhoyansk Foredeep Basin that had its main subsidence phase in the Neocomian (Parfenov and Kuzmin, 2001). The possible northern boundary of the Verkhoyansk-Chukotka Orogen takes course along the Zhokhov-Wrangell-Herald thrust belt (Drachev et al., 2010; Nikishin et al., 2017a, 2017b; Nikishin et al., 2015). A belt of possible sedimentary wedges of Late Jurassic-Early Cretaceous deposits is observed on a number of published and commercial seismic lines just to the north of this thrust front, with thicknesses as up to 4 s TWT (Nikishin et al., 2015). The Verkhoyansk-Chukotka Orogen consists of collisional orogens as deformed edges of the Asian Paleozoic continent (the Verkhoyansk-Chersky and Chukotka-New Siberian regions), and a system of terranes that formed on an oceanic crust in the Pacific Ocean. It should, however, be noted that it still remains an intricate problem how to draw boundaries of different areas (terrane) (Amato et al., 2015; Parfenov and Kuzmin, 2001; Sokolov et al., 2015, 2002; Toro et al., 2016; Zonenshain et al., 1990). Along the outer boundary of the system of accretional terranes, a system of Neocomian molasse basins is identified, which can be considered as foredeeps or as *syn*-collisional basins. The Rauchuan (Vatrushkina, 2018), Lyakhovskiy (Kuzmichev, 2009) and

Zyryanka (Nikishin et al., 2017a, 2017b; Nikishin et al., 2015) basins belong to them. It should be noted that ages of detrital zircons from Neocomian sandstones of the Stolbovoy Island (the Lyakhovskiy Basin) (Soloviev and Miller, 2014) and from sandstones of the Rauchuan Basin (Vatrushkina, 2018) mainly coincide: they have common peaks with values ca. 140–160 Ma, ca. 235–280 Ma, and ca. 1900 Ma.

In Alaska, the collision of the block of Arctic Alaska and the system of terranes of the Brooks Orogen started approximately at the Jurassic/Cretaceous boundary and the Colville Foredeep Basin started to form in the Neocomian (Houseknecht and Wartes, 2013; Moore et al., 2015; Toro et al., 2016).

As noted above, it is assumed for Canada Basin that the breakup unconformity has an age of about 135–130 Ma (Hadlari et al., 2016; Helwig et al., 2011; Nikishin et al., 2017a, 2017b). The time of opening of Canada Basin, as we already noted, is a highly debatable issue. According to our model, opening was completed at ca. 125 Ma, before the onset of emplacement of the HALIP superplume.

In the Neocomian, significant transport of clastic matter into the Barents Basin took place from the north. It is quite conceivable that the Lomonosov Ridge and the Alpha-Mendeleev ridges were uplifts and rivers transported clastic material from them toward the present-day Barents Sea.

We completed a kinematic reconstruction of the Arctic for the

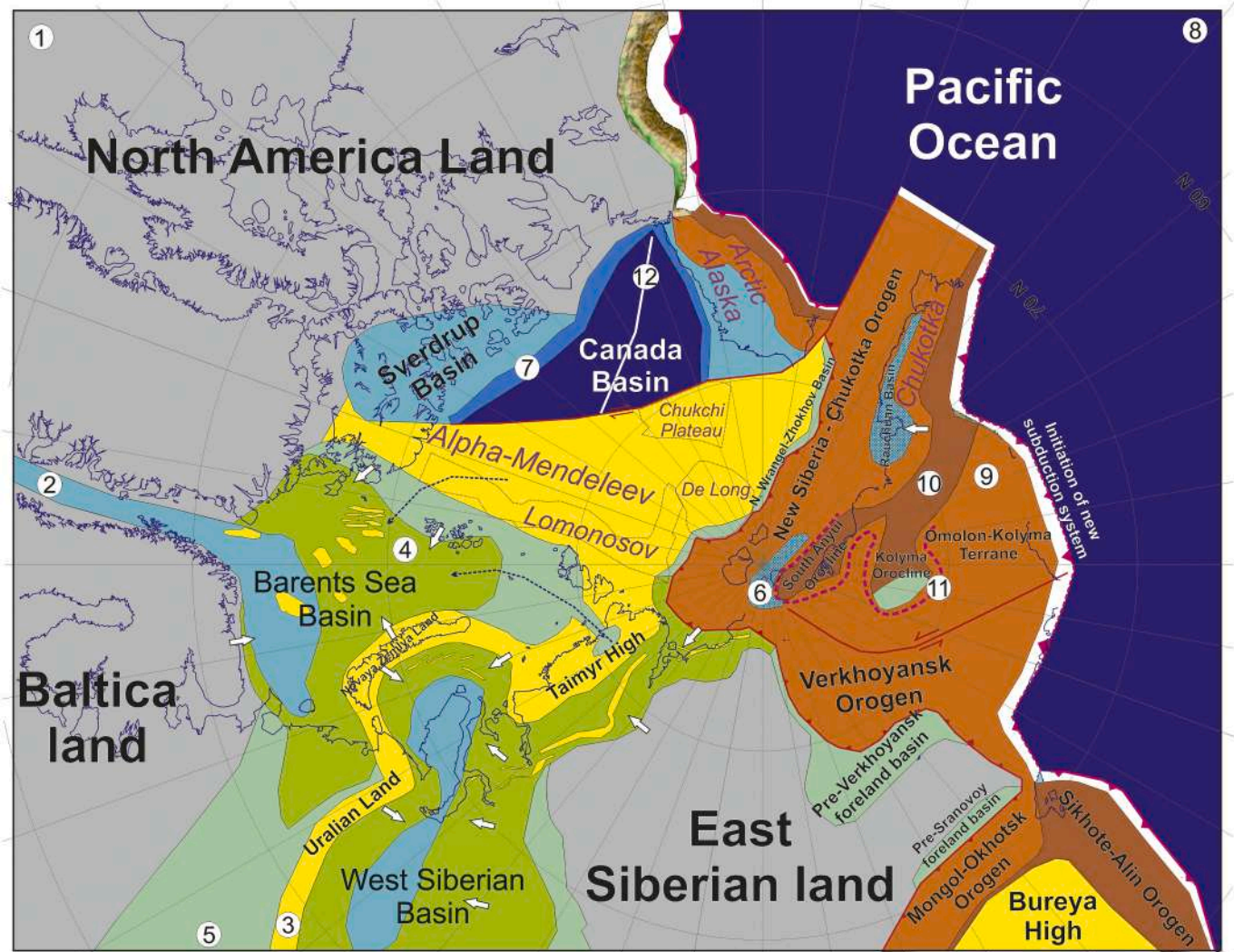


Fig. 5. Tectonic restoration of the Arctic region for the Early Cretaceous, Berriasian to Barremian (145–125 Ma). Kinematic restoration for the 128 Ma. Restoration was performed using GPlates programme. Legend is similar to Fig. 4. 1 – cratonic land, 2 – shelf basin, 3 – uplifted active land, 4 – prograding shelf basin, 5 – alluvial plain to shallow-marine, 6 – flysch to molasses synorogenic basin, 7 – continental slope, 8 – oceanic/deepwater basin, 9 – collision orogen, 10 – accretion-collision orogen, 11 – orocline, 12 – spreading axis. Violet outlines and letters mark position of some terranes and their names. (For interpretation of the references to colour in this figure legend, the reader is referred to the web version of this article.)

Barremian (128 Ma) within the framework of the GPlates software and our geodynamic concept (Freiman et al., 2018; Nikishin et al., 2015). The reconstruction is presented in Fig. 5. We superimposed data of our paleogeography onto the geometrical reconstruction.

According to our model, in the Late Jurassic, Chukotka and Alaska were part of a single continent with an active continental margin with the Anyui-Alazaea-Oloy Oceanic Bay of the Pacific Ocean. In the Neocomian, this oceanic bay was closed as a result of movement of continental and oceanic terranes northwards and eastwards. At that time, the large-size Kolyma Orocline and South Anyui Orocline formed. We do not associate closure of the Anyui-Alazaea-Oloy Oceanic Bay with opening of the Amerasia Basin. Our model is based on the concept that the continental Alpha-Mendeleev Terrane existed in the Neocomian which was situated north of the Verkhoyansk-Chukotka Orogen. In the Neocomian, final closure of the Mongol-Okhotsk Ocean took place and a major collisional orogen was formed along the southern edge of Siberia (Guo et al., 2017; Metelkin et al., 2010; Yang et al., 2015). The formation of the large Verkhoyansk-Chukotka and Mongol-Okhotsk orogens resulted

in availability of a significant source of clastic material in the Neocomian. Therefore, clinoform sedimentation was typical of the West Siberian and Barents megabasins. The significant collision resulted in the situation that intraplate tectonics in the form of formation of compressional anticlinal highs widely manifested itself in sedimentary basins.

The Canada Basin was opened in the Hauterivian-Barremian as a back-arc basin of the Pacific Ocean's subduction system. The basin was bounded in the north by the transform boundary which is named by us the Amerasian Transform Fault. It separated Arctic Alaska from Chukotka and its course was east of the Chukchi Plateau (Nikishin et al., 2017a, 2017b; Nikishin et al., 2015).

3.5. Aptian-Albian history of the Arctic

Fig. 6 shows our paleogeography map for the Aptian-Albian. To a considerable extent, it is compiled for its offshore part on the basis of our interpretation of seismic data. For the Norwegian Barents Sea, various

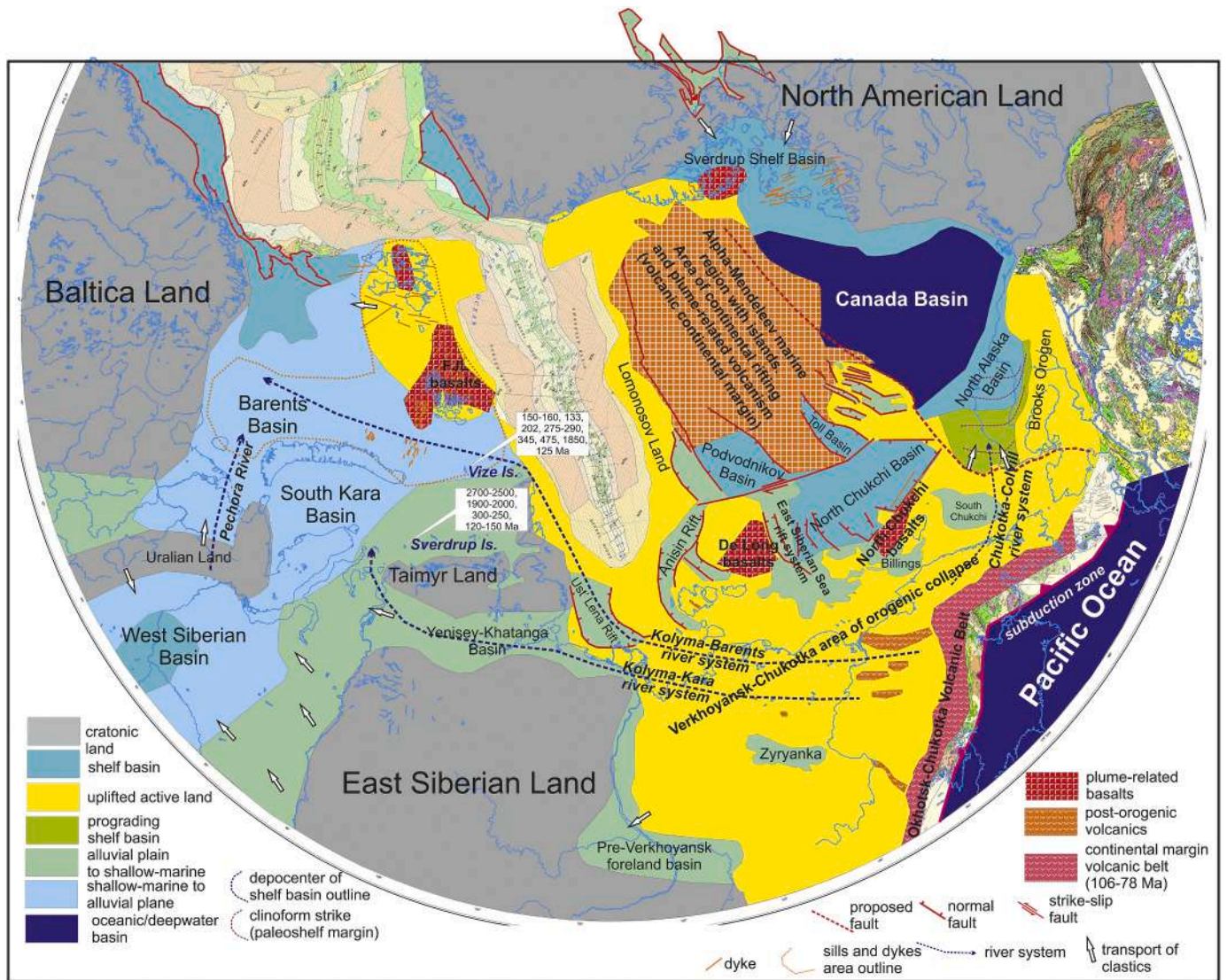


Fig. 6. Paleogeographic map of the Arctic for the Early Cretaceous, Aptian to Albian (125–100 Ma), on the present-day geographic framework. Geographic base map is Geological map of the Arctic (Harrison et al., 2011). Ages in the white boxes – ages of peaks of detrital zircons (our data), data for the Sverdrup Island are from Ershova et al., 2019.

studies (Blaich et al., 2017; Faleide et al., 2010; Grundvåg et al., 2017; Ziegler, 1988) were used. For the region of Alaska and Canada, the data in Houseknecht et al. (2009), Houseknecht and Wartes (2013), Moore et al. (2015) and Galloway et al. (2015) were used. For the onshore, the main studies were performed by Vinogradov (1968) and Kontorovich et al. (2014).

In the Russian part of the Barents Sea, the Neocomian clinofom complex is overlain by a sequence with horizontal layering which is considered by us as Aptian-Albian. The age of this seismostratigraphic complex is tied to available well data (Grundvåg et al., 2017; Midtkandal et al., 2016; Mordasova, 2018; Startseva, 2018). South and southwest of Franz Josef Land, approximately at the bottom of the horizontally layered Aptian sequence, a package with bright and chaotic reflections occurs. Its typical thickness is about 50–100 msec. We believe that this package of bright reflections corresponds to the strata of basalts on Franz Josef Land (see Paper 2, Fig. 56). This member of igneous rocks has an age of ca. 122–125 Ma (Corfu et al., 2013; Polteau et al., 2016). In the area of Svalbard, a horizon of bentonites with isotopic age of 123.1 ± 0.3 Ma is dated in the Cretaceous section (Midtkandal et al., 2016). These probable volcanites lay with an unconformity on the Neocomian

clinofom complex. This unconformity approximately corresponds to the Barremian/Aptian boundary.

At the bottom of the Aptian, an angular unconformity is observed in the area of the Barents and Kara Seas. Aptian deposits covered all relative anticlinal highs, including Novaya Zemlya (Mordasova, 2018; Nikishin et al., 2015; Nikishin, 2013; Startseva, 2018). The pre-Aptian angular unconformity on anticlinal highs is well known for the Yenisey-Khatanga and West Siberian basins (Afanasenkov et al., 2016; Kontorovich et al., 2014; Unger et al., 2017). In the Aptian-Albian in the area of the Barents and Kara Seas, an environment of a shelf sea and alluvial plain prevailed (Grundvåg et al., 2017; Mordasova, 2018; Smelror et al., 2009; Startseva, 2018).

In the north of the Kara Sea on the Vize Island, sandstones with an Upper Barremian-Aptian age were sampled. Peaks of ages of detrital zircons have values in the range from 150 to 160, 133, 202, 275–290, 345, 475, 1850, 125 Ma (Nikishin et al., 2014). According to our data (Nikishin et al., in preparation), Jurassic and Neocomian sandstones from Franz Josef Land and from Barents Sea offshore wells have typical ages of detrital zircons of 290–230, 415–435, 520–560, 1700, 1000–1400, 230–250 Ma. I.e., the ‘Uralian’ source of clastic matter

prevailed. From the Aptian on, the paleogeography pattern abruptly changed. The presence of Jurassic and Early Cretaceous zircons is indicative of a new source area from the Verkhoyansk-Chukotka Orogen (Nikishin et al., 2015), where Jurassic and Early Cretaceous magmatism widely manifested itself. The age data of detrital zircons for Aptian-Albian deposits of Chukotka coincide with ages for the Vize Island sandstones (Nikishin et al., 2014; Vatrushkina, 2018). Similar ages of detrital zircons are also available for Albian continental sandstones from the Kotelny Island of the New Siberian Islands, with peaks ca. 145, 240, 290, 330, 1700, 1880 Ma (Kuzmichev et al., 2018). Similar results were obtained for the Aptian sandstones of the South Kara Basin (Sverdrup Island) (Ershova et al., 2019). Hence, it is surmised that a major river system existed from Chukotka to the Barents-Kara Seas in the Aptian (see Fig. 6).

An Aptian-Albian deltaic system with clinoforms is identified in the Colville Basin on Alaska (Houseknecht et al., 2009; Houseknecht and Wartes, 2013; Moore et al., 2015). The river system had its start on Chukotka. The data in Moore et al. (2015) show that ages of detrital zircons in the Alaskan Aptian-Albian deposits almost coincide with ages

of zircons on Chukotka and on the Vize Island. This topic requires special analysis, but the hypothesis assumes that in the Aptian-Albian time, rivers from Chukotka were running both toward the Canada Basin and toward the area of the Barents Sea.

Within the Verkhoyansk-Chukotka region, collapse of the Early Cretaceous orogen took place and numerous post-collisional granitoids were formed in the Aptian-Albian (Amato et al., 2015; Khanchuk et al., 2019; Kuzmichev, 2009; Miller et al., 2018b, 2018a, 2010, 2008; Parfenov and Kuzmin, 2001; Sokolov et al., 2002; Toro et al., 2016). In the area of the strip of the South Anyui zone, a system of volcanic belts in an extensional environment was formed synchronously with collapse of the orogen (125–112 Ma). These belts are consisting of basalts, andesites, rhyolites and sedimentary rocks. The largest of these belts is the Tytylveyem belt (Tikhomirov, 2018; Tikhomirov et al., 2017). Similar volcanites are also encountered on the New Siberian Islands (Kos'ko and Trufanov, 2002; Nikitenko et al., 2017).

In the Arctic from the Laptev Sea up to the Chukchi Sea, continental rift systems were formed in the Aptian and Albian. The North Chukchi Basin, East Siberian Sea Basin, Anisin-Novosibirsk Basin, and Ust' Lena

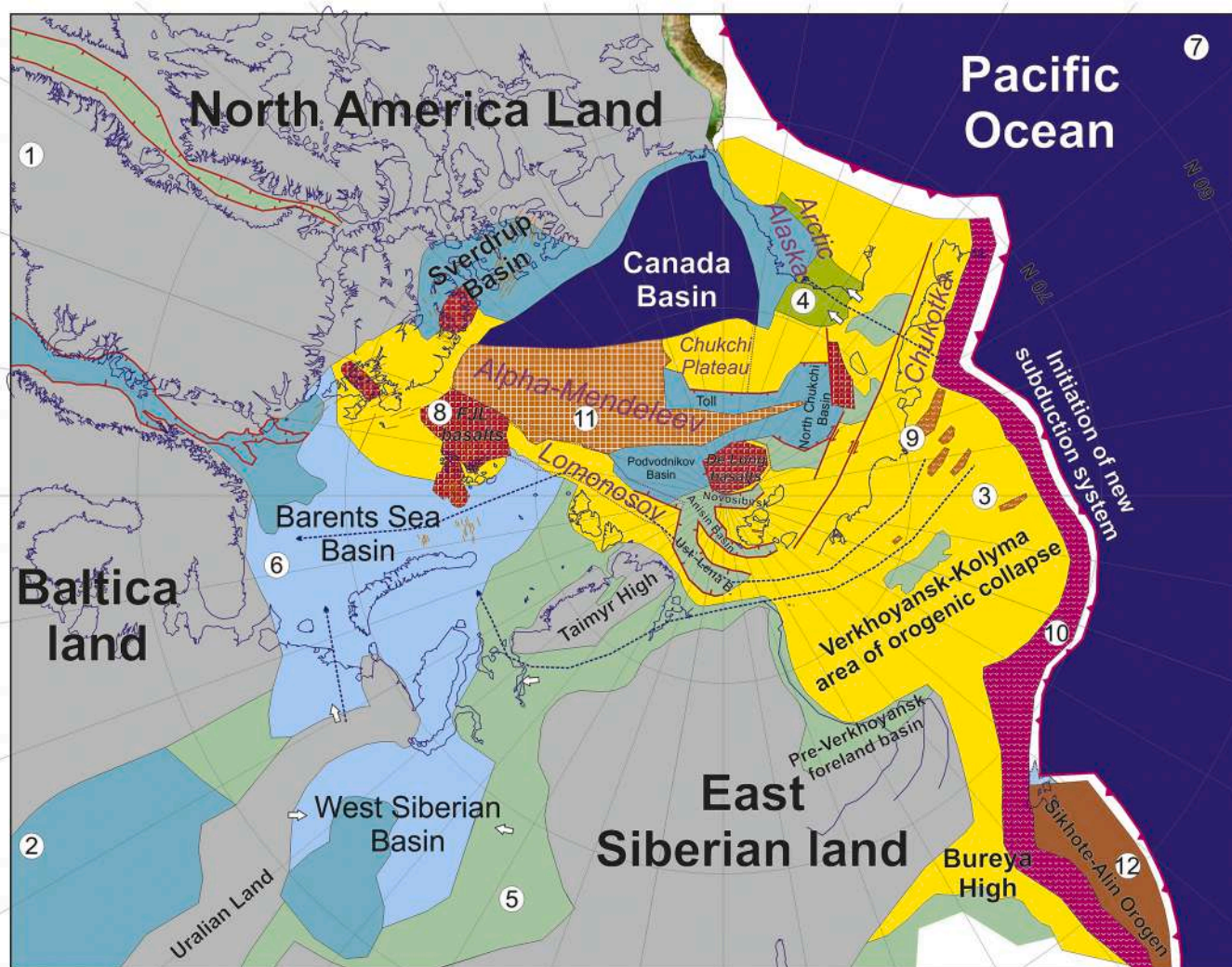


Fig. 7. Tectonic restoration of the Arctic region for the Early Cretaceous, Aptian to Albian (125–100 Ma). Kinematic restoration for the 115 Ma. Restoration was performed using GPlates programme. Legend is similar to Fig. 6. 1 – cratonic land, 2 – shelf basin, 3 – uplifted active land, 4 – prograding shelf basin with clinoform sedimentation mainly, 5 – alluvial plain to shallow-marine, 6 – shallow-marine to alluvial plane, 7 – oceanic/deepwater basin, 8 – plume-related basalts, 9 – post-orogenic volcanics, 10 – continental margin volcanic belt, 11 – area of continental rifting and plume-related volcanism, 12 – accretion orogen. Violet letters mark position of some terranes and their names. (For interpretation of the references to colour in this figure legend, the reader is referred to the web version of this article.)

Basin belong to them. On seismic lines, we observe normal faults of dominantly near north-south trends; we also observe possible strike-slip faults with dominantly near east-west trends. The Podvodnikov and Toll Basins probably started to form since the Aptian.

Aptian-Albian rifts are well known in the North Atlantic region (Ziegler, 1988) and in the Baffin Bay (Dickie et al., 2011; Gregersen et al., 2013).

We compiled a kinematic reconstruction of the Arctic for the Aptian (115 Ma) within the framework of GPlates software and our geodynamic concept (Freiman et al., 2018; Nikishin et al., 2017a, 2017b; Nikishin et al., 2015), presented in Fig. 7. We charted our paleogeography data onto the geometric reconstruction. For the Aptian, five areas of basaltic magmatism are identified on the shelf: Franz Josef Land, Svalbard, Sverdrup, De Long and North Chukchi areas. Ages of the onset of magmatism are not exactly dated, though they are likely close to 122–125 Ma. Probably magmatism started approximately simultaneously in all of the five igneous provinces.

The data for the area of the De Long Plateau show that basalts are present at the base of many rifts in the area of the Laptev Sea and the East Siberian Sea (see Paper 2). It is likely that after start of the magmatism, continental rifting widely manifested itself in the shelf areas from the Laptev Sea to the Chukchi Sea, as well as in the North Atlantic and in the Baffin Bay region. For the Alpha-Mendelev ridges, isotopic ages of basalts are known in the interval of 127–110 Ma. The volcanic Alpha-Mendelev ridges were together with the volcanic Franz Josef

Land Plateau and the volcanic De Long Plateau at the onset of its formation (e.g., Døssing et al., 2013; Nikishin et al., 2015). Such an interrelationship is typical for known volcanic continental margins (e.g., Geoffroy, 2005). Therefore, we assume that in the Aptian the Alpha-Mendelev ridges were formed as a volcanic continental margin on a continental crust. Such a hypothesis was discussed in Dove et al. (2010). Volcanic margins are typically associated with SDRs (e.g., Clerc et al., 2018; Geoffroy, 2005; Stica et al., 2014). In the area of the Toll Basin situated between the Mendelev Ridge and the Chukchi Plateau, half-grabens with probable SDRs were identified on two seismic sections (Ilhan and Coakley, 2018; Nikishin et al., 2015). This result shows that volcanism on the Alpha-Mendelev ridges was accompanied by continental rifting in the Aptian-Albian.

We find no indication for the presence of an oceanic spreading axis for the Aptian-Albian in the Alpha-Mendelev ridges. Extension in the area of the Alpha-Mendelev ridges and the rift systems of the Laptev-Chukchi Seas was probably associated with major strike-slip faults. These strike-slip faults might reach the Pacific Ocean and its subduction zone.

For the Aptian-Albian, many dyke belts and areas of development of sills are well known in the Arctic (e.g., Buchan and Ernst, 2018; Dockman et al., 2018; Døssing et al., 2013; Estrada et al., 2016; Kingsbury et al., 2018; Minakov et al., 2018; Shipilov, 2016). We refined these data for the Barents and Chukchi Seas on the basis of new seismic data and magnetic anomalies (Fig. 6).

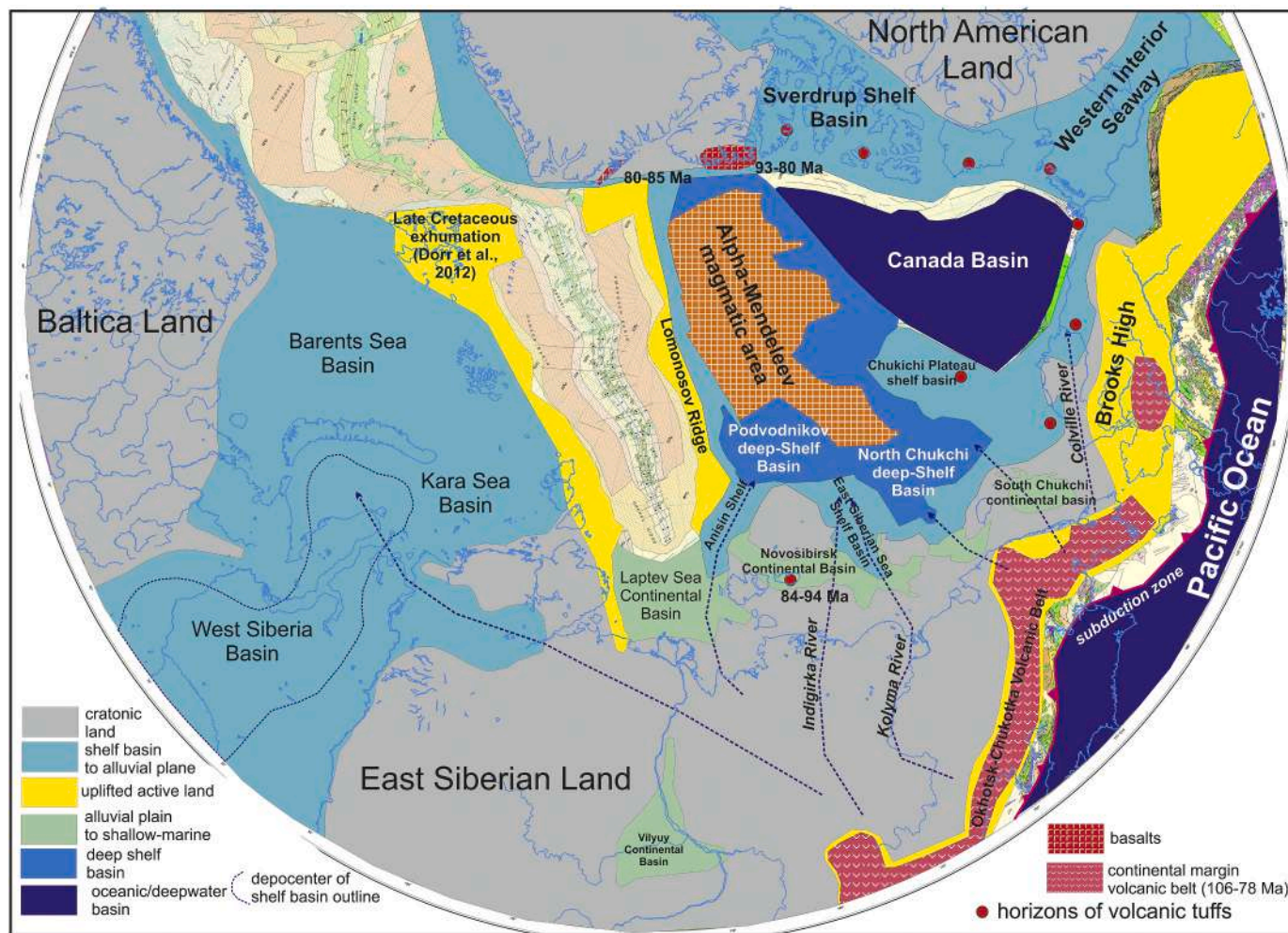


Fig. 8. Paleogeographic map of the Arctic for the Late Cretaceous, Cenomanian to Campanian (100–80 Ma), on the present-day geographic framework. Geographic base map is Geological map of the Arctic (Harrison et al., 2011).

3.6. Late Cretaceous history of the Arctic (100–80 Ma)

Fig. 8 shows our paleogeography map for the Late Cretaceous (Cenomanian – Middle Campanian). For its offshore part, it is compiled to a large extent on the basis of our interpretation of seismic data. For the Norwegian Barents Sea, the studies of Ziegler (1988) and Faleide et al. (2010) are used. For the region of North America, the data in Houseknecht and Connors (2016), Craddock and Houseknecht (2016), Moore et al. (2015), Schröder-Adams et al. (2014), Schröder-Adams et al. (2014) and Pugh et al. (2014) are utilized. For the Russian onshore, the main studies of Vinogradov (1968) and Kontorovich et al. (2014) are used.

Data of commercial drilling in the Russian part of the Barents Sea and in the South Kara Basin demonstrated that the Upper Cretaceous was widespread, but in the Barents Sea it was considerably eroded during the Quaternary glaciations (e.g., Henriksen et al., 2011a, 2011b).

In the South Kara Basin, the Upper Cretaceous is studied by several boreholes (Leningradskaya and Rusanovskaya, etc.) (Nikishin et al., 2015; Nikishin, 2013; Shishkin et al., 2015). Similar Upper Cretaceous deposits are penetrated by wells on Yamal (Kontorovich et al., 2014; Shishkin et al., 2015). In the South Kara Basin, the thickness of Upper Cretaceous deposits is about 700–1300 m, determined by drilling data. The Upper Cretaceous is represented mainly by marine and continental clays and siltstones including biosilica horizons. The Cenomanian is characteristic of sandstones (e.g., Nikishin, 2013; Shishkin et al., 2015).

The Upper Cretaceous is penetrated by several wells in the East Barents Megabasin. The most complete description is available for the Severo-Murmanskaya-1, Arkticheskaya, Shtokmanovskaya-1, Ledovaya-2 -1 wells (Mordasova, 2018). Thickness of Upper Cretaceous deposits in the wells reaches 300 m. Deposits are represented mainly by shelf clays and siltstones. It is observed on seismic lines that the thickness of Upper Cretaceous deposits exceeds more than 1 km (Mordasova, 2018; Nikishin et al., 2015; Startseva, 2018). The Upper Cretaceous biostratigraphy is poorly studied. On the Kolguyev Island, marine fauna from Cenomanian to Campanian are encountered in Upper Cretaceous deposits (Zhuravlev et al., 2014). Hence, it appears that shelf marine environments prevailed in the Barents Basin for this interval of time.

In the Norwegian part of the Barents Sea, a shelf sea was mainly present in the Late Cretaceous in the Cenomanian-Campanian, though these deposits have been eroded to a considerable extent (Faleide et al., 2010; Henriksen et al., 2011b, 2011a; Ziegler, 1988). Maastrichtian deposits are almost absent in the Barents Sea. It is assumed that a phase of regional erosion took place in the Maastrichtian (Henriksen et al., 2011b, 2011a).

Based on the available seismic data and analysis of lithofacies distribution in Upper Cretaceous deposits we assume that in the Upper Cretaceous all main uplifts in the region of the Barents and Kara Seas were covered by sediments. It is likely that integrated shelf basins existed which comprised the basins of the Barents Sea, Kara Sea and West Siberia.

A phase of uplift and exhumation occurred on Svalbard in the Late Cretaceous (Dörr et al., 2012). However, this issue is debatable at present. The Upper Cretaceous deposits of the Barents-Kara seas have no typical clinofolds. As a result, it is still unknown where the main sources of clastic material were situated.

In the Russian Far East, a well-known structure is the Okhotsk-Chukotka continental-marginal volcanic belt with an age of about 106–78 Ma (Akinin, 2012; Khanchuk et al., 2019; Parfenov, 1984; Tikhomirov, 2018). This belt separated the Asian continent from the Pacific Ocean. In the Arctic in the area of the Laptev, East Siberian and Chukchi Seas, formation of post-rift basins was underway. Data for the Upper Cretaceous are available for the New Siberian Islands only. Cenomanian, Turonian and Coniacian deposits are present there. Cenomanian deposits are probably represented by continental sandstones, while Turonian-Coniacian deposits form a coastal coal-bearing member up to 95 m thick (Kostyleva et al., 2018; Nikitenko et al., 2017). In

Turonian-Coniacian sandstones, many detrital zircons are present, with ages of ± 82 –94 Ma, whereas horizons of rhyolitic tuffs are also identified (Danukalova and Kuzmichev, 2014; Kostyleva et al., 2018). In the north of Siberia and south of the Lena River delta in the area of the town of Tiksi, volcanic centers and dykes composed of basalts were discovered. U–Pb SHRIMP zircon dating of 3 dykes yielded crystallization ages of 86 ± 4 , 86.2 ± 1.3 and 89 ± 2 Ma (Turonian to Santonian) (Prokopiev et al., 2013). In the Russian Far East, no marine Upper Cretaceous deposits are present. The only mountain belt appears to be the Okhotsk-Chukotka volcanic belt. It is likely, therefore, that the main river system was from the Okhotsk-Chukotka volcanic belt into the shelf sea of the North Chukotka Basin and into the Podvodniy Basin (Fig. 8).

A Late Cretaceous shelf of the Sverdrup Basin is located in northern Canada (Hadlari et al., 2016; Pugh et al., 2014; Schröder-Adams et al., 2014). It consists of shelf clays and sandstones. Volcanites are known from the Cenomanian and Campanian (Hadlari et al., 2016; Schröder-Adams et al., 2014). The maxima of dyke volcanism are of 95 ± 4 Ma and 81 ± 4 Ma (Buchan and Ernst, 2018; Dockman et al., 2018). For the Mackenzie Delta Basin and Arctic Alaska Basin, the Upper Cretaceous is mainly represented by shelf clays (Houseknecht and Bird, 2011).

Volcanic tephra of Cenomanian-Coniacian age (ca. 100–86 Ma) are widely known in Upper Cretaceous on the Alaskan Shelf. It is assumed that the volcanic material entered from the Okhotsk-Chukotka volcanic belt (Houseknecht and Connors, 2016; Houseknecht and Bird, 2011).

Late Cretaceous ages of basalts are known for the Alpha-Mendelev ridges (Coakley et al., 2016). We assume that a possible source of volcanic material for Late Cretaceous shelf deposits of the Arctic region was the area of the Alpha-Mendelev ridges (see Fig. 8). Volcanoes of rhyolitic composition are inferred for the Alpha Ridge based on seismic data (Brumley, 2014). We compared the Mendelev Ridge with the Vøring Plateau on the Norwegian continental margin in the North Atlantic. The Vøring Plateau is composed of basalts, but volcanites of acidic composition (dacites, ignimbrites), and pyroclastic material in the form of tuffs are also present (Abdelmalak et al., 2016). Thus, basaltic magmatism with possible acidic-composition, occurred in the area of the Alpha-Mendelev ridges in Late Cretaceous. Acidic composition is characteristic of plume magmatism on a continental crust, as known for the Vøring Plateau.

We compiled a kinematic reconstruction of the Arctic for the Late Cretaceous (88 Ma) within the framework of GPlates software and our geodynamic concept (Freiman et al., 2018; Nikishin et al., 2017a, 2017b; Nikishin et al., 2015), presented in Fig. 9. We superimposed our paleogeographic data onto the geometric reconstruction. It is likely that the main event in the Late Cretaceous was magmatism on the Alpha-Mendelev ridges. This magmatism was possibly accompanied by rifting on a not well-constrained scale. Magmatism manifested itself within shelf basins of the Arctic Ocean as well. It is likely that intraplate tectonics dominated in the Arctic Ocean in the Late Cretaceous.

3.7. Paleocene history of the Arctic

Fig. 10 shows our paleogeography map for the Paleocene. For its offshore part, it is to a considerable extent based on our interpretation of seismic data. For the Norwegian Barents Sea, the studies of Ziegler (1988), Faleide et al. (2010), Henriksen et al. (2011b), and Lasubada et al. (2018) are used. For the North American region, various data (Craddock and Houseknecht, 2016; Dixon et al., 2019; Houseknecht, 2019; Houseknecht and Connors, 2016) are used. For the Russian onshore, we compiled the main studies presented by Grossgeym and Korobkov (1975), Akhmetiev and Zaporozhets (2014), Yakovleva (2017) and Vasilieva (2017).

As in the Barents and Kara seas, Paleocene deposits were eroded to a considerable extent, making it difficult to restore paleogeography of this period of time. Paleocene deposits are penetrated by wells in West Siberia (Akhmet'ev et al., 2010; Grossgeym and Korobkov, 1975; Vasilieva, 2017; Volkova, 2014; Yakovleva, 2017; Zyleva et al., 2014). In the

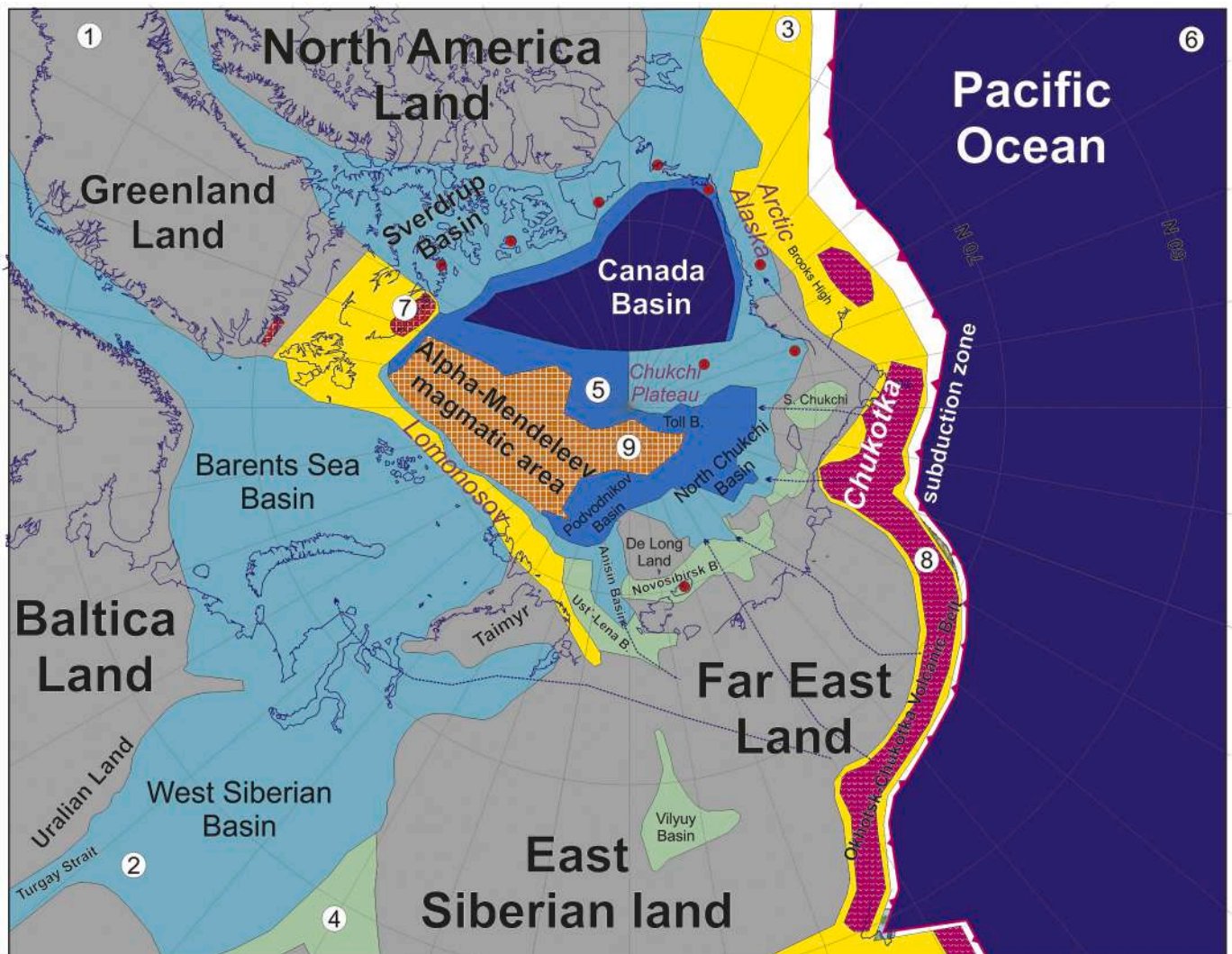


Fig. 9. Tectonic restoration of the Arctic region for the Late Cretaceous, Cenomanian to Campanian (100–80 Ma). Kinematic restoration for the 88 Ma. Restoration was performed using GPlates programme. Legend is similar to Fig. 8. 1 – cratonic land, 2 – shelf basin, 3 – uplifted active land, 4 – alluvial plain to shallow-marine, 5 – deep shelf basin, 6 – oceanic/deepwater basin, 7 – basalts, 8 – continental margin volcanic belt, 9 – Alpha-Mendelev intraplate magmatic area. Violet letters mark position of some terranes and their names. (For interpretation of the references to colour in this figure legend, the reader is referred to the web version of this article.)

Paleocene, shelf diatomites play an important role. Paleocene deposits are known from wells in the South Kara Basin and on Yamal (the Leningradskaya-1 well and others) (Shishkin et al., 2015). They are represented by continental and shelf deposits with horizons of diatomites. In the upper part of the Paleocene (the Serov Formation), horizons of volcanic ash with volcanic glass are known (Shishkin et al., 2015). In the Timan-Pechora Basin, Paleocene sections are studied in several wells (Oreshkina et al., 1998). The Paleocene is represented by shelf diatomites and clays. Marine shelf sediments are known for the western part of the Barents Sea, with a hiatus at the base of Paleocene in the Hammerfest Basin (Lasabuda et al., 2018). No adequate data on the presence of Paleocene are available for the Russian part of the Barents Sea (e.g., Smelror et al., 2009). The presence of marine Paleocene deposits in the West Siberian, Timan-Pechora and South Kara Basins makes it likely that the entire Barents-Kara region in the Paleocene was a shelf sea. Periods of emergence and desiccation are interpreted for this region. This region was situated in a stable intraplate tectonic setting.

On Svalbard, horizons of bentonites are encountered in the Paleocene Basilika Formation. Within these bentonites, ages of detrital zircons are studied (Elling et al., 2016). Many zircons have ages in the range of

200–650 Ma, though rare zircons are encountered with ages of about 88, 152, 154, 162 and 188 Ma (Elling et al., 2016). Cretaceous and Jurassic magmatic zircons in the Arctic are widely known in the Verkhoyansk-Chukotka region. That is why a probability exists that they were transported to the Svalbard region from the Russian Far East in the Paleocene (Elling et al., 2016). Our data on ages of detrital zircons in the North Kara Sea showed that many Cretaceous and Jurassic zircons with ages of ca. 150–160, 133, 202, 275–290 Ma are present within Aptian and Albian deposits (see Fig. 6). It can be assumed that erosion of Cretaceous sandstones took place in the north of the Barents-Kara Seas in the Paleocene. A shoulder of the Paleocene continental rift was possibly uplifted along the recent margin of the Eurasia Basin.

In the north of Greenland and on the Canadian Islands, the Eurekan Orogeny started in the Paleocene and the Central Tertiary Basin on Spitsbergen started to form as a foredeep basin (Elling et al., 2016; Lasabuda et al., 2018; Petersen et al., 2016; Piepjohn et al., 2015; Saalman et al., 2005). At that time, a continental rift system was formed in the North Atlantic (Faleide et al., 2010).

In the Russian Far East within the Verkhoyansk-Chukotka region, the Paleocene is only known in the Lower Kolyma Basin and in the north of

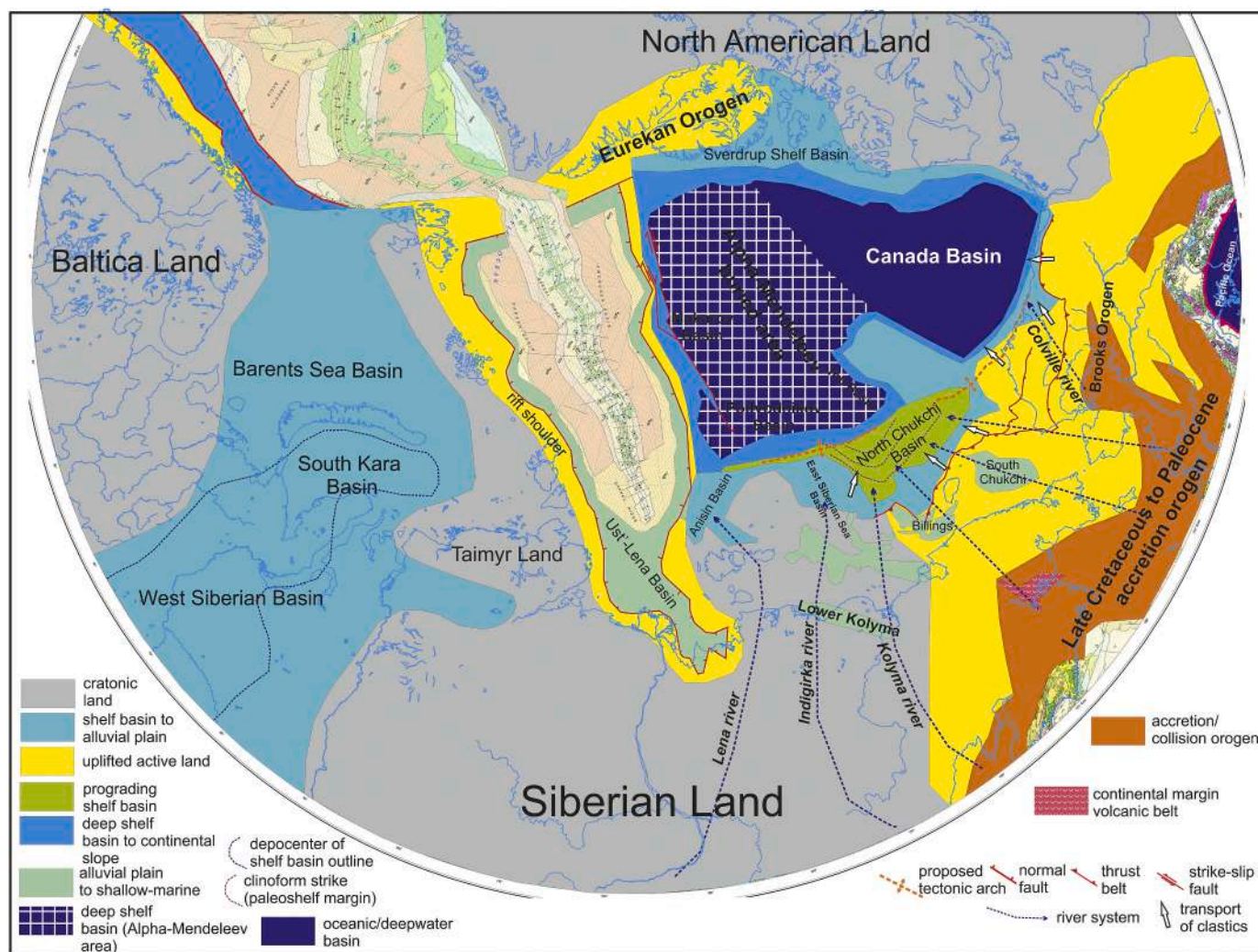


Fig. 10. Paleogeographic map of the Arctic for the Paleocene (66–56 Ma) on the present-day geographic framework. Geographic base map is Geological map of the Arctic (Harrison et al., 2011).

the Verkhoyansk Range near the Lena River delta (the Sogo Basin, Omoloy Basin, Ust'-Yana Basin). Paleocene deposits are known mainly from drilling data. The Paleocene is represented by continental deposits up to 200–300 m thick with horizons of coals (Gertseva et al., 2016; Grinenko, 1989; Grinenko et al., 1997; Grossgeym and Korobkov, 1975; Shulgina and Bashlavin, 2000). A regional weathering crust is well known at the Paleocene base; the Paleocene with erosional bottom overlies deposits of various ages (Grinenko, 1989; Grinenko et al., 1997). It is likely that a regional uplift phase took place at the Cretaceous/Paleocene boundary.

A well is available north of Chukotka on the Ayon Island in the area of the Rauchuan Basin. A weathering crust with kaolin clays is present in the well at the base of the Paleocene, Danian deposits are absent. The Selandian and Thanetian are represented by continental sediments with horizons of coals, with total thickness of about 50 m. Marine sediments might be present in the upper part of the Thanetian (Aleksandrova, 2016).

On the New Siberian Islands, a stratum of Thanetian age, up to 30 m thick, is known. It is represented by continental sediments with horizons of coal (Kos'ko and Trufanov, 2002; Kostyleva et al., 2018).

On the Alaska Shelf, three wells with Paleocene deposits are available. These are Klondike-1, Crackerjack-1, and Popcorn-1 (Craddock and Houseknecht, 2016; Houseknecht and Bird, 2011; Ilhan and

Coakley, 2018; Sherwood et al., 2002). In these wells, the Mid-Brookian Unconformity (MBU) is identified to which a major erosional boundary corresponds whose age has not been determined exactly though it is close to the Cretaceous/Paleogene boundary (Craddock and Houseknecht, 2016; Sherwood et al., 2002). In the Popcorn-1 well, Lower Paleocene deposits overlie Aptian deposits (Sherwood et al., 2002). The magnitude of erosion is evaluated to be on the order of hundreds of meters. The Paleocene is represented by clays with sandstone horizons. Marine fauna is present in the sediments.

In the Russian part of the North Chukchi Basin, the "lower" clinoform complex belongs to the Paleocene in accordance with our seismic-stratigraphy model (see Paper 2). We identified clinoforms on seismic data and traced their strikes (see Fig. 10). Transport of clastic material took place from the south from the Verkhoyansk-Chukotka region and from the side of West Alaska. North of the Wrangel and Herald islands, is a thrust belt, the Herald-Wrangel Ridge is situated to the south (Drachev et al., 2010; Nikishin et al., 2017a, 2017b; Nikishin et al., 2015). North of the Herald-Wrangel Thrust Belt, the MBU seismic boundary overlies a low-angle folded complex (Ikhsanov, 2014; Nikishin et al., 2017a, 2017b; Nikishin et al., 2015). Our analysis of seismic profiles shows that folding was accompanied by sedimentation with variable thicknesses in synclines. The folding took place not long before the MBU boundary. On the Chukchi Plateau, it is observed on seismic lines that Cretaceous

grabens experienced inversion accompanied by syntectonic sedimentation prior to the MBU boundary (Nikishin et al., 2015). As shown in Ilhan and Coakley (2018) in the eastern part of the North Chukchi Basin, significant erosion and, locally, an angular unconformity corresponds to the MBU boundary.

AFT data for the Brooks Range show that syntectonic uplift with kilometer-scale erosion took place at 60–65 Ma. This erosion encompassed the territories of the Alaska North Slope as well (Craddock et al., 2018; O’Sullivan et al., 1997). Modeling of subsidence history of the Alaska North Slope based on interpretation of seismic lines showed that an erosion phase with an amount up of 2–3 km took place at ca. 60 Ma (Peters et al., 2011). Our analysis of seismic lines for the MBU boundary shows that north of the Wrangel-Herald Thrust Belt, the amount of erosion below the MBU boundary reached the equivalent of 1–2 s TWT (the study was performed by M. Skaryatin). AFT data for the Wrangel Island show that a significant phase of erosion and uplift took place at about 72–64 Ma (Verzhbitsky et al., 2015, 2012). AFT data for the Herald High show that its uplifting started at ca. 74 Ma (Craddock and Houseknecht, 2016). It is likely that active uplift and erosion of the

Wrangel-Herald High started earlier than uplift of the Brooks Range area.

At the base of the Paleocene, an erosional boundary is identified on the Chukchi Plateau (Ilhan and Coakley, 2018). The Andrianov High is located in the eastern part of the North Chukchi Basin. On this high, a small angular unconformity is also present at the bottom of the MBU boundary (Ikhsanov, 2014; Nikishin et al., 2015). It is likely that this high experienced uplift in the Paleocene in the course of regional compression.

The following scenario of the Paleocene history can be proposed for the area of the Chukchi Sea. Regional compression and upthrusting of the Wrangel-Herald High and the Brooks system onto the North Chukchi Basin and the Chukchi Plateau started at the end of the Late Cretaceous at ca. 80–70 Ma, before the MBU boundary. The compression was accompanied by formation of mountain relief in the Wrangel-Herald and Brooks system strip of highs. The mountain belt became a source of a large amount of clastic material and a thick clinoform complex started to form in the North Chukchi Basin in the Paleocene.

In the area of the Laptev Sea, Paleocene deposits are exposed onshore

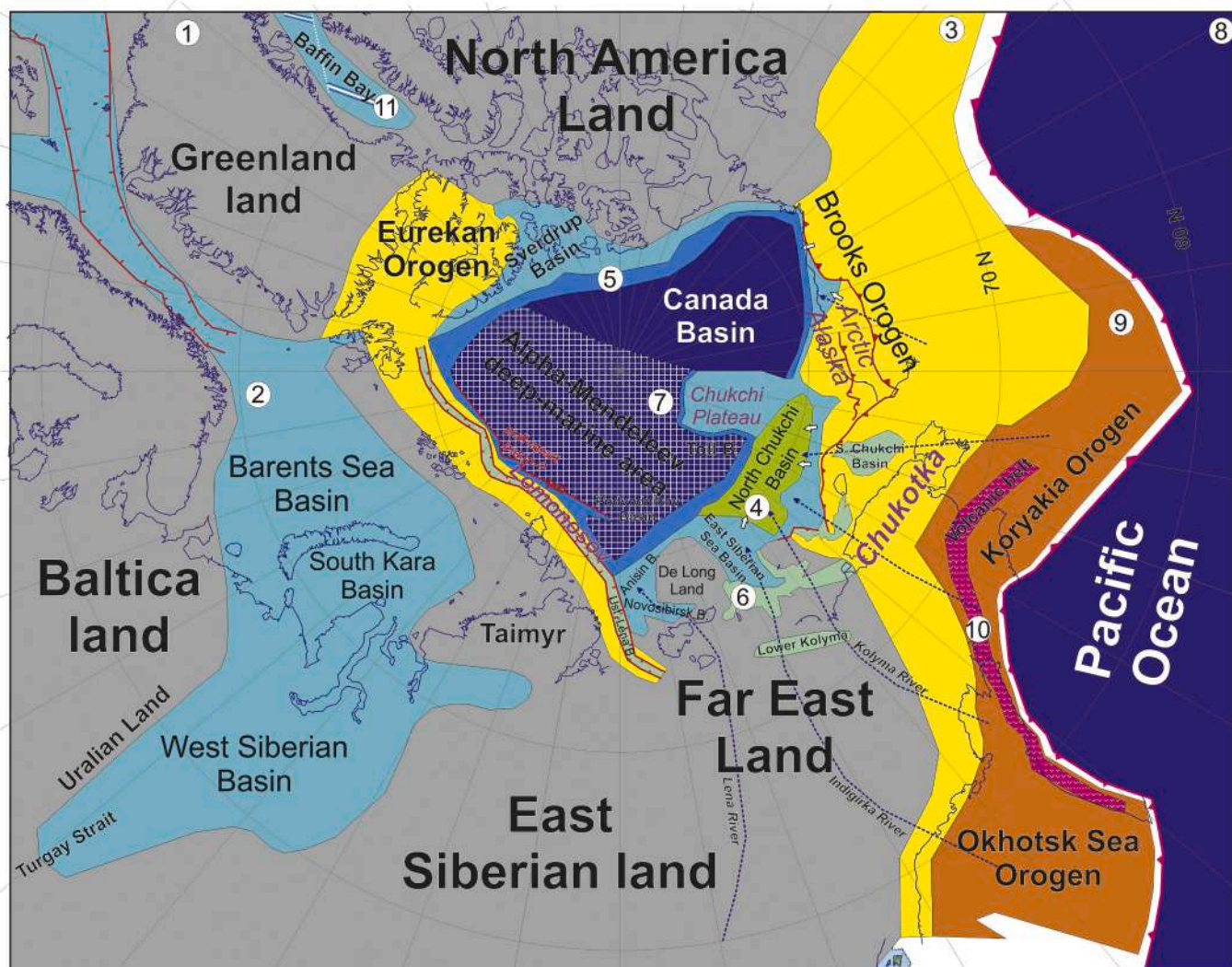


Fig. 11. Tectonic restoration of the Arctic region for the Paleocene (66–56 Ma). Kinematic restoration for the 65 Ma. Restoration was performed using GPlates programme. Legend is similar to Fig. 10. 1 – cratonic land, 2 – shelf basin, 3 – uplifted active land, 4 – prograding shelf basin with clinoform sedimentation mainly, 5 – deep shelf basin to continental slope, 6 – alluvial plane to shallow-marine, 7 – deep shelf basin, 8 – oceanic/deepwater basin, 9 – accretion/collision orogen, 10 – continental margin volcanic belt, 11 – spreading axis. Violet letters mark position of some terranes and their names. (For interpretation of the references to colour in this figure legend, the reader is referred to the web version of this article.)

east of the Lena River delta (the Sogo Basin, Omoloy Basin, Ust'-Yana Basin). These Paleocene deposits are known from well drilling data. These are continental sediments with horizons of coals. The typical thickness of the deposits is about 100–300 m (Gertseva et al., 2016; Grinenko, 1989). These basins are bounded by faults and probably are a continuation of the Laptev Sea rift system (the Ust'-Lena Basin).

In the Laptev Sea, the Paleocene is identified by interpretation of seismic lines (see Paper 2). In the Paleocene, the large-size Ust'-Lena Rift formed and postrift subsidence of the Anisin and New Siberian Basins continued; facies of shelf, alluvial plains and slopes are identifiable. The deepest-water portion of the marine basin was the area of the Anisin Basin which transited into the continental slope of the Podvodnikov Basin in the north.

We compiled a kinematic reconstruction of the Arctic for the Paleocene (65 Ma) within the framework of GPlates software and our geodynamic concept (Freiman et al., 2018; Nikishin et al., 2017a, 2017b; Nikishin et al., 2015), presented in Fig. 11. We superimposed our paleogeography data onto the geometric reconstruction.

At the end of Cretaceous and in the Paleocene, a major continental-marginal orogen formed which comprised the area from the Okhotsk Sea Orogen and the Koryak Orogen to the Brooks Orogen on Alaska (O'Sullivan et al., 1997; Sokolov, 2010; Soloviev, 2008). Formation of the thrust belt of the Brooks Orogen system and the Wrangel-Herald

Orogen is associated with formation of this orogen. Growth of mountain systems resulted in fast filling of the North Chukchi Basin with clinoform complexes. Synchronously with this "Laramide" Orogeny, the Eureka Orogeny was taking place.

In the North Atlantic and along the present-day Eurasia Basin, continental rifting took place in the Paleocene. For the Eurasia Basin, parts of these rifts remained on the slope of the Lomonosov Ridge (see Paper 1). A Paleocene rift system (the Ust'-Lena Rift) was formed in the Laptev Sea as well. Formation of the Ust'-Lena Rift and the Paleocene "pre-Gakkel Rift" was associated with the history of the Atlantic Ocean opening. The West Makarov Basin was formed in the Paleocene as a pull-apart basin and as a part of the Paleocene Gakkel (or "pre-Gakkel") rift system.

3.8. Early-Middle Eocene history of the Arctic

Fig. 12 shows our paleogeography map for the Early-Middle Eocene (56–45 Ma). For its offshore part, it was developed to a considerable extent on the basis of our seismic data interpretation. For the Norwegian Barents Sea, the studies by Ziegler (1988), Faleide et al. (2010), Henriksen et al. (2011b) and Lasubuda et al. (2018) were used. For the Alaska region, the data in Houseknecht and Connors (2016) and Craddock and Houseknecht (2016) were used. For the Russian onshore,

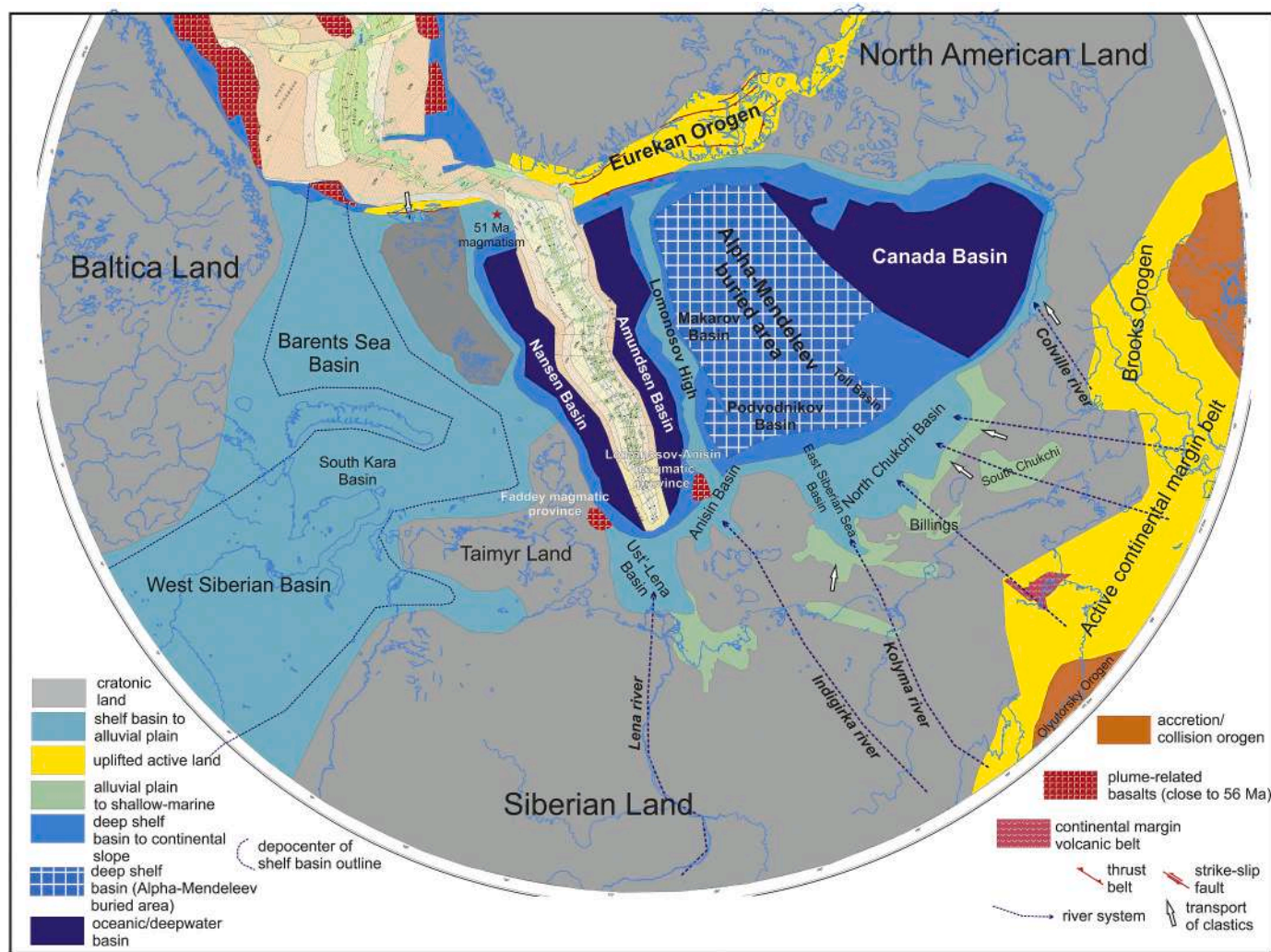


Fig. 12. Paleogeographic map of the Arctic for the Early-Middle Eocene (56–45 Ma) on the present-day geographic framework. Geographic base map is Geological map of the Arctic (Harrison et al., 2011).

the main studies are Grossgeym and Korobkov (1975), Akhmet'ev and Zaporozhets (2014), Yakovleva (2017) and Vasileva (2017).

In the North Atlantic region, plume magmatism widely manifested itself at the end of Paleocene and beginning of Eocene, which transitioned into formation of volcanic continental margins and subsequent formation of the North Atlantic Ocean in the Eocene. This classical history is described in numerous publications (e.g., Abdelmalak et al., 2016; Faleide et al., 2010; Funck et al., 2017; Gaina et al., 2017; Torsvik et al., 2002; Wilkinson et al., 2017; Ziegler, 1988). We identified two new magmatic provinces at the boundary of the Laptev Sea Shelf and the Eurasia Basin on the basis of analysis of seismic profiles and magnetic field anomalies (see Paper 2). They are situated symmetrically relative to the Gakkel Ridge. Based on analysis of linear magnetic anomalies, the opening of the Eurasia Basin is assumed to start at ca. 56 Ma (e.g., Glebovsky et al., 2006). It appears that volcanic passive margins might form at the Siberian termination of the Eurasia Basin.

On the Lomonosov Ridge slope from the side of the Amundsen Basin, a breakup type boundary is readily identified on seismic lines (see Paper 1). In the Ust'-Lena Rift, a breakup type boundary is also well expressed on the side of Taimyr (see Paper 2).

On shore, Early Eocene deposits form several grabens (Gertseva et al., 2016; Grinenko, 1989). The best studied of them is probably the Kengday Basin situated east of the Lena River delta. Its deposits are represented by Ypresian-Lower Lutetian which overlies Paleozoic deposits with an angular unconformity (Grinenko, 1989; Grinenko et al., 1997). The graben is filled with continental coal-bearing sediments of about 500–700 m thickness with individual horizons of marine deposits in the form of marls. The main phase of rifting was in the Ypresian-Early Lutetian (ca. 56–45 Ma) in accordance with the available stratigraphy schemes (Gertseva et al., 2016; Grinenko, 1989). Early Eocene coal-bearing deposits are present in the Lower Kolyma Basin as well (Grinenko, 1989; Shulgina and Bashlavin, 2000).

Analysis of seismic lines for the Laptev Sea demonstrates that the Lower-Middle Eocene deposits (56–45 Ma) are thickest in the Ust'-Lena Basin (about 1 s). A phase of rifting took place in this basin. Analysis of seismic facies shows that in the Ust'-Lena Basin, the Lower-Middle Eocene is likely to be represented by non-marine and shallow marine deposits. A weak phase of rifting possibly took place in the Anisin-New Siberian Basin.

On the New Siberian Islands, Lower Eocene (Ypresian) deposits are known on the New Siberia Islands. They are represented by continental coal-bearing deposits of about 50 m thickness (Kos'ko and Trufanov, 2002; Kostyleva et al., 2018).

In the Chukchi Sea on the Ayon Island north of Chukotka, Ypresian deposits of about 25 m thickness are known from drilling data. They are represented by non-marine deposits (Aleksandrova, 2016).

Analysis of seismic lines for the North Chukchi Basin shows that Lower-Middle Eocene deposits (56–45 Ma) form a sedimentary cover of approximately even thickness (see Paper 2). Analysis of seismofacies shows that in the North Chukchi Basin, Early-Middle Eocene deposits have a facies transition from non-marine facies in the south to shelf ones in the north.

On the Alaskan Shelf, Lower-Middle Eocene non-marine and shallow marine deposits were sampled by wells (Ilhan and Coakley, 2018; Sherwood et al., 2002).

For the Arctic Beaufort-Mackenzie Basin, Lower-Middle Eocene deposits have been studied in the offshore well Natsek E-56 (Neville et al., 2017). They are represented mainly by clays with horizons of siltstones and conglomerates, with a total thickness of about 2 km. Sediments were formed on the continental shelf and slope and contain marine fossils. On the whole, the Lower-Middle Eocene is represented for the Alaskan and Canadian shelf by continental and shelfal sediments (Helwig et al., 2011; Houseknecht and Bird, 2011; Peters et al., 2011).

In the Early-Middle Eocene, the Eurekan Orogeny manifested itself in the north of Canada and Greenland (Elling et al., 2016; Lasabuda et al., 2018; Petersen et al., 2016; Piepjohn et al., 2016, 2015; Saalman et al.,

2005; Tegner et al., 2011). At that time, ca. 53–47 Ma, a transpressional orogen was formed in the north of Canada and Greenland, while a collisional orogen was formed in the west of Spitsbergen (Piepjohn et al., 2015). In the Eocene, the main phase of formation of the Central Tertiary Basin of Spitsbergen as a foredeep basin took place. Analysis of ages of detrital zircons in this basin shows that it was from the early Eocene. At this time the transport of sediments into the Central Tertiary Basin of Spitsbergen was from the side of the Eurekan Orogen (Petersen et al., 2016). Prior to this time the main transport of sediments took place from the Barents region (Elling et al., 2016; Petersen et al., 2016).

Within the Barents and Kara seas and West Siberia, Early-Middle Eocene deposits (56–45 Ma) overlie Paleocene deposits and form continuous stratigraphic sections. Paleogeography environments were on the whole constant. In the Early-Middle Eocene, an integral sedimentary basin probably existed in the area of the Barents and Kara Seas and in West Siberia. Eocene deposits are penetrated by wells in West Siberia (Akhmet'ev et al., 2010; Grossgeym and Korobkov, 1975; Vasileva, 2017; Volkova, 2014; Yakovleva, 2017; Zyleva et al., 2014). Eocene deposits are known from wells in the South Kara Basin and on Yamal (Shishkin et al., 2015). They are represented by continental and shelf deposits with horizons of diatomites. In the Timan-Pechora Basin, Early-Middle Eocene sections are studied in several wells (Oreshkina et al., 1998). The Eocene is represented mainly by shelf diatomites. Marine shelf sediments are known for the western part of the Barents Sea only (Lasabuda et al., 2018). No reliable data are available on the presence of Eocene strata in the Russian part of the Barents Sea (Smelror et al., 2009). The presence of marine Early-Middle Eocene deposits in the West Siberian, Timan-Pechora and South Kara Basins suggests that the entire Barents-Kara region in the Early-Middle Eocene (56–45 Ma) was a shelf sea, that periodically desiccated and became a sub-aerial flatland.

Early-Middle Eocene deposits are studied for the Lomonosov Ridge based on data of ACEX boreholes (Backman et al., 2008; Backman and Moran, 2009; Brinkhuis et al., 2006). The lower unit with an age of ca. 56–50 Ma is represented by silty clay and clay. The upper unit with an age of ca. 50–45 Ma is represented by biosiliceous ooze. In the Early-Middle Eocene, euxinic shelf sedimentation prevailed (Backman et al., 2008; Backman and Moran, 2009; Brinkhuis et al., 2006; Moran et al., 2006).

In the Eurasia and Amerasia basins, Early-Middle Eocene deposits (56–45 Ma) are well traced as a package with bright reflections (see Paper 1). This distinctive acoustic signature is probably a result of a lithologic composition that is distinct from overlying and underlying deposits. We believe that siliceous deposits may be present in the composition of Lower-Middle Eocene deposits.

In the Early-Middle Eocene, an active orogeny along the Pacific margin of Asia and Alaska formed. A continental-marginal orogen was formed in the strip from Sakhalin and the Sea of Okhotsk to Koryakia and along the Brooks Range (Sokolov, 2010; Soloviev, 2008).

We compiled a kinematic reconstruction of the Arctic for the end of Paleocene and the Early-Middle Eocene (~56 Ma) within the framework of the GPlates software and our geodynamic concept (Freiman et al., 2018; Nikishin et al., 2017a, 2017b; Nikishin et al., 2015), presented in Fig. 13. We superimposed our paleogeography data onto the geometrical reconstruction. Three major tectonic events took place at that time: (1) opening of the North Atlantic Ocean and of the Eurasia Basin started after the epoch of plume magmatism; (2) the Eurekan Orogen developed; (3) a continental-marginal orogen was formed along the Pacific margin of Asia and North America.

3.9. Middle-Late Eocene history of the Arctic

Fig. 14 displays our paleogeography map for the Middle-Late Eocene for the time interval of 45–34 Ma. For the offshore part, it is developed to a considerable extent on the basis of our seismic data interpretation. For the Norwegian Barents Sea, the studies of Ziegler (1988), Faleide et al.

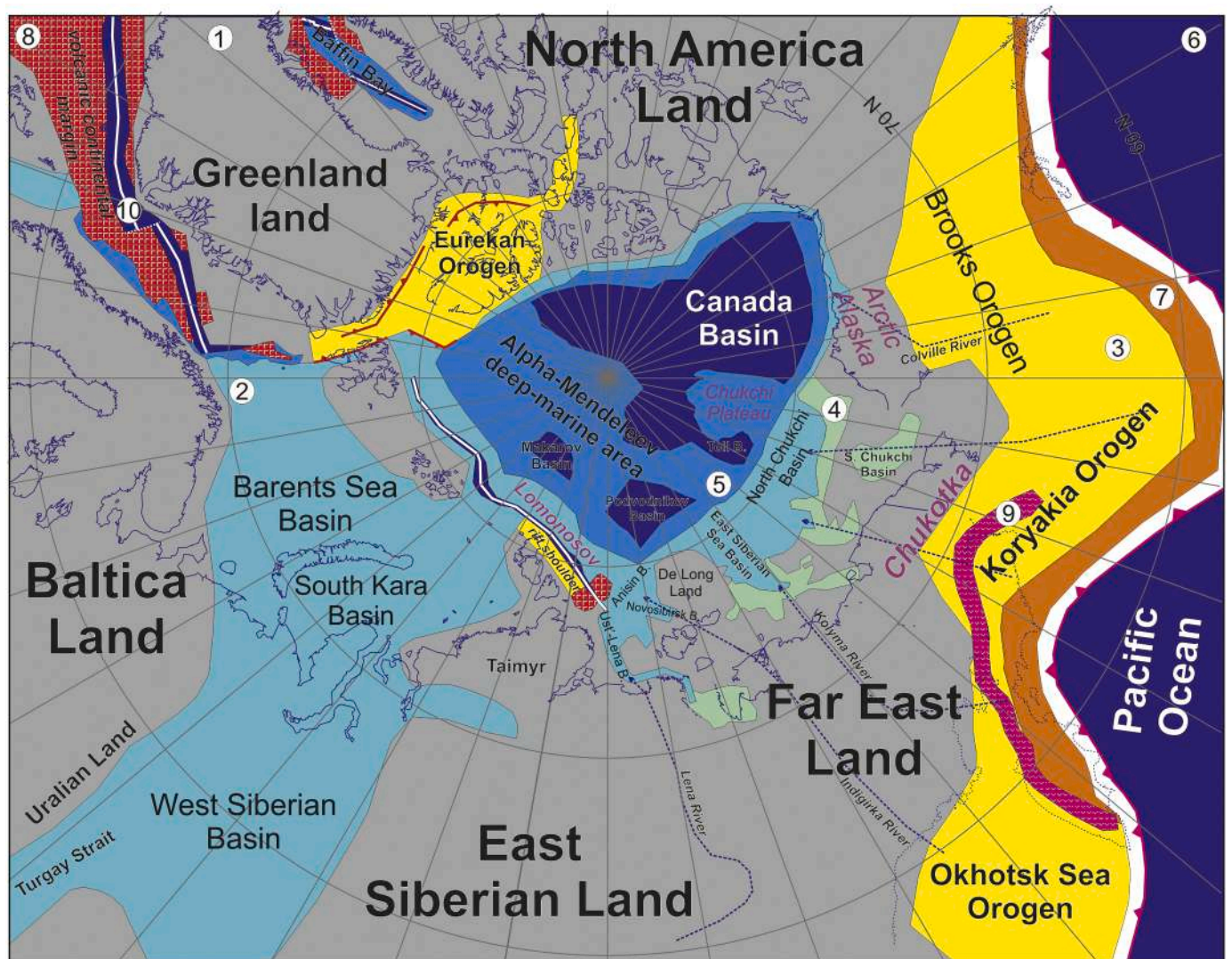


Fig. 13. Tectonic restoration of the Arctic region for the Early-Middle Eocene (56–45 Ma). Kinematic restoration for the 56 Ma. Restoration was performed using GPlates programme. Legend is similar to Fig. 12. 1 – cratonic land, 2 – shelf basin, 3 – uplifted active land, 4 – alluvial plain to shallow-marine, 5 – deep shelf basin to continental slope, 6 – oceanic/deepwater basin, 7 – accretion/collision orogen, 8 – plume-related basalts, 9 – continental margin volcanic belt, 10 – spreading axis. Violet letters mark position of some terranes and their names. (For interpretation of the references to colour in this figure legend, the reader is referred to the web version of this article.)

(2010), Henriksen et al. (2011b), and Lasabuda et al. (2018) were used. For the North American region, the data in Houseknecht and Connors (2016), Craddock and Houseknecht (2016) were used. For the Russian onshore, the main data are presented in Grossgeym and Korobkov (1975), Akhmetiev and Zaporozhets (2014), Yakovleva (2017) and Vasilieva (2017).

This interval of time is characterized by the diversity of tectonic processes. In the Arctic, there were three zones of formation of oceanic crust with spreading axes: the North Atlantic, Baffin Bay, and Eurasia Basin (e.g., Ziegler, 1988). In the Eurasia Basin, ultraslow spreading started at ca. 45 Ma (e.g., Glebovsky et al., 2006; Nikishin et al., 2018), which continues until the present time. The time interval of 45–34 Ma is characterized by the main compressional phase of the Eureka Orogen and formation of the Central Tertiary Basin of Spitsbergen as a foredeep basin (Døssing et al., 2014; Elling et al., 2016; Gaina et al., 2015; Kleinspehn and Teyssier, 2016; Lasabuda et al., 2018; Petersen et al., 2016; Piepjohn et al., 2015; Saalman et al., 2005).

Within the Barents and Kara Seas and the north of West Siberia and Yamal, Middle-Late Eocene deposits (45–34 Ma) are absent. Middle-Late

Eocene deposits are penetrated by wells in the central and southern parts of West Siberia (Akhmet'ev et al., 2010; Grossgeym and Korobkov, 1975; Vasilieva, 2017; Volkova, 2014; Yakovleva, 2017; Zyleva et al., 2014). They are represented mainly by marine clays and siltstones (siliceous deposits disappear at ca. 45 Ma) (Akhmet'ev et al., 2010; Vasilieva, 2017; Yakovleva, 2017). Marine shelf sediments are known for the westernmost part of the Barents Sea (Lasabuda et al., 2018; Smelror et al., 2009). Recent paleogeography reconstructions show that the West Siberian Basin was separated by a vast land mass from the Arctic water basin in the Lutetian time at ca. 48–43 Ma (Akhmet'ev et al., 2010; Shatsky, 1978; Vasilieva, 2017; Yakovleva, 2017).

In the area of Yamal and South Kara Basin, wells penetrated Paleocene and Eocene deposits (Kontorovich et al., 2010; Shishkin et al., 2015; Viskunova et al., 2004). The youngest Paleogene sediments are strata with diatomites with ages from the Thanetian to Middle Ypresian (about 58–52 Ma) (the Serov and Irbit Formations) (Shishkin et al., 2015; Viskunova et al., 2004; Yakovleva, 2017). Up the section, Pliocene strata occur with an angular unconformity. In the South Kara Basin, it is assumed on the basis of seismic data interpretation that Early Eocene

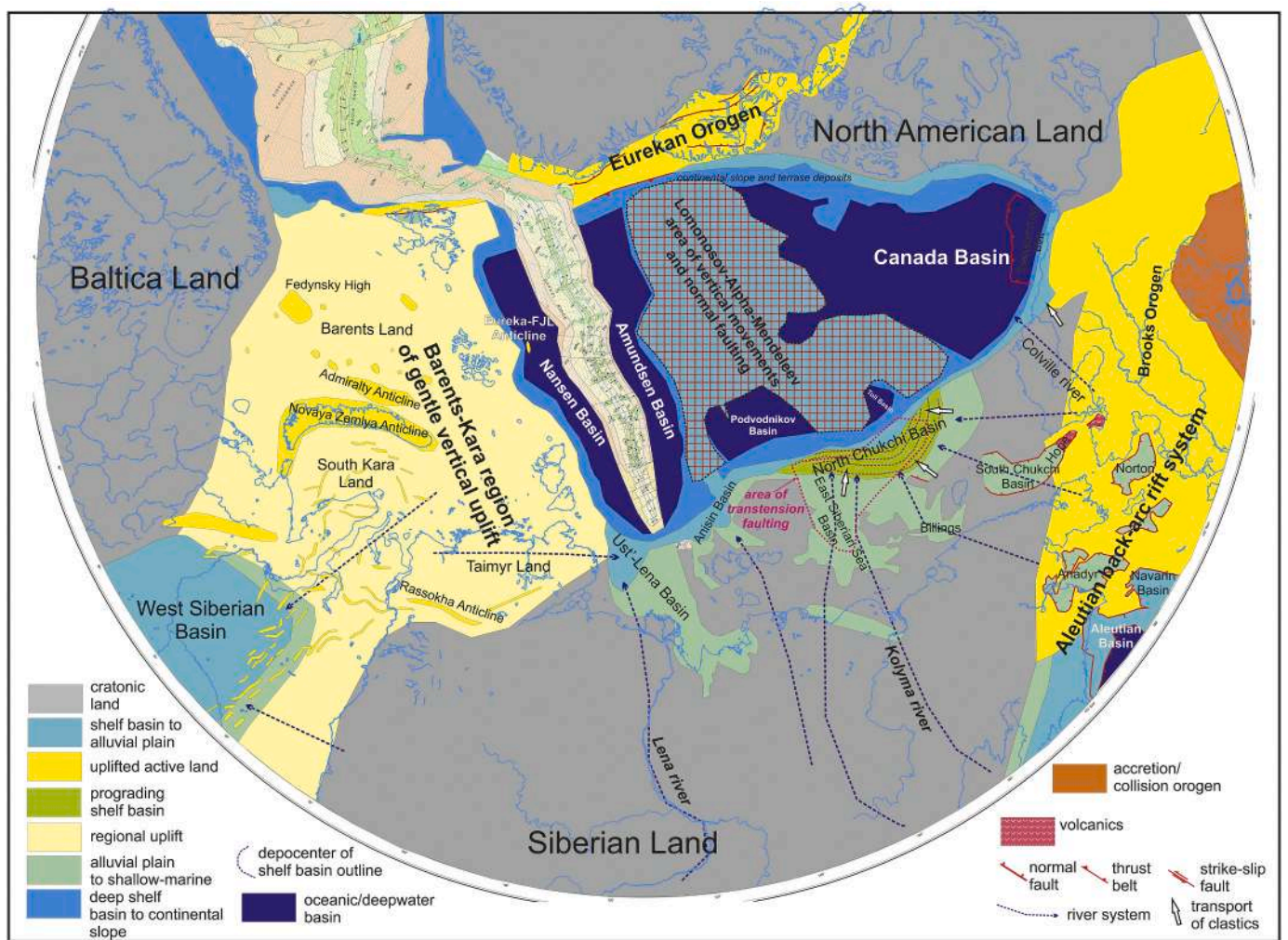


Fig. 14. Paleogeographic map of the Arctic for the Middle-Late Eocene (45–34 Ma) on the present-day geographic framework. Geographic base map is Geological map of the Arctic (Harrison et al., 2011).

deposits are overlain by thin Oligocene strata with an angular unconformity (Petrov, 2012; Viskunova et al., 2004). Data for the Yamal and the South Kara Basin show that starting from the Lutetian time, these areas experienced uplift and erosion. Probable low-angle folding took place before the Oligocene as presumed Oligocene deposits overlie the Paleocene-Eocene deposits with an angular unconformity. However, Oligocene deposits are not penetrated by wells at the present time and no stringent substantiation for this hypothesis is available yet. In West Siberia, a regional pre-Oligocene unconformity is known (Akhmet'ev and Zaporozhets, 2014; Grossgeym and Korobkov, 1975; Volkova, 2014; Volkova et al., 2016; Yakovleva, 2017). Oligocene and Miocene deposits are formed by a single series of mainly continental sedimentary rocks (Grossgeym and Korobkov, 1975; Volkova et al., 2016).

Within the West Siberian, Barents and South Kara basins, many anticlinal folds and anticlinal highs formed after the Cretaceous (Nikishin et al., 2015). In West Siberia, such anticline-like swells have been identified for a long time and they are known to have formed in the Cenozoic (exact time is not known) (Brekhtunsov et al., 2011; Kontorovich et al., 2010; Kontorovich et al., 2016). In the Yenisey-Khatanga Basin, Mesozoic, Paleocene and Early Eocene deposits make part of the stratigraphic section of swells (Afanasenkov et al., 2016; Unger et al., 2017). The last phase of their growth was after the Early Eocene. A large number of anticline-like swells are located in the South Kara Basin. Deposits from Jurassic to Late Cretaceous age make part of the structure

of these folds (Kontorovich et al., 2010; Nikishin et al., 2015; Nikishin, 2013) (Fig. 15). Since in the South Kara Basin, Paleocene and Lower Eocene deposits conformably overlie Cretaceous deposits, we anticipate that deposits up to the Lower Eocene were present in structure of these anticlinal swells. Analysis of seismic profiles shows that an angular unconformity is present in the South Kara Basin. Late Cenozoic sediments overlie Cretaceous and Paleocene-Lower Eocene sediments with an angular unconformity. Although ages of the Late Cenozoic (pre-Quaternary) deposits are not exactly dated, we assume an Oligocene age for this unit. In the Barents Sea, a large number of anticlinal swells are present; in which Upper Cretaceous deposits constitute part of the structure (presence of the Cenomanian is proved (e.g., Mordasova, 2018)). The following known structures belong to them: the Admiralty Swell, Fedynsky High, Shtokman High (e.g., Henriksen et al., 2011b, 2011a; Nikishin et al., 2015; Stoupakova et al., 2011) (Fig. 16). Our reconstructions show that deposits of the entire Upper Cretaceous and, possibly, of the Paleocene-Lower Eocene took part in the formation of these anticlinal highs. In the Barents Sea north of Novaya Zemlya, based on interpretation of commercial seismic lines, Jurassic-Cretaceous deposits are locally overlain by Cenozoic (pre-Quaternary) deposits with an angular unconformity. Although their age is not strictly dated, we assume that these are Oligocene-Neogene deposits. Seismic data interpretation shows that the time of formation of anticlinal highs was determined as between the middle of the Late Cretaceous and the

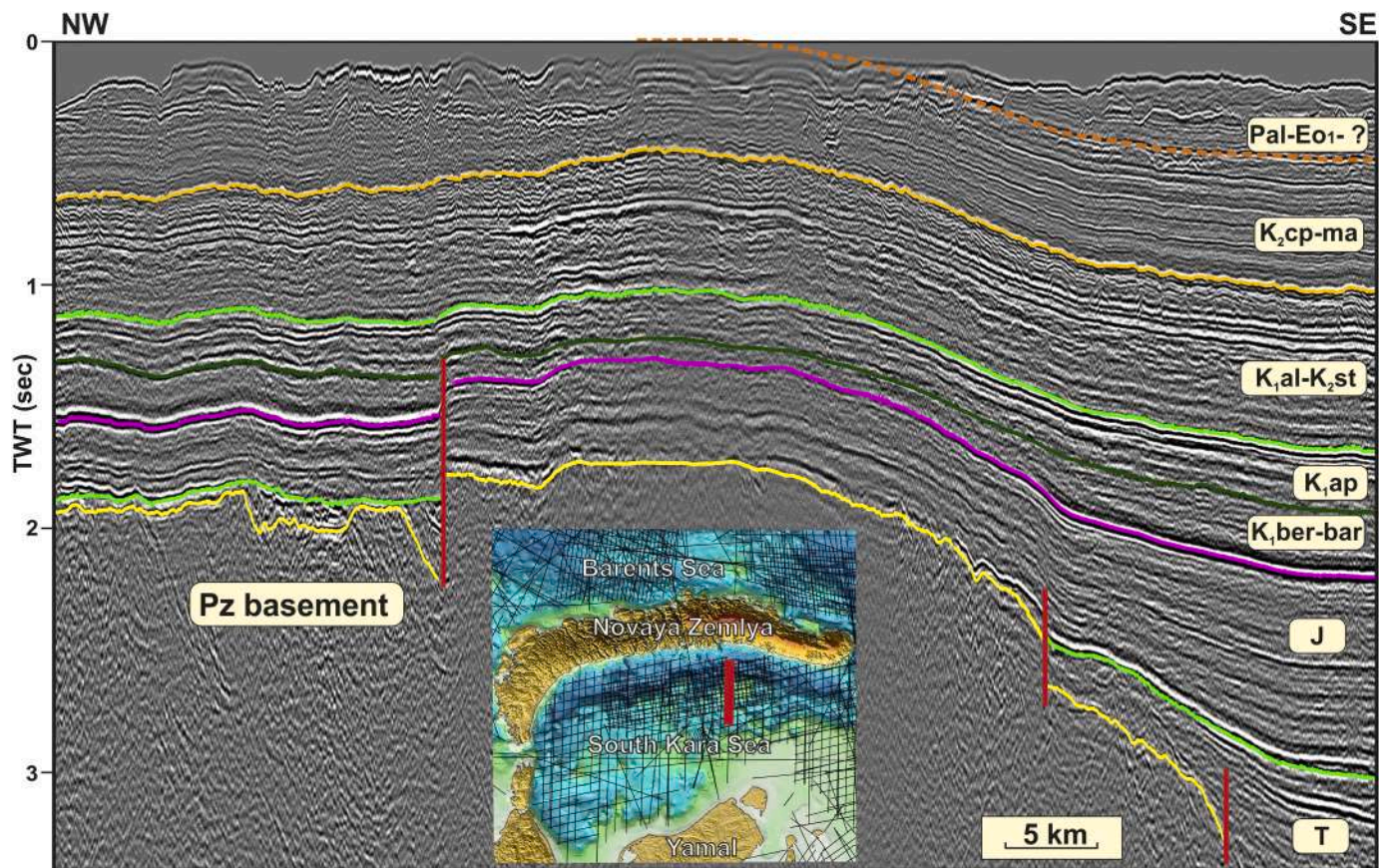


Fig. 15. Interpretation of seismic line for the Universitetskaya Swell, South Kara Basin (Nikishin et al., 2015; Nikishin, 2013, modified). The anticline structure originated after Late Cretaceous time, and possibly after Early Eocene time.

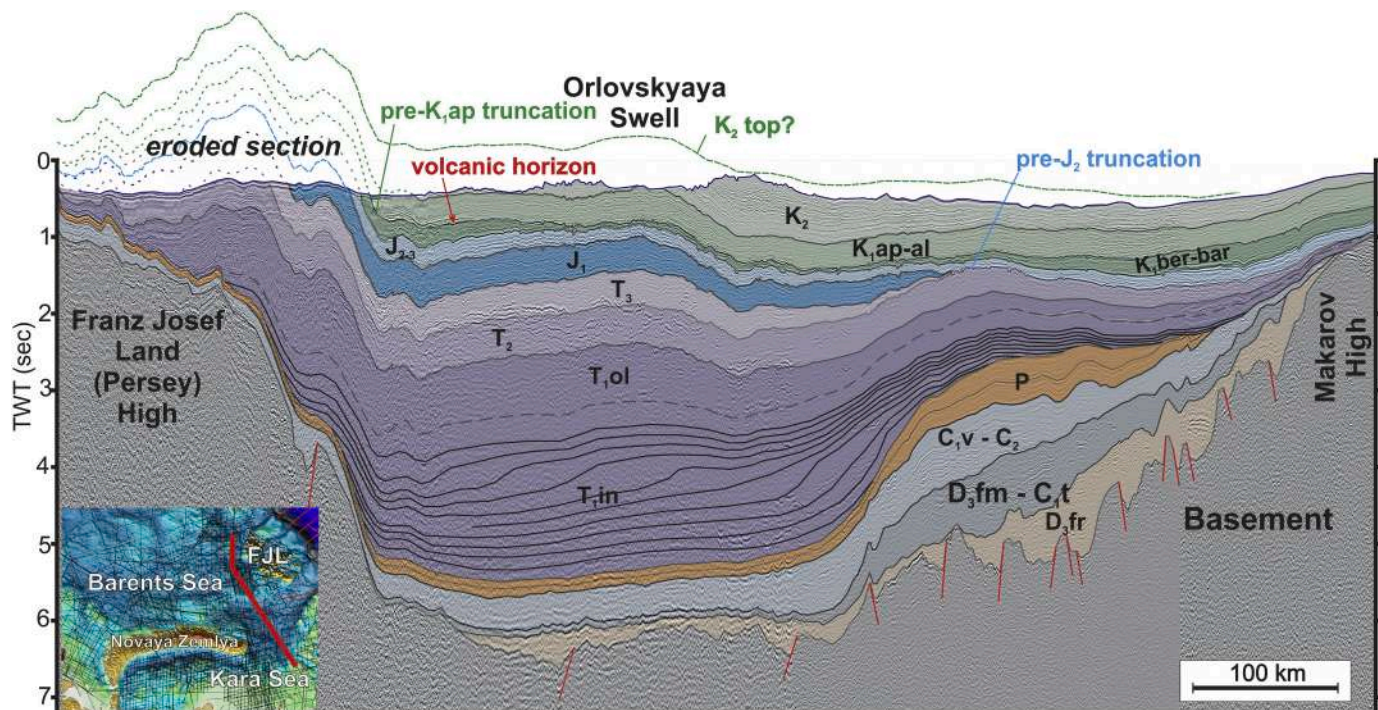


Fig. 16. Interpretation of regional seismic line 4-AR for the East Barents Magabasin. Modified after (Nikishin et al., 2015; Startseva et al., 2017). The anticline structures originated after Late Cretaceous time. Volcanic horizon is observed on a number of seismic lines. This is a prolongation of the Franz Josef Land volcanic province.

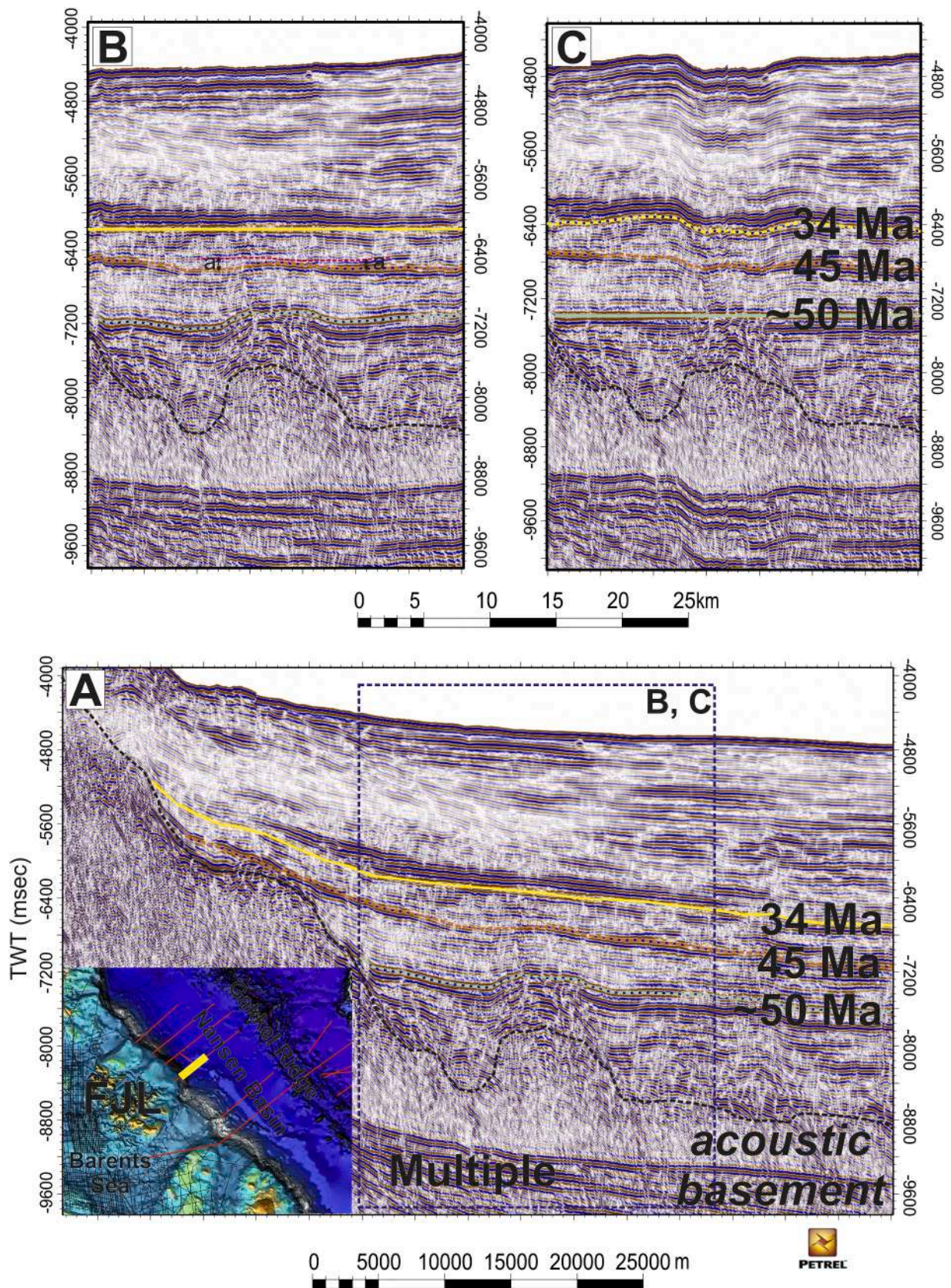


Fig. 17. A. Interpretation of seismic line ARC11-006 for the Amundsen Basin. Based on Nikishin et al. (2018) with additional data. A small anticline of the Eocene time origin can be recognized. B and C. Flattening for horizons 34 Ma and 50 Ma.

Neogene. The available data suggest that the main epoch of anticlinal folds formation was between the Lutetian (Eocene) and the Oligocene. The main argument in favor of our hypothesis is the observation that regional uplift in the north of West Siberia started in the Lutetian. In West Siberia, the Oligocene unconformably overlies Eocene and Paleocene deposits. Our preliminary and unpublished AFT data for Franz Josef Land show that maximum subsidence occurred in the Maastrichtian-Eocene. Regional uplift started from the end of Eocene and took place in the Oligocene-Neogene. AFT data available for the Fersmanovskaya-1 well on the Fersman High, show that uplift started in the Early Paleocene at ca. 60 Ma (Sobolev and Soloviev, 2013). These AFT data do not contradict our hypothesis that the main formation time of anticlinal highs was between the Lutetian and the Oligocene.

We studied seismic profiles for the Nansen Basin (Nikishin et al., 2018). Only seismic line ARC11-006 shows evidence for Cenozoic tectonic compressional deformation. Interpretation of this line demonstrates a small anticline structure originated before the Oligocene. Preliminary seismic stratigraphy based on linear magnetic anomalies points to a timing of anticline growth between 50 Ma and 34 Ma (Fig. 17).

The hypothetical time of formation of anticlines-swells in the vast

area from West Siberia to the Barents and Kara Seas, and Nansen Basin coincides with the epoch of maximum of the period of compression during the Eureka Orogeny.

In the Laptev Sea Basin, Middle-Upper Eocene deposits are known along the Laptev Sea coast and also in the Lower Kolyma Basin (Gertseva et al., 2016; Grinenko, 1989; Grinenko et al., 1997; Shulgina and Bashlavin, 2000). These are thin-thickness continental deposits (the Tenkichen and Parshinsky Horizons) which unconformably overlie underlying Early-Middle Eocene deposits. It is likely that a restructuring of the paleogeography took place at the Laptev Sea coast at circa 45 Ma.

Within the Laptev Sea, Upper Eocene deposits are known on the Belkovsky Island (Kuzmichev et al., 2013). Devonian deposits are overlain by strata of Upper Eocene – Lower Miocene continental deposits, of about 40 m thickness.

For the Laptev Sea Basin, it appears from our seismic data interpretation that continental and shelf sediments accumulated within it. The northern part of the basin is characteristic of clinoforms directed toward the Eurasia Basin. The time interval of 45–34 Ma is characterized by a weak manifestation of normal faults, i.e. a small-scale rifting was taking place, possibly in a transtensional tectonics regime.

Within the North Chukchi Basin and the East Siberian Sea Basin, the

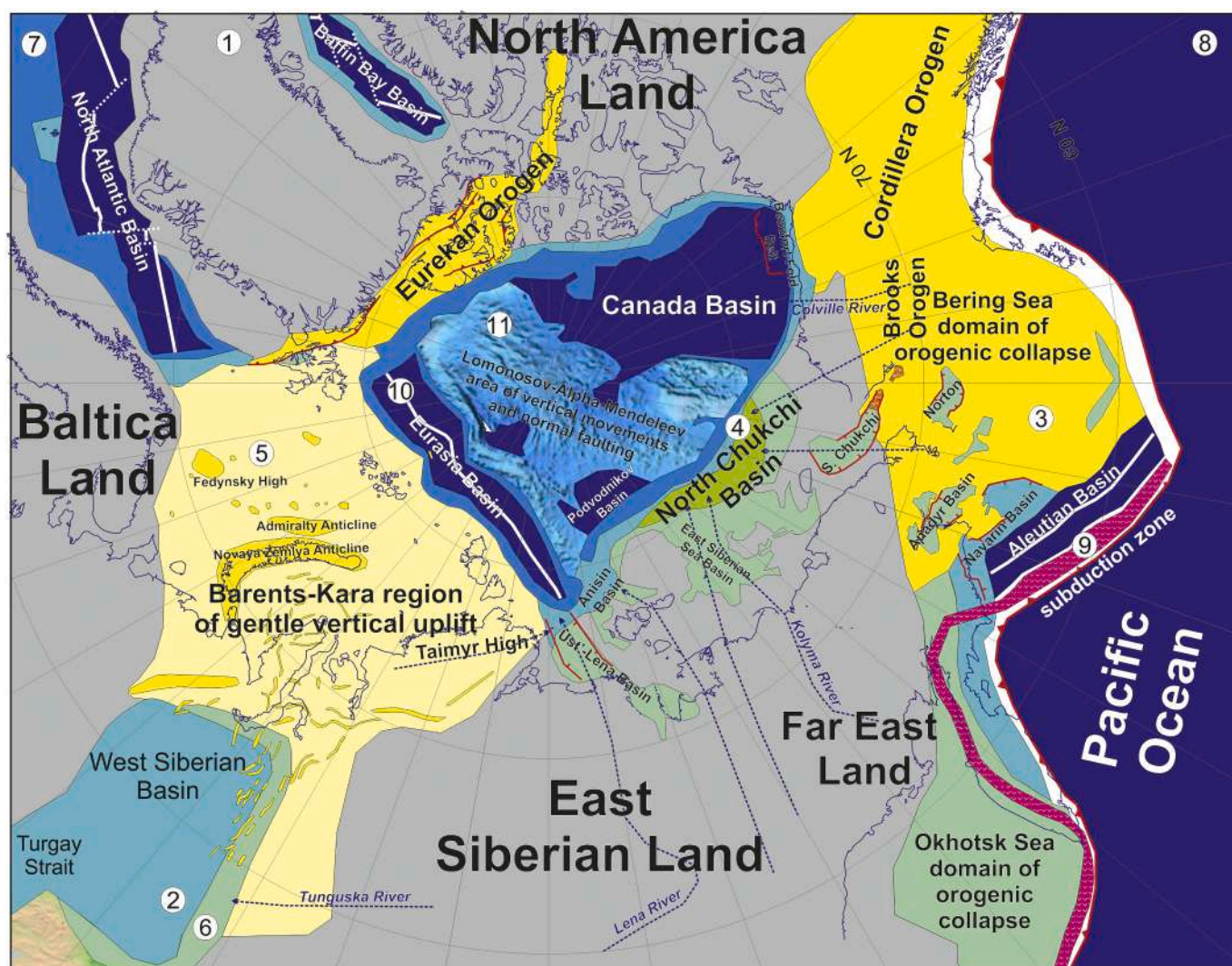


Fig. 18. Tectonic restoration of the Arctic region for the Middle-Late Eocene (45–34 Ma). Kinematic restoration for the 45 Ma. Restoration was performed using GPlates programme. Legend is similar to Fig. 14. 1 – cratonic land, 2 – shelf basin, 3 – uplifted active land, 4 – prograding shelf basin with clinoform sedimentation mainly, 5 – region of gentle vertical uplift, 6 – alluvial plain to shallow-marine, 7 – deep shelf basin to continental slope, 8 – oceanic/deepwater basin, 9 – continental margin volcanic belt, 10 – spreading axis, 11 area of vertical movements and normal faulting (main time of recent bathymetry generation).

main event in the Middle-Late Eocene (45–34 Ma) was formation of the “upper” clinoform complex with strongly pronounced progradation toward the Amerasia Basin (see Paper 2). At approximately 45 Ma, the shelf edge moved landward. As this transgression cannot be explained by eustasy alone, a short-term tectonic event is likely, which resulted in a rapid subsidence of the shelf area. Analysis of seismic data shows that within the North Chukchi Basin and East Siberian Sea Basin a facies transition takes place from continental deposits to shelf deposits and subsequently to deep-water deposits with turbidites.

Within the North Chukchi Basin and East Siberian Sea Basin, a large number of low-amplitude normal faults are identified, with ages of about 45 Ma (see Paper 2). We suppose that they formed during a short-term intensive regional phase of transtensional tectonics.

In the Chukchi Sea in the Ayon well on the Ayon Island, Lutetian and Bartonian deposits (48–38 Ma) are absent. The main hiatus occurs just at this time. Thin Priabonian deposits (38–34 Ma) are represented by

continental sediments (Aleksandrova, 2016).

On the Alaska Shelf, Middle-Upper Eocene deposits are penetrated by the Crackerjack-1 and Popcorn-1 wells (Sherwood et al., 2002). They are represented by sampled continental and shallow-water marine sediments.

The tectonic event at ca. 45 Ma and the onset of accumulating deposits of the “upper” clinoform complex of the North Chukchi Basin corresponds in time to the uplift phase of the Brooks Range in Alaska (~45 Ma) (Craddock et al., 2018; O’Sullivan et al., 1997).

In the South Chukchi Basin, continental sedimentation is inferred for the Middle-Late Eocene based on seismic data interpretation in the South Chukchi Basin. The Hope Basin is situated at the eastern continuation of the South Chukchi Basin. Wells are available within this basin. The Paleozoic basement is overlain by Middle-Upper Eocene strata with volcanites and tuffs. Isotopic ages of 42.3 Ma and 40.7 Ma are known for the volcanites (Sherwood et al., 2002). It is likely that rifting took place

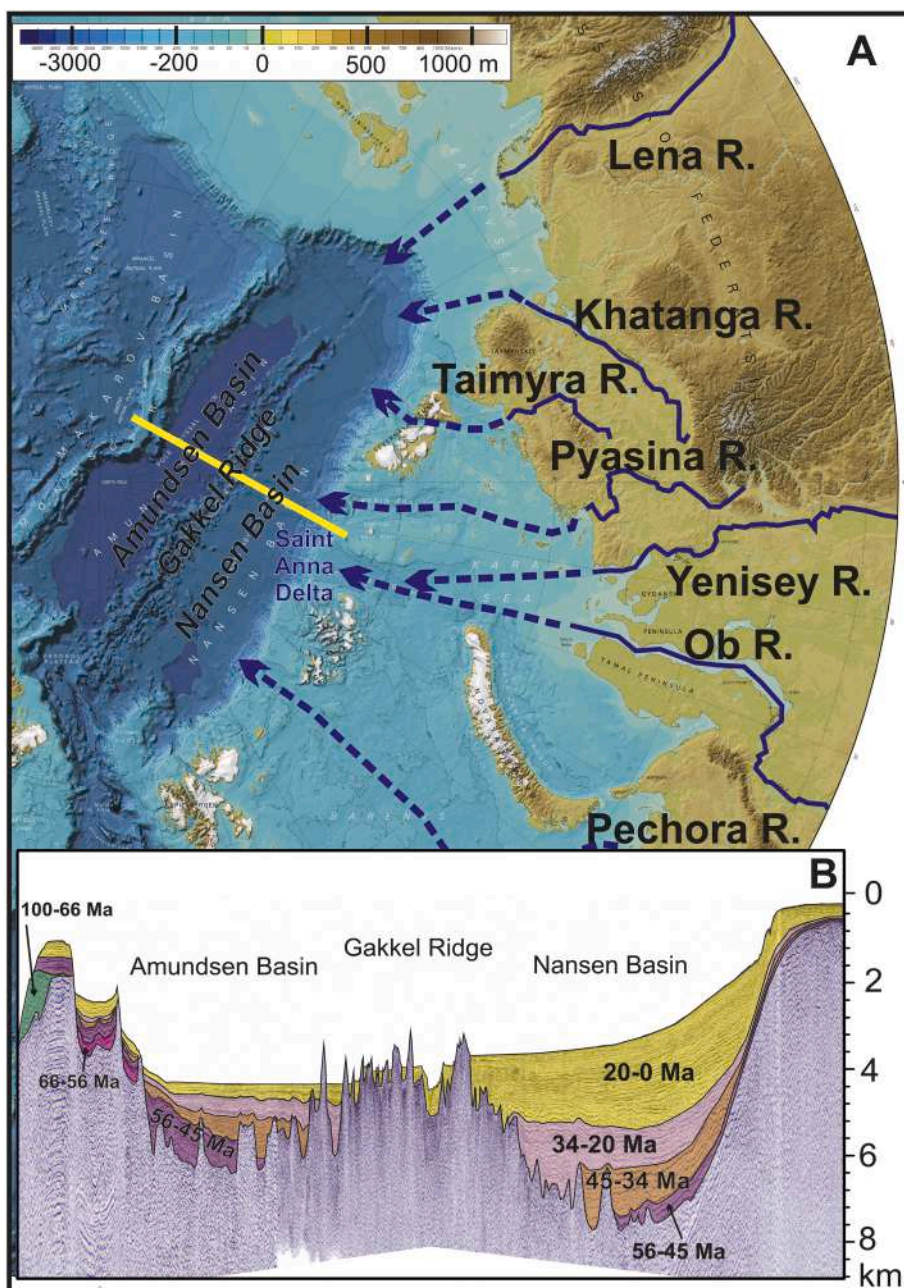


Fig. 19. A. Topographic map of part of Arctic region with proposed river systems for the Neogene to Quaternary time. B. Interpretation of seismic line ARC 14-07 for the Eurasian Basin. Location is yellow line in “A”. Asymmetry of the Eurasian Basin is well observed. Topographic map after Jakobsson et al. (2012). Saint Anna Delta is in our hypothesis partly based on limited seismic data. (For interpretation of the references to colour in this figure legend, the reader is referred to the web version of this article.)

during formation of the basin.

A system of Eocene sedimentary basins is situated within the Bering Sea Shelf and the Russian onshore area of Chukotka and Koryakia. The Anadyr Basin and Norton Basin belong to them (Kharakhinov et al., 2014; Klemperer et al., 2002; Nikishin et al., 2015). The Eocene Khatyrka and Navarin Basins are a part of the passive continental margin of the Aleutian Basin (Kharakhinov et al., 2014; Nikishin et al., 2015). Basic information concerning these basins, with wells and seismic lines, is presented in Kharakhinov et al. (2014). All these basins are characteristic of the lower rift complex represented by the Mainitsky stratigraphic horizon of Lutetian-Oligocene age. This is a synrift complex with prevalence of continental deposits. Rifting in these basins was probably synchronous with rifting in the Hope Basin. Rifting in the Khatyrka and Navarin Basins in the Late Eocene or Oligocene probably transited into opening of the back-arc Aleutian Basin with an oceanic crust.

Low-amplitude normal faults formed in Amerasia Basin on the Alpha-Mendelev and Lomonosov ridges in the Middle-Late Eocene (see Paper 2).

We compiled a kinematic reconstruction of the Arctic for the Middle-Upper Eocene (~45 Ma), presented in Fig. 18.

During this time, the following major tectonic events took place: (1) The Gakkell Ridge became an ultraslow spreading center after 45 Ma. (2) The maximum of the Eurekan Orogeny took place in the north of Greenland and the Canadian Arctic Archipelago Islands. (3) The vast area of the Barents and Kara seas and the north of West Siberia experienced syncompressional uplift and numerous anticline-like swells formed. (4) Within the Amerasia Basin on the Alpha-Mendelev and Lomonosov ridges and the Chukchi Plateau, low-amplitude faults were formed in extensional and transtensional environments together with differential vertical movements. (5) At circa 45 Ma, within the sedimentary basins of the Chukchi, East Siberian and Laptev seas, a restructuring of paleogeography occurred with vertical movements and formation of low-amplitude normal faults. (6) A continental rifting phase took place in the areas of the Chukchi and Bering Seas (e.g. Hope Basin and Anadyr Basin). It started with collapse of the orogen in the area from the Sea of Okhotsk and Kamchatka to the Bering Sea.

3.10. Oligocene-Neogene history of the Arctic (34–2.6 Ma)

The Oligocene-Neogene history of the Arctic is relatively well known and this topic is beyond the scope of the present paper. Here we will note three principal points. (1) Oligocene-Quaternary sediments are thicker in the Nansen Basin than in the Amundsen Basin (Fig. 19). A thick series of Neogene-Quaternary sediments is present in the Nansen Basin (see Paper 2). We suppose that at that time the main rivers of Siberia of the type of the Ob, Yenisey, etc. together with paleo-ice streams flowed into the Nansen Basin and formed numerous deltaic systems. We identify a major Saint Anna Delta. (2) Activation of several normal faults on slopes of Lomonosov and Alpha-Mendelev ridges continued (see Paper 2). (3) Within the East Siberian and Chukchi Seas, many faults and transpression zones were active post-34 Ma (Ikhsanov, 2014; Nikishin et al., 2015). Analysis of seismic profiles showed that there are many more of such zones than previously thought.

4. Discussion

In this study, we present new data together with a synthesis of published data on the geology of the Arctic. These data allow to resolve the history of the Arctic Ocean. Here we present several new concepts and approaches.

The new models presented in this study show that it is difficult to use the classical “rotational” model to explain the opening of Amerasia Basin with the main transform along the Lomonosov Ridge (e.g., Grantz et al., 2011b, 2011a). There are two groups of principal arguments against this model. (1) The Alpha-Mendelev ridges have continental (pre-Ordovician) basement and the Paleozoic cover was preserved within it. It

follows from this that in the course of opening of Canada Basin; the main transform boundary might run along the edge of these ridges rather than along that of the Lomonosov Ridge. (2) Preliminary data from interpretation of seismic lines show that in the area of the Alpha-Mendelev ridges and of contiguous basins of the type of Podvodnikov and Toll Basins, the main strike of structures is perpendicular relative to the strike of the spreading axis in Canada Basin. A similar conclusion was suggested in Hegewald and Jokat (2013).

The opening of Canada Basin, according to our model, had no geometrical relation with closure of the South Anyui Ocean (Orogen) as usually assumed in many recent studies (e.g., Grantz et al., 2011b, 2011a). The Verkhoyansk-Chukotka Orogen which includes the South Anyui Suture was a continental-marginal orogen of the “Cordillera” type. In the course of its formation, terranes were moving toward Asia and the Arctic accompanied by formation of oroclines. Synchronously with the Verkhoyansk-Chukotka and Mongol-Okhotsk orogenies, inversion tectonics with growth of numerous anticlinal highs manifested itself in the vast area of the Barents, South Kara, West Siberian and Yenisey-Khatanga Basins.

We consider the Alpha-Mendelev ridges as a volcanic edifice on a continental crust. Around this ridge, as a minimum five volcanic plateaus are identified: Sverdrup on the Canadian Islands, Svalbard and Franz Josef Land in the north of the Barents Sea, De Long in the north of the East Siberian Sea, and the proposed North Chukchi Plateau north of the Wrangel Island. Magmatism in these areas started at about ± 125 Ma. Near the same time, magmatism started on the Alpha-Mendelev ridges as well. Synchronously with the start of magmatism or somewhat later, large-scale continental rifting started in the North Chukchi Basin, in the Laptev Sea Basin, in the North Atlantic, and in the Baffin Bay. In the course of formation of the North Chukchi rift basin, strike-slip tectonics widely manifested itself. Magmatism within the Alpha-Mendelev Ridge was completed at ca. 80 Ma. We assume that the Alpha-Mendelev ridges started to form as a rift system with wide-scale magmatism, but rifting had not transited into oceanic crust spreading. We propose to classify the Alpha-Mendelev ridges as an aborted volcanic passive continental margin. Foulger et al. (2019) proposed a new geodynamic model for the Greenland-Iceland-Faroe Ridge. We propose that the early stage of the history of the Greenland-Iceland-Faroe Ridge represents a possible geodynamic model for the Alpha-Mendelev ridges.

Approximately at the Cretaceous/Paleocene boundary and in the Paleocene, formation of the major continental-marginal orogen was going on in the strip from the Sea of Okhotsk and West Kamchatka to Koryakia and the Brooks Orogen. Filling-up of the North Chukchi Basin with the thick sedimentary cover with cliniform structure was connected with this event. At that time, thrust belts were actively forming in the Chukchi Sea and on Alaska. Approximately simultaneously, continental rifting was underway in the Ust'-Lena Basin of the Laptev Sea and along the future Eurasia Basin.

At the Paleocene/Eocene boundary, plume basaltic magmatism widely manifested itself in the area of the North Atlantic, which was followed by opening of the North Atlantic Ocean and prevalence of volcanic continental margins (e.g., Torsvik et al., 2002; Ziegler, 1988). We have revealed two possible igneous provinces in the north of the Laptev Sea. The formation of these two provinces probably preceded opening of the Eurasia Basin. In this case, we observe similarity in the geodynamics of opening of the North Atlantic and Eurasia oceanic basins. Anomalies in the upper mantle in the eastern part of the Eurasia Basin (approximately at the place where we identify igneous provinces) on the whole resemble anomalies in the North Atlantic according to new seismic tomography data (Lebedev et al., 2018). This is an additional argument in favor of our hypothesis concerning new igneous provinces in the east of the Eurasia Basin.

At circa 45 Ma, a very interesting superregional complex tectonic event occurred; the chronology of which is uncertain: 1) the Gakkell Ridge started to experience ultraslow spreading (e.g., Glebovsky et al., 2006); 2) the maximum collision in the Eurekan Orogen started (e.g.,

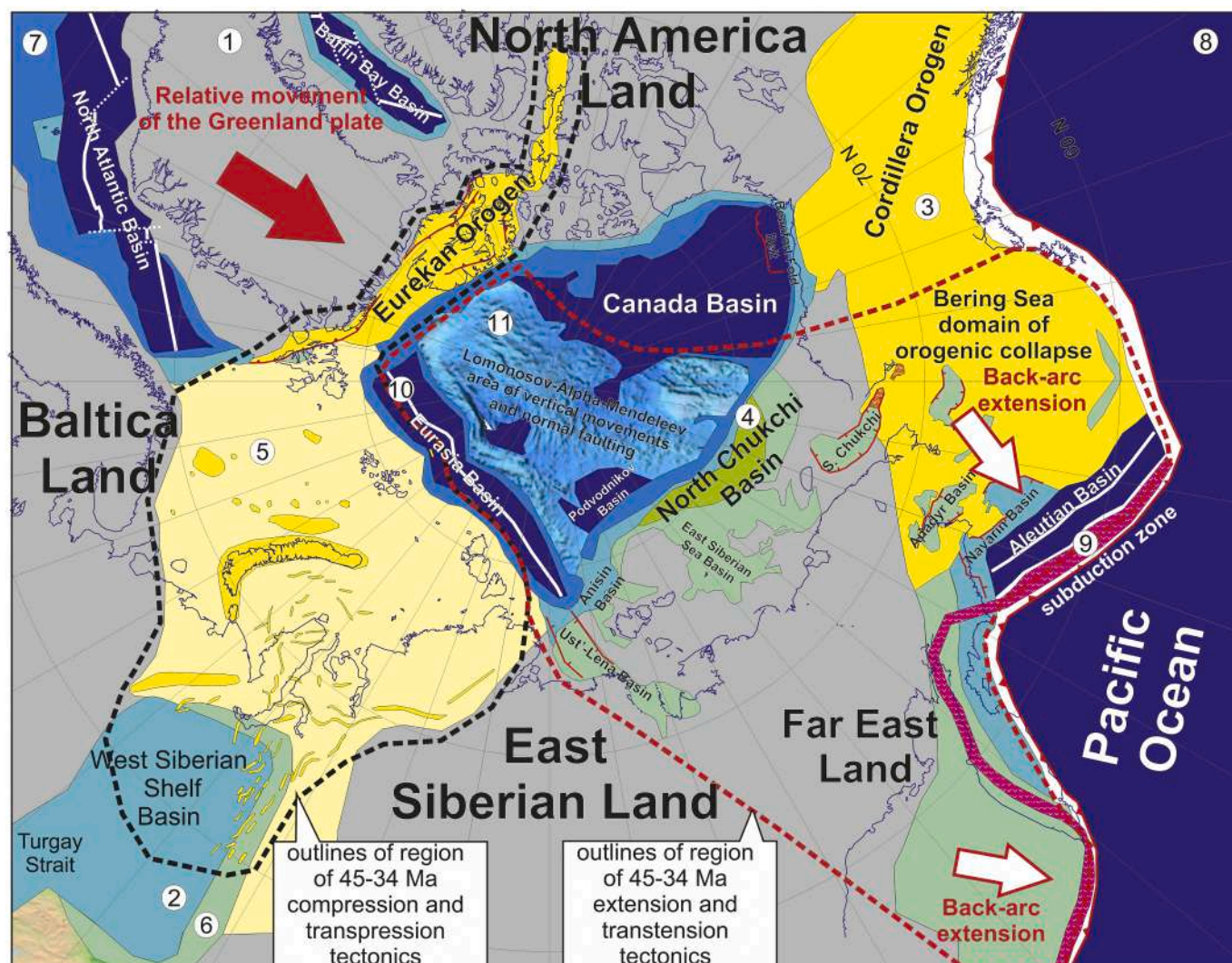


Fig. 20. Two superdomains of the 45–34 Ma regional intraplate tectonics in the Arctic region (see Fig. 18 for the legend). Relative movement of the Greenland plate led to Eurekan Orogeny and intensive compression/transpression intraplate tectonics in the Barents-Kara-West Siberia region. Gakkel Ridge, Alpha-Mendelev Ridge, and Chukchi-Bering-Okhotsk seas region underwent extension and transtension intraplate tectonics as a back-arc region for the Pacific subduction system.

Gaina et al., 2015). In the North Chukchi Basin, after a short-term tectonic event, the shelf edge sharply moved southward by 200–300 km; 3) in the area of the North Chukchi Basin, formation of low-amplitude normal faults in a possible transtensional environment widely manifested itself; 4) in the area of the Chukchi and Bering Seas, continental rifting widely manifested itself; 5) in the area of the Lomonosov and Alpha-Mendelev ridges, numerous normal faults reactivated in extension and transtensional environments. At that time, a paleogeographic restructuring with regional uplifting took place in the vast area of the Barents-Kara Seas and West Siberia. In the course of this process, growth of numerous intraplate anticlinal highs started in compressional or transpressional environments. On the whole, we see that the tectonic regime on either side of the Eurasia Basin was quite different. In the Barents-Kara region, compression prevailed, while in the area of the Amerasia Basin and the shelves of Siberia, extension prevailed. The simplest explanation comes down to the idea that the collision of the Greenland and Eurasian lithosphere plates in the area of Spitsbergen resulted in compression of the Barents-Kara region. This collision did not propagate to the area of the Amerasia Basin and its Russian-Alaskan shelf. The Amerasia-Chukotka-Bering superdomain had a possibility to stretch out toward the Pacific Ocean in a regional “back-arc” environment (Fig. 20). This issue obviously deserves further special analysis.

We do not know well the structure of the continental basement of the Arctic region. In accordance with the model presented in Fig. 1, the Eurasia Basin had opened along a possible Caledonian suture. The Caledonian suture was widely utilized for formation of strike-slip faults in the course of formation of the North Chukchi Basin. The Canada Basin probably formed along fabrics of the former Ellesmere Orogen.

The Arctic Ocean was always in the polar regions during the entire Cretaceous and Cenozoic time (e.g., Shephard et al., 2013). Sedimentation in polar regions is strongly dependent on paleoclimate. Therefore, study of the sedimentary cover will help us restore the history of global climate (e.g., Stein, 2008). Different types of sediments have different velocity characteristics on seismic sections. In the section of the Arctic Ocean, we observe as a minimum two sequences on seismic profiles with regionally developed bright reflection: HARS in the upper part of the section (Nikishin et al., 2015; Weigelt et al., 2014) and HARS-2 in the lower part of the section (see Paper 2). In accordance with our stratigraphic model, the HARS sequence corresponds to an age of 56–45 Ma and siliceous deposits, which are known for the ACEX boreholes, are present in its section. The epoch of 56–45 Ma is characteristic for several intervals of time with significant climate warming (Cramer et al., 2009; Gradstein et al., 2012; Stein, 2008).

The HARS-2, in accordance with our seismic stratigraphy model, has

an age of about 80–100 Ma. This period also corresponds to a time of global warming (e.g., O'Brien et al., 2017). It is probable that in the Arctic, rocks of this stratigraphic level have a special lithology. For example, siliceous deposits may be present. Deposits of the HARS and HARS-2 can be considered as regional source rocks in analysis of hydrocarbon systems of the Arctic. This is proven for deposits of the HARS (Mann et al., 2009).

According to our model for the paleogeographical history of the Arctic, significant changes in paleogeography happened at circa 45 Ma (see Fig. 18). The main event was connected with sub-aerial exposure of the shelves of the Barents and Kara Seas and the north of West Siberia. This event resulted in abrupt cooling in the Arctic and cessation of siliceous sediment production (e.g., Stein, 2008; Stein et al., 2015).

5. Conclusions

An atlas of paleogeographic and paleotectonic maps showing main events in the history of the Arctic during the period of 0–157 Ma is presented in this paper. The following main conclusions obtained by us are:

1. There are Timanides, Caledonides, Ellesmerides, and Uralides-Taimyrides terranes within continental basement rocks underlying the greater Arctic Basin.
2. The Mendeleev Ridge has a possible continental pre-Ordovician basement.
3. The classical rotational model for opening of the Amerasia Basin with the main transform fault along the Lomonosov Ridge likely can be revised. The data suggesting that the Mendeleev (or Alpha-Mendeleev) Ridge possibly has a continental basement contradicts this model. Additional investigations are needed to resolve this question.
4. The following chronology of events in the history of the Arctic Ocean is proposed since Kimmeridgian: (1) Kimmeridgian-Tithonian (157–145 Ma): continental rifting occurred in the area of the Sverdrup-Banks basins and in the area of the present-day Canada Basin; a system of continental-margin volcanic belts was formed in the area of Chukotka and the Verkhoyansk-Omolon area; closure of the hypothetical South Anyui Ocean was not associated with opening of Canada Basin; (2) Berriasian-Barremian (145–125 Ma): formation of the Verkhoyansk-Chukotka continental-margin orogen with the South Anyui and Kolyma oroclinal; fast opening of Canada Basin (~133–125 Ma); intraplate compressional and transpressional tectonics in the basins of the Barents and South Kara Seas and in the north of West Siberia; (3) Aptian-Albian (125–100 Ma): formation of continental igneous provinces (for the Aptian, five areas of basaltic magmatism are identified on the shelf: Franz Josef Land, Svalbard, Sverdrup, De Long and North Chukchi areas); rifting and magmatism in the area formed the Alpha-Mendeleev ridges; rifting in the Ust'-Lena, Anisin, North-Chukchi, Podvodnikov and Toll Basins; synchronous rifting in the North Atlantic and in Baffin Bay; (4) Cenomanian-Campanian (100–80 Ma): intraplate magmatism in the area of the Alpha-Mendeleev ridges; basaltic magmatism in the north of North America; (5) Campanian-Maastrichtian (80–66 Ma): a likely start of compressional deformations in the area of the Chukchi Sea; a likely start of transtensional tectonics in the area of the Makarov and Ust'-Lena Basins; (6) Paleocene (66–56 Ma): in the wide strip from the Sea of Okhotsk to Koryakia and Alaska, formation of a continental-margin orogen; continental rifting took place along the present-day Eurasia Basin and the Ust'-Lena Basin; the Makarov Basin was likely formed as a pull-apart basin; (7) Early-Middle Eocene (56–45 Ma): after the epoch of plume magmatism, opening of the North Atlantic Ocean and of the Eurasia Basin started; a continental-margin orogen was formed along the Pacific margin of Asia and North America; the Eureka Orogen was actively developed; (8) Middle-Late Eocene (45–34 Ma): at about 45 Ma, a major restructuring of the Arctic's paleogeography and paleotectonics took place with subaerial emergence of the Barents and Kara Sea shelves, onset of ultra-slow spreading at Gakkel Ridge, formation of normal and strike-slip faults on Lomonosov and Alpha-Mendeleev ridges and on the Chukchi Sea and East Siberian Sea shelves; collapse of orogens in the Bering and Okhotsk seas; maximum compression in the Eureka Orogen; (9) Oligocene-Neogene (34–2.6 Ma): formation of the Eurasia Basin continued; activation of normal faults in the Amundsen Basin and on the Lomonosov, Alpha-Mendeleev ridges.
5. We assume that the Alpha-Mendeleev ridges started to form as a rift system with wide-scale magmatism, though rifting had not progressed into oceanic crust spreading. These processes were connected with possible HALIP mantle plume. We propose to classify the Alpha-Mendeleev ridges as an aborted volcanic passive continental margin.
6. The ~45 Ma event in the Arctic is a unique short-duration event in the history of the Earth: the ultra-slow spreading of the Gakkel Ridge started and approximately synchronously therewith, a major part of the lithospheric plate experienced intraplate compression and transpression, while another part of the lithospheric plate, probably synchronously, experienced intraplate tension and transtension. This short-duration tectonic event resulted in a considerable restructuring of paleogeography and climate.
7. Analysis of seismic stratigraphy of the Arctic suggests that the intervals of 100–80 Ma and 56–45 Ma are characteristic for the formation of sediments with some specific lithology. These sediments are possibly presented not by clay but, for instance, characterized by deposition of siliceous sediments. We assume that a climatic warming took place in the Arctic at these times. These periods coincide with global intervals of a relatively hot climate.

Declaration of Competing Interest

Reviewer-3 disagrees with our model of the Arctic history. Reviewer-3 believes to the classical rotation model, it is very difficult to discuss with him any alternative tectonic scenarios.

He sent a political paper to editors with the title: "Worrisome Political Overtones of the Nikishin et al papers". We do not want political discussions in the scientific journal.

We have no any other conflicts of interest.

Acknowledgements

The authors are thankful to Ministry of Natural Resources and Ecology of Russia for the possibility to publish this paper. Discussions with C. Gaina, E. Miller, V. Pease, W. Jokat, J.I. Faleide, S. Drachev, R. Stephenson, D. Franke, A. Escalona, I. Norton, N. Lebedeva-Ivanova, E. Lundin, A. Doré, E. Weigelt stimulated our work. We are grateful to many Russian geologists from different scientific organizations with which we conducted numerous discussions: L.I. Lobkowsky, V.A. Vernikovskiy, S.D. Sokolov, A.K. Khudoley, A.V. Prokopiev, O.V. Petrov, E. V. Shipilov, A.V. Stoupakova, E.A. Gusev, V.A. Poselov, S.N. Kashubin, G.N. Aleksandrova, A.S. Alekseev, V.B. Ershova, A.B. Herman, and others. In the course of studying the Arctic, we had the possibility to conduct scientific discussions with geologists from different companies: Rosneft, ExxonMobil, Statoil, Total, BP, Gazprom Neft, Gazprom. We thank our colleagues E.A. Bulgakova, M.S. Doronina, L.N. Kleschina, V. A. Nikishin, A.B. Popova, M.V. Skaryatin, M.A. Baklan and M.A. Rogov for important contribution in preparation our paleogeographic maps. The work of AMN, SIF, KFS and NNZ was supported by RFBR grants (18-05-70011 and 18-05-00495). We thank François Roure, David Mosher and an anonymous reviewer for generous, detailed, and constructive criticism.

References

- Abdelmalak, M.M., Meyer, R., Planke, S., Faleide, J.I., Gernigon, L., Frieling, J., Sluijs, A., Reichart, G.-J., Zastrozhnov, D., Theissen-Krah, S., Said, A., Myklebust, R., 2016. Pre-breakup magmatism on the Vøring Margin: Insight from new sub-basalt imaging and results from Ocean Drilling Program Hole 642E. *Tectonophysics* 675, 258–274. <https://doi.org/10.1016/j.tecto.2016.02.037>.
- Afanasenkov, A.P., Nikishin, A.M., Unger, A.V., Bordunov, S.I., Lugovaya, O.V., Chikishev, A.A., Yakovishina, E.V., 2016. The tectonics and stages of the geological history of the Yenisei–Khatanga Basin and the conjugate Taimyr Orogen. *Geotectonics* 50, 161–178. <https://doi.org/10.1134/S0016852116020023>.
- Akhmet'ev, M.A., Zaporozhets, N.I., 2014. Paleogene events in Central Eurasia: their role in the flora and vegetation cover evolution, migration of phytochore boundaries, and climate changes. *Stratigr. Geol. Correl.* 22, 312–335. <https://doi.org/10.1134/S0869593814030022>.
- Akhmet'ev, M.A., Zaporozhets, N.I., Yakovleva, A.I., Aleksandrova, G.N., Beniamovsky, V.N., Oreshkina, T.V., Gnididenkov, Z.N., Dolya, Z.A., 2010. Comparative analysis of marine paleogene sections and biota from West Siberia and the Arctic Region. *Stratigr. Geol. Correl.* 18, 635–659. <https://doi.org/10.1134/S0869593810060043>.
- Akinin, V.V., 2012. Late Mesozoic and Cenozoic Magmatism and Lower Crust Modifications in the Northern Framing of Pacific. IGEM RAS, Moscow.
- Akinin, V.V., Gottlieb, E.S., Miller, E.L., Polzunenkov, G.O., Stolbov, N.M., Sobolev, N.N., 2015. Age and composition of basement beneath the De Long archipelago, Arctic Russia, based on zircon U–Pb geochronology and O–Hf isotopic systematics from crustal xenoliths in basalts of Zhokhov Island. *arXiv* 1, 9. <https://doi.org/10.1007/s41063-015-0016-6>.
- Aleksandrova, G.N., 2016. Geological evolution of Chauna Depression (North-Eastern Russia) during Paleogene and Neogene. 1. Paleogene. (in Russian). *Bull. Moscow Soc. Nat. Geol. Ser.* 91, 148–164 (in Russian).
- Alvey, A., Gaina, C., Kuszmir, N.J., Torsvik, T.H., 2008. Integrated crustal thickness mapping and plate reconstructions for the high Arctic. *Earth Planet. Sci. Lett.* 274, 310–321. <https://doi.org/10.1016/j.epsl.2008.07.036>.
- Amato, J.M., Toro, J., Akinin, V.V., Hampton, B.A., Salmikov, A.S., Tuchkova, M.I., 2015. Tectonic evolution of the Mesozoic south Anya suture zone, eastern Russia: a critical component of paleogeographic reconstructions of the Arctic region. *Geosphere* 11, 1530–1564. <https://doi.org/10.1130/GES01165.1>.
- Backman, J., Moran, K., 2009. Expanding the Cenozoic paleoceanographic record in the Central Arctic Ocean: IODP Expedition 302 Synthesis. *Open Geosci.* 1 <https://doi.org/10.2478/v10085-009-0015-6>.
- Backman, J., Jakobsson, M., Frank, M., Sangiorgi, F., Brinkhuis, H., Stickley, C., O'Regan, M., Lovlie, R., Pälke, H., Spofford, D., Gattacecca, J., Moran, K., King, J., Heil, C., 2008. Age model and core-seismic integration for the Cenozoic Arctic Coring Expedition sediments from the Lomonosov Ridge. *Paleoceanography* 23. <https://doi.org/10.1029/2007PA001476> n/a–n/a.
- Bénard, F., Callot, J.-P., Vially, R., Schmitz, J., Roest, W., Patriat, M., Loubrieu, B., 2010. The Kerguelen plateau: Records from a long-living/composite microcontinent. *Mar. Pet. Geol.* 27, 633–649. <https://doi.org/10.1016/j.marpetgeo.2009.08.011>.
- Blaich, O.A., Tsigalas, F., Faleide, J.I., 2017. New insights into the tectono-stratigraphic evolution of the southern Stappen High and its transition to Bjørnøya Basin, SW Barents Sea. *Mar. Pet. Geol.* 85, 89–105. <https://doi.org/10.1016/j.marpetgeo.2017.04.015>.
- Borissova, I., Coffin, M.F., Charvis, P., Operto, S., 2003. Structure and development of a microcontinent: Elan Bank in the southern Indian Ocean. *Geochem. Geophys. Geosyst.* 4 n/a–n/a. [doi:10.1029/2003GC000535](https://doi.org/10.1029/2003GC000535).
- Borodkin, V.N., Kurchikov, A.R., 2010. Materials for refining the stratigraphic chart of the Berriasian–lower Aptian in West Siberia with regard to the clinoforn subsurface structure. *Russ. Geol. Geophys.* 51, 1267–1274. <https://doi.org/10.1016/j.rgg.2010.11.001>.
- Brekhtunsov, A.M., Monasteyrev, B.V., Nesterov, I.I., 2011. Distribution patterns of oil and gas accumulations in West Siberia. *Russ. Geol. Geophys.* 52, 781–791. <https://doi.org/10.1016/j.rgg.2011.07.004>.
- Brinkhuis, H., Schouten, S., Collinson, M.E., Sluijs, A., Damsté, J.S.S., Dickens, G.R., Huber, M., Cronin, T.M., Onodera, J., Takahashi, K., Bujak, J.P., Stein, R., van der Burgh, J., Eldrett, J.S., Harding, I.C., Lotter, A.F., Sangiorgi, F., Cittert, H. van K., de Leeuw, J.W., Matthiessen, J., Backman, J., Moran, K., 2006. Episodic fresh surface waters in the Eocene Arctic Ocean. *Nature* 441, 606–609. <https://doi.org/10.1038/nature04692>.
- Brumley, K., 2014. *Geologic History of the Chukchi Borderland*. Arctic Ocean. Stanford University.
- Brumley, K., Miller, E.L., Konstantinou, A., Grove, M., Meisling, K.E., Mayer, L.A., 2015. First bedrock samples dredged from submarine outcrops in the Chukchi Borderland, Arctic Ocean. *Geosphere* 11, 76–92. <https://doi.org/10.1130/GES01044.1>.
- Bruvold, V., Kristoffersen, Y., Coakley, B.J., Hopper, J.R., 2010. Hemipelagic deposits on the Mendeleev and northwestern Alpha submarine Ridges in the Arctic Ocean: acoustic stratigraphy, depositional environment and an inter-ridge correlation calibrated by the ACEX results. *Mar. Geophys. Res.* 31, 149–171. <https://doi.org/10.1007/s11001-010-9094-9>.
- Bruvold, V., Kristoffersen, Y., Coakley, B.J., Hopper, J.R., Planke, S., Kandilarov, A., 2012. The nature of the acoustic basement on Mendeleev and northwestern Alpha ridges, Arctic Ocean. *Tectonophysics* 514–517, 123–145. <https://doi.org/10.1016/j.tecto.2011.10.015>.
- Buchan, K.L., Ernst, R.E., 2018. A giant circumferential dyke swarm associated with the High Arctic large Igneous Province (HALIP). *Gondwana Res.* 58, 39–57. <https://doi.org/10.1016/j.gr.2018.02.006>.
- Chernova, A.I., Metelkin, D.V., Matushkin, N.Y., Vernikovskiy, V.A., Travin, A.V., 2017. Geology and paleomagnetism of Jeannette Island (De Long Archipelago, Eastern Arctic). *Russ. Geol. Geophys.* 58, 1001–1017. <https://doi.org/10.1016/j.rgg.2017.08.001>.
- Chian, D., Lebedeva-Ivanova, N., 2015. Atlas of Sonobuoy Velocity Analyses in Canada Basin. <https://doi.org/10.4095/295857>.
- Chian, D., Jackson, H.R., Hutchinson, D.R., Shimeld, J.W., Oakey, G.N., Lebedeva-Ivanova, N., Li, Q., Saltus, R.W., Mosher, D.C., 2016. Distribution of crustal types in Canada Basin, Arctic Ocean. *Tectonophysics* 691, 8–30. <https://doi.org/10.1016/j.tecto.2016.01.038>.
- Clerc, C., Ringenbach, J.-C., Jolivet, L., Ballard, J.-F., 2018. Rifted margins: Ductile deformation, boudinage, continentward-dipping normal faults and the role of the weak lower crust. *Gondwana Res.* 53, 20–40. <https://doi.org/10.1016/j.gr.2017.04.030>.
- Coakley, B., Ilhan, I., 2012. Developing Geophysical Constraints on the History of the Amerasian Basin of the Arctic Ocean. In: OTC Arctic Technology Conference. Offshore Technology Conference. <https://doi.org/10.4043/23795-MS>.
- Coakley, B., Brumley, K., Lebedeva-Ivanova, N., Mosher, D., 2016. Exploring the geology of the Central Arctic Ocean; understanding the basin features in place and time. *J. Geol. Soc. Lond.* 173, 967–987. <https://doi.org/10.1144/jgs2016-082>.
- Cocks, L.R.M., Torsvik, T.H., 2011. The Palaeozoic geography of Laurentia and western Laurussia: a stable craton with mobile margins. *Earth Sci. Rev.* 106, 1–51. <https://doi.org/10.1016/j.earscirev.2011.01.007>.
- Colpron, M., Nelson, J.L., 2011. Chapter 31 A Palaeozoic NW Passage and the Timanian, Caledonian and Uralian connections of some exotic terranes in the North American Cordillera. *Geol. Soc. Lond. Mem.* 35, 463–484. <https://doi.org/10.1144/M35.31>.
- Corfu, F., Polteau, S., Planke, S., Faleide, J.I., Svensen, H., Zayoncheck, A., Stolbov, N., 2013. U–Pb geochronology of cretaceous magmatism on Svalbard and Franz Josef Land, Barents Sea large Igneous Province. *Geol. Mag.* 150, 1127–1135. <https://doi.org/10.1017/S0016756813000162>.
- Craddock, W.H., Houseknecht, D.W., 2016. Cretaceous–Cenozoic burial and exhumation history of the Chukchi shelf, offshore Arctic Alaska. *Am. Assoc. Pet. Geol. Bull.* 100, 63–100. <https://doi.org/10.1306/09291515010>.
- Craddock, W.H., Moore, T.E., O'Sullivan, P.B., Potter, C.J., Houseknecht, D.W., 2018. Late Cretaceous–Cenozoic Exhumation of the Western Brooks Range, Alaska, Revealed from Apatite and Zircon Fission Track Data. *Tectonics* 37, 4714–4751. <https://doi.org/10.1029/2018TC005282>.
- Cramer, B.S., Toggweiler, J.R., Wright, J.D., Katz, M.E., Miller, K.G., 2009. Ocean overturning since the late cretaceous: Inferences from a new benthic foraminiferal isotope compilation. *Paleoceanography* 24. <https://doi.org/10.1029/2008PA001683>.
- Danukalova, M.K., Kuzmichev, A.B., 2014. Wood Mountain (Novaya Sibir Island): fold-thrust orogeny of Neo-Pleistocene age. Tectonics of thrust belts of Eurasia: similarities, differences, features of recent orogeny, and regional reviews. In: *Proceeding of XLVI Tectonic Conference*. GEOS, Moscow, pp. 104–106 in Russian.
- Danukalova, M.K., Kuzmichev, A.B., 2018. Shallow-marine and deep-water Carboniferous deposits of New Siberian Islands: Restoration of late Paleozoic margin of the Siberian paleocontinent. In: Degtyarev, K.E. (Ed.), *Problems of Tectonics and Geodynamics of the Earth Crust and Mantle*, 1. GEOS, Moscow, pp. 135–138. *Proceedings of 50th Tectonic Conference*. (in Russian).
- Danukalova, M.K., Kuzmichev, A.B., Aristov, V.A., 2014. Upper Devonian depositional system of Bel'kov Island (New Siberian Islands): an intracontinental rift or a continental margin? *Geotectonics* 48, 390–412. <https://doi.org/10.1134/S0016852114050021>.
- Danukalova, M.K., Kuzmichev, A.B., Gatovsky, Y.A., Ganelin, V.G., Kossovaya, O.L., Isakova, T.N., 2017. The Upper Paleozoic reference section of the New Siberian Islands (Tas-Ary Peninsula, Kotel'ny Is.) and its significance for Eastern Arctic paleogeography. In: Nurgaliev, D.K., Silantiev, V. (Eds.), *Kazan Golovkinsky Stratigraphic Meeting – 2017 and Fourth All-Russian Conference "Upper Palaeozoic of Russia" Upper Palaeozoic Earth Systems High-Precision Biostratigraphy, Geochronology and Petroleum Resources*. Kazan University Press, Kazan, Russia, pp. 37–38.
- Dickie, K., Keen, C.E., Williams, G.L., Dehler, S.A., 2011. Tectonostratigraphic evolution of the Labrador margin, Atlantic Canada. *Mar. Pet. Geol.* 28, 1663–1675. <https://doi.org/10.1016/j.marpetgeo.2011.05.009>.
- Didenko, A.N., Bondarenko, G.Y., Sokolov, S.D., Kravchenko-Berezhnoy, I.R., 2002. Jurassic–Cretaceous history of the Omolon massif, northeastern Russia: Geologic and paleomagnetic evidence. In: Miller, E.L., Grantz, A., Klemperer, S.L. (Eds.), *Special Paper 360: Tectonic Evolution of the Bering Shelf–Chukchi Sea–Arctic Margin and Adjacent Landmasses*. Geological Society of America, Boulder, Colorado, pp. 225–241. <https://doi.org/10.1130/0-8137-2360-4.225>.
- Dixon, J., Lane, L.S., Dietrich, J.R., McNeil, D.H., Chen, Z., 2019. Geological History of the Late Cretaceous to Cenozoic Beaufort–Mackenzie Basin, Arctic Canada. In: *The Sedimentary Basins of the United States and Canada*. Elsevier, pp. 695–717. <https://doi.org/10.1016/B978-0-444-63895-3.00017-6>.
- Dockman, D.M., Pearson, D.G., Heaman, L.M., Gibson, S.A., Sarkar, C., 2018. Timing and origin of magmatism in the Sverdrup Basin, Northern Canada—Implications for lithospheric evolution in the High Arctic large Igneous Province (HALIP). *Tectonophysics* 742–743, 50–65. <https://doi.org/10.1016/j.tecto.2018.05.010>.
- Doré, A.G., Lundin, E.R., Gibbons, A., Sømme, T.O., Torudbakken, B.O., 2016. Transform margins of the Arctic: a synthesis and re-evaluation. *Geol. Soc. Lond. Spec. Publ.* 431, 63–94. <https://doi.org/10.1144/SP431.8>.
- Dörr, N., Lisker, F., Clift, P.D., Carter, A., Gee, D.G., Tebenkov, A.M., Spiegel, C., 2012. Late Mesozoic–Cenozoic exhumation history of northern Svalbard and its regional significance: Constraints from apatite fission track analysis. *Tectonophysics* 514–517, 81–92. <https://doi.org/10.1016/j.tecto.2011.10.007>.

- Døssing, A., Jackson, H.R., Matzka, J., Einarsson, I., Rasmussen, T.M., Olesen, A.V., Brozna, J.M., 2013. On the origin of the Amerasia Basin and the High Arctic large Igneous Province—results from new aeromagnetic data. *Earth Planet. Sci. Lett.* 363, 219–230. <https://doi.org/10.1016/j.epsl.2012.12.013>.
- Døssing, A., Hansen, T.M., Olesen, A.V., Hopper, J.R., Funck, T., 2014. Gravity inversion predicts the nature of the Amundsen Basin and its continental borderlands near Greenland. *Earth Planet. Sci. Lett.* 408, 132–145. <https://doi.org/10.1016/j.epsl.2014.10.011>.
- Dove, D., Coakley, B., Hopper, J., Kristoffersen, Y., Team, H.G., 2010. Bathymetry, controlled source seismic and gravity observations of the Mendeleev ridge; implications for ridge structure, origin, and regional tectonics. *Geophys. J. Int.* 183, 481–502. <https://doi.org/10.1111/j.1365-246X.2010.04746.x>.
- Drachev, S.S., 2016. Fold belts and sedimentary basins of the Eurasian Arctic. *arkots* 2, 21. <https://doi.org/10.1007/s41063-015-0014-8>.
- Drachev, S., Saunders, A., 2006. The early Cretaceous Arctic LIP: its geodynamic setting and implications for Canada Basin opening. In: Scott, R.A., Thurston, D.K. (Eds.), *Proceedings of the Fourth International Conference on Arctic Margins*. US Department of the Interior MMS, Dartmouth, Nova Scotia, Canada, pp. 216–223.
- Drachev, S.S., Malyshev, N.A., Nikishin, A.M., 2010. Tectonic history and petroleum geology of the Russian Arctic Shelves: an overview. *Geol. Soc. London, Pet. Geol. Conf. Ser.* 7, 591–619. <https://doi.org/10.1144/0070591>.
- Elling, F.J., Spiegel, C., Estrada, S., Davis, D.W., Reinhardt, L., Henjes-Kunst, F., Allroggen, N., Dohrmann, R., Piepjohn, K., Lisker, F., 2016. Origin of Bentonites and Detrital Zircons of the Paleocene Basilaika Formation, Svalbard. *Front. Earth Sci.* 4 <https://doi.org/10.3389/feart.2016.00073>.
- Embry, A., 2011. Chapter 36 Petroleum prospectivity of the Triassic–Jurassic succession of Sverdrup Basin, Canadian Arctic Archipelago. *Geol. Soc. Lond. Mem.* 35, 545–558. <https://doi.org/10.1144/M35.36>.
- Embry, A., Beauchamp, B., 2008. Chapter 13 Sverdrup Basin. In: *Sedimentary Basins of the World*, pp. 451–471. [https://doi.org/10.1016/S1874-5997\(08\)00013-0](https://doi.org/10.1016/S1874-5997(08)00013-0).
- Embry, A., Beauchamp, B., Dewing, K., Dixon, J., 2018. Episodic Tectonics in the Phanerozoic Succession of the Canadian High Arctic and the “10-Million-Year Flood”. *Geol. Soc. Am. Spec. Pap.* 2541, 1–18. [https://doi.org/10.1130/2018.2541\(11\)](https://doi.org/10.1130/2018.2541(11)).
- Ershova, V.B., Prokopiiev, A.V., Khudoley, A.K., 2015a. Integrated provenance analysis of Carboniferous deposits from Northeastern Siberia: Implication for the late Paleozoic history of the Arctic. *J. Asian Earth Sci.* 109, 38–49. <https://doi.org/10.1016/j.jseas.2015.04.046>.
- Ershova, V.B., Prokopiiev, A.V., Nikishin, V.A., Khudoley, A.K., Malyshev, N.A., Nikishin, A.M., 2015b. New data on Upper Carboniferous–lower Permian deposits of Bol'shevik Island, Severnaya Zemlya Archipelago. *Polar Res.* 34, 24558 <https://doi.org/10.3402/polar.v34.24558>.
- Ershova, V.B., Lorenz, H., Prokopiiev, A.V., Sobolev, N.N., Khudoley, A.K., Petrov, E.O., Estrada, S., Sergeev, S., Larionov, A., Thomsen, T.B., 2016a. The De Long Islands: a missing link in unraveling the Paleozoic paleogeography of the Arctic. *Gondwana Res.* 35, 305–322. <https://doi.org/10.1016/j.gr.2015.05.016>.
- Ershova, V.B., Prokopiiev, A.V., Khudoley, A.K., 2016b. Devonian–Permian sedimentary basins and paleogeography of the Eastern Russian Arctic: an overview. *Tectonophysics* 691, 234–255. <https://doi.org/10.1016/j.tecto.2016.03.026>.
- Ershova, V.B., Prokopiiev, A., Andersen, T., Khudoley, A., Kullerud, K., Thomsen, T.B., 2018. U–Pb and Hf isotope analysis of detrital zircons from Devonian–Permian strata of Kotel'ny Island (New Siberian Islands, Russian Eastern Arctic): Insights into the Middle–late Paleozoic evolution of the Arctic. *J. Geodyn.* 119, 199–209. <https://doi.org/10.1016/j.jog.2018.02.008>.
- Ershova, V., Stockli, D., Khudoley, A., Gaina, C., 2019. When big river started to drain to Arctic Basin: view from the Sverdrup Well (Kara Sea). *Geophys. Res. Abstr. EGU2019-9720*. EGU Gen. Assem. 2019. 21.
- Estrada, S., Damaske, D., Henjes-Kunst, F., Schreckenberger, B., Oakey, G.N., Piepjohn, K., Eckelmann, K., Linnemann, U., 2016. Multistage Cretaceous magmatism in the northern coastal region of Ellesmere Island and its relation to the formation of Alpha Ridge – evidence from aeromagnetic, geochemical and geochronological data. *Nor. J. Geol.* 96 (2), 65–95. <https://doi.org/10.17850/njg96-2-03>.
- Estrada, S., Mende, K., Gerdes, A., Gärtner, A., Hofmann, M., Spiegel, C., Damaske, D., Koglin, N., 2018. Proterozoic to cretaceous evolution of the western and central Pearya Terrane (Canadian High Arctic). *J. Geodyn.* 120, 45–76. <https://doi.org/10.1016/j.jog.2018.05.010>.
- Evangelatos, J., Mosher, D.C., 2016. Seismic stratigraphy, structure and morphology of Makarov Basin and surrounding regions: tectonic implications. *Mar. Geol.* 374, 1–13. <https://doi.org/10.1016/j.margeo.2016.01.013>.
- Faleide, J.I., Bjørlykke, K., Gabrielsen, R.H., 2010. *Geology of the Norwegian Continental Shelf*. In: *Petroleum Geoscience*. Springer Berlin Heidelberg, Berlin, Heidelberg, pp. 467–499. https://doi.org/10.1007/978-3-642-02332-3_22.
- Fouler, G.R., Doré, T., Emeleus, C.H., Franke, D., Geoffroy, L., Gernigon, L., Hey, R., Holdsworth, R.E., Hole, M., Höskuldsson, Á., Julian, B., Kuszniir, N., Martinez, F., McCaffrey, K.J.W., Natland, J.H., Peace, A., Petersen, K., Schiffer, C., Stephenson, R., Stoker, M., 2019. A continental Greenland-Iceland-Faroe Ridge. *Earth Sci. Rev.* 102926 <https://doi.org/10.1016/j.earscirev.2019.102926>.
- Freiman, S., Nikishin, A.M., Gaina, C., Petrov, E., 2018. Cretaceous plate tectonic model of Russian Arctic shelf. In: 20th EGU General Assembly. Austria, Vienna, p. 2200.
- Funck, T., Erlendsson, Ö., Geissler, W.H., Gradmann, S., Kimbell, G.S., McDermott, K., Petersen, U.K., 2017. A review of the NE Atlantic conjugate margins based on seismic refraction data. *Geol. Soc. Lond. Spec. Publ.* 447, 171–205. <https://doi.org/10.1144/SP447.9>.
- Gaina, C., Werner, S.C., Saltus, R., Maus, S., 2011. Chapter 3 Circum-Arctic mapping project: new magnetic and gravity anomaly maps of the Arctic. *Geol. Soc. Lond. Mem.* 35, 39–48. <https://doi.org/10.1144/M35.3>.
- Gaina, C., Nikishin, A.M., Petrov, E.L., 2015. Ultraslow spreading, ridge relocation and compressional events in the East Arctic region: a link to the Eurekan orogeny? *arkots* 1, 16. <https://doi.org/10.1007/s41063-015-0006-8>.
- Gaina, C., Nasuti, A., Kimbell, G.S., Blischke, A., 2017. Break-up and seafloor spreading domains in the NE Atlantic. *Geol. Soc. Lond. Spec. Publ.* 447, 393–417. <https://doi.org/10.1144/SP447.12>.
- Galloway, J.M., Tullius, D.N., Evenchick, C.A., Swindles, G.T., Hadlari, T., Embry, A., 2015. Early cretaceous vegetation and climate change at high latitude: Palynological evidence from Isachsen Formation, Arctic Canada. *Cretac. Res.* 56, 399–420. <https://doi.org/10.1016/j.cretres.2015.04.002>.
- Galloway, B.J., Dewing, K., Beauchamp, B., 2018. Upper Paleozoic hydrocarbon systems in the Sverdrup Basin, Canadian Arctic Islands. *Mar. Pet. Geol.* 92, 809–821. <https://doi.org/10.1016/j.marpetgeo.2017.12.013>.
- Gee, D.G., Bogolepova, O.K., Lorenz, H., 2006. The Timanide, Caledonide and Uralide orogens in the Eurasian high Arctic, and relationships to the palaeo-continent Laurentia, Baltica and Siberia. *Geol. Soc. Lond. Mem.* 32, 507–520. <https://doi.org/10.1144/GSL.MEM.2006.032.01.31>.
- Geoffroy, L., 2005. Volcanic passive margins. *Compt. Rendus Geosci.* 337, 1395–1408. <https://doi.org/10.1016/j.crte.2005.10.006>.
- Gertseva, M.V., Borisova, T.P., Chibisova, E.D., Emelianov, E.N., Cherenkov, V.G., Ignat'eva, L.M., Kotov, E.B., Istoshina, E.B., Fedoseev, I.F., Al, E., 2016. State Geological Map of Russian Federation. Scale 1:1 000 000 (third generation). In: *Verkhoyansk-Kolyma Seria. Quadrangle R-52, Tiksi. Explanatory note*. VSEGEI, St. Petersburg.
- Glebovsky, V.Y., Kaminsky, V.D., Minakov, A.N., Merkur'ev, S.A., Childers, V.A., Brozna, J.M., 2006. Formation of the Eurasia Basin in the Arctic Ocean as inferred from geohistorical analysis of the anomalous magnetic field. *Geotectonics* 40, 263–281. <https://doi.org/10.1134/S0016852106040029>.
- Golonka, J., 2011. Chapter 6 Phanerozoic palaeoenvironment and palaeolithofacies maps of the Arctic region. *Geol. Soc. Lond. Mem.* 35, 79–129. <https://doi.org/10.1144/M35.6>.
- State geological map of Russian Federation. Scale 1:1 000 000 (new seria). In: *Gorodinsky, M.E. (Ed.), 1999a. Quadrangle R-(60)-2. Wrangel Island. Explanatory note*. VSEGEI, St. Petersburg.
- State geological map of Russian Federation. Scale 1:1 000 000 (new seria). In: *Gorodinsky, M.E. (Ed.), 1999b. Quadrangle R-58-(60). Bilibino. Explanatory note*. VSEGEI, ed. St. Petersburg.
- Gottlieb, E.S., Meisling, K.E., Miller, E.L., Mull, C.G., 2014. Closing the Canada Basin: Detrital zircon geochronology relationships between the North Slope of Arctic Alaska and the Franklinian mobile belt of Arctic Canada. *Geosphere* 10, 1366–1384. <https://doi.org/10.1130/GES01027.1>.
- Gottlieb, E.S., Pease, V., Miller, E.L., Akinin, V.V., 2018. Neoproterozoic basement history of Wrangel Island and Arctic Chukotka: integrated insights from zircon U–Pb, O and Hf isotopic studies. *Geol. Soc. Lond. Spec. Publ.* 460, 183–206. <https://doi.org/10.1144/SP460.11>.
- Gradstein, F.M., Ogg, J.G., Schmitz, M.D., Ogg, G.M. (Eds.), 2012. *The Geologic Time Scale*. Elsevier. <https://doi.org/10.1016/C2011-1-08249-8>.
- Grantz, A., Hart, P.E., Childers, V.A., 2011a. Chapter 50 Geology and tectonic development of the Amerasia and Canada Basins, Arctic Ocean. *Geol. Soc. Lond. Mem.* 35, 771–799. <https://doi.org/10.1144/M35.50>.
- Grantz, A., Scott, R.A., Drachev, S.S., Moore, T.E., Valin, Z.C., 2011b. Chapter 2 Sedimentary successions of the Arctic Region (58–64° to 90°N) that may be prospective for hydrocarbons. *Geol. Soc. Lond. Mem.* 35, 17–37. <https://doi.org/10.1144/M35.2>.
- Gregersen, U., Hopper, J.R., Knutz, P.C., 2013. Basin seismic stratigraphy and aspects of prospectivity in the NE Baffin Bay, Northwest Greenland. *Mar. Pet. Geol.* 46, 1–18. <https://doi.org/10.1016/j.marpetgeo.2013.05.013>.
- Grinenko, O.V., 1989. *The Paleogene and Neogene of the North-Eastern USSR*. Yakut Scientific Center SB AS USSR, Yakutsk.
- Grinenko, O.V., Sergeenko, A.I., Beloyubsky, I.N., 1997. *Stratigraphy of the Paleogene and Neogene deposits of Russian Far East. Otchechestvennaya Geol.* 8, 14–20 in Russian.
- Grossgeym, V.A., Korobkov, I.A. (Eds.), 1975. *Straigraphy of the USSR. Paleogene System*. Nedra, Moscow.
- Grundvåg, S.-A., Marin, D., Kairanov, B., Śliwińska, K.K., Nøhr-Hansen, H., Jelby, M.E., Escalona, A., Olaussen, S., 2017. The lower cretaceous succession of the northwestern Barents Shelf: Onshore and offshore correlations. *Mar. Pet. Geol.* 86, 834–857. <https://doi.org/10.1016/j.marpetgeo.2017.06.036>.
- Guo, Z.-X., Yang, Y.-T., Zhabrev, S., Hou, Z.-H., 2017. Tectonostratigraphic evolution of the Mohe-Upper Amur Basin reflects the final closure of the Mongol-Okhotsk Ocean in the latest Jurassic–earliest cretaceous. *J. Asian Earth Sci.* 145, 494–511. <https://doi.org/10.1016/j.jseas.2017.06.020>.
- Hadlari, T., Davis, W.J., Dewing, K., 2014. A pericratonic model for the Pearya terrane as an extension of the Franklinian margin of Laurentia, Canadian Arctic. *Geol. Soc. Am. Bull.* 126, 182–200. <https://doi.org/10.1130/B30843.1>.
- Hadlari, T., Midwinter, D., Galloway, J.M., Dewing, K., Durbano, A.M., 2016. Mesozoic rift to post-rift tectonostratigraphy of the Sverdrup Basin, Canadian Arctic. *Mar. Pet. Geol.* 76, 148–158. <https://doi.org/10.1016/j.marpetgeo.2016.05.008>.
- Harrison, J.C., Brent, T.A., 2005. Basins and fold belts of Prince Patrick Island and adjacent area. *Canadian Arctic Islands*. <https://doi.org/10.4095/220345>.
- Harrison, J.C., St-Onge, M.R., Petrov, O.V., Strelnikov, S.I., Lopatin, B.G., Wilson, F.H., Tella, S., Paul, D., Lynds, T., Shokalsky, S.P., Hulst, C.K., Bergman, S., Jepsen, H.F.,

- Solli, A., 2011. Geological map of the Arctic; Geological Survey of Canada, Map 2159A, scale 1:5 000 000. Geological Survey of Canada.
- Hegewald, A., Jokat, W., 2013. Tectonic and sedimentary structures in the northern Chukchi region, Arctic Ocean. *J. Geophys. Res. Solid Earth* 118, 3285–3296. <https://doi.org/10.1002/jgrb.50282>.
- Helwig, J., Kumar, N., Emmet, P., Dinkelman, M.G., 2011. Chapter 35 Regional seismic interpretation of crustal framework, Canadian Arctic passive margin, Beaufort Sea, with comments on petroleum potential. *Geol. Soc. Lond. Mem.* 35, 527–543. <https://doi.org/10.1144/M35.35>.
- Henriksen, E., Bjørnseth, H.M., Hals, T.K., Heide, T., Kiryukhina, T., Kløvjan, O.S., Larssen, G.B., Ryseth, A.E., Rønning, K., Sollid, K., Stoupakova, A., 2011a. Chapter 17 Uplift and erosion of the greater Barents Sea: impact on prospectivity and petroleum systems. *Geol. Soc. Lond. Mem.* 35, 271–281. <https://doi.org/10.1144/M35.17>.
- Henriksen, E., Ryseth, A.E., Larssen, G.B., Heide, T., Rønning, K., Sollid, K., Stoupakova, A.V., 2011b. Chapter 10 Tectonostratigraphy of the greater Barents Sea: implications for petroleum systems. *Geol. Soc. Lond. Mem.* 35, 163–195. <https://doi.org/10.1144/M35.10>.
- Hoiland, C.W., Miller, E.L., Pease, V., Hourigan, J.K., 2018. Detrital zircon U–Pb geochronology and Hf isotope geochemistry of metasedimentary strata in the southern Brooks Range: constraints on Neoproterozoic–cretaceous evolution of Arctic Alaska. *Geol. Soc. Lond. Spec. Publ.* 460, 121–158. <https://doi.org/10.1144/SP460.16>.
- Houseknecht, D.W., 2019. Evolution of the Arctic Alaska Sedimentary Basin. In: *The Sedimentary Basins of the United States and Canada*. Elsevier, pp. 719–745. <https://doi.org/10.1016/B978-0-444-63895-3.00018-8>.
- Houseknecht, D.W., Bird, K.J., 2011. Chapter 34 Geology and petroleum potential of the rifted margins of the Canada Basin. *Geol. Soc. Lond. Mem.* 35, 509–526. <https://doi.org/10.1144/M35.34>.
- Houseknecht, D.W., Connors, C.D., 2016. Pre-Mississippian tectonic affinity across the Canada Basin–Arctic margins of Alaska and Canada. *Geology* 44, 507–510. <https://doi.org/10.1130/G37862.1>.
- Houseknecht, D.W., Wartes, M.A., 2013. Cliniform deposition across a boundary between orogenic front and foredeep - an example from the lower cretaceous in Arctic Alaska. *Terra Nova* 25, 206–211. <https://doi.org/10.1111/ter.12024>.
- Houseknecht, D.W., Bird, K.J., Schenk, C.J., 2009. Seismic analysis of cliniform depositional sequences and shelf-margin trajectories in Lower Cretaceous (Albian) strata, Alaska North Slope. *Basin Res.* 21, 644–654. <https://doi.org/10.1111/j.1365-2117.2008.00392.x>.
- Hutchinson, D.R., Jackson, H.R., Houseknecht, D.W., Li, Q., Shimeld, J.W., Mosher, D.C., Chian, D., Saltus, R.W., Oakey, G.N., 2017. Significance of Northeast-Trending Features in Canada Basin, Arctic Ocean. *Geochem. Geophys. Geosyst.* 18, 4156–4178. <https://doi.org/10.1002/2017GC007099>.
- Ikhсанov, B., 2014. Late Mesozoic and Cenozoic Deformations of Sedimentary Basins of Chukchi Sea. PhD Thesis. In: Moscow State University.
- Ilhan, I., Coakley, B.J., 2018. Meso–Cenozoic evolution of the southwestern Chukchi Borderland, Arctic Ocean. *Mar. Pet. Geol.* 95, 100–109. <https://doi.org/10.1016/j.marpetgeo.2018.04.014>.
- Jakobsson, M., Mayer, L., Coakley, B., Dowdeswell, J.A., Forbes, S., Fridman, B., Hodnesdal, H., Noormets, R., Pedersen, R., Rebesco, M., Schenke, H.W., Zarayskaya, Y., Accettella, D., Armstrong, A., Anderson, R.M., Bienhoff, P., Camerlenghi, A., Church, I., Edwards, M., Gardner, J.V., Hall, J.K., Hell, B., Hestvik, O., Kristoffersen, Y., Marcussen, C., Mohammad, R., Mosher, D., Nghiem, S. V., Pedrosa, M.T., Travaglini, P.G., Weatherall, P., 2012. The International Bathymetric Chart of the Arctic Ocean (IBCAO) Version 3.0. *Geophys. Res. Lett.* 39, n/a/n/a. [doi:10.1029/2012GL052219](https://doi.org/10.1029/2012GL052219).
- Jokat, W., Ickrath, M., 2015. Structure of ridges and basins off East Siberia along 81°N, Arctic Ocean. *Mar. Pet. Geol.* 64, 222–232. <https://doi.org/10.1016/j.marpetgeo.2015.02.047>.
- Kairanon, B., Escalona, A., Mordasova, A., Śliwińska, K., Suslova, A., 2018. Early cretaceous tectonostratigraphic evolution of the north Central Barents Sea. *J. Geodyn.* 119, 183–198. <https://doi.org/10.1016/j.jog.2018.02.009>.
- Kashubin, S.N., Pavlenkova, N.I., Petrov, O.V., Mil'shteyn, E.D., Shokalsky, S.P., Erinchek, Y.M., 2013. Earth crust types of the Circum-Polar Arctics. *Reg. Geol. i Metallog.* 55, 5–20 in Russian.
- Kashubin, S.N., Petrov, O.V., Artemieva, I.M., Morozov, A.F., Vyatkina, D.V., Golyshova, Y.S., Kashubina, T.V., Mil'shteyn, E.D., Rybalka, A.V., Erinchek, Y.M., Sakulina, T.S., Krupnova, N.A., Shulgin, A.A., 2018. Crustal structure of the Mendeleev rise and the Chukchi Plateau (Arctic Ocean) along the Russian wide-angle and multichannel seismic reflection experiment “Arctic-2012”. *J. Geodyn.* 119, 107–122. <https://doi.org/10.1016/j.jog.2018.03.006>.
- Khanchuk, A.I., Grebennikov, A.V., Ivanov, V.V., 2019. Albian–Cenomanian Orogenic Belt and Igneous Province of Pacific Asia. *Russ. J. Pacific Geol.* 13, 187–219. <https://doi.org/10.1134/S1819714019030035>.
- Kharakhinov, V.V., Shlenkin, S.I., Vashkevich, A.A., Agapitov, D.D., Obukhov, A.N., 2014. Oil and Gas Basins of the Bering Sea Area (Results of Exploration Works in 2000–2009). Scientific World, Moscow.
- Khudoley, A.K., Verzhbitsky, V.E., Zastrozhnov, D.A., O'Sullivan, P., Ershova, V.B., Proskurnin, V.F., Tuchkova, M.I., Rogov, M.A., Kyser, T.K., Malyshev, S.V., Schneider, G.V., 2018. Late Paleozoic – Mesozoic tectonic evolution of the Eastern Taimyr-Severnaya Zemlya Fold and Thrust Belt and adjoining Yenisey-Khatanga Depression. *J. Geodyn.* 119, 221–241. <https://doi.org/10.1016/j.jog.2018.02.002>.
- Kingsbury, C.G., Kamo, S.L., Ernst, R.E., Söderlund, U., Cousins, B.L., 2018. U–Pb geochronology of the plumbing system associated with the late cretaceous Strand Fiord Formation, Axel Heiberg Island, Canada: part of the 130–90 Ma High Arctic large igneous province. *J. Geodyn.* 118, 106–117. <https://doi.org/10.1016/j.jog.2017.11.001>.
- Kleinspehn, K.L., Teysier, C., 2016. Oblique rifting and the late Eocene–Oligocene demise of Laurasia with inception of Molloy Ridge: Deformation of Forlandsundet Basin, Svalbard. *Tectonophysics* 693, 363–377. <https://doi.org/10.1016/j.tecto.2016.05.010>.
- Klemperer, S.L., Miller, E.L., Grantz, A., Scholl, D.W., 2002. Crustal structure of the Bering and Chukchi shelves: Deep seismic reflection profiles across the North American continent between Alaska and Russia, in: *Special Paper 360: Tectonic Evolution of the Bering Shelf-Chukchi Sea-Artic Margin and Adjacent Landmasses*. *Geol. Soc. Am.* 1–24. <https://doi.org/10.1130/0-8137-2360-4.1>.
- Knudsen, C., Hopper, J.R., Bierman, P.R., Bjerager, M., Funck, T., Green, P.F., Ineson, J. R., Japsen, P., Marcussen, C., Sherlock, S.C., Thomsen, T.B., 2018. Samples from the Lomonosov Ridge place new constraints on the geological evolution of the Arctic Ocean. *Geol. Soc. Lond. Spec. Publ.* 460, 397–418. <https://doi.org/10.1144/SP460.17>.
- Kontorovich, A.E., Epov, M.I., Burshtein, L.M., Kaminskii, V.D., Kurchikov, A.R., Malyshev, N.A., Prischepa, O.M., Safronov, A.F., Stupakova, A.V., Suprunenko, O.I., 2010. Geology and hydrocarbon resources of the continental shelf in Russian Arctic seas and the prospects of their development. *Russ. Geol. Geophys.* 51, 3–11. <https://doi.org/10.1016/j.rgg.2009.12.003>.
- Kontorovich, A.E., Kontorovich, V.A., Ryzhikova, S.V., Shurygin, B.N., Vakulenko, L.G., Gaideburova, E.A., Danilova, V.P., Kazanenkov, V.A., Kim, N.S., Kostyeva, E.A., Moskvina, V.I., Yan, P.A., 2013. Jurassic paleogeography of the West Siberian sedimentary basin. *Russ. Geol. Geophys.* 54, 747–779. <https://doi.org/10.1016/j.rgg.2013.07.002>.
- Kontorovich, A.E., Ershov, S.V., Kazanenkov, V.A., Karogodin, Y.N., Kontorovich, V.A., Lebedeva, N.K., Nikitenko, B.L., Popova, N.I., Shurygin, B.N., 2014. Cretaceous paleogeography of the West Siberian sedimentary basin. *Russ. Geol. Geophys.* 55, 582–609. <https://doi.org/10.1016/j.rgg.2014.05.005>.
- Kontorovich, A.E., Ayunova, D.V., Gubin, I.A., Ershov, S.V., Kalinin, A.Y., Kalinina, L. M., Kanakov, M.S., Solov'ev, M.V., Surikova, E.S., Shestakova, N.I., 2016. Seismic stratigraphy, formation history and gas potential of the Nadym–Pur interfluve area (West Siberia). *Russ. Geol. Geophys.* 57, 1248–1258. <https://doi.org/10.1016/j.rgg.2016.08.010>.
- Korago, E.A., Kovaleva, G.N., Il'in, V.F., Pavlov, L.G., 1992. *Tektonika i Metallogeniya Rannikh Kimmerid Novoy Zemli (Tectonics and Metallogeny of Early Cimmerides of New Earth)*. VNIIOkeangeologiya, Nedra, Saint Petersburg.
- Kos'ko, M.K., Trufanov, G.V., 2002. Middle cretaceous to Eocene sequences on the New Siberian Islands: an approach to interpret offshore seismic. *Mar. Pet. Geol.* 19, 901–919.
- Kos'ko, M.K., Cecile, M.P., Harrison, J.C., Ganelin, V.G., Khandoshko, N.V., Lopatin, B. G., 1993. Geology of Wrangel Island, between Chukchi and East Siberian seas, northeastern Russia. *Geol. Surv. Canada Bull.* 461, 101.
- Kostyleva, V., Shchepetova, E., Kotelnikov, A., 2018. Upper Cretaceous rhyolite ash beds from the New Siberian Islands. In: *ICAM8 (Stockholm)*.
- Kumar, N., Granath, J.W., Emmet, P.A., Helwig, J.A., Dinkelman, M.G., 2011. Chapter 33 Stratigraphic and tectonic framework of the US Chukchi Shelf: exploration insights from a new regional deep-seismic reflection survey. *Geol. Soc. Lond. Mem.* 35, 501–508. <https://doi.org/10.1144/M35.33>.
- Kurchikov, A.R., Borodkin, V.N., 2011. Stratigraphy and paleogeography of Berriassian–lower Aptian deposits of West Siberia in connection with the cliniform structure of the section. *Russ. Geol. Geophys.* 52, 859–870. <https://doi.org/10.1016/j.rgg.2011.07.009>.
- Kuzmichev, A.B., 2009. Where does the south Anyui suture go in the New Siberian islands and Laptev Sea? Implications for the Amerasia basin origin. *Tectonophysics* 463, 86–108. <https://doi.org/10.1016/j.tecto.2008.09.017>.
- Kuzmichev, A.B., Aleksandrova, G.N., Herman, A.B., Danukalova, M.K., Simakova, A.N., 2013. Paleogene–Neogene sediments of Bel'kov Island (New Siberian Islands): Characteristics of sedimentary cover in the eastern Laptev shelf. *Stratigr. Geol. Correl.* 21, 421–444. <https://doi.org/10.1134/S0869593813040059>.
- Kuzmichev, A.B., Danukalova, M.K., Aleksandrova, G.N., Zakharov, V.A., Herman, A.B., Nikitenko, B.L., Khubanov, V.B., Korostylev, E.V., 2018. Mid-cretaceous Tuor-Yuryakh section of Kotelnii Island, New Siberian Islands: how does the Probable Basement of Sedimentary Cover of the Laptev Sea look on Land? *Stratigr. Geol. Correl.* 26, 403–432. <https://doi.org/10.1134/S0869593818040044>.
- Kuznetsov, N.B., Natapov, L.M., Belousova, E.A., O'Reilly, S.Y., Griffin, W.L., 2010. Geochronological, geochemical and isotopic study of detrital zircon suites from late Neoproterozoic clastic strata along the NE margin of the east European Craton: Implications for plate tectonic models. *Gondwana Res.* 17, 583–601. <https://doi.org/10.1016/j.gr.2009.08.005>.
- Lane, L.S., 2007. Devonian–Carboniferous paleogeography and orogenesis, northern Yukon and adjacent Arctic Alaska. *Can. J. Earth Sci.* 44, 679–694. <https://doi.org/10.1139/e06-131>.
- Lasabuda, A., Laberg, J.S., Knutsen, S.-M., Høgseth, G., 2018. Early to middle Cenozoic paleoenvironment and erosion estimates of the southwestern Barents Sea: Insights from a regional mass-balance approach. *Mar. Pet. Geol.* 96, 501–521. <https://doi.org/10.1016/j.marpetgeo.2018.05.039>.
- Laverov, N.P., Lobkovsky, L.I., Kononov, M.V., Dobretsov, N.L., Vernikovskiy, V.A., Sokolov, S.D., Shipilov, E.V., 2013. A geodynamic model of the evolution of the Arctic basin and adjacent territories in the Mesozoic and Cenozoic and the outer limit of the Russian Continental Shelf. *Geotectonics* 47, 1–30. <https://doi.org/10.1134/S0016852113010044>.
- Lawver, L.A., Gahagan, L.M., Norton, I., 2011. Chapter 5 Palaeogeographic and tectonic evolution of the Arctic region during the Palaeozoic. *Geol. Soc. Lond. Mem.* 35, 61–77. <https://doi.org/10.1144/M35.5>.

- Lawver, L., Norton, I., Garagan, L., 2015. The Bigger Picture: A Need for the Whole Earth Plate Tectonic Setting when Reconstructing Greenland, in: 3P Arctic. The Polar Petroleum Potential. Conference & Exhibition. Abstract Book. Stavanger, p. 61.
- Lebedev, S., Schaeffer, A.J., Pulla, J., Pease, V., 2018. Seismic tomography of the Arctic region: inferences for the thermal structure and evolution of the lithosphere. *Geol. Soc. Lond. Spec. Publ.* 460, 419–440. <https://doi.org/10.1144/SP460.10>.
- Lobkovsky, L.L., 2016. Deformable plate tectonics and regional geodynamic model of the Arctic region and Northeastern Asia. *Russ. Geol. Geophys.* 57, 371–386. <https://doi.org/10.1016/j.rgg.2016.03.002>.
- Luchitskaya, M.V., Sokolov, S.D., Kotov, A.B., Natapov, L.M., Belousova, E.A., Katkov, S. M., 2015. Late Paleozoic granitic rocks of the Chukchi Peninsula: Composition and location in the structure of the Russian Arctic. *Geotectonics* 49, 243–268. <https://doi.org/10.1134/S0016852115040056>.
- Luchitskaya, M.V., Moiseev, A.V., Sokolov, S.D., Tuchkova, M.I., Sergeev, S.A., O'Sullivan, P.B., Verzhbitskii, V.E., Malyshev, N.A., 2017. Marginal continental and within-plate neoproterozoic granites and rhyolites of Wrangel Island, Arctic region. *Geotectonics* 51, 17–39. <https://doi.org/10.1134/S0016852117010034>.
- Makariev, A.A. (Ed.), 2013. Geological Map of Russian Federation, Scale 1:1000000, T-45-48 (Cape Chelyuskin). Explanatory Notes. St. Petersburg, VSEGEI.
- Malyshev, N.A., Nikishin, V.A., Nikishin, A.M., Obmetko, V.V., Martirosyan, V.N., Kleshchina, L.N., Reydik, Y.V., 2012. A new model of the geological structure and evolution of the North Kara Sedimentary Basin. *Dokl. Earth Sci.* 445, 791–795. <https://doi.org/10.1134/S1028334X12070057>.
- Mann, U., Knies, J., Chand, S., Jokat, W., Stein, R., Zweigel, J., 2009. Evaluation and modelling of Tertiary source rocks in the Central Arctic Ocean. *Mar. Pet. Geol.* 26, 1624–1639. <https://doi.org/10.1016/j.marpetgeo.2009.01.008>.
- Metelkin, D.V., Vernikovskiy, V.A., Kazansky, A.Y., Wingate, M.T.D., 2010. Late Mesozoic tectonics of Central Asia based on paleomagnetic evidence. *Gondwana Res.* 18, 400–419. <https://doi.org/10.1016/j.gr.2009.12.008>.
- Metelkin, D.V., Vernikovskiy, V.A., Tolmacheva, T.Y., Matushkin, N.Y., Zhdanova, A.I., Pisarevskiy, S.A., 2016. First paleomagnetic data for the New Siberian Islands: Implications for Arctic paleogeography. *Gondwana Res.* 37, 308–323. <https://doi.org/10.1016/j.gr.2015.08.008>.
- Midtkandal, I., Svensen, H.H., Planke, S., Corfu, F., Polteau, S., Torsvik, T.H., Faleide, J. I., Grundvåg, S.-A., Selnes, H., Kürschner, W., Olausson, S., 2016. The Aptian (early cretaceous) oceanic anoxic event (OAE1a) in Svalbard, Barents Sea, and the absolute age of the Barremian-Aptian boundary. *Palaeogeogr. Palaeoclimatol. Palaeoecol.* 463, 126–135. <https://doi.org/10.1016/j.palaeo.2016.09.023>.
- Miller, E.L., Verzhbitsky, V.E., 2009. Structural studies near Pevek, Russia: implications for formation of the East Siberian Shelf and Makarov Basin of the Arctic Ocean. *Stephan Mueller Spec. Publ. Ser.* 4, 223–241. <https://doi.org/10.5194/smeps-4-223-2009>.
- Miller, E.L., Gelman, M., Parfenov, L., Hourigan, J., 2002. Tectonic setting of Mesozoic magmatism: A comparison between northeastern Russia and the North American Cordillera, in: Special Paper 360: Tectonic Evolution of the Bering Shelf-Chukchi Sea-Arctic Margin and Adjacent Landmasses. *Geol. Soc. Am.* 313–332. <https://doi.org/10.1130/0-8137-2360-4.313>.
- Miller, E.L., Soloviev, A., Kuzmichev, A., Gehrels, G.E., Toro, J., Tuchkova, M., 2008. Jura-cretaceous foreland basin deposits of the Russian Arctic: Separated by birth of Makarov Basin? *Nor. J. Geol.* 201–226.
- Miller, E.L., Gehrels, G.E., Pease, V., Sokolov, S., 2010. Paleozoic and Mesozoic stratigraphy and U–Pb detrital zircon geochronology of Wrangel Island, Russia: constraints on paleogeography and paleocontinental reconstructions of the Arctic. *Am. Assoc. Pet. Geol. Bull.* 94, 665–692.
- Miller, E.L., Akinin, V.V., Dumitru, T.A., Gottlieb, E.S., Grove, M., Meisling, K., Seward, G., 2018a. Deformational history and thermochronology of Wrangel Island, East Siberian Shelf and coastal Chukotka, Arctic Russia. *Geol. Soc. Lond. Spec. Publ.* 460, 207–238. <https://doi.org/10.1144/SP460.7>.
- Miller, E.L., Meisling, K.E., Akinin, V.V., Brumley, K., Coakley, B.J., Gottlieb, E.S., Hoiland, C.W., O'Brien, T.M., Soboleva, A., Toro, J., 2018b. Circum-Arctic Lithosphere Evolution (CALE) Transect c: displacement of the Arctic Alaska–Chukotka microplate towards the Pacific during opening of the Amerasia Basin of the Arctic. *Geol. Soc. Lond. Spec. Publ.* 460, 57–120. <https://doi.org/10.1144/SP460.9>.
- Minakov, A., Yarushina, V., Faleide, J.I., Krupnova, N., Sakoulina, T., Dergunov, N., Gלבovsky, V., 2018. Dyke emplacement and crustal structure within a continental large igneous province, northern Barents Sea. *Geol. Soc. Lond. Spec. Publ.* 460, 371–395. <https://doi.org/10.1144/SP460.4>.
- Moore, T.E., O'Sullivan, P.B., Potter, C.J., Donelick, R.A., 2015. Provenance and detrital zircon geochronologic evolution of lower Brookian foreland basin deposits of the western Brooks Range, Alaska, and implications for early Brookian tectonism. *Geosphere* 11, 93–122. <https://doi.org/10.1130/GES01043.1>.
- Moran, K., Backman, J., Brinkhuis, H., Clemens, S.C., Cronin, T., Dickens, G.R., Eynaud, F., Gattacceca, J., Jakobsson, M., Jordan, R.W., Kaminski, M., King, J., Koc, N., Krylov, A., Martinez, N., Matthiessen, J., McInroy, D., Moore, T.C., Onodera, J., O'Regan, M., Pälke, H., Rea, B., Rio, D., Sakamoto, T., Smith, D.C., Stein, R., St John, K., Suto, I., Suzuki, N., Takahashi, K., Watanabe, M., Yamamoto, M., Farrell, J., Frank, M., Kubik, P., Jokat, W., Kristoffersen, Y., 2006. The Cenozoic palaeoenvironment of the Arctic Ocean. *Nature* 441, 601–605. <https://doi.org/10.1038/nature04800>.
- Mordasova, A.V., 2018. Conditions of formation and prospects of oil and gas efficiency of Upper Jurassic and lower cretaceous deposits of Barents Sea shelf. PhD Thesis. In: Moscow State University.
- Petroleum exploration in northern Canada: a guide to oil and gas exploration potential. In: Morrell, G.R. (Ed.), 1995. Minister of Indian Affairs and Northern Development Report.
- Mosher, D.C., Shimeld, J., Hutchinson, D., Chian, D., Lebedeva-Ivanova, N., Jackson, R., 2012. Canada Basin revealed. In: Society of Petroleum Engineers - Arctic Technology Conference, 2012, pp. 805–815.
- Natapov, L.M., Surmilova, E.P., 1992. Geological map of the USSR. Scale 1:1 000 000 (new seria). Quadrangle R-53-(55). Deputatskiy. In: Explanatory Note. St. Petersburg, VSEGEI and Aerogeologia.
- Neville, L.A., McNeil, D.H., Grasby, S.E., Ardakani, O.H., Sanei, H., 2017. Late Paleocene-middle Eocene hydrocarbon source rock potential in the Arctic Beaufort-Mackenzie Basin. *Mar. Pet. Geol.* 86, 1082–1091. <https://doi.org/10.1016/j.marpetgeo.2017.06.042>.
- Nikishin, V.A., 2013. Intraplate and near-plate boundary deformations of the Kara Sea sedimentary basins. In: PhD Thesis. Moscow State University.
- Nikishin, A.M., Ziegler, P.A., Stephenson, R.A., Cloetingh, S.A.P.L., Furne, A.V., Fokin, P. A., Ershov, A.V., Bolotov, S.N., Korotaev, M.V., Alekseev, A.S., Gorbachev, V.I., Shipilov, E.V., Lankreijer, A., Bembinova, E.Y., Shalimov, I.V., 1996. Late Precambrian to Triassic history of the east European Craton: dynamics of sedimentary basin evolution. *Tectonophysics* 268, 23–63. [https://doi.org/10.1016/S0040-1951\(96\)00228-4](https://doi.org/10.1016/S0040-1951(96)00228-4).
- Nikishin, A.M., Malyshev, N.A., Nikishin, V.A., Soloviev, A.V., Aleksandrova, G.N., Escalona, A., 2014. Aptian paleogeography of North Kara Sea Region: Provenance Analyses Based on Detrital Zircon Ages from Vize Island Aptian Sandstones. In: AAPG 3P Arctic Polar Petroleum Potential Conference & Exhibition. Stavanger, Norway, p. 29.
- Nikishin, A.M., Petrov, E.I., Malyshev, N.A., 2015. Geological Structure and History of the Arctic Ocean. EAGE Publications bv. <https://doi.org/10.3997/9789462821880>.
- Nikishin, V.A., Malyshev, N.A., Golovanov, D.Y., Kleshchina, L.N., Nikitina, V.A., Nikishin, A.M., Ulianov, G.V., Cherepanov, D.E., 2016. The geological aspects of evolution of the North Kara basin and East Barents megabasin. In: 7th EAGE Saint Petersburg International Conference and Exhibition.
- Nikishin, A.M., Petrov, E.I., Malyshev, N.A., Ershova, V.P., 2017a. Rift systems of the Russian Eastern Arctic shelf and Arctic deep water basins: link between geological history and geodynamics. *Geodyn. Tectonophysics* 8, 11–43. <https://doi.org/10.5800/GT-2017-8-1-0231>.
- Nikishin, V.A., Malyshev, N.A., Nikishin, A.M., Golovanov, D.Y., Proskurnin, V.F., Soloviev, A.V., Kulemin, R.F., Morgunova, E.S., Ulyanov, G.V., Fokin, P.A., 2017b. Recognition of the Cambrian Timan–Severnaya Zemlya orogen and timing of geological evolution of the North Kara sedimentary basin based on detrital zircon dating. *Dokl. Earth Sci.* 473, 402–405. <https://doi.org/10.1134/S1028334X17040146>.
- Nikishin, A.M., Gaina, C., Petrov, E.I., Malyshev, N.A., Freiman, S.I., 2018. Eurasia Basin and Gakkel Ridge, Arctic Ocean: Crustal asymmetry, ultra-slow spreading and continental rifting revealed by new seismic data. *Tectonophysics* 746, 64–82. <https://doi.org/10.1016/j.tecto.2017.09.006>.
- Nikitenko, B.L., Devyatov, V.P., Lebedeva, N.K., Basov, V.A., Goryacheva, A.A., Pestchevskaya, E.B., Glinkikh, L.A., 2017. Jurassic and cretaceous stratigraphy of the New Siberian Archipelago (Laptev and East Siberian Seas): facies zoning and lithostratigraphy. *Russ. Geol. Geophys.* 58, 1478–1493. <https://doi.org/10.1016/j.rgg.2017.11.012>.
- Oakey, G.N., Saltus, R.W., 2016. Geophysical analysis of the Alpha–Mendelev ridge complex: Characterization of the High Arctic large Igneous Province. *Tectonophysics* 691, 65–84. <https://doi.org/10.1016/j.tecto.2016.08.005>.
- O'Brien, T.M., Miller, E.L., Benowitz, J.P., Meisling, K.E., Dumitru, T.A., 2016. Dredge samples from the Chukchi Borderland: Implications for paleogeographic reconstruction and tectonic evolution of the Amerasia Basin of the Arctic. *Am. J. Sci.* 316, 873–924. <https://doi.org/10.2475/09.2016.03>.
- O'Brien, C.L., Robinson, S.A., Pancost, R.D., Sinnighe Damsté, J.S., Schouten, S., Lunt, D.J., Alsenz, H., Bornemann, A., Bottini, C., Brassell, S.C., Farnsworth, A., Forster, A., Huber, B.T., Inglis, G.N., Jenkens, H.C., Linnert, C., Littler, K., Markwick, P., McAnena, A., Mutterlose, J., Naafs, B.D.A., Püttmann, W., Sluijs, A., van Helmond, N.A.G.M., Vellekoop, J., Wagner, T., Wrobel, N.E., 2017. Cretaceous sea-surface temperature evolution: Constraints from TEX 86 and planktonic foraminiferal oxygen isotopes. *Earth Sci. Rev.* 172, 224–247. <https://doi.org/10.1016/j.earscirev.2017.07.012>.
- Omosanya, K.O., Johansen, S.E., Abrahamson, P., 2016. Magmatic activity during the breakup of Greenland-Eurasia and fluid-flow in Stappen High, SW Barents Sea. *Mar. Pet. Geol.* 76, 397–411. <https://doi.org/10.1016/j.marpetgeo.2016.05.017>.
- Oreshkina, T.V., Alekseev, A.S., Smirnova, S.B., 1998. Cretaceous and Paleogene deposits of polar Pre-Uralian area: Biostratigraphic and paleogeographic features. In: Knipper, A.L., Kurenkov, S.A., Semikhatov, M.A. (Eds.), *Urals: Fundamental Problems of Geodynamics and Stratigraphy*. Proceedings, 500. Nauka, Moscow, pp. 183–192 (in Russian).
- O'Sullivan, P.B., Murphy, J.M., Blythe, A.E., 1997. Late Mesozoic and Cenozoic thermotectonic evolution of the Central Brooks Range and adjacent North Slope foreland basin, Alaska: Including fission track results from the Trans-Alaska Crustal Transect (TACT). *J. Geophys. Res. Solid Earth* 102, 20821–20845. <https://doi.org/10.1029/96JB03411>.
- Parfenov, L.M., 1984. Continental Margins and Island Arcs of the North-East Asia. Nauka, Novosibirsk.
- Parfenov, L.M., 1991. Tectonics of the Verkhoyansk-Kolyma Mesozoids in the context of plate tectonics. *Tectonophysics* 199, 319–342.
- Parfenov, L.M., Kuzmin, M.I. (Eds.), 2001. Tectonics, Geodynamics and Metallogeny of the Territory of the Sakha Republic (Yakutia). MAIK “Nauka/Interperiodika,” Moscow.
- Parfenov, L.M., Natal'in, B.A., 1986. Mesozoic tectonic evolution of Northeastern Asia. *Tectonophysics* 127, 291–304.

- Pease, V., 2011. Chapter 20 Eurasian orogens and Arctic tectonics: an overview. *Geol. Soc. Lond. Mem.* 35, 311–324. <https://doi.org/10.1144/M35.20>.
- Pease, V., Scott, R.A., 2009. Crustal affinities in the Arctic Uralides, northern Russia: significance of detrital zircon ages from Neoproterozoic and Palaeozoic sediments in Novaya Zemlya and Taimyr. *J. Geol. Soc. Lond.* 166, 517–527. <https://doi.org/10.1144/0016-76492008-093>.
- Pease, V., Drachev, S., Stephenson, R., Zhang, X., 2014. Arctic lithosphere — a review. *Tectonophysics* 628, 1–25. <https://doi.org/10.1016/j.tecto.2014.05.033>.
- Peters, K., Schenk, O., Bird, K., 2011. Timing of Petroleum System Events Controls Accumulations on the North Slope, Alaska. In: AAPG Memoir.
- Petersen, T.G., Thomsen, T.B., Olausen, S., Stemmerik, L., 2016. Provenance shifts in an evolving Eureka foreland basin: the Tertiary Central Basin, Spitsbergen. *J. Geol. Soc. Lond.* 173, 634–648. <https://doi.org/10.1144/jgs2015-076>.
- Petrov, O.V. (Ed.), 2012. *Geological Map of Russia and Adjoining Water Areas, Scale 1: 2500000* (St. Petersburg).
- Petrov, O.V., 2017. *Tectonic Map of the Arctic*. VSEGEI Publishing House, St. Petersburg.
- Petrov, O., Morozov, A., Shokalsky, S., Kashubin, S., Artemieva, I.M., Sobolev, N., Petrov, E., Ernst, R.E., Sergeev, S., Smelror, M., 2016. Crustal structure and tectonic model of the Arctic region. *Earth Sci. Rev.* 154, 29–71. <https://doi.org/10.1016/j.earscirev.2015.11.013>.
- Piepjoh, K., von Gosen, W., Tessensohn, F., Reinhardt, L., McClelland, W.C., Dallmann, W., Gaedicke, C., Harrison, J.C., 2015. Tectonic map of the Ellesmerian and Eureka deformation belts on Svalbard, North Greenland, and the Queen Elizabeth Islands (Canadian Arctic). *arkots* 1, 12. <https://doi.org/10.1007/s41063-015-0015-7>.
- Piepjoh, K., von Gosen, W., Tessensohn, F., 2016. The Eureka deformation in the Arctic: an outline. *J. Geol. Soc. Lond.* 173, 1007–1024. <https://doi.org/10.1144/jgs2016-081>.
- Piepjoh, K., Lorenz, H., Franke, D., Brandes, C., von Gosen, W., Gaedicke, C., Labrousse, L., Sobolev, N.N., Solobov, P., Swan, G., Mrugalla, S., Talarico, F., Tolmacheva, T., 2018. Mesozoic structural evolution of the New Siberian Islands. *Geol. Soc. Lond. Spec. Publ.* 460, 239–262. <https://doi.org/10.1144/SP460.1>.
- Piskarev, A., Poselov, V., Kaminsky, V. (Eds.), 2019. *Geologic Structures of the Arctic Basin*. Springer International Publishing, Cham. <https://doi.org/10.1007/978-3-319-77742-9>.
- Pogrebitsky, Y.E., 1971. *Paleotectonic Analysis of the Taimyr Folded System*. Nedra, Leningrad.
- Polteau, S., Hendriks, B.W.H., Planke, S., Ganerød, M., Corfu, F., Faleide, J.I., Midtkandal, I., Svensen, H.S., Myklebust, R., 2016. The early cretaceous Barents Sea Sill complex: distribution, 40Ar/39Ar geochronology, and implications for carbon gas formation. *Palaeogeogr. Palaeoclimatol. Palaeoecol.* 441, 83–95. <https://doi.org/10.1016/j.palaeo.2015.07.007>.
- Prokopyev, A.V., Khudoley, A., Egorov, A., Gertseva, M., Afanasieva, E., Sergeenko, A., Ershova, V., Vasiliev, D., 2013. Late Cretaceous-Early Cenozoic indicators of continental extension on the laptev Sea Shore (North Verkhoyansk). In: *3P Arctic. The Polar Petroleum Potential*. Conference & Exhibition. Abstract Book, Stavanger p. Abstract 1663486.
- Prokopyev, A.V., Ershova, V.B., Anfinson, O., Stockli, D., Powell, J., Khudoley, A.K., Vasiliev, D.A., Sobolev, N.N., Petrov, E.O., 2018. Tectonics of the New Siberian Islands archipelago: Structural styles and low-temperature thermochronology. *J. Geodyn.* 121, 155–184. <https://doi.org/10.1016/j.jog.2018.09.001>.
- Proskurnin, V.F., Vernikovskiy, V.A., Metelkin, D.V., Petrushkov, B.S., Vernikovskaya, A. E., Gavrilish, A.V., Bagaeva, A.A., Matushkin, N.Y., Vinogradova, N.P., Larionov, A.N., 2014. Rhyolite-granite association in the Central Taimyr zone: evidence of accretionary-collisional events in the Neoproterozoic. *Russ. Geol. Geophys.* 55, 18–32. <https://doi.org/10.1016/j.rgg.2013.12.002>.
- Pugh, A.T., Schröder-Adams, C.J., Carter, E.S., Herrle, J.O., Galloway, J., Haggart, J.W., Andrews, J.L., Hatsukano, K., 2014. Cenomanian to Santonian radiolarian biostratigraphy, carbon isotope stratigraphy and paleoenvironments of the Sverdrup Basin, Ellef Ringnes Island, Nunavut, Canada. *Palaeogeogr. Palaeoclimatol. Palaeoecol.* 413, 101–122. <https://doi.org/10.1016/j.palaeo.2014.06.010>.
- Puscharovsky, Y.M., 1960. Some general problems of the Arctic tectonics. *Reports Acad. Sci. USSR* 9, 15–28 (in Russian).
- Rekant, P., Sobolev, N., Portnov, A., Belyatsky, B., Dipre, G., Pakhalko, A., Kaban'kov, V., Andreeva, I., 2019. Basement segmentation and tectonic structure of the Lomonosov Ridge, arctic Ocean: Insights from bedrock geochronology. *J. Geodyn.* 128, 38–54. <https://doi.org/10.1016/j.jog.2019.05.001>.
- Rippington, S., Scott, R.A., Smyth, H., Bogolepova, O., Gubanov, A., 2010. *The Ellesmerian Orogeny: fact or fiction?*. In: *GeoCanada 2010 – Working with the Earth*. Saalman, K., Tessensohn, F., Piepjoh, K., von Gosen, W., Mayr, U., 2005. Structure of Palaeogene sediments in East Ellesmere Island: Constraints on Eureka tectonic evolution and implications for the Nares Strait problem. *Tectonophysics* 406, 81–113. <https://doi.org/10.1016/j.tecto.2005.06.005>.
- Schröder-Adams, C.J., Herrle, J.O., Embry, A.F., Haggart, J.W., Galloway, J.M., Pugh, A. T., Harwood, D.M., 2014. Aptian to Santonian foraminiferal biostratigraphy and paleoenvironmental change in the Sverdrup Basin as revealed at Glacier Fiord, Axel Heiberg Island, Canadian Arctic Archipelago. *Palaeogeogr. Palaeoclimatol. Palaeoecol.* 413, 81–100. <https://doi.org/10.1016/j.palaeo.2014.03.010>.
- Shatskiy, N.S., 1935. On the tectonics of the Arctic, in: *The Geology and Mineral Resources of the Northern USSR* Glavsnemortputi. 1st Geological Invitational Conference, Moscow, pp. 149–168 in Russian.
- Shatskiy, S.B., 1978. Main questions of stratigraphy and paleogeography of Paleogene of the West Siberia. In: Shatskiy, S.B. (Ed.), *Paleogene and Neogene of Siberia (Paleontology and Stratigraphy)*. Nauka, Novosibirsk, pp. 3–21 (in Russian).
- Shephard, G.E., Müller, R.D., Seton, M., 2013. The tectonic evolution of the Arctic since Pangea breakup: Integrating constraints from surface geology and geophysics with mantle structure. *Earth Sci. Rev.* 124, 148–183. <https://doi.org/10.1016/j.earscirev.2013.05.012>.
- Sherwood, K.W., Johnson, P.P., Craig, J.D., Zerwick, S.A., Lothamer, R.T., Thurston, D. K., Hurlbert, S.B., 2002. Structure and stratigraphy of the Hanna Trough, U.S. Chukchi Shelf, Alaska. In: Miller, E.L., Grantz, A., Klempner, S.L. (Eds.), *Special Paper 360: Tectonic Evolution of the Bering Shelf-Chukchi Sea-Arctic Margin and Adjacent Landmasses*. Geological Society of America, Boulder, Colorado, pp. 39–66. <https://doi.org/10.1130/0-8137-2360-4.39>.
- Shipilov, E.V., 2016. Basaltic magmatism and strike-slip tectonics in the Arctic margin of Eurasia: evidence for the early stage of geodynamic evolution of the Amerasia Basin. *Russ. Geol. Geophys.* 57, 1668–1687. <https://doi.org/10.1016/j.rgg.2016.04.007>.
- Shishkin, M.A., Faybusovich, Y.E., Shkarubo, S.I., Nazarov, D.V., Abakumova, L.A., Borozdina, Y.A., Voronin, A.S., Gerasicheva, A.V., Gorelina, T.E., Zavarzina, G.A., Zinchenko, A.G., Zuykova, O.N., Kostin, D.A., Lang, E.I., Likhotin, V.G., Markina, T. V., Petrov, S.Y., Petrova, M.N., Pushka, D.V., Radchenko, M.S.M., Rubin, L.I., Seregin, S.V., Solonina, S.F., Sychev, S.N., Tortsov, Y.I., Bazhko, S.F., Vasilenko, E. P., Ivanova, E.I., Perlov, D.K., Ruchkin, M.V., Stepanova, A.P., 2015. *State Geological Map of Russian Federation. Scale 1:1 000 000 (third generation)*. In: *West Siberian Seria. Quadrangle R-42, Yamal Peninsular*. Explanatory notes. VSEGEI, St. Petersburg.
- Shulgina, V.S., Bashlavin, D.K. (Eds.), 2000. *State Geological Map of Russian Federation. Scale 1:1 000 000 (New Seria)*. Nizhnekolymsk. Quadrangle R-(55)-57, Explanatory Note. VSEGEI, St. Petersburg.
- Skolotnev, S.G., Fedonkin, M.A., Korniychuk, A.V., 2017. New data on the geological structure of the southwestern Mendeleev rise, Arctic Ocean. *Dokl. Earth Sci.* 476, 1001–1006. <https://doi.org/10.1134/S1028334X17090173>.
- Skolotnev, S., Aleksandrova, G., Isakova, T., Tolmacheva, T., Kurilenko, A., Raevskaya, E., Rozhnov, S., Petrov, E., Korniychuk, A., 2019. Fossils from seabed bedrocks: Implications for the nature of the acoustic basement of the Mendeleev rise (Arctic Ocean). *Mar. Geol.* 407, 148–163. <https://doi.org/10.1016/j.margeo.2018.11.002>.
- Smelror, M., Petrov, O.V., Larssen, G.B., Werner, S. (Eds.), 2009. *Geological History of the Barents Sea. Atlas. Geological Survey of Norway, Trondheim*.
- Sobolev, P.O., Soloviev, A.V., 2013. Constraints on the Magnitude and timing of Cenozoic Exhumation for the Russian Barents Sea. In: 75th EAGE Conference & Exhibition Incorporating SPE EUROPEC 2013. London, United Kingdom. <https://doi.org/10.3997/2214-4609.20131053>.
- Sokolov, S.D., 2010. Tectonics of Northeast Asia: an overview. *Geotectonics* 44, 493–509. <https://doi.org/10.1134/S001685211006004X>.
- Sokolov, S.D., Bondarenko, G.Y., Morozov, O.L., Shekhovtsov, V.A., Glotov, S.P., Ganelin, A.V., Kravchenko-Berezhnoy, I.R., 2002. South Anyui suture, Northeast Arctic Russia: Facts and problems. In: Miller, E.L., Grantz, A., Klempner, S. (Eds.), *Special Paper 360: Tectonic Evolution of the Bering Shelf-Chukchi Sea-Arctic Margin and Adjacent Landmasses*. Geological Society of America, Boulder, Colorado, pp. 209–224. <https://doi.org/10.1130/0-8137-2360-4.209>.
- Sokolov, S.D., Tuchkova, M.I., Ganelin, A.V., Bondarenko, G.E., Layer, P., 2015. Tectonics of the South Anyui Suture, Northeastern Asia. *Geotectonics* 49, 3–26. <https://doi.org/10.1134/S0016852115010057>.
- Sokolov, S.D., Tuchkova, M.I., Moiseev, A.V., Verzhbitskii, V.E., Malyshev, N.A., Gushchina, M.Y., 2017. Tectonic zoning of Wrangel Island, Arctic region. *Geotectonics* 51, 3–16. <https://doi.org/10.1134/S0016852117010083>.
- Soloviev, A.V., 2008. *Investigation of the Tectonic Processes of the Convergent Setting of Lithosphere Plates: Fission-Track Dating and Structural Analysis*. Nauka, Moscow.
- Soloviev, A.V., Miller, E.L., 2014. The U-Pb age dating of detrital zircons from Upper Jurassic-lower cretaceous deposits of Stolbovoy Island (New Siberian Islands). *Stratigr. Geol. Correl.* 22, 507–517. <https://doi.org/10.1134/S0869593814050086>.
- Sømme, T.O., Doré, A.G., Lundin, E.R., Tørrudbakken, B.O., 2018. Triassic-Paleogene paleogeography of the Arctic: Implications for sediment routing and basin fill. *Am. Assoc. Pet. Geol. Bull.* 102, 2481–2517. <https://doi.org/10.1306/05111817254>.
- Startseva, K.F., 2018. *Stages of history of origin the East Barents and North Kara basins based on seismic stratigraphy analyses*. PhD Thesis. In: Moscow State University.
- Startseva, K.F., Nikishin, A.M., Malyshev, N.A., Nikishin, V.A., Yalushchega, A.A., 2017. Geological and geodynamic reconstruction of the East Barents megabasin from analysis of the 4-AR regional seismic profile. *Geotectonics* 51, 383–397. <https://doi.org/10.1134/S0016852117030104>.
- Stein, R., 2008. *Arctic Ocean Sediments: Processes, Proxies, and Paleoenvironment, 1st ed.* Elsevier Science.
- Stein, R., Jokat, W., Niessen, F., Weigelt, E., 2015. Exploring the long-term Cenozoic Arctic Ocean climate history: a challenge within the International Ocean Discovery Program (IODP). *arkots* 1, 3. <https://doi.org/10.1007/s41063-015-0012-x>.
- Stica, J.M., Zalan, P.V., Ferrari, A.L., 2014. The evolution of rifting on the volcanic margin of the Pelotas Basin and the contextualization of the Paraná-Étendeka LIP in the separation of Gondwana in the South Atlantic. *Mar. Pet. Geol.* 50, 1–21. <https://doi.org/10.1016/j.marpetgeo.2013.10.015>.
- Stoupakova, A.V., Henriksen, E., Burlin, Y.K., Larsen, G.B., Milne, J.K., Kiryukhina, T.A., Golynchik, P.O., Bordunov, S.I., Ogarkova, M.P., Suslova, A.A., 2011. Chapter 21 the geological evolution and hydrocarbon potential of the Barents and Kara shelves. *Geol. Soc. Lond. Mem.* 35, 325–344. <https://doi.org/10.1144/M35.21>.
- Suslova, A.A., 2013. *Conditions of formation of natural reservoirs of Jurassic oil and gas bearing complex of the Barents Sea Shelf*. PhD Thesis. In: Moscow State University.
- Tegner, C., Storey, M., Holm, P.M., Thorarinnsson, S.B., Zhao, X., Lo, C.-H., Knudsen, M.F., 2011. Magmatism and Eureka deformation in the High Arctic large Igneous Province: 40Ar–39Ar age of Kap Washington Group volcanics, North Greenland. *Earth Planet. Sci. Lett.* 303, 203–214. <https://doi.org/10.1016/j.epsl.2010.12.047>.

- Tikhomirov, P.L., 2018. Cretaceous Continental-Margin Magmatism of North-East Asia and Questions of Large Phanerozoic Acidic Volcanic Provinces. Moscow State University, Doctor of Sci. Dissertation.
- Tikhomirov, P.L., Prokofev, V.Y., Kal'ko, I.A., Apletalin, A.V., Nikolaev, Y.N., Kobayashi, K., Nakamura, E., 2017. Post-collisional magmatism of western Chukotka and early cretaceous tectonic rearrangement in northeastern Asia. *Geotectonics* 51, 131–151. <https://doi.org/10.1134/S0016852117020054>.
- Toro, J., Miller, E.L., Prokopiev, A.V., Zhang, X., Veselovskiy, R., 2016. Mesozoic orogens of the Arctic from Novaya Zemlya to Alaska. *J. Geol. Soc. Lond.* 173, 989–1006. <https://doi.org/10.1144/jgs2016-083>.
- Torsvik, T.H., Cocks, L.R.M., 2017. *Earth History and Palaeogeography*. Cambridge University Press, Cambridge. <https://doi.org/10.1017/9781316225523>.
- Torsvik, T.H., Carlos, D., Mosar, J., Cocks, L.R.M., Malmé, T.N., 2002. Global reconstructions and North Atlantic paleogeography 440 Ma to recent. In: Eide, E.A. (Ed.), *BATLAS – Mid Norway Plate Reconstructions Atlas with Global and Atlantic Perspectives*. Geological Survey of Norway, pp. 48–59.
- Unger, A.V., Nikishin, A.M., Kuzlyapina, M.A., Afanasenkov, A.P., 2017. Evolution of the inversion megaswells of the Yenisei–Khatanga Basin. *Mosc. Univ. Geol. Bull.* 72, 164–171. <https://doi.org/10.3103/S0145875217030097>.
- Vasilieva, O.N., 2017. *Dinocysts and Biostratigraphy of Paleogene of Trans-Uralian Area, Turgay Basin and Precaspian Basin*. Doctor of Sci. Dissertation, Zavaritsky Institute of Geology and Geochemistry.
- Vatruschkina, E.V., 2018. *Upper Jurassic and Lower Cretaceous deposits of Western Chukotka: composition, provenance, sedimentological environments and geodynamic regimes*. In: PhD Thesis. Academy of Sciences.
- Vernikovskiy, V.A., 1996. *Geodynamic Evolution of Taimyr Folded Area*. SB RAS, SPC UIGGM, Novosibirsk.
- Vernikovskiy, V.A., Vernikovskaya, A.E., 2001. Central Taimyr accretionary belt (Arctic Asia): Meso–Neoproterozoic tectonic evolution and Rodinia breakup. *Precambrian Res.* 110, 127–141. [https://doi.org/10.1016/S0301-9268\(01\)00184-X](https://doi.org/10.1016/S0301-9268(01)00184-X).
- Vernikovskiy, V.A., Dobretsov, N.L., Metelkin, D.V., Matushkin, N.Y., Koulakov, I.Y., 2013. Concerning tectonics and the tectonic evolution of the Arctic. *Russ. Geol. Geophys.* 54, 838–858. <https://doi.org/10.1016/j.rgg.2013.07.006>.
- Verzhbitsky, V.E., Sokolov, S.D., Tuchkova, M.I., Frantzen, E.M., Little, A., Lobkovsky, L. I., 2012. The South Chukchi Sedimentary Basin (Chukchi Sea, Russian Arctic). In: *Tectonics and Sedimentation*. American Association of Petroleum Geologists, Tulsa, Oklahoma, pp. 267–290. <https://doi.org/10.1306/13351557M1003534>.
- Verzhbitsky, V.E., Sokolov, S.D., Tuchkova, M.I., 2015. Present-day structure and stages of tectonic evolution of Wrangel Island, Russian eastern Arctic Region. *Geotectonics* 49, 165–192. <https://doi.org/10.1134/S001685211503005X>.
- Vinogradov, A.P. (Ed.), 1968. *Atlas of the lithological-paleogeographical maps of the USSR*. Vol. 3. Triassic, Jurassic and Cretaceous. Ministry of Geology of the USSR, Moscow.
- Viskunova, K.G., Zinchenko, A.G., Kalenich, A.P., Kiyko, O.A., Kozlov, S.A., Kostin, D.A., Kuzin, I.L., Lopatin, B.G., Orgo, V.V., Penedyuk, E.V., Ustinov, N.V., Shkarubo, S.I., Yakovleva, T.V., 2004. State geological map of Russian federation. Scale 1:1 000 000 (new Series). Quadrangle S-41-43. Belyi Island. In: *Explanatory Note*. St. Petersburg, VSEGEI.
- Volkova, V.S., 2014. Geologic stages of the Paleogene and Neogene evolution of the Arctic shelf in the Ob' region (West Siberia). *Russ. Geol. Geophys.* 55, 483–494. <https://doi.org/10.1016/j.rgg.2014.03.006>.
- Volkova, V.S., Kuz'mina, O.B., Gnibidenko, Z.N., Golovina, A.G., 2016. The Paleogene/Neogene boundary in continental deposits of the West Siberian Plain. *Russ. Geol. Geophys.* 57, 303–315. <https://doi.org/10.1016/j.rgg.2016.02.007>.
- Weigelt, E., Jokat, W., Franke, D., 2014. Seismostratigraphy of the Siberian Sector of the Arctic Ocean and adjacent Laptev Sea Shelf. *J. Geophys. Res. Solid Earth* 119, 5275–5289. <https://doi.org/10.1002/2013JB010727>.
- Wilkinson, C.M., Ganerød, M., Hendriks, B.W.H., Eide, E.A., 2017. Compilation and appraisal of geochronological data from the North Atlantic Igneous Province (NAIP). *Geol. Soc. Lond. Spec. Publ.* 447, 69–103. <https://doi.org/10.1144/SP447.10>.
- Yakovleva, A.I., 2017. *Dinocysts of Late Paleocene and Eocene Marine Basins of the Eurasia: Systematics, Detailed Biostratigraphy and Restorations of Paleoenvironments*. Doctor of Sci. Dissertation, Russian Academy of Sci.
- Yang, Y.-T., Guo, Z.-X., Song, C.-C., Li, X.-B., He, S., 2015. A short-lived but significant Mongol–Okhotsk collisional orogeny in latest Jurassic–earliest cretaceous. *Gondwana Res.* 28, 1096–1116. <https://doi.org/10.1016/j.gr.2014.09.010>.
- Zhang, X., Omma, J., Pease, V., Scott, R., 2013. Provenance of late Paleozoic–Mesozoic Sandstones, Taimyr Peninsula, the Arctic. *Geosciences* 3, 502–527. <https://doi.org/10.3390/geosciences3030502>.
- Zhang, X., Pease, V., Skogseid, J., Wohlgenuth-Ueberwasser, C., 2016. Reconstruction of tectonic events on the northern Eurasia margin of the Arctic, from U-Pb detrital zircon provenance investigations of late Paleozoic to Mesozoic sandstones in southern Taimyr Peninsula. *Geol. Soc. Am. Bull.* 128, 29–46. <https://doi.org/10.1130/B31241.1>.
- Zhuravlev, V.A., Korago, E.A., Kostin, D.A., Zuykova, O.N., Goncharov, A.V., Gusev, E.A., Zinchenko, A.G., Ivanova, V.V., Kovaleva, G.N., Kozlov, S.A., Krasilova, M.V., Lopatin, B.G., Mintseva, E.I., Nagaytseva, N.N., Povyshcheva, L.G., Preobrazhenskaya, E.N., Radchenko, M.S., Rudenko, O.V., Solonina, S.F., Ustinov, N. V., Shkarubo, S.I., 2014. *State Geological Map of Russian Federation. Scale 1:1 000 000 (Third Generation)*. North Kara-Barents Sea Series. Quadrangle R-39. Kolguev Island-Kara Gate Strait. Explanatory note. VSEGEI, St. Petersburg, p. 40.
- Ziegler, P.A., 1988. Evolution of the Arctic-North Atlantic and the Western Tethys. *Am. Assoc. Pet. Geol. Mem.* 43, 1–198.
- Ziegler, P.A., 1989. *Evolution of Laurussia. A Study in Late Palaeozoic Plate Tectonics*. Kluwer Academic Publishers.
- Zonenshain, L.P., Kuzmin, M.I., Natapov, L.M., 1990. *Geology of the USSR: A Plate-Tectonic Synthesis*, Geodynamics Series. American Geophysical Union, Washington, D. C. <https://doi.org/10.1029/GD021>.
- Zyleva, L.I., Kononov, A.L., Kazak, A.P., Zhdanov, A.V., Korkunov, K.V., Denisov, V.A., Novikova, L.P., Rumyantseva, N.A., Cherepanov, Y.P., Cherkashin, A.V., Khyrskova, L.A., 2014. *State Geological Map of Russian Federation. Scale 1:1 000 000 (third generation)*. West Siberian Series. Quadrangle R-39, Q-42, Salekhard. In: *Explanatory Note*. St. Petersburg, VSEGEI.